UNIVERSITÀ DEGLI STUDI DELL'AQUILA
DIPARTIMENTO DI Ingegneria Industriale, dell'Informazione ed Economi

Dottorato di Ricerca in Ingegneria industriale dell'informazione e di economia

Curriculum ingegneria chimicae materiali

ciclo **XXXVII**

Titolo della tesi

Treatments of macro-organic and micropollutants contained in wastewater using advanced oxidation processes

ICHI 02/A

Dottoranda

Karima AYEDI

Coordinatore del corso

Prof..ssa Katia Gallucci

Tutor

Prof..ssa Marina Prisciandaro

Prof..ssa Valentina Innocenzi

a.a. 2023/2024

ABSTRACT

Water pollution has been a persistent environmental concern, driving extensive research into effective wastewater treatment methods. Among the advanced oxidation processes (AOPs), cavitation-based treatments have emerged as promising technologies due to their high efficiency in pollutant removal. The objective of this doctoral research focuses on the degradation of dyes, hydrocarbons, and phenols from industrial wastewater, particularly from the textile, pharmaceutical, and agro-industries.

Hydrodynamic cavitation (HC) has shown significant potential in treating dyeing solutions, even at low concentrations, and achieving the mineralization of organic pollutants. The study investigates the degradation of Methyl Blue (MB) using HC and evaluates the effectiveness of a hybrid process combining ozone (O3) with HC. Optimal operating conditions were determined, including pressure (4.5 bar), pH (2), and O3 dosage (7.5 mg/L). Results showed that the hybrid process significantly enhances degradation efficiency, achieving a 100% decolorization yield for MB at an initial concentration of 10 mg/L within 30 minutes.

Additionally, the research explores the treatment of winery wastewater (WW) using the Fenton process, which demonstrated up to 85% COD removal under optimal conditions (pH 3, $[H_2O_2]$ = 0.5 mol/L, $[H_2O_2]/[Fe2+]$ = 2.5) within 1 hour. The integration of membrane processes with HC and Fenton treatment for dyeing wastewater was also examined, highlighting the potential for water reuse and safe discharge of treated effluents.

The research investigates the removal of polycyclic aromatic hydrocarbons (PAHs) from soil washing emulsions using Fenton and solar photo-Fenton processes, emphasizing the recovery and reuse of surfactants. Soil was artificially contaminated with anthracene (ANT) and benzo[a]pyrene (BaP) and subsequently washed using sodium dodecyl sulfate (SDS). Complete removal of PAHs was achieved with the Fenton process, with BaP consistently degraded across all conditions, while ANT required the highest H_2O_2 (240 mg dm^{-3}) and Fe (10 mg dm^{-3}) concentrations over 6 hours. The solar photo-Fenton process achieved 100% removal of BaP and up to 70% removal of ANT. Notably, minimal SDS degradation and negligible emulsion mineralization were observed, indicating preservation of the surfactant's integrity post-treatment.

This study presents a comparative analysis of traditional wastewater treatment processes and innovative approaches incorporating hydrodynamic cavitation. The

findings reveal substantial improvements in pollutant removal efficiencies and cost-effectiveness. Notably, the innovative process achieved a 95% reduction in COD, underscoring the efficacy of the combined operation. Significant enhancements in TOC and BOD5 reductions further highlight the potential of these methods to produce high-quality effluent suitable for industrial reuse. Additionally, the process analysis of the Takeda wastewater treatment plant demonstrated the effectiveness of integrating hydrodynamic cavitation with advanced oxidation processes. The plant's comprehensive multi-stage process, A detailed cost analysis further supports the economic feasibility of these innovative treatment methods.

In conclusion, this thesis underscores the potential of hydrodynamic cavitation and its combination with other advanced processes as sustainable and effective wastewater treatment technologies. The findings contribute to advancing knowledge in the field and provide valuable insights for developing innovative remediation strategies.

Keywords: Hydrodynamic cavitation, Advanced oxidation processes, Wastewater treatment, Methyl Blue, Ozone, Fenton process, Winery wastewater, Textile industry, Polycyclic aromatic hydrocarbons, Soil remediation, Surfactant Recovery

CONTENTS

Abstract II

List of figures iv

List OF TABLES vii

List of abbreviations ix

Nomenclature ix

Latin ix

Greek ix

1.1 Background and Motivation x

2. Literature review 1

2.1 Background of Cavitation Process 1

2.1.1 Cavitation Process 2

2.1.2 **HC Generation and Mechanisms** 6

2.1.3 HC Flow Regimes 7

2.1.4 Mechanisms of Pollutant Degradation 13

2.1.5 The Effect of Various Parameters on HC Effectiveness 14

2.1.6 Device Construction Parameters 14

2.1.7 Properties of the Liquid Medium 22

2.2 Methods to Evaluate Cavitation Efficiency 25

2.2.1 Conventional Scheme of HC Experimental System 27

3. Water reuse 29

3.1 Water Reuse Quality Criteria 31

3.2 Review on Urban Water Allocation and Reuse Modeling 36

3.3 Wastewater Treatment Technologies Used in Water Reuse 37

3.4 energy-approach-carbon 37

3.4.1 Emission Limits for Water Discharges 40

3.4.2 Emerging Pollutants 43

3.4.3 Agricultural and Green Space Irrigation 44

3.4.4 Industrial Use 45
4. Wastewater Contaminants: Types and Treatment Methods 48
4.1 Introduction to Wastewater Contaminants 48
4.2 . Types 49
4.2.1 Dyes 49
4.2.2 Textile Wastewater 52
4.2.3 Winery wastewater 56
4.2.4 The Stages of Wine Production 57
4.2.5 Production of Winery Wastewater 59
4.3 Possible Applications of Treated Winery Wastewater: Advantages and Limitations ... 61
4.4 hydrocarbones 62
4.4.1 Physical and Chemical Characteristics of Polycyclic Aromatic Hydrocarbon 63
4.4.2 Occurrence and Environmental Fate of PAHs 64
4.4.3 Reactivity of PAHs 65
4.4.4 Analytical Procedures for the Measurement of PAHs 66
4.5 Treatment Methods 67
4.5.1 . Primary Processes 67
4.5.2 . Secondary Treatment Processes 68
4.5.3 Tertiary Treatment Processes 69
4.5.4 Acoustic and Hydrodynamic Cavitation 72
4.5.5 . The Fenton Process 76
4.5.6 Innovative Treatments of Textile Wastewater 80
5. Materials and methods 87
5.1 Materials and Methods 87
5.2 cavitation system 87
5.2.1 chemicals 87
5.2.2 Experimental Setup and Procedure 87
5.2.3 Analytical procedure 93
5.3 Fenton and Solar photo-Fenton SYSTEM 95
5.3.1 chemicals 95
5.3.2 Experimental Setup and Procedure 95

5.3.3 Analytical procedure 98
6. Experimetal results 101
6.1 Dyes and textiles treatments results 102
6.1.1 dyes results 102
6.1.2 textiles results 114
6.2 winery treatments results 128
6.2.1 . Results and discussion 128
6.3 hydrocarbons treatments results 135
6.3.1 Soil characterization 135
6.3.2 . Surfactant soil washing 135
6.3.3 Treatment of polluted emulsion 137
6.4 water reuse results 148
6.5 . Process analysis 150
6.5.1 Textile wastewater 151
6.5.2 Pharmaceutical wastewater of Takeda 154
6.5.3 Results and discussion 161
7. Conclusions 167
Appendix A 170
Addendum B 174
Bibliograph 175
Acknowledgements 202

LIST OF FIGURES

Figure 1:Diagram phase [Brennen 27]..... 4

Figure 2:Simple steps of hydrodynamic cavitation: nucleation, bubble growth, bubble implosion with arrows to show the flow of events [Brennen 27] 5

Figure 3:effect of constriction on flow velocity and pressure in a venturi system, a) contours of flow velocity magnitude, b) contours of flow pressure magnitude, c) high speed camera frames [Brennen 27]..... 7

Figure 4**:**Attached cavitation on hydrofoil and bluff body and describe the attached cavitation [Brennen 27] 10

Figure 5:Shematic representation of developed HC(a) where highly dynamical vapour cloud shedding associated with high pressure pulsation is expected and super cavitation (b) which is characteristic of large cavitation pocket reproduced from Dular et al 11

Figure 6:Convected cavitation [Brennen 27]..... 12

Figure 7:vortex cavitation [Brennen 27]..... 13

Figure 8:Linear (a) and circular (b) urban metabolism systems Source: Novotny (2013), page 591 30

Figure 9:Electricity in different wastewater technologies Source: Lee et al. [101] p. 599. 38

Figure 10: Water in the Industrial World..... 45

Figure 11: Difference Between Water Treatments in the Industrial Field..... 46

Figure 12:Absorption Spectrum of Methylene Blue Showing Three Distinct Peaks At Wavelengths Of 290 Nm, 590 Nm, And 670 Nm. 51

Figure 13: Chemical structures indicating numbered positions PAHs 66

Figure 14:Various stages of cavitation events with a pressure profile in the hydrodynamic cavitation reactor..... 73

Figure 15:Formation and collapse of bubbles in a Venturi tube..... 74

Figure 16: Phases of Cavitation..... 81

Figure 17: Venturi Tube - Hydrodynamic Cavitation..... 81

Figure 18:Lab-scale experimental apparatus. 88

Figure 19:Process flowsheet diagram for winery wastewater treatment. 90

Figure 20:Spectrophotometer used for the evaluation of chlorides, phenols, and sulfates 94

Figure 21: Scheme of the experimental set-up Fenton and Solar photo-Fenton. 96

Figure 22:Simulated solar light received in the reactor 96

Figure23:Effect of the inlet pressure on MB decolorization (C0 = 5 mg/L, V = 1 L, pH = 2, T = 20°± 2°C)..... 104

Figure 24: Kinetic analysis for the experiment conducted at 4.5 bar..... 104

Figure 25:Comparison between methyl orange (MO) and methyl blue (MB)..... 105

Figure 26: Effect of the initial solution concentration (in ppm) on the degradation of MB (Pin = 4.5 bar; V = 1 L; pH = 2; T = 20 ± 2 °C)..... 106

Figure 27:Effect of O3 dosage on the degradation of MB (C0=10mg/L; V = 1 L; pH = 2; T = 20 ± 2 °C)..... 107

Figure 28:Effect of pH on the degradation of MB (C0=10 mg/L; O3=8 LPM; V = 1 L; pH = 2; T = 20 ± 2 °C) 108

Figure 29: Effect of O_3 on the degradation of MB at high concentration (Pin=4.5 bar; O3=8 LPM; V = 1 L; pH = 2; T = 20± 2 °C) 109

Figure 30: Main effect and interaction 110

Figure 31: Effect of HC combined with O3 on the degradation of MB (Pin=4.5 bar; O3=8 LPM; V = 1L; pH = 2; T = 20± 2 °C)..... 111

Figure 32:the Hydraulic curve..... 116

Figure 33:UV-vis spectra of textile wastewater degradation before and after HC +H_2O_2 treatments 118

Figure 34:Extent of COD and Color reduction obtained in the presence of oxygen peroxide (Experimental conditions: pressure= 4.5 bar, pH = 2, Temperature = 25 ± 2 ◦C). 119

Figure 35: Extent of COD and color reduction obtained for HC+H_2O_2 and HC+Ozone (Experimental conditions: pH = 2, Temperature = 25 ± 2 ◦C, Ozone flow rate = 7.5 mg/L [H_2O_2] = 0.3 mol/L, pressure = 4.5 bar) 122

Figure 36:COD concentration as a function of the treatment 123

Figure 37 :Process analysis for the traditional process 127

Figure 38:Response surface for COD removal as a function of [H2O2] and [H2O2/Fe2+]..... 133

Figure 39: Comparison between experimental and model predicted values for CODremoval..... 134

Figure 40**:** a) Adsorption isotherm of SDS in the contaminated soil and, b) K_d of ANT (triangles) and BaP (squares) after soil washing with SDS (V_L/W = 2 mL g^{-1}, 24 h). 136

Figure 41:Normalized concentration of PAHs ([SDS]$_0$ = 4500 mg dm^{-3}, [ANT]$_0$ = 5 mg dm^{-3}, [BaP]$_0$ = 5 mg dm^{-3}) without reagents, in the presence of H_2O_2 (120 mg dm^{-3}), and Fe (5 mg dm^{-3}) (E1-E3). Black bars: ANT; white bars: Ba, pH=7..... 138

Figure 42:Influence of H_2O_2 concentration (60 (●), 120 (■), and 240 mg dm^{-3} (▲)) on the degradation of PAHs in the emulsion by Fenton process (E4-E6). [SDS]$_0$ = 4500 mg dm^{-3}; [ANT]$_0$ = 5 mg dm^{-3}; [BaP]$_0$ = 5 mg dm^{-3}; [Fe]$_0$ = 5 mg dm^{-3}, pH=3..... 139

Figure 43: Influence of iron concentration (2.5 (●), 5 (■), and 10 mg dm^{-3} (▲)) on the degradation of PAHs in the emulsion in the Fenton process (E5, E7-E8). $[SDS]_0$ = 4500 mg dm^{-3}; $[ANT]_0$ = 5 mg dm^{-3}; $[BaP]_0$ = 5 mg dm^{-3}; $[H_2O_2]_0$ = 120 mg dm^{-3}, pH=3..... 140

Figure 44**:**Influence of H_2O_2 concentration (60 (●), 120 (■) and 240 mg dm^{-3} (▲)) on the degradation of PAHs in the solar Photo-Fenton process (E12-E14). $[SDS]_0$ = 4500 mg dm^{-3}; $[ANT]_0$ = 5 mg dm^{-3}; $[BaP]_0$ = 5 mg dm^{-3}; $[Fe]_0$ = 5 mg dm^{-3}, pH=7..... 142

Figure 45**:** Influence of iron concentration (2.5 (●), 5 (■), and 10 mg dm^{-3} (▲)) on the degradation of PAHs in the solar photo-Fenton process (E15, E13, E16). $[SDS]_0$ = 4500 mg dm^{-3}; $[ANT]_0$ = 5 mg dm^{-3}; $[BaP]_0$ = 5 mg dm^{-3}; $[H_2O_2]_0$ = 120 mg dm^{-3}, pH=7..... 143

Figure 46**:**PAHs degradation at 6 h by Fenton and solar photo-Fenton with varying oxidant and catalyst dosages. ANT: orange bars; BaP: blue bars. Fenton: stripped bars; solar photo-Fenton: full bars 145

.Figure 47:Surfactant capacity of the emulsion (SDS and TOC) after the (a) Fenton and (b) solar-Fenton processes at different oxidant and catalyst doses. CMC values remain unchanged after oxidation treatment. 148

Figure 48:*(a) Process analysis with hydrodynamic cavitation alone and (b)q process analysis with hydrodynamic cavitation preceded by adding a solution of H2O2 +metals 151

Figure 49 : The Takeda process..... 157

LIST OF TABLES

Table 1: Concentration in mg/L of main pollutants in effluents from domestic appliances, greywater, domestic and municipal wastewater 32

Table 2 :The water reuse percentages 35

Table 3: An equivalent inhabitant also corresponds to a chemical oxygen demand (COD) of 130 grams of O2 per day or a discharge volume of 200 liters of wastewater per inhabitant per day, referring to the highest value (D.P.G.R. 28/R/03).Table 4: Emission Limits for Urban Wastewater Treatment Plants 41

Table 5: Emission Limits for Urban Wastewater Treatment Plants Discharging in Sensitive Areas 42

Table 6: Physicochemical characteristics of methylene 51

Table 7: Textile Effluent Parameters 54

Table 8: Dyes Used in the Textile Sector (Tecnotessile, 2007)[118] 54

Table 9: COD of Wastewater Resulting from Wool Dyeing [118] 55

Table 10: Pollutants in Washing Water (Tecnotessile, 2007)[118] 55

Table 11: BOD5 and COD Values in Finishing (Tecnotessile, 2007)[118] 56

Table 12: Operational Structures in the Wine Production Sector (ISTAT data)[121] 60

Table 13: Possible Applications of Treated Water with Respective Limits 62

Table 14: Summary of Primary Treatment Processes 68

Table 15: Winery Wastewater Treatment Methods with Corresponding Efficiencies[123] 71

Table 16: Table Summary of Experimental Conditions for Treating Wastewaters 93

Table 17: Experimental conditions for treating contaminated emulsions (4500 mg dm^{-3} of SDS and 5 mg dm^{-3} of BaP and ANT) 98

Table 18: Factorial plan and experimental results 109

Table 19: Analysis of the variance 110

Table 20: Comparison with other studies of MB Degradation using hydrodynamic cavitation. 112

Table 21: Energy consumption for the degradation of 95% of dye solutions 114

Table 22: Characteristics of effluent 115

Table 23 : Characteristics of effluent after H2O2 treatment 117

Table 24 :the kinetic constant for different approaches. 118

Table 25:Characteristics of effluent after HC+H_2O_2 treatment 119

Table 26:Estimation of cost for various approaches coupled with HC 126

Table 27:Comparison between traditional and innovative process 128

Table 28:Characteristics of effluent. 129

Table 29:Independent Variable Actual and Coded Values Used for Two-Factor, Three-Level. 130

Table 30:Observed and predicted COD removal for the two factors used to assess performance of the Fenton-like process for the treatment of actualWWpre-treated via centrifugation. 131

Table 31:ANOVA results for the development of quadratic models to predict COD removal. 132

Table 32:Pseudo-first order kinetic constants calculated for the degradation of PAHs with the Fenton and photo-Fenton processes at different oxidant and catalyst doses. 144

Table 33:Typical performance summary for reverse osmosis process 152

Table 34:The characteristics of stream 153

Table 35: Characteristics of effluent 161

Table 36: Concentration of Parameters Before and After Treatment 163

Table 37: Degradation Rates Achieved Through Hydrodynamic Cavitation (HC) 163

LIST OF ABBREVIATIONS

NOMENCLATURE

LATIN

AOPs: Advanced oxidation processes

ANT: anthracene

BaP: benzo[a]pyrene

BOD: Biochemical Oxygen Demand

COD: Chemical Oxygen Demand

C.Y.: Cavitation Yield

EVV: management of winemaking wastewater

ED: Extent of Degradation

HC: Hydrodynamic cavitation

PHCs : Petroleum hydrocarbons

PV : vapor pressure

PAHs: polycyclic aromatic hydrocarbons

SDS: sodium dodecyl sulfate

TOC: Total Organic Carbon

TDS: Dissolved Inorganics: Measured as Total Dissolved Solid

GREEK

ΔP	pressure difference
ρ	*the liquid density*
P	*pressure*

1.1 Background and Motivation

Industrialization has revolutionized global economies but has also introduced significant environmental concerns, particularly regarding the management and treatment of wastewater pollutants. Industries across sectors such as manufacturing, chemical processing, mining, and textiles generate vast quantities of wastewater containing a complex array of contaminants. These include heavy metals, persistent organic pollutants like dyes and solvents, hydrocarbons, and various chemical byproducts, each presenting distinct challenges for environmental stewardship and public health [1]

The discharge of untreated or inadequately treated industrial effluents into natural water bodies poses immediate and long-term risks. Pollutants can persist in aquatic environments, bioaccumulate in organisms, and enter the food chain, thereby threatening both aquatic biodiversity and human health through exposure via drinking water and agricultural produce [2].This cumulative impact underscores the urgent need for effective and sustainable wastewater treatment solutions.

Conventional treatment methods, while foundational in water treatment practices, often fall short when dealing with recalcitrant pollutants found in industrial effluents. Organic compounds such as synthetic dyes used extensively in textiles and hydrocarbons from petroleum refining processes are notable examples of contaminants that resist degradation by traditional means due to their complex molecular structures and chemical stability([3] Incomplete degradation of these pollutants can lead to the formation of toxic intermediates, further complicating environmental remediation efforts.

Advanced oxidation processes (AOPs) have emerged as promising alternatives for tackling the persistence and toxicity of industrial wastewater pollutants. Among AOPs, hydrodynamic cavitation (HC) has gained prominence for its ability to induce powerful physical and chemical transformations in aqueous solutions. HC operates by creating and rapidly collapsing vapor-filled cavities within turbulent flows, generating localized extremes of temperature and pressure that facilitate the

production of highly reactive hydroxyl radicals (•OH) and other oxidative species [4]

The unique role of hydrodynamic cavitation lies in its capacity to enhance the breakdown of complex organic molecules present in industrial wastewater. Through the intense cavitation-induced processes, HC generates conditions where organic bonds are effectively cleaved, leading to the fragmentation of pollutants into simpler, more biodegradable forms. This mechanism not only accelerates the degradation kinetics but also promotes the mineralization of contaminants, reducing them to harmless substances such as carbon dioxide and water.

The application of HC in industrial wastewater treatment offers several strategic advantages. It enables enhanced removal rates of diverse pollutants, including dyes, solvents, and hydrocarbons, while reducing reliance on chemical additives and energy-intensive processes associated with traditional treatment methods [5] Moreover, HC has the potential to mitigate environmental impacts by facilitating the complete mineralization of contaminants, thereby preventing the accumulation of harmful residues in natural ecosystems.

However, the successful implementation of HC in industrial settings hinges on optimizing operational parameters and system configurations to suit specific wastewater compositions and treatment objectives. Tailoring HC setups to accommodate variations in flow dynamics, reactor designs, and cavitation intensity is essential for maximizing treatment efficacy and ensuring consistent performance across different industrial sectors and pollutant profiles.

In conclusion, addressing the complex challenges posed by industrial wastewater requires innovative and sustainable approaches that integrate advanced technologies like HC. By advancing our understanding of cavitation-induced processes and optimizing their application in wastewater treatment, we can enhance environmental stewardship, safeguard water resources, and promote the long-term sustainability of industrial activities on a global scale.

OBJECTIVES AND SCOPE

The goal of this doctoral research is to develop effective treatment methods for the removal of pollutants i.e. dye, hydrocarbon, organic substances, phenols from wastewater coming from different industrial sector, mainly textile, pharmaceutical and winery industries. The study begins with an introduction that outlines the research questions, scope, and the environmental impact of dye pollution, hydrocarbon contamination, and textile and winery waste. The literature review covers various treatment methods, including physicochemical techniques like adsorption, membrane filtration, coagulation-flocculation, and ion exchange, as well as advanced oxidation processes (AOPs) such as photocatalysis, chemical oxidation, and electrochemical treatment. Biological methods, including microbial degradation and enzymatic approaches, are also discussed.

For hydrocarbon treatment, the focus is on bioremediation, phytoremediation, and chemical methods. The treatment of textile and winery waste is explored through hydrodynamic cavitation, highlighting its application, results, and advantages. The experimental methods section details the materials and methods, study areas, experimental set-up, and analytical methods used for data processing.

The results and discussion chapter presents data on dye and hydrocarbon removal efficiency, comparing the effectiveness of different methods. It also discusses the impact of hydrodynamic cavitation on textile and winery waste treatment. The scope of this research includes also a comprehensive process analysis of traditional and innovative wastewater treatment methods, with a specific focus on the Takeda wastewater treatment plant. This analysis highlights the operational improvements and cost-effectiveness achieved through the implementation of hydrodynamic cavitation and advanced oxidation processes.

Finally, the challenges faced during the research and future directions for further study and practical applications are outlined

2. LITERATURE REVIEW

2.1 BACKGROUND OF CAVITATION PROCESS

Hydrodynamic cavitation (HC) has emerged as a transformative technique for intensifying chemical and mechanical processes, particularly within the field of wastewater treatment. This process leverages the formation, growth, and collapse of bubbles to generate extreme conditions that facilitate the degradation of pollutants and the solubilization of organic matter.[6]

The effectiveness of HC is rooted in its dual mechanisms: chemical and mechanical. Chemically, HC promotes the thermal decomposition of volatile pollutants and the interaction of hydroxyl radicals with contaminants at the cavity-water interface. Mechanically, the process generates shock waves, liquid micro-jets, and interfacial turbulence, all of which contribute to the breakdown of complex molecules and enhance mass and heat transfer.[3], [7]

[8]. Factors such as flow velocity, inlet pressure, temperature, pH, viscosity, and surface tension significantly influence cavitational effects. For instance, increasing flow velocity and inlet pressure generally enhances cavitation, although supercavitation at very high pressures can reduce efficiency. Optimal temperatures balance increased kinetic rates with the drawbacks of higher vapor content in bubbles, while acidic conditions favor pollutant degradation due to the availability of hydroxyl radicals. Additionally, the presence of dissolved gases enhances cavitation by providing nuclei and affecting collapse dynamics.[9]

Evaluating the efficiency of HC involves metrics like the Extent of Degradation (ED) and Cavitational Yield (C.Y.), which allow for comparisons between different setups. HC also improves biological treatment processes by enhancing sludge solubilization and accelerating both aerobic and anaerobic digestion through the breakdown of bacterial cell walls and the release of intracellular matter [10,11].

Due to its elevated oxidative capability, hydrodynamic cavitation (HC), either as a standalone technique or in combination with other methods, has been utilized for a variety of applications. These range from biological uses, such as cell disruption, to chemical reactions like the oxidation of organic pollutants in aqueous effluents, including bio-refractory toxic chemicals [11, 12]

Generally, the effectiveness of the cavitation process in wastewater treatment has been widely demonstrated using acoustic cavitation (AC) [13, 14] which has shown to overcome some limitations of advanced oxidation processes (AOPs) that are commonly incapable of completely degrading complex compounds. In the last decade, the high costs associated with AC have been mitigated by the development of HC technologies. HC is proving to be characterized by higher removal efficiencies compared to other conventional treatment techniques, higher energy efficiencies, and fewer issues of secondary contamination. [8, 15, 16]

While many studies have focused on the application of AC in wastewater treatments, HC has also been extensively researched, showing promising outcomes in fields such as sludge and biomass pretreatment, denitrification processes, activated sludge reduction, and the removal of carcinogens, toxic dyes, and pharmaceuticals [17, 18, 19]

2.1.1 Cavitation Process

Cavitation is described as the process where bubbles or cavities are generated (inception), grow, merge, split, and collapse violently within a liquid in less than a few microseconds. This phenomenon results in extremely high local temperatures (500-5000 K) and pressures (up to 5000 atm), leading to various physical, chemical, and mechanical effects.[20]

Depending on the mode of its generation, cavitation can be classified into:

- **Acoustic Cavitation (AC)**: Generated by ultrasound waves.
- **Hydrodynamic Cavitation (HC)**: Caused by local pressure fluctuations.
- **Optic Cavitation (OC)**: Occurs when a liquid is irradiated with high-intensity light or lasers.
- **Particle Cavitation (PC)**: Induced by elementary particles such as protons and neutrinos.

OC and PC occur when a liquid is exposed to high-intensity light or lasers. In OC, photons rupture the liquid, while in PC, other elementary particles like protons and neutrinos are used [21] Conversely, AC and HC rely on local pressure fluctuations causing pressure drops. Although all four types generate bubbles, only AC and HC have been found to induce the desired chemical changes in treated materials in the environmental field. [21, 22, 23]

To better understand the cavitation process based on local pressure drops, the well-known thermodynamic concept of vapor pressure can be considered.[24, 25] . As shown in the phase diagram of water, the curve from the triple point to the critical point separates the liquid and vapor domains. Crossing this curve represents a reversible transformation under static or equilibrium conditions. Phase transformations from liquid to vapor (evaporation) or vice versa (condensation) occur at a specific pressure known as the vapor pressure (Pv) for each temperature. Cavitation is like boiling, except that the main driving mechanism is a pressure change rather than a temperature change. [26, 27, 28] Cavitation bubbles in a liquid typically grow in a low-pressure region and are transported by convection into a higher-pressure region where they collapse.

When cavitation occurs, it is possible to observe a breakdown or void creation in the fluid. This void is then filled by vapor with eventual saturation. All these phases occur simultaneously, and the instantaneous saturation of the void with vapor can be justifiably assumed. [6, 29, 30]

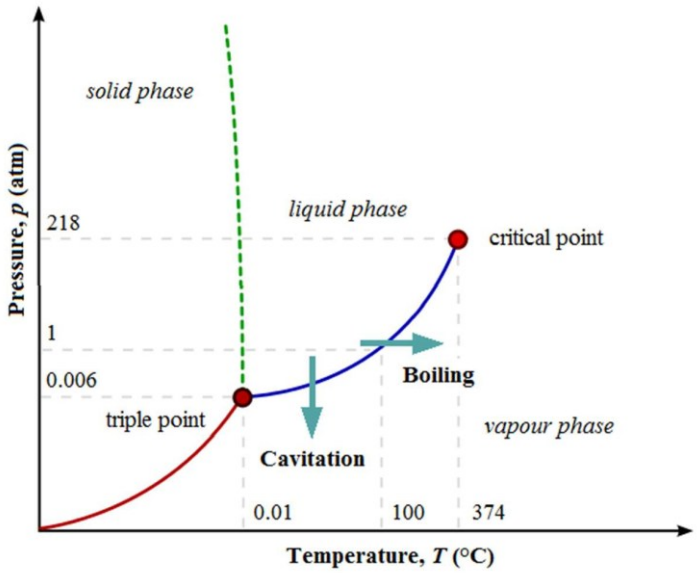


Figure 1:diagram phase [Brennen 27]

It is widely accepted that cavitation inception strongly depends on water quality and nuclei concentrations in water. The occurrence of cavitation bubbles initiates from weak points in water, namely bubble nuclei, which break the bond between water molecules. These are generally tiny gas bubbles or solid nuclei.

Despite some differences in cavitation bubble generation using AC and HC, on a small scale, the principles governing hydrodynamic and acoustic bubble growth are the same. In AC, when an ultrasound wave propagates into a liquid, it generates compressions and rarefactions. The compression cycles exert positive pressure on the liquid by pushing the molecules together, whereas the rarefaction cycles exert a negative pressure by pulling the molecules apart. Due to the low pressure, cavitation bubbles form in the rarefaction regions. These bubbles grow in successive cycles and reach an unstable diameter, collapsing violently. In HC, due to the presence of constrictions in the fluid, low flow pressures are achieved, resulting in cavitation bubble generation. Downstream of the constriction, as the liquid expands, the flow pressure recovers, causing the bubbles to grow and collapse violently.[31] Bubbles in a cavitating flow are often far from spherical, but spherical analysis often provides satisfactory higher-level bubble dynamic modeling. It is often assumed that an isothermal bubble growth up to the maximum radius occurs, with the bubble mainly filled by vapor at equilibrium at the ambient temperature. [32, 33]

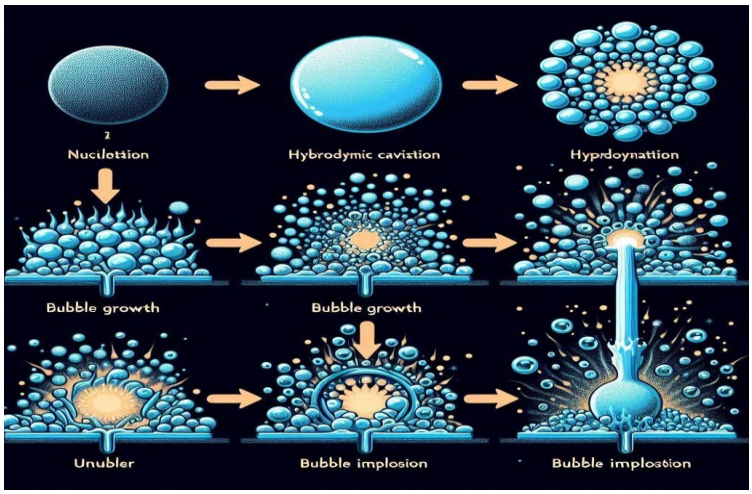


Figure 2:simple steps of hydrodynamic cavitation: nucleation, bubble growth, bubble implosion with arrows to show the flow of events [Brennen 27]

Many studies have been conducted on bubble collapse dynamics, showing the presence of several peculiar phenomena that can occur in very short periods, while the overall environment remains at ambient atmospheric conditions. After the growth phase, bubbles can collapse, generating new rebound bubbles that can sometimes break into several smaller bubbles [34, 35] The shape of rebound bubbles depends on the symmetry or asymmetry of the collapse dynamics. A perfectly spherical collapse produces a spherical rebound bubble, while asymmetry leads to bubble deformation and the generation of a microjet emerging from the rebound bubble. Microjets can reach velocities of up to 100 m/s, [36] increasing turbulence and the mass transport coefficient. Due to their high velocity, microjets can promote changes in water clusters and agglomerations of fibers and molecules. During the collapse, the high velocity of the bubble interface and the compressibility of the liquid lead to the generation of shock waves in the liquid. At this stage, very high temperatures of several thousand Kelvin occur, but these last for a very short time before dropping to the surrounding fluid's temperature. Such extreme conditions are sufficient to dissociate vapors trapped in the cavitating bubbles, resulting in the generation of free radicals, such as ·H and. OH, which are very strong and non-specific oxidizing species. At the final stage of the collapse, the pressure and temperature inside the bubbles are so high that light is emitted, a phenomenon known as luminescence. [37, 38, 39]

Based on the intensity, in terms of pressure or temperature magnitude, cavitation can be classified as either transient or stable. In transient cavitation, bubble radius expands to at least twice the initial size. During the collapse, bubbles can shrink to a minute size of their original size within a limited time frame, resulting in no mass flow of permanent gas through the bubble-liquid interface and causing a very violent implosion. This allows the release of a significant amount of energy. [9, 22]

This process releases a significant amount of energy in the form of acoustic shock wave and visible light. At this stage, the temperature of the vapor within the bubble and the pressure can reach several thousand Kelvin and several hundred atmospheres, respectively. In stable cavitation, however, bubbles contain more gas and thus have a less violent collapse compared to transient bubbles. The shock waves and microjets caused by stable bubble implosions generate lower pressure compared to transient ones.

In hydrodynamic cavitation (HC), it was demonstrated that if the intensity of turbulence is quite low, the pressure recovery downstream of the constriction can be approximated by a linear expression with respect to the distance downstream of the constriction where stable cavitation occurs [40]. When the intensity of turbulence increases and pressure recovery is no longer linear, the cavitation bubble behavior can be defined as transient. [41, 42]

2.1.2 HC GENERATION AND MECHANISMS

HC is produced by pressure variations in a flowing liquid caused by flow velocity variations in the system by introducing constrictions, such as an orifice plate, venturi, or throttling valve. According to Bernoulli's principle, when the liquid passes through the constriction, the flow velocity increases, and the flow kinetic energy increases at the expense of the flow pressure.[41]

Where V is the flow velocity at a point on a streamline, g is the acceleration due t o gravity, z is the elevation of the point above a reference plane, p is the pressure at the chosen point, and ρ is the density of the fluid at all points in the fluid. [43, 44]

The total energy of the cavitation process is constant, but some of the

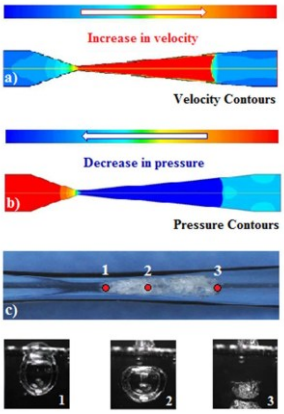


Figure 3:effect of constriction on flow velocity and pressure in a venturi system, a) contours of flow velocity magnitude, b) contours of flow pressure magnitude, c) high speed camera frames [Brennen 27]

energy is converted to turbulence and heat during the process. Therefore, the downstream flow pressure will always be less than the upstream flow pressure. If the throttling of the constriction is sufficient, the flow pressure at the throat of the constriction equals or falls below the vapor pressure of the liquid at the given temperature, and vaporous cavities are formed.

Where P_{minis} the minimum static flow pressure and Pv is the vapor pressure at a gi ven temperature of the liquid.Depending on the geometry of the constriction, with further lowering of the pressure, the cavities continue to grow, reaching their maximum size at the lowest pressure. Subsequently, when the liquid flow expands, resulting in a decrease in flow velocity, the flow pressure recovers, leading to the implosion and collapse of these cavities.[45]

2.1.3 HC Flow Regimes

In characterizing cavitating flows, the most used parameter is the cavitation number (Cv). It is a dimensionless number that can be expressed as follows:

$$C_v = \frac{2\Delta p}{\rho V^2} \qquad \textit{Equation 1}$$

Where (pr) is the measured downstream recovery pressure in the undisturbed flow, (pa) is a conventional reference point close to the point where cavitation inception is expected and where flow pressure is easily measured, (pv) is the vapor pressure of the liquid at the operative temperature (e.g., 2.35 kPa at 25°C), Δp is the pressure

difference that characterizes the system, and ρ and (V) are the liquid density (kg/m³) and the measured liquid velocity (m/s) at the cavitating constriction, respectively.[43], [45], [46]

This parameter indicates the probability of cavitation occurring in a flow regime. High values of Cv involve more collapsing forces and lower initiating forces, indicating lower cavitation activity. Cavitation may occur because of either a decrease in flow pressure at the reference point or an increase in the (Δp) value.[47]

Cavitation begins to occur at values below the cavitation inception number (Cv). In most studies, it was observed that cavity formation starts at Cv equal to 1. However, due to the presence of dissolved gases in the liquid and other solid particles, cavitation can start for Cv greater than 1. Typical values of Cv range from 1 to 2.5 for orifice flow in pipes.[48]

Many reports indicate that with a decrease in Cv below 1, more cavities are formed, resulting in an increase in cavitation effects. It was also observed that further decreases in Cv imply the achievement of a condition where cavities start coalescing with each other due to a large number and volumetric concentration of cavities, forming vaporous clouds (choked cavitation or super cavitation), resulting in a decrease in cavitation intensity.

The threshold Cv depends on various factors considered in fluid mechanics, such as flow geometry, viscosity, gravity, surface tension, turbulence levels, thermal parameters, wall roughness, and gas content of the liquid in terms of dissolved and free gases. [49, 50]

In HC, five different flow regimes can be identified depending on the cavitation number value compared to the threshold value Cv [46, 51]

Non-Cavitating Flow

When the pressure of the liquid is higher than the saturated vapor pressure, cavitation does not occur (Cv > Cv*)). In this stage, known as the non-cavitating flow phase, there is no evidence of cavitation bubbles in the liquid.[50]

Cavitation Inception or Limited Cavitation

In this phase, the pressure of the liquid equals or falls below the vapor pressure of the liquid ((Cv <=Cv*)). Cavitation is just barely detectable, resulting in the appearance of scattered cavitation bubbles in the fluid. This phase is always characterized by the strong noise of collapsing bubbles due to the instability of the generated cavities.[52]

Developed Cavitation

Even lower values of the cavitation number ((Cv <<Cv*)) allow the complete development of cavitation bubbles.[53]

Supercavitation

This stage represents the final state of cavitation ((Cv <<<Cv*)). In this regime, the pressure in the cavitating area is low, and a large, fixed cavity is formed. Compared with other types of cavitation, the interface of supercavitation is stable. The cavity stays attached to the constriction, and its length does not vary significantly, although considerable oscillations can occur at its closure.[54]

Desinent Cavitation

In this phase, cavitation bubbles completely disappear because of raising the downstream flow pressure. Desinent cavitation is often used as the threshold between cavitating and non-cavitating flows.

Recently, it was proven that (Cv) cannot be used as a single parameter in providing cavitation conditions, and there are large inconsistencies regarding its determination in previous reports. Moreover, (Cv) is not always determinable in HC devices due to some operational difficulties in measuring flow velocity or pressure in the cavitating zone, especially when the complexity of the geometry of the cavitating device is increased.[55]

2.1.3.1 HC TYPES

Cavitating flows can exhibit different kinds of cavitation depending on the flow configuration. Three main classification families are attached cavitation, convicted cavitation, and vortex cavitation.

a. **Attached Cavitation**

In the attached cavitation, a wake or region of separated flow filled with vapor can be observed. The cavity interface is partly attached to the solid surface. The liquid-vapor interface can be smooth and transparent or have the shape of a highly turbulent boiling surface. Attached cavitation can be partial or appear as supercavitation when the cavity grows to completely envelop the solid body. This type of cavitation on a hydrofoil or propeller blade is usually termed sheet cavitation, whereas in the context of pumps, it is known as blade cavitation. In the context of bluff bodies, a vapor-filled wake is often called a fully developed or attached cavity. Clearly, sheet, blade, fully developed, and attached cavities are terms for the same large-scale cavitation structure.[6] attached cavities are terms for the same large-scale cavitation structure.

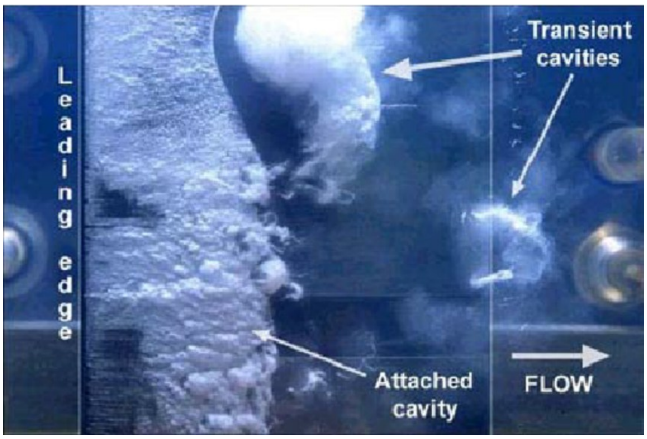


*Figure 4**: attached cavitation on hydrofoil and bluff body and describe the attached cavitation [Brennen 27]***

When generated transient cavities are of the same order as the main attached cavity, attached cavitation is also called cloud cavitation, where periodic formation and collapse of a cloud of cavitation bubbles can be observed. The temporal periodicity may occur naturally or may be the response to a periodic disturbance imposed on the flow. A very common example of imposed fluctuations can be provided by the interaction between rotor and stator blades in a pump or turbine. Recently, in a shear-induced HC reactor where two facing rotors with special radial grooves are spinning in opposite directions, the developed cavitation was studied by Petkovsek et al [56]. Attached cavitation and bubbles shed from the attached cavitation were

observed on the solid surface of the teeth rotors, in the gap between the rotor and the housing. A cavitation cloud between the aligned grooves was also detected.

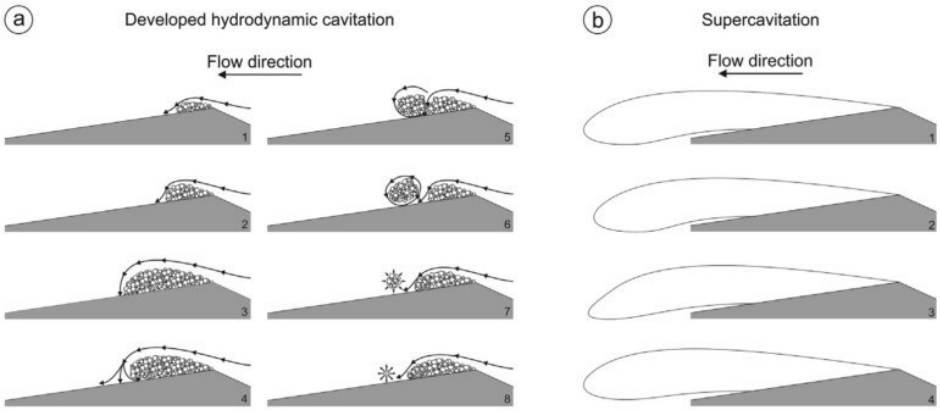


*Figure 5:**shematic representation of developed HC(a) where highly dynamical vapour cloud shedding associated with high pressure pulsation is expected and super cavitation (b) which is characteristic of large cavitation pocket reproduced from Dular et al***

To effectively exploit the positive effects of HC, the developed cavitation must be studied and controlled in HC reactors. For instance, recently Dular et al. [57] studied a venturi device where attached cavitation occurred and showed the progress of the developed cavitation. It was observed that the flow followed a distinctive pattern where cavitation structures of different shapes and sizes were shed from the attached cavity. Due to the pressure difference between the outer flow and the inside of the attached cavity, the streamline curves towards the cavity and the surface beneath it. This caused the attached cavity to close, and the formation of a stagnation point at which the flow was split into outer flow, which reattached to the wall, and the re-entrant jet, which traveled upstream, carrying a small quantity of the liquid to the inside of the cavity. As the re-entrant jet traveled upstream, it lost momentum, turned upwards, and cut the attached cavity, causing cavitation clouds to separate and shed. The cloud was then entrained downstream by the main flow and violently collapsed in a region of pressure recovery. During the separation, circulation around the structure can appear, causing it to reshape and break up. Meanwhile, the attached cavity began to grow, and the process was periodically repeated. As the system pressure decreased, and consequently the flow velocity increased, a small cavity extended and grew more and more. It became a

supercavity as soon as it stopped closing on the cavitator wall but inside the liquid, downstream of the cavitator. Supercavitating flow is not characterized by noise, vibration, and erosion.

a. Convected Cavitation

While in attached cavitation the cavity surface is partly attached to the solid surface, in convected cavitation the entire cavity interface moves with the flow. Cavitation bubbles are generated in the liquid for low-pressure gradients and move with it as they expand and collapse during their life cycles.[28]



Figure 6:convected cavitation [Brennen 27]

b. Vortex Cavitation

Many flows with high Reynolds numbers contain a region of concentrated vorticity where the pressure in the vortex core is often significantly smaller than in the flow, and thus cavitation inception can occur. With further reduction of the cavitation number, the entire core of the vortex may become filled with vapor. It may happen that the vortex cavitation bubbles remain smaller compared to the vortex core radius, with nearly spherical rapidly growing and collapsing bubbles entirely within the confines of the vortex core. However, at lower flow pressure, the initially near-spherical bubble can expand and elongate to fill the core of the vortex and continue to grow along the vortex axis, becoming highly **elongated**.[58]

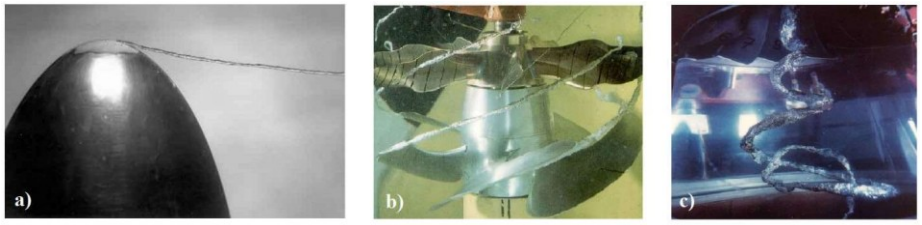
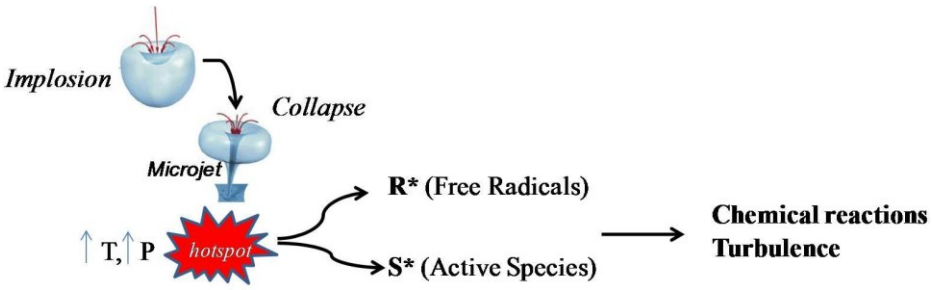


Figure 7:vortex cavitation [Brennen 27]

2.1.4 Mechanisms of Pollutant Degradation

The violent collapse of the cavities in cavitating systems results in the formation of reactive hydrogen atoms and hydroxyl radicals, as well as gives rise to thermal hot spots, which can yield pyrolytic cleavage of chemicals. Thus, HC results in several effects (both chemical and mechanical) in the system.



The two main chemical mechanisms for the degradation of pollutants using hydrodynamic cavitation (HC) are:[59, 60]

Thermal Decomposition: Volatile pollutant molecules entrapped inside the cavity undergo thermal decomposition during the collapse of the cavity.

Radical Reactions: The reaction of hydrogen (H) and hydroxyl (OH) radicals with the pollutant occurs at the interface cavity-water. For non-volatile pollutants, the primary degradation mechanism is the attack of hydroxyl radicals on the pollutant molecules at the cavity-water interface and in the bulk fluid medium.Mechanical effects are also significant and include:

1. Generation of shock waves by the collapsing cavities.
2. Formation of liquid micro-jets.

3. Creation of interfacial turbulence and powerful hydraulic shear stress due to high flow velocity.

These mechanical effects can directly rupture molecular bonds on the macromolecular main chain, especially in complex large molecular weight compounds, thus degrading refractory organic matter. The broken-down intermediates are more amenable to OH attack as well as biological oxidation, which can further enhance the rate of oxidation and mineralization of the pollutants. Furthermore, the high-velocity micro-jets (>100 m/s) disturb the boundary layer at the solid surface, leading to the breakdown of the liquid film responsible for resistance to mass transfer. Additionally, chemical and mechanical effects are responsible for the enhancement of heat transfer, with the heat transfer rate almost doubling in the presence of cavitation in a conduit.[53, 61]

2.1.5 The Effect of Various Parameters on HC Effectiveness

Overall, a significant number of parameters affect HC effectiveness, influencing the number of generated reactive bubbles and the collapse conditions. An overview of the effective parameters in HC was suggested by Braeutigam et al.

The main factors determining the HC field, and its effectiveness are:

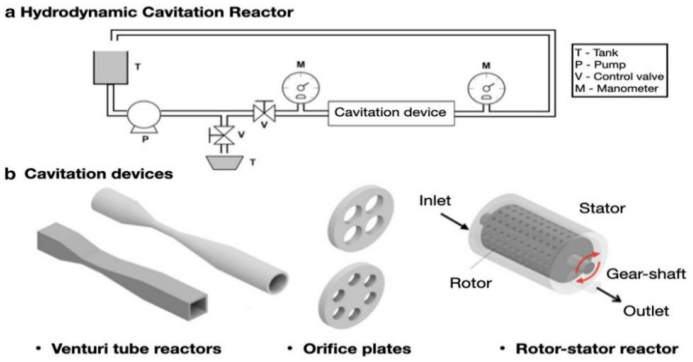
1. Device construction parameters.
2. Technological process parameters.
3. Properties of the liquid medium.

The influence of all these aspects on HC effectiveness is separately analyzed in the following paragraphs.

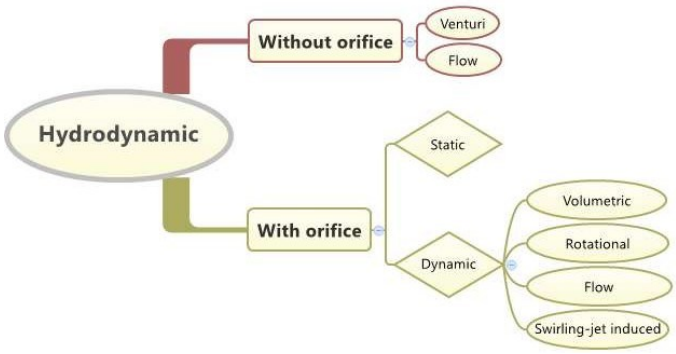
2.1.6 Device Construction Parameters

HC effectiveness depends on the size and shape of the cavitation inducer and flow chamber, which both affect the cavitation number and the collapse intensity. Recently, many researchers have focused on optimizing cavitating device geometries to obtain maximum cavitational effects, in terms of both the number of cavitation events and significant pressure drops, thus decreasing energy consumption. Various HC devices have been developed, including static orifice plates, nozzles, venturi, swirling jets, and rotor/stator systems.[34,62]

Different geometric configurations of each device have been investigated. For example, Sarc et al. considered four very similar venturi shapes and exposed them to the same operative conditions (constant flow pressure, constant flow velocity, constant temperature).[63] Significant differences in typology, dynamics, and aggressiveness of cavitation were found. By using a high-speed camera, they observed how cavitation size and appearance could vary significantly when the divergence angle of the venturi system was changed. Similarly, Kim et al. investigated the effect of different venturi outlet inclination angles on the performance of their HC system used to increase sludge solubilization.[64]



Several researchers have investigated. The highest cavitation intensity is generated by using the lowest free area. However, for the same free area, plates with a higher diameter of the hole and a lower number of holes generate relatively lower intensities.



A swirling jet cavitation device was investigated by Wang et al [6]. An innovative swirling jet-induced cavitation device was proposed by Mancuso et al[65]. and Langone et al., studying the influence of the number of injection slots, the geometry of the double cone, and the number of HC devices in series on HC effectiveness.

Patil et al. developed an efficient stator and rotor assembly. A novel stator and rotor configuration was later developed by Petkovsek et al., who studied the effect of different shapes of the teeth of one rotor on the cavitation process [56, 66].

2.1.6.1 Technological Process Parameters

This second group includes parameters associated with the characteristics of the technological process, such as liquid flow velocity/kinetic energy, pressure at the inlet to the HC system, liquid temperature, liquid pH, and HC processing time (the number of times the liquid passes through the cavitation region).

a. Effect of Liquid Flow Velocity

In an HC device, the number of cavitation bubbles is mainly related to an increase in the velocity/kinetic energy of the liquid. Increasing flow velocity leads to higher local pressure oscillations, and pressure may fall below the vapor pressure of the liquid at the operating temperature, causing partial vaporization of the liquid and generation of cavities. As can be deduced from the equation, an increase in flow velocity implies a decrease in cavitation number, resulting in an increase in cavitational effects. Higher flow velocities further imply higher turbulence levels.

The flow velocity can be varied either by adjusting the pump flow rate (and thus the pump discharge pressure) or by changing the geometry of the cavitating device (i.e., reducing the constriction area).

Sarc et al. [67]observed different cavitation conditions by changing the flow velocity at the throat of the venturi system by varying the inlet pressure while keeping the cavitation number and the geometry of their HC system constant. They observed a slight increase in cavity growth when the flow velocity was increased. Using venturi systems, Sharan et al.[68] studied the effect of flow velocity on the degradation of RR120 by increasing the inlet pressure from 3 to 10 bar. It was observed that the degradation rate increased with an increase in the inlet pressure, reaching a maximum at 5 bars and then dropping due to the onset of supercavitation. Similar results using venturi systems were reported by Prajpat and Gogate and Gore et al.[4, 69]

Similarly, Joshi and Gogate investigated the influence of flow velocity at the throat of a single orifice plate by varying the inlet pressure. In their experiments, the inlet

pressures were varied in the range from 3 to 6 bar by varying the flow rate [70]. They observed that the extent of degradation of dichlorvos increased as the inlet pressure was increased from 3 bar to an optimum value of 5 bar. In this range, higher inlet pressures, and thus higher flow velocities, promoted an increasingly violent collapse of cavities, resulting in increased hydroxyl ion generation and an enhancement in the extent of degradation. However, at a pressure of 6 bar, the extent of degradation decreased, indicating the onset of supercavitation, resulting in an extremely rapid growth of bubbles downstream of the orifice, leading to splashing and vaporization in the flow.

Wang and Zhang reported a continuous increase in the degradation rate of alachlor with increasing flow velocity using a swirling jet-induced reactor[71]. The authors increased the flow velocity by raising the inlet pressure from 2 to 6 bars while keeping the geometry of their HC system constant. These results align with the study by Mancuso et al. [7, 20], which observed an increase in sludge disintegration degree by increasing the inlet pressure from 2 to 4 bars due to higher flow velocities in a novel swirling jet-induced cavitation reactor. However, using the same HC device to degrade a waste dye aqueous solution (rhodamine B), supercavitation occurred at 3 bars [16].

In a rotor-stator system, Badve et al. [63] varied the velocity of the liquid on the surface of the rotor by changing the rotor's rotation speed. Their results showed that as the rotation speed increased, the liquid surface velocities increased as well, and the cavitation number decreased.

Nevertheless, geometry is also essential to increase flow velocity and maximize cavitational effects. Sivakumar and Pandit [72,29] using multiple hole orifice plates operating at the same inlet pressure, showed an increase in the cavitation process efficiency with the increase in flow velocity due to geometry variations. In an innovative swirling jet-induced reactor, Mancuso et al. [7] obtained increasing effectiveness of the HC process, in terms of activated sludge solubilization, by increasing the flow velocity due to the decrease in the number of injection slots while keeping the inlet pressure constant.

b. Effect of Liquid Inlet Pressure

Fluid inlet pressure influences both the number of cavitation bubbles and collapse intensity. In HC systems, an increase in the inlet pressure always implies an increase in flow rate and vice versa. Higher inlet pressures involve higher flow rates and thus higher flow velocities, increasing turbulence levels and local pressure oscillations. Therefore, increasing the inlet pressure accelerates the HC process. Furthermore, higher inlet pressures involve higher pressure drops through the HC device, resulting in both higher shear forces that break down bacterial cell walls and higher release of organic matter [9]. Treating wastewaters containing RhB using both a multi-hole orifice plate system and a swirling jet reactor, a higher extent of degradation was observed at higher pressure drops obtained by increasing the inlet pressure [8]. Kumar and Pandit [29]also showed that with an increase in the venturi inlet pressure, the pressure drops across the venturi increased, resulting in an increase in the cluster collapse pressure.

c. Effect of Cavitation Number

Cavitation number is interrelated with the previously described parameters: flow velocity and inlet pressure. Many studies on the influence of cavitation number on the effectiveness of cavitation have been carried out. However, missing or inaccurate information about the position at which the pressure and the flow velocity were measured or calculated implies that researchers commonly tend to use inappropriate values of cavitation number, taking advantage of the lack of standard methods for its determination [44]. Most studies on HC are not repeatable because of a poor definition of the cavitation number in the manuscripts. Nevertheless, for completeness, some results on the influence of cavitation number on HC effectiveness are reported here.

Sahran et al. [73]used a venturi system to degrade reactive Red 120 dye. It was observed that the rate of degradation increased with a reduction in cavitation number, reaching a maximum and then dropping. The authors explained this finding by considering two separate stages depending on the cavitation number value. In the first stage, a decrease in cavitation number allowed an increase in the number of cavitation bubbles generated. The increase in the number of cavitational collapse pulses and generated OH radicals resulted in an increased degradation rate. In the second stage, the degradation rate decreased with a further decrease in cavitation number. This may be due to reduced cavitational intensity caused by the excess

number of cavities inside the venturi at very low cavitation numbers. When there is a large number of cavities, they can start coalescing to form larger bubbles that can escape the liquid without collapsing or result in an incomplete collapse, reducing the generation of OH radicals.

Gore et al. [69] investigated the influence of cavitation number, ranging from 0.210 to 0.095, on the degradation of reactive orange 4 dye using a venturi system. It was found that the decolorization rate increased with a decrease in cavitation number, reaching a maximum at 0.15 and then decreasing. The authors attributed these findings to an increase in the number of cavities and thus in the number of collapsing events, resulting in the generation of more OH radicals. However, a further decrease in cavitation number below 0.15 implied a decrease in the extent of degradation due to the occurrence of choked cavitation/supercavitation conditions. Under choked cavitation conditions, cavities no longer behaved as individual cavities. They coalesced with each other to form larger vaporous bubbles, which were carried away with the flowing liquid without collapsing.

Therefore, for a decrease in cavitation number, an increase in the number of cavities is expected, resulting in an increase in the overall collapse intensity of cavities. However, depending on the specific HC device configuration, after a certain value of cavitation number, the number of cavities can become very high, causing these cavities to start coalescing with each other and form a cavity cloud. Energy produced by the collapse of some cavities can be absorbed by neighboring cavities, resulting in cavity cloud formation (choked cavitation). Hence, it is important to optimize HC cavitation devices to operate between these two limits, i.e., cavitation inception and choked cavitation/supercavitation, to achieve maximum effect Furthermore, it should be noted that to compare two or more HC systems, parameters other than the cavitation number, such as vibrations and noise measurements, and indexes can be used to measure the intensity and efficiency of the HC system.

d. Effect of Liquid Temperature

The influence of temperature on HC is complex, with both positive and negative effects on HC treatment efficiency. Temperature affects the dynamics of the cavity through the properties of the liquid, such as vapor pressure, viscosity, surface

tension, and gas solubility. The vapor pressure of a fluid is dependent on its temperature and increases exponentially with temperature. Thus, an increase in the operative temperature can enhance the kinetic rate. The increase in temperature implies a decrease in viscosity and surface tension, leading to easier bubble formation [51]. However, these generated bubbles are richer in vapor content, which cushions their implosion, reducing the intensity of bubble collapse [51]. A rise in temperature reduces gas solubility, which is the chief source of cavity nuclei, thus reducing the rate of occurrence of cavitation events.

It is likely that an optimum operative temperature exists for specific conditions. When the temperature of the solution increases beyond the optimum value, the increase in the vapor pressure of the liquid might result in higher vapor content in the cavitating bubbles, leading to a cushioning effect and a reduction in HC effectiveness.

With this background, Wang and Zhang [71]reported a positive effect on the degradation of alachlor with an increase in temperature from 30°C to 40°C, but the degradation rate decreased with a further increase in temperature over the range of 40°C to 60°C. Joshi and Gogate [74]investigated the effect of operative temperature over the range of 31°C to 39°C. In their experiments on the degradation of dichlorvos, the maximum degradation rate was achieved at the lowest temperature. Mancuso et al. [20], [35] investigated the influence of temperature, ranging from 20°C to 35°C, on sludge disintegration. The authors observed that in this temperature range, HC efficiency was more effective in terms of sludge solubilization at higher temperatures. Sarc et al. demonstrated that the magnitude of the pressure oscillations, which occur due to cavitation bubble collapse, increased for temperatures up to 40°C but then dropped significantly for higher temperatures.[67]

e. Effect of Liquid pH

Typically, acidic or basic conditions can be favorable for the degradation of chemical pollutants using HC reactors. The optimal pH value depends on the pollutants to be treated. Many studies have been carried out to remove dye pollutants from wastewaters. Their degradation is strongly dependent on medium pH, as pH can influence the presence of OH free radicals available for pollutant

removal and change pollutant structure, resulting in a more biodegradable form that can be easily attacked by OH free radicals. Usually, acidic conditions are recommended for pollutant degradation by HC because such conditions favor the generation of hydroxyl radicals and impede the recombination reactions among free radicals [60].

Joshi and Gogate [74]investigated the influence of solution pH on the degradation of dichlorvos using an orifice plate as the cavitating device. Among the investigated pH values, lower pH provided a higher extent of degradation. Gore et al. [69]investigated the effect of solution pH on the degradation of reactive orange 4 dye using a venturi system, ranging from 2 to 10. The authors observed that the decolorization rate increased with both a decrease and an increase in solution pH starting from a neutral polluted solution. However, the highest extent of degradation was obtained for lower pH solutions, indicating a lower rate of recombination of generated OH radicals in acidic conditions and hence the presence of more OH radicals available for the oxidation of the dye. Moreover, under acidic conditions, the orange 4 molecules change from ionic to molecular. This alteration in the state of the molecules makes them hydrophobic and more easily attacked by OH free radicals. On the contrary, in a basic medium, the extent of the degradation of orange 4 was not as high as in acidic conditions because its molecules remained in an ionic state, resulting in an increase in their hydrophilic behavior that implied their persistence in the liquid bulk. Similar behaviors were reported for rhodamine B degradation. Mancuso et al. [8] treated polluted aqueous solutions of rhodamine B using a multi-hole orifice plate system and observed the highest degradation rate of the dye at pH 2, while it dropped significantly and remained constant in the pH range of 5-8. This was due to the prevalence of rhodamine B in the cationic form rather than the zwitterionic form in acidic conditions [75]. Previous research on rhodamine B in the cationic form revealed that it is easier to breakdown [76], resulting in greater oxidation of rhodamine B at low pH levels. Mishra and Gogate [77] used a venturi device to achieve similar results, as did Wang et al. [78], who used a swirling jet-induced cavitation system. Sharan et al. [79] studied the influence of medium pH on reactive Red 120 dye degradation by conducting experiments at pH levels ranging from 2 to 11. Their findings showed that the rate

of degradation increased as the pH of the solution decreased, confirming that an acidic medium was more suited for the degradation of reactive Red 120 dye.

Alkaline conditions are better for treating sludge because they promote organic hydrolysis [76]. When HC was pre-treated with NaOH at a pH of 9–10, the best results in terms of organic matter release were achieved, encouraging the formation of biogas through anaerobic digestion [77].

2.1.7 PROPERTIES OF THE LIQUID MEDIUM

This final group includes metrics that describe the liquid medium's qualities, primarily pollutant concentration, liquid viscosity, surface tension, and dissolved gas content.

a. Effect of Pollutant Concentration

When the cavitation conditions are consistent, the amount of OH radicals produced in the HC system remains constant. As a result, increasing the starting pollutant concentration would reduce the rate of pollutant removal because hydroxyl radicals may not be enough to totally eliminate the pollutant.

This holds true for the elimination of chemical contaminants dissolved in water solutions. Parsa et Zonouzain [76] investigated the influence of dye starting concentration on rhodamine B degradation utilizing a submerged multi-hole orifice plate device. In their trials, the starting dye concentration ranged between 2 and 12 mg/L. They discovered that the efficiency of the method was inversely proportional to the starting dye concentration. The authors proposed that this could be attributable to a rise in the overall number of dye molecules while the total number of free hydroxyl radicals remained These results are consistent with research on the degradation of rhodamine B conducted by Mancuso et al. [75] and Wang et al. [76], in which the authors found that the degree of dye degradation increased as the original dye concentration decreased.
Higher initial total solid concentration (TS) can, however, favorably affect the degree of sludge disintegration when sludge with particle organic matter is treated to promote its solubilization. Using a venturi system as the cavitating device, Kim

et al. [77] examined the impact of starting sludge concentration, which ranged from 5 to 40 g/L, on sludge solubilization.

As the initial TS concentration increased, the scientists saw a rise in sludge solubilization. These findings are consistent with a study by Mancuso et al. [20], in which the authors found that the maximum COD solubilization occurred for the highest starting sludge content, ranging from 4 to 40 g/L. Because of interactions between and within particles, the increased TS content produces more cells and aggregates, which raises the sludge's viscosity. The rise in TS increases the collisions between sludge flocs and cavitation bubbles, allowing for a subsequent increase in sludge disintegration, even if viscosity in HC slows down both the growth and collapse of bubbles [46]. Therefore, in comparison to the beneficial effect, the detrimental effect of a high TS concentration was minimal compared to the positive effect on sludge disintegration.

The initial size of the nuclei can also be influenced by the presence of solids, and the impact of the initial radius needs to be considered when selecting a certain liquid medium and process parameters.

Effect of Liquid Viscosity

Viscosity is the primary characteristics that reflects the rheology of the treated material. This critical parameter has the potential to alter HC intensity and the flow of dirty liquids into HC devices. Viscosity influences both the distribution of nuclei and bubble behaviours. Typically, a rise in viscosity in both Newtonian and non-Newtonian fluids affects the efficiency of the cavitation action, resulting in a slower growth and collapse of bubbles in HC [28]. Indeed, water is commonly utilized as a liquid medium in most applications due to its low viscosity, which aids in the formation of cavitation.

Yet, the HC process is also employed as a pretreatment for wastewater treatment plant sludge, which increases in viscosity as the TS concentration increases due to inter and intra-particle interactions [76]. Experimental results demonstrated that the negative effect of viscosity on sludge solubilization is minor when compared to the favorable effect of sludge concentration on cavitation formation [20,76]. Furthermore, when sludge is treated with the HC process, its viscosity lowers,

implying that energy requirements for heating, mixing, and pumping during anaerobic digestion may be reduced [71]. Kim et al. [76] used a venturi system as the cavitating device and found that sludge viscosity fell dramatically during the first 30 minutes of treatment before remaining basically constant after 1 hour. The reduction in viscosity was mostly due to a rise in temperature, shear forces, and cavitation bubble collapse. These findings are consistent with a study by Mancuso et al. [20], who used swirling jet-induced cavitation to improve sludge solubilization. During their HC testing, the authors gradually lowered the frequency of the pump inverter to maintain a constant inlet pressure value, and hence flow rate and velocity. This was attributable to the gradual changing of the sludge's rheology, resulting in a decrease in viscosity during the HC treatment. Similarly, Prajapat and Gogate [77] studied the influence of intake pressure on the depolymerization of an aqueous polyacrylamide solution using a venturi system. Their experimental results demonstrated that as the inlet pressure increased, so did the reduction of intrinsic viscosity.

Effect of Surface Tension

Surface tension controls the nucleation stage of the HC process by regulating the number and size of stable gas or vapor nuclei in the liquid, hence influencing HC process efficiency [55]. For a bubble in stable equilibrium with the surrounding liquid, the pressure inside the bubble equals the sum of the exterior liquid pressure and surface tension. Before cavitation, higher surface tensions cause faster dissolution of gas nuclei into the liquid due to surface tension forces, resulting in a reduced number of gas nuclei present in the liquid at any one time. Thus, in the beginning of the HC process, the nuclei may not be present in sufficient quantities to have any substantial impact on cavitation. However, during collapse, the cavities are broken at high implosive velocities, and these fragments might then become nuclei for the following cycle. Thus, the nuclei accumulate in sufficient numbers over time, allowing the cavitational effect to be observed. Surface tension varies with the type of liquid and temperature. A rise in temperature reduces surface tension, allowing for quicker evaporation [27], [61]. The presence of a little amount of surfactant allows for a drop in surface tension, drastically reducing the cavitation threshold and facilitating the development of bubbles, hence producing hydroxyl radicals Although a drop in the liquid's surface tension

facilitates cavitation formation, it should be highlighted that this also has an impact on the collapse of cavities, making it less violent.

Effect of Dissolved Gas Content

The presence of dissolved gases considerably improves the cavitational impact by providing nuclei for the HC reaction. Furthermore, the quality of the gas inside the cavity influences the final collapse temperature and pressure [76]. The majority of HC applications take place in the presence of a gas atmosphere; however, the effect of other gases (for example, argon) has been explored [77]. Different dissolved gas qualities, such as gas solubility, have been found to have a major impact on the cavitational process [78].

2.2 Methods to Evaluate Cavitation Efficiency

In recent years, many parameters have been presented to study the efficiency of various HC systems in terms of treatment removal efficiency as well as total energy supplied to the system. These parameters are primarily determined by the properties of the treated material.can significantly impact the cavitational process, such as gas solubility [78].

Pollutant Degradation in Wastewaters

The HC approach has lately been employed alone or with additions to breakdown hazardous and carcinogenic colors in polluted water bodies. In many investigations, the extent of degradation (ED) of dyes, such as rhodamine B (RhB) [75, 76, 77, 78], orange 4 dye [69], orange acid II [79], pharmaceuticals [80], and pharmaceutical micropollutants [81], was evaluated by considering the percentage of removal. The ED was calculated as reported in Eq. 2.

$$ED = \frac{C_0 - C}{C_0} \times 100 \qquad \textit{Equation 2}$$

Where (C0) [mg/L] is the initial pollutant concentration and (C) [mg/L] is the residual pollutant concentration at any given time. HC efficiency was more effective in terms of dye degradation at higher ED levels. Another investigated defined is the cavitational yield (C.Y) [28], [38], [55], [82], calculated as in Eq. 3

and defined as the ratio of the observed cavitational effect, in terms of the amount of degraded pollutant (typically expressed in mg/L) using HC, to the total energy provided to the system.

$$C.Y = \frac{Degraded\ matter}{Power\ density} \qquad Equation\ 3$$

Where (C_0) [mg/L] is the initial pollutant concentration and (C) [mg/L] is the residual pollutant concentration at a gi. The degraded matter is the amount of dye eliminated in mg/L throughout the experiment, and the power density, in [J/L], is given by the following equation (Eq. 4):

$$Power\ density\ = \frac{V*Pabs}{t} \qquad Equation\ 4$$

Where (V) is the volume of treated matter [L], (P_{abs}) is the pump-absorbed power by the HC system [W], and (t) is the treatment period [s]. The greater the C.Y. value, the more efficient the HC treatment is in terms of both degradation and total energy input to the HC system. When treating the same pollutant, C.Y. can be utilized to compare two or more distinct HC systems.

a. Biological Wastewater Treatment

The Cavitation acts by breaking down bacterial cell walls and membranes, which releases intracellular and extracellular matter [16]. Many of the intracellular constituents, such as cytoplasm and nucleic acids, are easily biodegradable, which either accelerates the aerobic and anaerobic digestion processes in sludge treatment or promotes denitrification in the wastewater treatment process [10], [65]. In this situation, HC efficiency can be measured by measuring (i) the improvement of sludge solubilization in terms of the soluble chemical oxygen demand (SCOD) increase (Eq. 7) and (ii) the ratio of change in soluble chemical oxygen demand after cavitation to particulate chemical oxygen demand.

2.2.1 CONVENTIONAL SCHEME OF HC EXPERIMENTAL SYSTEM

Various schemes of HC experimental systems have been used in the wastewater treatment sector. Closed-loop circuits are the most typical experimental designs employed in HC investigations. Among these, the continuous HC test is the most widely used [82], [83]. It includes a reservoir (1), a pump (2), control valves (V1, V2, V3, V4, V5), a cavitation reactor (4), and a sampling port (5).

Measurement gauges (P1 and P2). Control valves (V1, V2, and V3) are installed at strategic locations to regulate the flow rate through the mainline [84]. Inverters (3), rather than control valves, can be utilized to regulate the pump flow rate by modifying the frequency [85]. Water is pumped from the reservoir branches into the main line via control valves, which includes a main line for HC and a bypass line for controlling flow rate and pressure. Using the inverter, the solution to be treated is pumped straight from the reservoir into a channel that houses the cavitating device. The solution treated with HC is then recirculated and reintroduced into the reservoir. The pump could be a single screw pump [8, 9].

In this situation, the pump's suction side is linked to the reservoir's bottom, as with a centrifugal pump [92]. Because temperature has a considerable impact on cavitation, a cooling system is typically included to manage the liquid temperature.

Concluding Comment

Hydrodynamic cavitation (HC) is a highly effective method for enhancing chemical and mechanical processes, especially in wastewater treatment. It uses bubble dynamics to create extreme conditions that degrade pollutants and solubilize organic matter. Key factors influencing HC efficiency include flow velocity, inlet pressure, temperature, pH, viscosity, surface tension, and dissolved gas content. Optimal conditions for these parameters can significantly enhance cavitational effects, improving pollutant degradation and sludge solubilization. The presence of dissolved gases, for instance, enhances cavitation by providing nuclei and affecting collapse dynamics. Evaluation metrics like the extent of degradation (ED) and cavitational yield (C.Y.) are crucial for assessing HC system efficiency. Experimental setups, typically involving closed-loop systems, are designed to

maintain optimal conditions for HC processes. Overall, HC technology is a versatile and powerful tool for wastewater treatment, significantly improving pollutant degradation and organic matter solubilization. As research progresses, HC is expected to play an increasingly important role in sustainable and efficient wastewater management.

HC is very effective for intensifying chemical and mechanical processes in wastewater treatment. Among mechanical treatments, it is gaining prominence due to its ease of operation, flexibility, and ability to vary cavitational conditions. This work explains the importance of HC phenomena in wastewater treatment engineering by detailing the basic principles and critically examining different types of HC

3. WATER REUSE

The opening section explains the idea of sustainable development, highlighting its significance and its link to urban water systems and the reuse of water. The next section delves into the specifics of urban water reuse. The third section analyzes current models for managing water reuse. The final section provides a detailed summary of the topics covered.

As water scarcity necessitates sourcing water from more distant locations, the costs associated with meeting water demands are escalating rapidly, potentially threatening larger aquatic ecosystems. In essence, long-distance water supplies may not be sustainable. So, what constitutes a sustainable urban water system? According to the ASCE [76], sustainable urban water systems should, over the long term, provide necessary services while safeguarding human health and the environment, using minimal scarce resources.

In other words, the goal of sustainable urban water system development is to meet water demands at a cost that society can afford, with minimal environmental and social impacts. Reusing treated wastewater for beneficial purposes offers a potential new water supply that can replace existing freshwater sources for certain uses. Additionally, water reuse reduces the stringent and costly treatment requirements for effluent discharge into surface waters. For instance, removing nutrients like nitrogen and phosphorus is very expensive, but for most non-potable water reuse applications, such nutrient removal is unnecessary and even counterproductive when used for irrigation. Moreover, by eliminating effluent discharges through

water reuse, a community may avoid or reduce the need for expanding costly advanced wastewater treatment processes. In summary, a water reuse program can support both water conservation and pollution reduction efforts EPA, [77] Therefore, water reuse is a crucial component of sustainable urban water resource management.

This section provides an in-depth look at urban water reuse, starting with key terminologies. It explains wastewater reclamation, which involves treating wastewater to specific quality standards for reuse and defines wastewater as including urban discharges and stormwater. Water reuse broadly covers the use of treated water for various purposes, while reclaimed water is treated to meet specific reuse standards. Direct reuse refers to the planned transport of treated water to reuse points, whereas indirect reuse involves discharging treated effluent into natural water bodies for later use. Water recycling is typically applied within industrial systems. In urban water systems, reclaimed water can substitute potable water for various uses. Engineered urban water reuse creates a looped system where water is reclaimed and reused, as illustrated by Asano et al. [78]. Freshwater enters the system from surface or groundwater sources, goes through municipal water treatment, distribution, use, wastewater discharge, treatment, and then reuse. n a linear consumption model, resources like water and materials are used, and waste and emissions are expelled beyond city limits. Conversely, a circular approach aims to close resource loops by reducing external inputs (such as energy and food) and minimizing outputs (like wastewater and emissions) through recycling waste for self-consumption [79]. Figure 8 illustrates two metabolic patterns: City A depends on non-renewable materials and does not reuse emissions and waste, while City B promotes recycling, reducing pollution and emphasizing renewable resources.

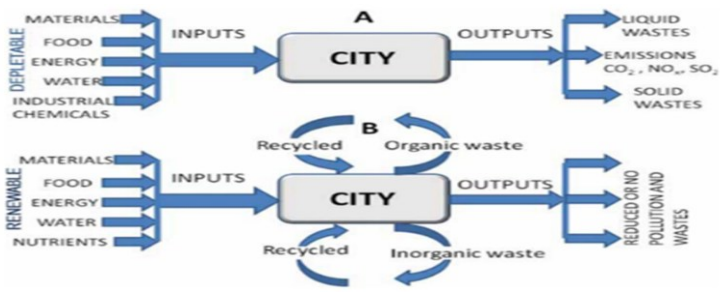


Figure 8:Linear (a) and circular (b) urban metabolism systems Source: Novotny (2013), page 591

The feasibility of water reuse depends on the quality required for specific applications and the available water quality. According to the U.S. EPA's Guidelines for Water Reuse 1992, water reuse applications are categorized by water quality requirements:[80]

Potable Reuse: Requires the highest water quality due to public health concerns and is not widely practiced.

Unrestricted Urban and Recreational Uses, and Agricultural Irrigation of Food Crops: Requires very high treatment levels, including secondary treatment, filtration, and disinfection.

Restricted-Access Urban Use, Restricted Recreational Use, and Agricultural Irrigation of Non-Food Crops: Involves limited access to reclaimed water, beneficial for irrigation due to nutrient content, with slightly lower treatment requirements.

Industrial Reuse: Focuses on recycling within industrial processes, with typical treatment including secondary treatment and disinfection.

The study emphasizes planned direct urban water reuse, excluding indirect reuse and water recycling due to their different scales.

3.1 Water Reuse Quality Criteria

The primary consideration in developing a water reuse system is ensuring that the reclaimed water's quality is suitable for its intended use. Key quality parameters include pathogens and chemical constituents. Pathogens are a major concern for non-potable reuse of municipal water due to the risk of infectious disease transmission. Chemical constituents in municipal wastewater can affect its suitability for food crop irrigation, indirect potable reuse, and certain industrial applications.

Typical water constituents and quality parameters include:

- Suspended Solids: Measured as Total Suspended Solids (TSS).

- Organics: Measured as Biochemical Oxygen Demand (BOD), Chemical Oxygen Demand (COD), and Total Organic Carbon (TOC).
- Dissolved Inorganics: Measured as Total Dissolved Solids (TDS) and specific elements like calcium (Ca) and magnesium (Mg).

These constituents impact water reuse applications in various ways. For example, suspended solids can absorb organic contaminants and heavy metals, clog equipment, and cause fouling. Organics can promote the growth of slime-forming organisms, create aesthetic and nuisance issues, and reduce heat transfer efficiency and water flow. Dissolved inorganics can increase water's electrical conductivity, leading to corrosion and scaling.

Therefore, these parameters are essential considerations in water reuse studies and application.

Chemical Oxygen Demand (COD) is the most extensively studied parameter, along with Biological Oxygen Demand (BOD), both indicating the presence of organic matter from food waste and hygiene products. Kitchen effluents, including those from dishwashers and washing machines, contribute 50-90% of the organic load [81], [82]. COD and BOD levels in mixed greywater are like those found in municipal or industrial [82]

The concentrations of Total Nitrogen (TN) and Total Phosphorus (TP) in greywater vary depending on the domestic appliance, reaching up to 50 mg/L in shower effluents for TN and TP and up to 74 mg/L in kitchen effluents[83]. The highest concentrations are found in toilet flushing, which is separate from greywater inputs, but phosphorus levels in some samples are higher than those in municipal wastewater, ranging from 3.7-11 mg/L Detergents and food waste are primary sources of TP and TN, which can cause adverse effects in water bodies due to eutrophication.

Table 1: Concentration in mg/L of main pollutants in effluents from domestic appliances, greywater, domestic and municipal wastewater

Component	COD	BOD	TN	TP	TSS	Reference
Handbasin						
1	1171.0	568.0	14.3	2.3	-	Oktor and Çelik, 2019

Component	COD	BOD	TN	TP	TSS	Reference
2	427.0	305.0	2.5	1.3	90.5	Noutsopoulos et al., 2018
3	208.1	101.0	5.1	3.3	18.5	Cardoso-Chrispim and Antunes-Nolasco, 2017
4	653.0	265.0	-	-	-	Zipf et al., 2016
5	225.0	43.0	-	-	48.0	Vakil et al., 2014
6	335.0	-	-	-	61.0	Antonopoulou et al., 2013
7	1489.0	597.0	105.0	26.0	573.0	Halalsheh et al., 2008
Kitchen						
1	1119.0	831.0	5.5	2.7	319.0	Noutsopoulos et al., 2018
2	602.0	293.0	-	-	308.0	Vakil et al., 2014
3	775.0	-	-	-	299.0	Antonopoulou et al., 2013
4	26.0	536.0	11.4	2.9	134.0	Li et al., 2009
5	2050.0	1460.0	74.0	74.0	1300.0	
6	2244.0	1100.0	51.0	18.3	644.0	Halalsheh et al., 2008
7	936.0	536.0	-	-	235.0	Mandal et al., 2011
Washing machine						
1	2072.0	1363.0	6.2	1.2	169.0	Noutsopoulos et al., 2018
2	274.1	77.0	4.3	2.3	32.7	Cardoso-Chrispim and Antunes-Nolasco, 2017
3	824.0	269.0	-	-	1852.0	Vakil et al., 2014
4	231.0	48.0	1.1	0.0	68.0	Li et al., 2009
5	2950.0	472.0	40.3	171.0	465.0	Li et al., 2009
6	725.0	472.0	-	-	165.0	Mandal et al., 2011
Bath/shower						
1	654.0	385.0	10.6	1.7	-	Oktor and Çelik, 2019
2	112.0	-	5.1	-	86.9	Mohamed et al., 2018
3	390.0	263.0	2.7	0.1	73.5	Noutsopoulos et al., 2018
4	272.8	123.1	50.3	5.3	155.8	Cardoso-Chrispim and Antunes-Nolasco, 2017
5	461.0	81.0	-	-	148.0	Vakil et al., 2014
6	399.0	-	-	-	63.0	Antonopoulou et al., 2013
7	424.0	216.0	17.0	-	120.0	Mandal et al., 2011
8	100.0	50.0	3.6	0.1	7.0	Li et al., 2009
9	633.0	300.0	19.4	48.8	505.0	Li et al., 2009

Component	COD	BOD	TN	TP	TSS	Reference
Toilet						
1	5160.0	1245.0	492.9	86.0	3740.0	Molla, 2013
2	900.0	300.0	100.0	20.0	-	Henze 1997 in Henze and Comeau, 2008
Mixed greywater						
1	194	157	-	-	1.33	Patil and Munavalli, 2016
2	244-284	56-100	12-17.6	-	42.84-57.7	Mandal et al., 2011
3	100-700	47-466	25-183	1.7-34.3	0.11-22.8	Li et al., 2009
4	-	208-688	85-285	25-45.2	17.2-27	Gross et al., 2007
5	425-1583	215	-	17.2-47.8	5.7-9.9	Hernández Leal et al., 2007
Domestic WW	250-800	110-350	20-70	4-12	120-400	Metcalf and Eddy, 2003
Stormwater	40-73	8-10	0.4-1	1-2	67-101	Metcalf and Eddy, 2003
Municipal WW	260-900	120-380	20-705	4-12	120-370	Metcalf and Eddy, 2003

Eutrophication, as explained by Morelli et al , occurs when nutrient loading in ecosystems increases. This rise in TP and TN, typically limiting nutrients, stimulates the rapid growth of algae and cyanobacteria, known as algal blooms. The death and microbial decomposition of algae reduce dissolved oxygen (DO) levels, leading to hypoxia, the death of benthic organisms, and habitat compression. Continuous nutrient and organic matter accumulation causes long-term changes in ecosystems, negatively impacting aquatic environments and potentially altering the taste, odor, and safety of drinking water due to algal toxins.[84]

The United Nations advocates for a fundamental shift in viewing wastewater as a valuable resource rather than waste to be discarded. This perspective encourages leveraging wastewater for water reclamation and reuse projects, which can yield significant benefits. For instance, reusing water for gardening, toilet flushing, and laundry within households could potentially replace 30-50% of domestic freshwater

usage [83]Phosphorus recovery through sludge application in agriculture is cost-effective but limited due to risks of pathogen or heavy metal contamination [85]. Urine separation at a decentralized level is promising, as it contains 80% of nitrogen and 56% of phosphorus from domestic sources[86] though it requires new pipeline installations. Additionally, energy recovery options include producing electricity from methane in anaerobic reactors or generating hydrogen [87]

Sustainable Development Goal (SDG) aims to reduce untreated wastewater and increase water reuse [88] However, water reuse practices vary globally. For example, Cyprus and Namibia reuse 95% of treated municipal wastewater, while other water-stressed countries reuse less than 50%. Table 3 shows the water reuse percentages and volumes for selected countries, highlighting significant disparities and gaps in global data collection

Table 2 :the water reuse percentages

Country	Water reuse (%)	Treated municipal wastewater (1x109 m3/year)	Direct use3 of treated municipal wastewater (1x109 m3/year
Cyprus	99%	0.030	0.030
Namibia			
Namibia	97%	0.006	0.0058
Qatar	47%	0.204	0.095
Singapore	38%	0.511	0.194
Mexico	23%	3.897	0.898
Australia	21%	2.000	0.420
Saudi Arabia	16%	1.600	0.254
China	8%	49.31	3.860

3.2 Review on Urban Water Allocation and Reuse Modeling

The rise of personal computers has enabled the use of advanced numerical modelling techniques and scenario analyses to better understand and address urban water resource challenges. Integrative management modelling is crucial for optimizing wastewater treatment and reuse. Water reuse planning and management modelling offer a systematic approach to evaluating potential reuse markets and identifying opportunities among major users. This section reviews existing research on water reuse modelling and highlights areas for improvement.

In the 1970s, several studies on water reuse management were conducted. Bishop and Hendriks [89]presented one of the first models, treating the problem as an un-capacitated transshipment issue with linear treatment and transportation costs, focusing on biological oxygen demand (BOD) and total dissolved solids (TDS). Mulvihill and Dracup aimed to minimize water supply costs, including reclaimed water, but their model treated all users as one entity with a single quality requirement and did not allow water reuse among users[90]. Rios et al. allowed water recycling and reuse, assuming a super source and super sink for water distribution and discharge.[91] Pingry et al. developed a nonlinear model considering flow requirements and water quality but did not include different treatment levels.[92]

In the last decade, environmental and health risk issues have been integrated into water reuse studies. Jacques and Anastasia (1996) discussed risk analysis for wastewater reclamation and reuse, suggesting the use of Geographic Information Systems (GIS) for data processing. Oron (1996) proposed an integrative approach for reusing domestic treated wastewater, considering treatment levels, supply and demand, transportation, storage, and environmental and health risks.

Despite existing studies, uncertainty in water demand and treatment quality has not been adequately addressed. Variations in reclaimed water demand due to weather conditions and economic factors, as well as treatment instability, pose significant challenges. Incorporating stochastic programming and enhancing GIS capabilities

for data processing and visualization are necessary for improving water reuse models.

Continued research is needed to fully integrate urban water systems, improve cost estimation accuracy, model demand and quality uncertainties, and utilize GIS for better data processing and presentation.

3.3 WASTEWATER TREATMENT TECHNOLOGIES USED IN WATER REUSE

The goal of treatment technologies is to produce effluent that meets the quality requirements for its intended use, following established safety guidelines. Various technologies are available for water reclamation in both decentralized and centralized systems, often integrating secondary and tertiary treatments. Typically, secondary treatments in municipal wastewater involve biological processes. The Conventional Activated Sludge (CAS) system employs oxygen-supply bioreactors and settling tanks to remove suspended solids. Membrane Biological Reactors (MBRs) are highly effective in semi-centralized units due to their over 90% BOD removal efficiency, compact size, and minimal sludge production. However, MBRs face challenges such as membrane fouling and high chemical costs [93] quential Batch Reactors (SBRs) are modified activated sludge processes that produce high-quality effluent quickly and at 60% lower operational costs than CAS[94] While SBRs have high COD removal efficiency (~90%), they are less effective at removing nutrients (11% TN and 32% TP) [82]. Rotating Biological Contactors (RBCs) are efficient for treating both heavy and light greywater, often achieving over 95% BOD removal when coupled with primary and secondary units [95] However, RBCs require significant energy and space.

3.4 ENERGY-APPROACH-CARBON

The water sector consumes about 7% of the world's total energy, which is crucial for various processes such as extracting fresh or groundwater, treating drinking water, distributing potable water, household uses (like heating), and treating and reusing wastewater. This energy includes both direct electricity and indirect energy,

which is embedded in chemicals, fuels, construction materials, and their production inputs.

Numerous studies have quantified the energy inputs in different urban water systems (UWS) and compared their performance based on the kilowatt-hours (kWh) used to treat or allocate 1 cubic meter of water at a specific [96], [97]. Recent reviews of energy use in the water cycle across various case [97] have concluded that energy consumption varies significantly along the UWS, depending on geographic, distance, climatic, and technological factors.[36]

Groundwater abstraction and wastewater treatment are among the most energy-intensive subsystems. Groundwater abstraction, which supplies a significant portion of global water demands, uses less than 0.8 kWh/m³, depending on factors such as elevation, flow, and pump type. Treating groundwater typically involves simple chlorination and is less energy-intensive than treating surface water, which may require coagulation-flocculation and chlorination. In contrast, treating saline water is much more energy-intensive, requiring processes like reverse osmosis and ultrafiltration, which can consume up to 5 kWh/m³ [98]

The collection and treatment of wastewater demand substantial energy, with the required amount varying according to the treatment level (Figure 10). Wastewater treatment is a vital component of urban water systems (UWS) for eliminating pollutants, consuming electricity, and releasing nutrients. Research shows that energy usage in wastewater treatment is influenced by local operational conditions, such as the scale of operations, the technology implemented, and overall efficiency [99][100].

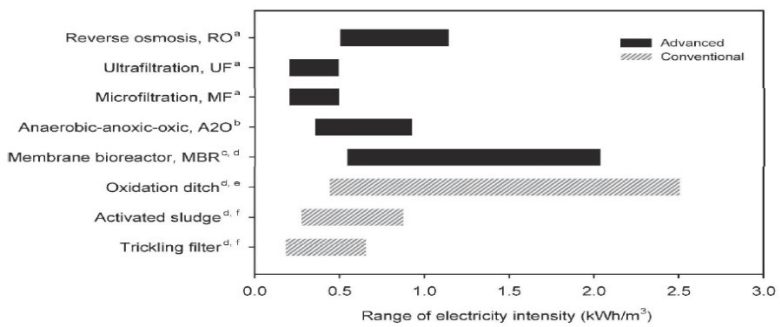


Figure 9:Electricity in different wastewater technologies Source: Lee et al. [101] p. 599.

The Water-Energy-Carbon (WEC) nexus highlights the interconnectedness of energy production and consumption, water delivery, and greenhouse gas (GHG) emissions. These emissions, measured in CO_2 equivalents, arise from both direct and indirect energy uses, as well as fugitive emissions [102] Analyzing the WEC nexus helps identify key areas for reducing carbon emissions. Various water supply sources, such as reclaimed water, greywater, rainwater, and groundwater, have been compared to conventional freshwater or transboundary inputs to assess potential water and energy savings. In some cases, reclaimed water has proven to be the most sustainable option.

A study by Mo et al. compared tertiary wastewater effluent, desalinated water, and freshwater supply in Tampa Bay (TB) and San Diego (SD), USA. Reusing reclaimed water showed the best performance against desalination, saving 0.2% (5,550 TJ) and 1.3% (35,540 TJ) of total electricity generation in TB and SD, respectively. Additionally, using reclaimed water could reduce GHG emissions by 0.25 million metric tonnes in TB and 1.05 million metric tonnes in SD annually. This is because the energy required for reverse osmosis and ultrafiltration is higher than that needed for water reclamation.[103]

Implementing water-saving techniques, such as efficient toilets, can achieve significant reductions at lower financial costs [103]. Increasing the use of renewable energy sources in regional electricity grids, such as solar-powered cells or biogas from wastewater treatment, can further reduce GHG emissions. Other energy conservation strategies, like extending the lifespan of water infrastructure through maintenance, are more energy-efficient than building new facilities[103]

The WEC nexus is crucial for assessing the environmental impacts of decentralizing wastewater treatment. Some studies have found that decentralized greywater systems can reduce energy use and emissions compared to centralized systems while others have reported contradictory results. An inventory of 50 wastewater treatment works (WWTW) in India and the UK showed that small-scale plants consume twelve times more energy than large-scale plants, at 4.67 kWh/m^3 and 0.40 kWh/m^3, respectively. Additionally, small plants emit almost four times more carbon (3.04 $kgCO_2eq/m^3$) than large ones (0.78 $kgCO_2eq/m^3$), due to differences in operation capacity, technology, and treated wastewater quality [99]

Silva-Vieira and Ghisi demonstrated a potential 48% energy saving when comparing decentralized greywater systems to centralized systems over a 20-year period in Florianopolis, Brazil. They found that greywater reuse energy consumption (0.5 kWh/m³) is lower than centralized systems (0.78 kWh/m³) only when demand exceeds 300 L/d, and benefits are directly linked to reducing effluents into centralized systems rather than the water source. [99]

Finally, Duong et al. analysed reuse strategies at household and cluster scales, concluding that on-site wastewater treatment energy prevents household-scale systems from achieving the same energy reductions as cluster-scale systems. These studies suggest that water reuse management must consider local conditions. While semi-centralized water reuse may be more suitable than household-level reuse, this might be more evident on a larger scale [104]

3.4.1 Emission Limits for Water Discharges

Discharges from wastewater treatment plants can be urban or industrial; in both cases, they must comply with the limit values defined by the Regions, according to temporal schedules and referring to quality objectives present in the decrees of the Environmental Consolidation Act (TUA). The limits imposed for sensitive areas are obviously different from those generally imposed.

3.4.1.1 Urban Wastewater

An equivalent inhabitant (PE), or specific organic load, indicates, in the field of sanitary engineering, the amount of biodegradable organic substances derived from a civil or similar user, conveyed into the sewer system over a 24-hour period, corresponding to a 5-day biochemical oxygen demand (120 hours) of 60 grams of O_2 per day (Legislative Decree 152/06 Art. 74-Definitions).[78], [80]

Table 3:An equivalent inhabitant also corresponds to a chemical oxygen demand (COD) of 130 grams of O2 per day or a discharge volume of 200 liters of wastewater per inhabitant per day, referring to the highest value (D.P.G.R. 28/R/03).Table 4: Emission Limits for Urban Wastewater Treatment Plants

Plant Capacity in PE (Population Equivalent)	2000-10000	>10000
Parameters (daily average) (1)	Concentration	% Reduction
BOD5 (without nitrification) mg/L (2)	≤ 25	70-90 (5)
COD mg/L (3)	≤ 125	75
Suspended Solids mg/L (4)	≤ 35 (5)	90 (5)

(1) Analyses of discharges from lagooning or phytoremediation must be carried out on filtered samples, and the concentration of suspended solids must not exceed 50 mg/L.

(2) Measurement must be made on a homogenized, unfiltered, and undecanted sample. The determination of dissolved oxygen is performed before and after a 5-day incubation period at 20°C ± 1°C in complete darkness, with the addition of nitrification inhibitors.

(3) Measurement must be made on a homogenized, unfiltered, and undecanted sample with potassium dichromate.

(4) Measurement must be made by filtering a representative sample through a 0.45 μm porosity membrane filter and drying at 105°C, followed by weight calculation, or by centrifugation for at least 5 minutes (average acceleration of 2800-3200 g), drying at 105°C, and weight calculation.(5) The percentage reduction of BOD5 must not be less than 40%. For suspended solids, the concentration must not exceed 70 mg/L, and the reduction percentage must not be less than 70%.

Table 5: Emission Limits for Urban Wastewater Treatment Plants Discharging in Sensitive Areas

Parameters (annual average)	Plant Capacity in PE (Population Equivalent)	10000-100000	>100000
Concentration	% Reduction	Concentration	% Reduction
Total Phosphorus (P mg/L) (1)	≤ 2	80	≤ 1
Total Nitrogen (N mg/L) (2) (3)	≤ 15	70-80	≤ 10

(1) The reference method for measurement is molecular absorption spectrophotometry.

(2) Total nitrogen means the sum of Kjeldahl nitrogen (organic N + NH_3) + nitric nitrogen + nitrous nitrogen. The reference method for measurement is molecular absorption spectrophotometry.

(3) As an alternative to the reference to the annual average concentration, provided that a similar level of environmental protection is achieved, reference can be made to the daily average concentration, which must not exceed 20 mg/L for any sample where the effluent temperature is equal to or greater than 12 degrees Celsius. The daily average concentration limit can be applied for a limited operational time that considers local climatic conditions.

The regulations also provide information regarding sampling: the sampling point must always be the same and must be upstream of the point of discharge into the receiving water body. If the percentage reduction of the pollutant is to be controlled, it is essential to take a sample at the entrance of the treatment plant: this is a factor to consider during the design and modification phase of the plant itself. Sampling takes into account the size of the plant and occurs periodically. Managers are responsible for both sampling and ensuring a sufficient number of self-checks on treatment schemes and incoming water.

If the characteristics of the waste to be disposed of require it, the authorization provides for:

- The adoption of pretreatment techniques suitable for ensuring pollutant concentrations that do not compromise the purification efficiency of the plant itself at the entrance of the wastewater treatment plant;
- The implementation of a qualitative and quantitative characterization program that allows systematic controls at the entrance and exit of the plant;
- The adoption of storage systems for the separation of treated wastewater from those to be treated.
- Adequate management standards for the purification process and specific plans for controlling purification efficiency.
- The use of self-control systems based on statistical or random criteria that represent the trend over time of the concentrations of substances to be measured analytically and verified with a confidence coefficient of at least 90%; the results obtained are kept available to the competent authorities for four years following the date of issuance/renewal of the authorization;
- Checks on the suitability or otherwise of the use in agriculture of biological sludge produced by the wastewater treatment plant in relation to the provisions of Legislative Decree 99/1992.

3.4.2 EMERGING POLLUTANTS

The main causes of surface or groundwater pollution are attributed to industrial discharges containing a large amount of pollutants, whose composition varies depending on the type of production process. Their impact on the environment is complex: often the toxic substances contained in these discharges reinforce each other's harmful effects, and thus the overall damage is greater than the sum of the individual effects. Examples include chemical fertilizers used in agriculture and waste produced by livestock farms: they are rich in organic substances that, washed away by rain, end up in aquifers or surface water bodies. These substances are often accompanied by debris of various sizes, which settle at the bottom of the basins.

Emerging pollutants (EPs) are a heterogeneous group of chemical and biological agents whose effects are causing growing concern due to the inability of traditional wastewater treatment systems to remove them and the great diversity of their chemical structures; they include both natural and synthetic substances not commonly involved in routine monitoring of environmental samples, although they

can severely affect the environment and human health. They derive from both point and diffuse pollution sources.

Among EPs are pharmaceuticals, personal care products, surfactants, disinfection by-products, nanomaterials, and solid organic pollutants; although present in small quantities (at parts per million, ppm), their effects on human health are related to genotoxicity and cytotoxicity, causing obesity, diabetes, and cardiovascular and reproductive disorders, the latter related to estrogenic activity.

In February 2016, a database with more than 1,000 available emerging contaminants was established, including flame retardants, pesticides, gasoline additives with related degradation products, and various proven and suspected emerging pollutants.

However, it is still difficult to analyze these compounds. Some of the systems developed today to detect EPs use nanomaterials to mimic enzyme behavior. Nanomaterials, in fact, are more stable under extreme reaction conditions and are among the most convenient candidates. These detection systems allow monitoring of emerging pollutants in the nanomolar, picomolar, and femtomolar quantitative range.

Once in the water, depending on their physicochemical properties, EPs undergo partial degradation such as biodegradation, photodegradation, adsorption on sediments along watercourses, or remain unchanged, accumulating over time. This creates the need to assess the potential risks from these sources of pollution, studying effective removal techniques and setting limits with controls to also monitor potential effects on human health.

To date, the Water Framework Directive (Directive, 2000) requires the development of an EP Watch List from national monitoring programs

3.4.3 Agricultural and Green Space Irrigation

In arid and semi-arid areas of the world, water reuse for agricultural purposes is well established, but today it is also an accepted practice in humid and temperate areas; agricultural activities, in fact, account for 72% of global freshwater withdrawals. The reuse of wastewater not only provides a significant amount of irrigation water but also helps preserve potable resources and reduces the

environmental impact related to the discharge of effluents into water bodies: the water naturally contains nutrients that have a positive impact on agriculture such as nitrogen, phosphorus, and potassium. Nitrogen and phosphorus have a positive effect on plant growth, while potassium has a much lesser effect.[105]

However, the quality of the water must be rigorously monitored to avoid imbalances in vegetation growth, irregular ripening, and reduced crop quality. They can contain a variety of pollutants, such as salts, heavy metals, organic compounds, enteric bacteria, and viruses.[106]

An accumulation of metals, even in trace amounts, such as cadmium, copper, iron, manganese, lead, and zinc, in soils through irrigation creates problems for agricultural production and leads to the absorption of metals by crops, thus compromising food quality and safety for both humans and the environment. Advanced processes for the removal of such pollutants are often considered.

3.4.4 Industrial Use

It is estimated that half of the wastewater produced comes from industrial activities (over 25,000 million m³): recovering 80% of this water would increase industrial energy consumption by only 4.1%, while investment costs would amount to 1.5% of the EU's GDP .[107]0]

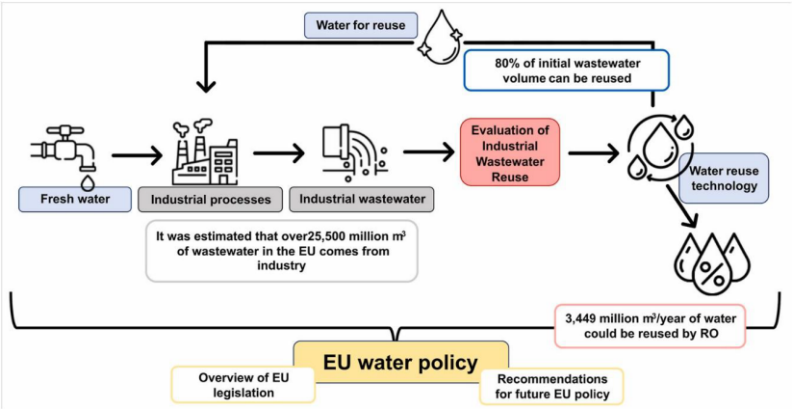


Figure 10: Water in the Industrial World

Typical industrial applications, depending on the sector, include the reuse of water for boiler feed, cooling towers, process water, and washing purposes. Although such practices are not widespread in the EU, successful cases of water reuse in

thermal power plants have been recorded in other parts of the world, such as Japan, the United States, and Mexico.

Based on a review of the literature and trends in wastewater treatment with respect to the level of purity at which water can be reused, three scenarios are introduced: only filtration, MLD, and ZLD:

- Only Filtration, with a reuse rate of 40%, involves the application of ultrafiltration (UF) as a pretreatment phase and reverse osmosis;
- MLD (Minimal Liquid Discharge), with a reuse rate of 80%, where filtration is combined with forward osmosis (FO);
- ZLD (Zero Liquid Discharge), with a reuse rate of 95%, where MLD is integrated with a concentrator and crystallizer.

ZLD differs from water recycling because it not only maximizes water efficiency but can also recover nutrients or metals from industrial wastewater, bringing wastewater discharge to zero [107]

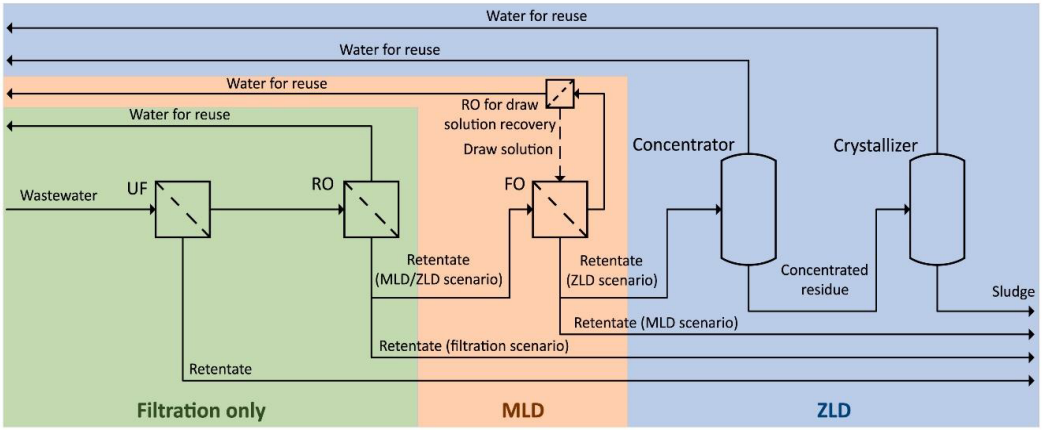


Figure 11: Difference Between Water Treatments in the Industrial Field

The concept of potability is associated with health risks, which can be chemical or biological. The risk is assessed based on the potability parameters established by Legislative Decree 31/2001, but also considers emerging pollutants that pose a risk to human health. In this case, water is used for street cleaning, vehicle washing, monumental fountains, and fire extinguishing systems.

Recreational Use

Aesthetic-recreational uses of water include those intended for bathing, safeguarding natural and environmental heritage, and fishery activities with the development of lakes, as well as the maintenance of parks and gardens.

Potable Use

For industrialized continents, the current and future trend is in the field of potable water reuse for human consumption. There are two types of potable reuse:

- Indirect Potable Reuse (IPR)
- Direct Potable Reuse (DPR)

In the first case, treated water is fed into an environmental reserve, aquifer, or surface water body, with the intent of achieving such mixing with fresh water as to ensure the safety of the water itself.

In the second case, treated water and raw water are mixed before reaching the drinking water treatment plant to increase supply; the treatment cost is higher than the previous one [107].

Concluding comments

Water reuse has been practiced for centuries, but it is gaining renewed attention in the context of circular economy and urban sustainability. Embracing circularity in water systems, such as using greywater, can enhance sustainability. Viewing wastewater as a resource rather than waste promotes trade-offs through controlled water reclamation and reuse projects. Decentralized water reuse strategies are expected to become more prevalent, but more evidence on their trade-offs is needed. Current literature indicates that data on greywater characteristics is limited and scattered, necessitating tailored regulatory guidelines. Generating city-scale water quality data is essential for developing clear greywater discharge standards. Additionally, there are conflicting findings on the energy savings potential of centralized versus decentralized reuse systems, highlighting the need for further research in this area. any studies focus on wastewater treatment technologies or compare different water sources, but often omit water reuse and sludge management, lacking an integrated management perspective. Including pollutants and environmental impacts in these analyses can provide a more comprehensive approach to comparing water reuse at different scales.

4. Wastewater Contaminants: Types and Treatment Methods

4.1 Introduction to Wastewater Contaminants

In the quest for sustainable industrial practices and environmental protection, effective wastewater management stands as a critical challenge. Industries such as textiles, petroleum refining, and wineries produce significant volumes of wastewater, each containing a unique blend of contaminants. Without proper treatment, these pollutants can cause severe ecological damage and pose serious health risks to humans.

This chapter delves into the primary types of wastewater contaminants, focusing on textile wastewater, hydrocarbons, winery wastewater, and dyes. Each section will explore the specific characteristics and challenges associated with these pollutants, as well as the advanced treatment technologies employed to mitigate their impact.

Textile Wastewater: The textile industry is notorious for generating wastewater with a complex composition, including dyes, heavy metals, and various chemicals used in the dyeing and finishing processes. These substances are often toxic and persistent, requiring advanced treatment methods such as membrane filtration,

advanced oxidation processes, and biological treatments to ensure safe discharge and environmental protection.

Hydrocarbons in Industrial Wastewater: Hydrocarbons, commonly found in wastewater from petroleum refining and other industrial activities, are organic compounds that can be harmful to aquatic ecosystems and human health. Effective treatment strategies typically involve a combination of physical, chemical, and biological processes, such as oil-water separation, adsorption, and bioremediation, to remove these contaminants and minimize their environmental impact.

Winery Wastewater: The production of wine generates wastewater characterized by high levels of organic matter, acidity, and sometimes alcohol. This type of wastewater requires specialized treatment processes, including anaerobic digestion, aerobic treatment, and constructed wetlands, to reduce its organic load and prevent environmental harm. These methods help in breaking down organic compounds and stabilizing the wastewater before discharge.

Dyes in Wastewater: Dyes, particularly from textile and dye manufacturing industries, are often resistant to conventional treatment methods and can be toxic to aquatic life. Advanced treatment techniques such as advanced oxidation processes (AOPs), adsorption using activated carbon, and biological treatments are employed to degrade these complex molecules and reduce their environmental impact.

By understanding the nature and treatment of these contaminants, we can develop more effective and sustainable approaches to wastewater management. This knowledge is crucial for protecting our water resources, promoting environmental sustainability, and ensuring public health.

4.2. TYPES

4.2.1 DYES

Dyes are complex unsaturated organic substances capable of absorbing light within the visible range (from 380 to 750 nm), thereby transforming white light into colored light through reflection on a surface, transmission, or diffusion [108]8]. Before the mid-19th century, natural dyes derived from plants, insects, animals, and

minerals [109]were commonly used. These dyes were generally less allergenic and toxic and could generate wastewater treatable through biodegradation

Today, the increased production of textile fibers corresponds to a corresponding growth in the number and types of dyes: approximately 7 × 10^7 tons of synthetic dyes are produced annually, 10% of which are discharged into the environment as effluent.

There are three essential groups in dye molecules: the chromophore, the auxochrome, and the matrix. The active site of the dye is the chromophore, which determines the spatial arrangement of atoms that absorb light energy; it consists of groups of atoms, the most common of which are nitro (NO_2), azo (-N═N-), nitroso (-N═O), thiocarbonyl (-C═S), carbonyl (-C═O), and alkenes (-C═C-). The absorption of electromagnetic waves by the chromophore is due to the excitation of electrons within the molecule [110]0], rendering it chromogenic. Dyeing capability is enhanced with the addition of other atom groups called "auxochromes" [13], which allow for dye fixation and can modify the dye color. These groups can be acidic (COOH, SO_3, and OH) or basic (NH_2, NHR, and NR_2). The remaining atoms of the molecule constitute the matrix, the third part of the dye. Textile dyes also contain functional groups such as carboxylic, amino, and azo groups, which are challenging to treat with traditional methods [111]

Classification of dyes has become mandatory due to the environmental hazards they pose and the global increase in production: it is estimated that there are approximately 8000 synthetic dyes listed in the Color Index (C.I) , under 40,000 commercial names. Each dye is classified with a name, a code indicating its class, its color, and an order number.

There are two methods for classifying dyes:

Based on chemical structure: Azo dyes, anthraquinone dyes, arylmethane dyes, indigo dyes, sulfur dyes, phthalocyanine dyes, nitro and nitroso dyes, as well as other structural types of dyes such as methylene and polymethine dyes, stilbenes, and various heterocyclic dyes.[19]

Based on application methods: Direct dyes, acid dyes, cationic dyes, reactive dyes, insoluble azo dyes, dispersed dyes, vat dyes, sulfur dyes, polycondensate dyes,

fluorescent whitening agents, oxidative dyes for fabrics (such as aniline black), solvent dyes, polypropylene dyes, and food dyes for edible products.[112]

4.2.1.1 METHYLENE BLUE

Methylene blue is an organic compound belonging to the class of aromatic heterocycles. At room temperature, it appears as a dark green crystalline solid, odorless, and stable to air and light. When dissolved in an aqueous solution, it exhibits an intense dark blue color.

In Table 7, some of the main physicochemical characteristics of methylene blue are listed:

Table 6: physicochemical characteristics of methylene

Chemical Formula	$C_{16}H_{18}ClN_3S$
Molecular Weight	Approximately 319.85 g/mol
Physical State	Dark green crystalline solid
Odor	Odorless
Color	Dark blue when dissolved in aqueous solution
Solubility	Soluble in water, forms a blue solution
Stability	Stable to air and light
Melting Point	Approximately 100-110°C
Structure	Aromatic heterocyclic compound

These characteristics highlight the stable nature of methylene blue in its solid form and its vivid blue color in solution, making it valuable in various applications, including medicine and biology.[113].

In Figure 13, the absorption spectrum of methylene blue is depicted, showing three distinct peaks that are highly pronounced both in the ultraviolet and visible regions. These peaks occur at wavelengths of 290 nm, 590 nm, and 670 nm.[114].

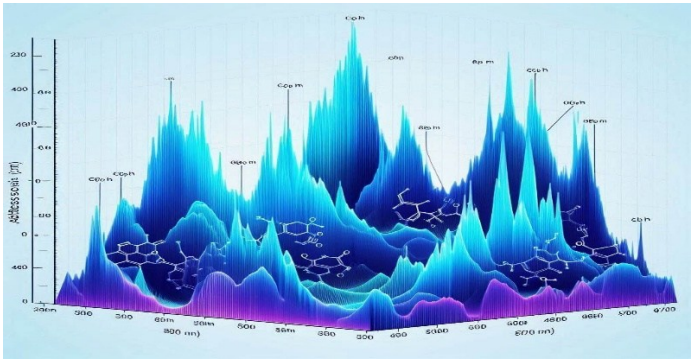


Figure 12:Absorption Spectrum of Methylene Blue Showing Three Distinct Peaks At Wavelengths Of 290 Nm, 590 Nm, And 670 Nm.

4.2.1.2. Industrial Synthesis of Methyl Orange and Methylene Blue

Dye production is among the oldest human activities, with recipes for the best dyes being passed down through generations since ancient times. Until the mid-19th century, basic ingredients were extracted from plants. However, with the advent of the industrial revolution and rapid development in the textile industry, natural dyes could no longer meet the growing demand.In this historical context, researchers began working on a wide range of synthetic dyes, characterized by vivid colors and higher prices. Science and industry forged a closer and more profitable cooperation from this point onwards.[115], [116]

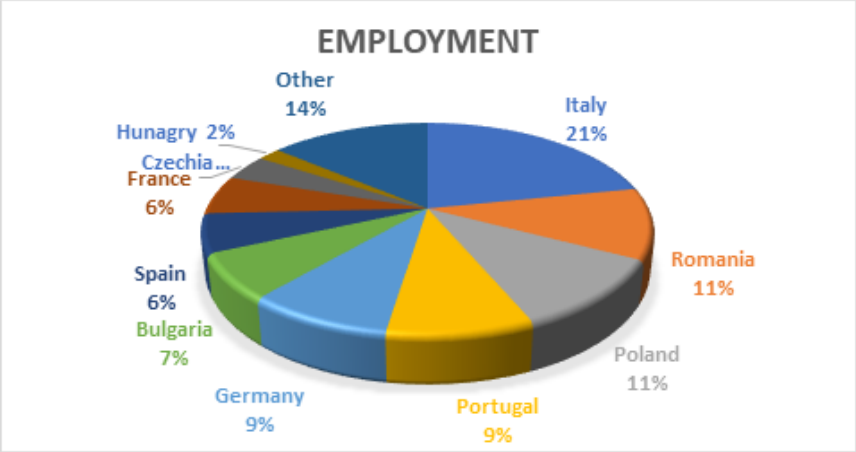
Methyl orange is a synthetic organic compound belonging to the category of azo dyes, synthesized for the first time by two German chemists: Johann Peter Griess in 1875 and Otto Nikolaus Witt in 1876. It is derived from sulfanilic acid, also known as 4-aminobenzenesulfonic acid ($NH_2C_6H_4SO_3H$), which is treated with sodium carbonate (Na_2CO_3) to form its sodium salt. In the subsequent stage, sodium nitrite and hydrochloric acid are added to form a diazonium salt. Reaction with N,N-dimethylaniline in the presence of sodium hydroxide leads to the formation of methyl orange.[14]

Methylene blue is industrially produced by oxidizing a mixture of dimethyl-phenylenediamine, sodium thiosulfate, and dimethylaniline. Its first synthesis dates to 1876. Robert Koch and Paul Ehrlich, scientists of the time, discovered its ability to selectively stain and inactivate various microbial species. This led to intensive research on its use in treating tropical diseases. Thus, methylene blue became the first synthetic compound in the history of medicine used as an antiseptic, predating sulfonamides and penicillin.[116]

4.2.2 Textile Wastewater

The textile industry is an important manufacturing activity from an economic point of view because it encompasses a variety of very different aspects. From a production perspective, the supply chain begins with the procurement of resources and the processing of raw materials, then moves on to the production and transformation phase, and ends with the distribution and sale of the product. From a commercial perspective, the entire chain is driven by consumer demand, whose

purchasing choices are regularly monitored through a lean retailing system that collects information directly from shopping centers and transmits it to manufacturing companies. The textile industry is a fundamental component of the European manufacturing sector in terms of production, value creation, and employment; in particular, the Italian textile industry is the largest in Europe, with activities that show the highest levels of employment and export value concentrated in Lombardy, Veneto, Emilia-Romagna, and Tuscany, accounting for 60% of the workforce employed and 80% of the sector's exports. According to data released by EURATEX (2022), Italy provides the greatest contribution to the textile industry



Furthermore, according to EURATEX estimates, the turnover of the textile and clothing industry in the EU-27 region was 147 billion euros in 2021, an increase of 11% compared to 2020. The textile activity in the EU has indeed recovered from the sharp contraction caused by the Covid-19 pandemic, while clothing companies have almost returned to pre-pandemic levels Although the number of companies has slightly decreased to 143,000, the EU's commercial performance has improved with exports reaching 58 billion euros in products, an increase of 10.6%.

The highest water consumption in the textile industry is associated with so-called "wet processes" such as pretreatment, dyeing, washing, and printing, which are also linked to the most significant environmental aspects. Generally, almost all the water used (about 95%) during the production process is discharged, as only a small part is dispersed as vapor during steaming operations. Additionally, there is extensive

use of chemicals (dyes, softeners, surfactants), which is why these discharges contain a significant amount of pollutants. According to the manual issued in 2007 by Tecnotessile – National Society of Technological Research, the main ranges for some typical parameters related to textile effluents are observed:[117] as shown in table 7.

Table 7: Textile Effluent Parameters

Parameters	Values
COD	150 – 5000
BOD5	50 – 700
SST	50 – 500
TOTAL SURFACTANTS	5 – 120
TOTAL NITROGEN	18 – 39
TOTAL PHOSPHORUS	0.3 – 15

4.2.2.1 Dyeing Process

These processes are characterized by high water consumption and effluents with a high load of pollutants such as dyes, metals, electrolytes, surfactants, organic auxiliaries, acids, or bases. The residual dye represents the part that does not bind to the fibers and is about 15% of the initial amount. Depending on the type of material treated, there will be different types of dyes as shown below:

Table 8:Dyes Used in the Textile Sector (Tecnotessile, 2007)[118]

Material	Dye Used
Wool	Pre-metallized (so-called due to the presence of a metal atom, generally chromium, bonded to two dye molecules), acid or reactive
Artificial fibres	Cationic, dispersed
Cellulosic fibres	Direct, reactive, sulphur, oxidation, analogizable, and couplable

Depending on the type of dyeing carried out, the effluent will have different chemical-physical characteristics; moreover, each phase of the dyeing process contributes differently to the pollutant load of the effluent. For example, the COD

value in the wastewater produced by the wool dyeing process with acid dyes and a bath ratio of 20:1 is reported (this value is expressed as a function of the discharged water and the amount of fiber processed).

Table 9: COD of Wastewater Resulting from Wool Dyeing [118].

Process Stage	COD (mg O_2/L of bath)	COD (g O_2/kg of Fiber)
Dye bath	982	19.6
Exhaust bath	995	19.9
First rinse	233	4.6
Second rinse	74	1.5
Third rinse	55	1.1

Washing Wastewater the pollutant load of these waters can vary depending on the products removed from the fibres, the chemicals used in the baths, and the phase of the washing process that produced them (discharge of the washing bath or rinse). Fabrics subjected to washing can come from various stages of the textile chain, such as weaving, dyeing, etc. Surfactants, softeners, various auxiliaries, and oxidants are the main classes of pollutants present in the effluents. The COD has high values, reaching up to 4000 mg/L, but is associated with lower BOD values (6 g/L), indicating the low biodegradability of this type of effluent. Some examples are provided below:

Table 10: Pollutants in Washing Water (Tecnotessile, 2007)[118].

Process Stage	Description
Wool degreasing	Produces an effluent with a high content of organic matter. The removal of auxiliaries such as knitting oils or preparation agents can lead to the discharge of hazardous substances like polychromatic hydrocarbons and bio acids. These wastewaters have COD values up to 40 - 80 g/kg of treated fibres.
Cotton desizing	95 g of COD/kg of fabric with COD concentrations often exceeding 20000 mg COD/L, with a COD to BOD ratio unfavourable to biodegradability
Bleaching of natural fibres	Metals are released into the discharge, which, due to complexing agents, give rise to secondary reactions forming halogenated organic compounds (AOX). Concentrations of 90 – 100 mg Cl/L of AOX are found in the exhausted bath if NaClO is used in bleaching and concentrations up to 6 mg Cl/L if H2O2 is used.

It is evident that in washing, the chemical-physical characteristics of the effluent vary based on the treatment employed.Special Refinishing Wastewater. Among the various finishing processes, those involving chemicals have the greatest environmental impact.

Table 11: BOD5 and COD Values in Finishing (Tecnotessile, 2007)[118]

BOD5 (mg/L of O_2)	COD (mg/L of O_2)
60 – 400	200 – 2500

The contaminants most frequently found in this wastewater are:

Softeners: Used in clothing, generally obtained with surfactants (cationic and non-ionic), sometimes mixed with resins or waxes.

Easy-care treatment: Performed on cellulosic fibers to increase washability and resistance using cross-linking agents.

Oiling agents: Based on mineral oils.

Mold inhibitors: Molds attack all fibers, particularly cellulosic ones if used or stored in a humid environment. Typical mold inhibitors are pyrethrins (highly toxic to insects).

Antibacterials: Use of formaldehyde, metal salts, phenols, posing a serious health risk. Less risky but less effective are cationic surfactants.

Flame retardants: Based on phosphate organic compounds and polybrominated organic compounds.

Antistatic agents: Alkyl phosphates and alkyl ether phosphates.

4.2.3 WINERY WASTEWATER

For several years, sustainability has become a central topic in all fields, from industrial to agricultural. The definition of sustainability is not unique, but one of the most used is that of the UN, dating back to the first environmental conference in 1972: “in environmental and economic sciences, the condition of development

capable of ensuring the satisfaction of the needs of the present generation without compromising the ability of future generations to meet their own needs." Around this definition revolves the intersection of three macro-systems: environmental, social, and economic; regardless of the sector, the aim is to define economically feasible projects that respect human rights, are beneficial to the community, and do not negatively impact the environment. This is where the 17 goals of the 2030 Agenda come from, an action program for both people and the planet, aimed at ending poverty, inequality, and addressing climate change.

Of particular interest for the Hydrocavi-Tech project are Goal 6 and Goal 12, which revolve around topics such as universal and equitable access to water and sanitation facilities, with a commitment to the sustainable and efficient use of natural resources, minimizing waste and promoting recycling and reuse.

Recovering and reusing the water that humans use daily, both for personal private use and in large-scale industrial productions, allows us to move closer to these key points, which are particularly important today. One of the popular fields for wastewater treatment applications is the wine sector.

In 2022, Italy was the nation with the highest wine production in the world, with 49,066,000 hectolitres, followed by France, Spain, and the United States of America. This sector uses a significant amount of water; the water footprint is generally more than 1 liter of water per liter of wine: in the European context, this amounts to over one hundred million hectolitres of water each year, most of which ends up as wastewater.

4.2.4 The Stages of Wine Production

Wine production involves a series of stages that follow in chronological order:

Harvesting: It is correct to say that winemaking begins before harvesting the grapes from the vine, as the care of the vineyard requires attention from cultivation with specific products. It is essential to stop treatments from the end of July so that the vine is cleaned by the August rain. Once fully ripe, the grapes are harvested. For white grapes, the harvest is slightly anticipated, while for red grapes, it is delayed. In this phase, healthy bunches are selected, separating them from those with mold or those still green.

Crushing: The technical start of winemaking begins with crushing and ends with the alcoholic fermentation process that transforms the sugars and water in the grape into alcohol and carbon dioxide. Crushing is usually done with special machines capable of crushing the grapes and discarding the stems. Consequently, the must, which increases in volume during fermentation, is pumped into the vat until it is three-quarters full.

Fermentation: This phase begins when the must is in the vat. To control this phase, selected yeasts are added to the must, which activate separately in a part of the must that will then be combined with the rest. For organic farming standards, a bit of grapes is harvested a few days before the main harvest and crushed by hand to obtain a fermenting must. The temperature of the process is very important and should never be below 18°C; sometimes special machinery is used to maintain a constant temperature. At this point, the so-called cap forms through the fermenting must, which releases gas that pushes the pomace upwards. To give color to the wine, periodic operations of punching down (breaking the cap with a stick to oxygenate the must) and pumping over (taking some must from the bottom and pouring it directly on the cap) are performed. The must can macerate in the vat for a couple of weeks depending on the type of wine, such as aged wine. If the wine is not aged, the time is reduced compared to the two weeks.

Racking: Using an electric pump, the wine is removed from the vat and transferred to a clean barrel.

Pressing: At a certain point, only wet pomace will remain in the vat, which will then be pressed, from which excellent material for distillation or fertilization can be obtained.

Slow Fermentation: While the wine is in wooden barrels or steel containers, fermentation occurs slowly for about a month until it is completely exhausted and the wine stops “fizzing.”

Storage: With the end of the slow fermentation process, the wine becomes vulnerable to air, and the risk of diseases multiplies. It is essential to take some precautions such as filling the barrels to the brim, keeping the floating lid always full, etc.

Racking: Around mid-November, the first racking takes place, necessary to remove residues and impurities from the wine. At this point, the wine is ready for aging, which could take place in a barrel or bottle.

Bottling: It is very important for this phase to respect strict hygiene standards. Regarding the bottling day, unfortunately, few (except biodynamic farming) consider the lunar phases and tend to follow the climate, preferring sunny days with high pressure.

Storage: Once bottled, the wine should be stored in a cool environment all year round at a temperature of about 15°C, in the dark, with low humidity, and away from harmful odors like gasoline. For about ten days, the bottles should be kept upright to allow the corks to expand, then they can be laid down.

4.2.5 Production of Winery Wastewater

The management of wastewater in wineries (WWW) falls under activities aimed at protecting water from pollution as provided in Part III of Legislative Decree 152 of 2006. This section includes regulatory requirements for:

- Soil protection and combating desertification
- Water pollution prevention
- Water resource management

Improving water quality is managed by monitoring chemical-physical-biological parameters, with both qualitative and quantitative analysis, capable of representing and respecting the aquatic ecosystem. Below is the regulation of surface discharges.

According to the definition in Article 74 of the Environmental Consolidation Act (TUA), discharge means “any release of wastewater carried out exclusively through a stable collection system that continuously connects the wastewater production cycle with the receiving body (surface water, soil, subsoil, and sewer network), regardless of their polluting nature, even if subjected to prior purification treatment.”[120]

The key aspects to focus on are the presence of a stable collection system and the continuity between the system generating wastewater and the receiving water body.

The fundamental rule is that "all discharges must be authorized" (Art. 124, paragraph 1, Legislative Decree 152/2006) by the competent authority as they are regulated based on compliance with the quality objectives of the receiving water bodies and must in any case comply with the limit values provided in Annex 5 to Part III of the TUA. The limit values are indicated in differentiated tables, contained in said annex, depending on the type of discharge and the receiving body.[120]

To understand how to manage a discharge of wastewater produced by a winery, it is useful to refer to the production chain to identify the factors to be investigated in an analysis and the parameters that influence the quality of the discharge.

Different categories of producers can be distinguished, depending on the supply chain, into:

- Private wineries that produce wine using their own grapes
- Private wineries that produce wine using grapes produced by third parties
- Cooperative wineries that produce wine using grapes provided by their members

Table 12: Operational Structures in the Wine Production Sector (ISTAT data)[121]

Production Structure	*Production % of Total*
Producers who vinify their own grapes	*42-46%*
Cooperatives	*42-46%*
Wine industry	*8-16%*

The main constituents of concern in winery wastewater are biodegradable organic substances, solids, and nitrogen. The quality of wastewater varies based on the winemaking phase (vintage, racking, bottling), the winemaking technique (production of red, white, and special wines), the operational scheme of the plant, and the chemicals used for cleaning. Wineries can reduce the strength of their wastewater by 90% by screening or filtering organic materials such as pomace and lees out of the water system.[122], [123]

Winery wastewater is generally acidic and has high concentrations of total solids (TS), volatile solids (VS), dissolved solids (DS), 5-day biochemical oxygen demand (BOD5), chemical oxygen demand (COD), total nitrogen (TKN), total phosphorus (TP), polyphenols, and turbidity.[123]

The high BOD concentration is largely attributed to biodegradable alcohols (mainly ethanol), sugars (mainly glucose and fructose), organic acids (e.g., lactic, tartaric, citric, malic, and succinic acids), and glycerin, while COD can also include recalcitrant organic substances such as polyphenols, tannins, and lignins. The average and maximum polyphenol concentrations are 67.5 and 268 mg/L, respectively, with gallic acid being one of the representative species. Other frequently found phenolic compounds include ethyl ester of 3,4,5-trihydroxybenzoic acid; 1,2-dihydroxyanthraquinone; trimethyl(2-phenylethoxy) phenol; and 2,4,6-tris-(1-methylethyl) phenol. Experimentally, it has been observed that some of these species were removed by conventional oxidation processes and others were not.[122,124].

4.3 Possible Applications of Treated Winery Wastewater: Advantages and Limitations

Previous regulations mostly dealt with the issue of discharge into a receiving water body, but evolving towards a circular economy reveals the use of treated water in many applications.

As shown in Table 13, the applications are numerous although there are important limitations to consider. The seasonality of demand, interventions on existing structures, and the impact on human health and nature are stringent constraints for the application of treated wastewater in any sector. Analytical evaluations are carried out to exclude environmental damage, as well as an economic analysis of the treatment to be used before the water can be reused [125].

Table 13: Possible Applications of Treated Water with Respective Limits.

Applications	*Major Constraints*
Agricultural irrigation	*Seasonal demand variability*
Landscape irrigation	*Seasonal demand variability*
Industrial	*Constant but site-specific demand*
Urban	*Need for a dual water distribution system; limited demand; costs*
Environmental/recreational use	*Site-specific*
Aquifer recharge for saline wedge reduction	*Presence of suitable aquifers near the treatment plant*
Indirect potable use	*Existence of an adequate environmental buffer; costs; health risks; social acceptance; lack of regulation*
Direct potable use	*Costs; health risks; social acceptance; lack of regulation*

4.4 HYDROCARBONES

Petroleum hydrocarbons (PHCs) represent significant organic contaminants, predominantly sourced from petrogenic activities, industrial coking residues, and other anthropogenic processes, contributing substantially to soil pollution [126] These compounds are characterized by high hydrophobicity and a notable octanol-water partition coefficient. As the number of benzene rings in PHCs increases, their degradation becomes increasingly challenging [127] The persistence of PHCs in soil is exacerbated by their low degradability and their documented carcinogenic, teratogenic, and ecotoxic properties, underscoring their global environmental and health impacts.

Efforts to address PHC contamination in the soil have become a critical area of research. Advanced oxidation processes (AOPs) and electrochemical advanced oxidation processes (EAOPs) have emerged as leading strategies for remediating PHCs from soil due to their efficacy in restoring contaminated environments [128,129]. AOPs such as H_2O_2/UV, $Fe^{2+/}H_2O_2$, various Fenton-like processes, ozonation, and photocatalysis are notable examples that leverage hydroxyl radicals (•OH) to degrade organic contaminants [130]

Among these processes, electro-Fenton techniques have gained prominence for their rapid kinetics, high efficiency, and versatility in treating PHCs However, traditional Fenton methods involving H_2O_2 and Fe^{2+} catalysts can be costly and may lead to secondary contamination issues, necessitating additional treatment steps

([131] Research has focused on innovations such as in situ H_2O_2 generation and cathodic Fe^{2+} regeneration to mitigate these challenges within electro-Fenton applications. The use of boron-doped diamond (BDD) electrodes has also been explored for their stability and ability to generate hydroxyl radicals (OH) effectively, thereby enhancing pollutant degradation on their surfaces.[132]

Despite the advantages of electro-Fenton, challenges remain, including the high cost of electrodes and energy consumption. In contrast, bioslurry processes offer an environmentally friendly approach to pollutant remediation but require careful control of operational parameters 2015[133] The sensitivity of microbial communities to toxic substances can limit the efficiency of bioslurry technologies, particularly at higher pollutant concentrations [134] Combining bioslurry with additives like biosurfactants or integrating it with AOPs presents promising synergistic approaches to enhance pollutant bioavailability and overall treatment efficacy [135]

Recognizing the strengths and limitations of both biological treatments and advanced oxidation methods, integrating these approaches has gained traction as a pragmatic solution[136]This hybrid approach holds potential for optimizing PHC biodegradation in soil, potentially reducing reliance on Fenton reagents and stabilizing waste products [137]

4.4.1 Physical and Chemical Characteristics of Polycyclic Aromatic Hydrocarbon

Polycyclic aromatic hydrocarbons (PAHs) possess distinct physical and chemical attributes. While traditionally defined as compounds with two or more fused benzene rings, the classification among environmental chemists often focuses on the presence of at least two benzene rings in the structure. Biphenyl, although its rings are connected by a single bond rather than fused, is commonly regarded as a PAH in this context. However, the criterion of "fused aromatic rings" remains widely accepted as the most accurate definition. In some contexts, these compounds are also referred to as "carbocyclic systems".[134, 138]

PAHs are known for their moderate resistance to biodegradation and are classified as persistent organic pollutants (POPs) in the environment. Their hydrophobic nature, low water solubility, and electrochemical stability significantly contribute to their environmental persistence. Among the extensive list of agents identified by the International Agency for Researc.[134]

The properties and environmental fate of PAHs depend largely on their molecular weight and the number of fused benzene rings. High molecular weight (HMW) PAHs, which consist of four or more fused benzene rings, exhibit distinct environmental behaviors compared to low molecular weight (LMW) PAHs, which typically have two to three fused benzene rings [139] Low molecular weight PAHs are characterized by their lower persistence, high volatility, slight water solubility, and reduced carcinogenicity. However, they pose significant risks to aquatic organisms such as fish due to their tendency to accumulate in tissues (bioaccumulation) and magnify up the food chain (biomagnification), potentially impacting humans through consumption [139]

In contrast, high molecular weight PAHs exhibit greater persistence, being less volatile and more resistant to oxidation. When alkyl or chlorine substituents are attached to their rings, these PAHs become more insoluble and can display increased reactivity and toxicity compared to their unmodified forms [140]

The effects of PAHs encompass carcinogenicity, mutagenicity, teratogenicity, direct toxicity, or combinations thereof [140] PAHs typically occur as complex mixtures rather than single compounds, totaling several hundred variants .

Common PAHs include anthracene, benzo(a)pyrene, chrysene, fluorene, and pyrene. Benzo[a]pyrene (BaP) is widely used as an indicator of PAH contamination, with a majority of available data focusing on this compound.

4.4.2 Occurrence and Environmental Fate of PAHs

Polycyclic aromatic hydrocarbons (PAHs) originate from both natural and human-made sources, with the latter contributing significantly to their associated hazards. Natural sources include biosynthesis by algae and bacteria, volcanic activity, and forest fires. Additionally, the formation of fossil fuels through the diagenesis of organic material is a natural source of PAHs.

Human-made sources primarily involve the incomplete combustion of organic materials in industries such as coal, petroleum, and metal smelting. Urban runoff, asphalt pavement deterioration, and car tire wear also contribute to PAH pollution.

PAHs are widespread in the environment, existing in mixtures of two or more compounds. Pure PAHs are typically colorless, white, or pale yellow-green solids with little to no odor. They are used in various applications, including medicines, dyes, plastics, and pesticides, and are found in substances like crude oil, coal, and asphalt.

The global distribution of PAHs results from both natural and anthropogenic activities, leading to their presence in air, water, soil, and sediments. In the air, PAHs can be gaseous or attached to particulates, depending on their molecular structure. In water, they can volatilize, undergo photolysis, oxidation, biodegradation, or bind to particles and sediments. In soil, PAHs can volatilize, degrade, or accumulate in plants and groundwater.

Due to their widespread release and associated health and environmental risks, regulatory agencies like the European Union and the United States Environmental Protection Agency (USEPA) have set permissible limits for 16 priority PAHs.

4.4.3 Reactivity of PAHs

PAHs are generally chemically inert and undergo transformation mainly through electrophilic substitution reactions. Significant energy is required to convert aromatic compounds into non-aromatic products. The reactivity of PAHs depends on the electron distribution within the molecule, determining the most reactive positions.

For example, naphthalene is more reactive at position 1 than 2, while anthracene and phenanthrene react at positions 9 and 10, with anthracene being more reactive. Fluorene is most reactive at position 9, and other PAHs like fluoranthene and pyrene exhibit similar reactivity patterns to anthracene and phenanthrene. The localization energy concept helps explain the mechanisms of PAH degradation and derivative formation. The numbering system for carbon atoms in PAHs follows a systematic order, except for anthracene and phenanthrene. Fig13 shows the **Chemical structures indicating numbered positions PAHs.**

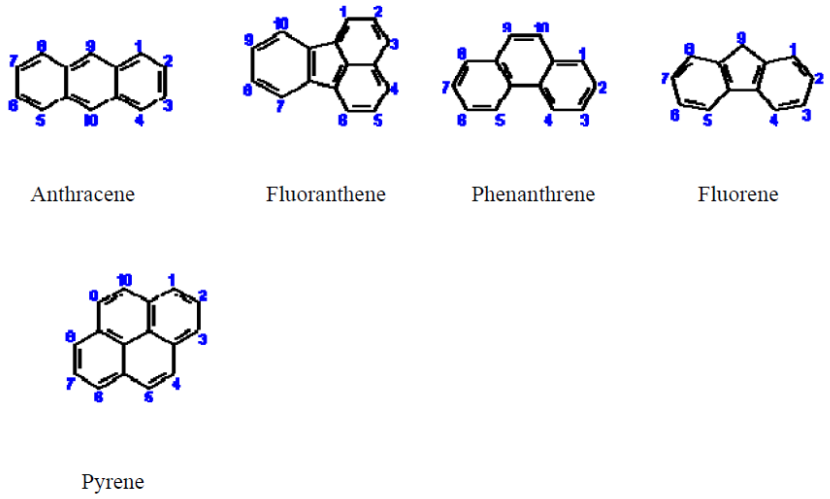


*Figure 13**: Chemical structures indicating numbered positions PAHs***

4.4.4 Analytical Procedures for the Measurement of PAHs

Measurements of PAHs in environmental matrices mostly require difficult analytical chemical procedures because of the complexity encountered in environmental samples. This complexity is readily seen when one considers the general categories of phases into which environmental samples may be categorized, namely, aqueous, air (gaseous or condensates/particulate matter), oil or organic liquid, solids or sludge, biological samples and even multiphase samples [141].

Sampling, sample preparation, isolation and concentration from sample matrices are critical in the analytical determination of PAHs. Typical sample preparation procedures include extraction, concentration and clean-up [141] Extraction methods explored over the years include: Soxhlet, sonication, liquid-liquid extraction, purge and trap, headspace, shaking, vortex, solid-phase, supercritical fluid extraction, solid-phase micro extraction (SPME), stir-bar sorptive extraction (SBSE), miniaturized solid-phase extraction (SPE), liquid-phase micro extraction (LPME), membrane-assisted solvent extraction techniques (MASE) etc., (Tang and Isacsson, 2008). Sample concentration methods employed include nitrogen

blowing, vacuum evaporation, micro-Snyder column technique and adsorbent or cryogenic trapping.

Some identification and quantification methods include the use of Gas Chromatography (GC), Gas Chromatography-Mass Spectrometry (GC-MS) and High-Performance Liquid chromatography (HPLC).

4.5 TREATMENT METHODS

Wastewater can generally be classified into:

Cooling Water: Characterized by medium to high temperatures but with a low pollutant load.

Washing Water: Features considerable flow rates with a non-negligible pollutant load.

Process Water: Does not have high flow rates but shows a significant pollutant load.

Increasingly stringent legislative requirements have driven companies to seek technological solutions aimed at reducing consumption and enabling water reuse.

There are numerous existing and innovative purification solutions, making it challenging to determine the most suitable techniques without considering the fate of the water (recirculation, discharge into surface water, discharge into the sewer) and the quality of the final product. The experience of individual operators also plays a significant role in the adoption of one system over another.

4.5.1 . PRIMARY PROCESSES

Primary processes, which are physicochemical in nature, represent the initial treatments to which wastewater is subjected. Their goal is to eliminate suspended solids(TSS), predominantly organic in nature, using flocculating substances to promote precipitation and increase sedimentability., homogenize the effluent, and regulate its pH. These processes can include:

Screening: Used for the removal of coarse substances (>2 cm) through bars or meshes of various shapes, with manual or automatic cleaning.

Oil Removal: Involves the gravitational separation of oils, fats, and foams, often facilitated using demulsifiers and air insufflation, through the use of flow deflectors that aid in the separation and collection of oil particles.

Primary Sedimentation: Occurs in special tanks where gravity allows the separation of even the smallest and lightest particles from the liquid medium, which settles at the bottom forming sludge.

Table 14: Summary of Primary Treatment Processes

Process	*Purpose*	*Method*	*Applications:*
Screening	*Remove large debris and coarse materials*	*Wastewater passes through screens with different mesh sizes*	*Commonly used in municipal and industrial wastewater treatment plants.*
Oil Removal	*Separate oils, fats, and greases*	*Gravitational separation, often enhanced*	*Essential in industries such as food processing, petrochemicals, and automotive.*
Primary Sedimentation	*Remove suspended solids and reduce organic load*	*Gravity allows solids to settle at the bottom, forming sludge*	*Used in both municipal and industrial wastewater treatment to improve the efficiency of subsequent treatment processes.*

4.5.2 . SECONDARY TREATMENT PROCESSES

Secondary treatment processes form the core of the purification plant and allow for the partial or total reduction of the pollutant load. Industrially, biological oxidation processes have shown great effectiveness, enabling the oxidation of dissolved organic and colloidal substances in the effluent through vigorous aeration, thanks to the intervention of a complex community of microorganisms.[11], [142]

These processes can be carried out through:

Activated Sludge: This is the most widely applied and efficient process, as it allows for the removal of BOD, COD, suspended solids, nitrogen, and phosphorus through aerobic bacterial fermentation in aerated tanks where the wastewater comes into contact with bacterial sludge.[143]

Trickling Filters: Microorganisms adhere to gravel, and the effluent trickles over it, reducing the risk of foam formation but also the process efficiency due to the limited contact time between the effluent and the microorganisms.

Anaerobic Processes: These can be of various types, heated or unheated; they have the advantage of producing less sludge and generating biogas (used as an energy source), but are disadvantaged by low purification efficiency and large size. These treatments are applicable only to highly concentrated effluents.[144]

Secondary processes also include denitrification and nitrification, which allow for the biological removal of ammoniacal, nitric, and nitrous nitrogen, as well as secondary sedimentation, which involves the sedimentation of microorganisms aggregated in sludge flocs. The produced sludge is partly recirculated into the oxidation tank to reintroduce perfectly efficient microorganisms, and partly extracted and sent to the sludge line for proper treatment and disposal.[145]

4.5.3 Tertiary Treatment Processes

Tertiary treatment processes have become increasingly important for achieving the quality standards necessary for discharge, especially into surface water, and even more so if the water is intended for recycling. These include:

Activated Carbon Adsorption: This involves filtration through an adsorbent medium capable of interacting with various substances present in the water, especially organic substances such as solvents, surfactants, pesticides, and dyes.[146]

Ozonation: Ozone is a powerful oxidant used industrially to oxidize, decolorize, and disinfect water, making it reusable.

Filtration: Used to eliminate particles ranging from millimeters to microns in size; the most common is sand filtration, useful for reducing suspended solids and non-settled sludge microflocs from secondary sedimentation. More advanced filtration is membrane filtration, which includes microfiltration, ultrafiltration, nanofiltration, and reverse osmosis, all high-pressure filtration processes on microporous membranes that allow high-purity water to flow through while

retaining solutes. However, these are still rarely used on an industrial scale due to high costs.[17]

According to ISPRA classifications, the following processes are included:

Anaerobic Digestion: Stabilizes organic substances through hydrolysis, acidogenesis, acetogenesis, and methanogenesis, with a long hydraulic retention time. The use of facultative ponds as a pretreatment process reduces organic strength, like upflow anaerobic sludge blanket reactors, but with low microbial biomass concentration under natural conditions. COD removal is less than 90%, while BOD, COD, and TSS remain below 81%. The reactors are quite complex and require highly qualified personnel to manage them. They are difficult to scale due to flow variation issues.

Aerobic Processes Combined with Activated Sludge and Membrane Bioreactors: Since the substances present in winery wastewater are easily degradable (BOD_5/COD=0.54) with the aerobic process, combining it with activated sludge processes and membrane bioreactors has achieved COD removal efficiencies between 89% and 99%. Although the treatment operation is simpler and more common, it is not at all economical. In this case, flow fluctuation can lead to difficulties in maintaining the system in the right conditions for microorganism life: during periods of high wastewater production, the number of microorganisms produced can cause problems in sludge disposal.[147]

Physico-Chemical Treatment: Physico-chemical methods such as coagulation-flocculation have been used for efficient removal of TSS, turbidity, natural organic matter, and dissolved inorganic constituents from winery wastewater. However, chemical methods are rarely used as they are particularly expensive.[148]

Although biological methods provide high organic load removals, they require relatively long residence times associated with extensive equipment. Aerobic methods require high energy consumption for aeration, which is a disadvantage compared to their anaerobic counterpart, which can also produce biogas as a byproduct.[149]

With the help of these secondary treatments, TSS, COD, and BOD are removed: COD removal is the most common measure of wastewater treatment efficiency, as

well as the factor that typically limits effluent discharge into the receiving water body.[150]

Pollutant removal efficiencies, in terms of COD, are reported. It is interesting to observe that the highest efficiencies are obtained in advanced oxidation processes, conducted following evaporation and air striping for the removal of volatile components. Advanced oxidation processes are innovative technologies used both as pretreatment or post-treatment to biological processes due to their ability to remove or inactivate persistent microcontaminant residues such as pharmaceuticals, endocrine-disrupting compounds, caffeine, or antibiotic-resistant compounds, some of which are classified as emerging pollutants.[151]

Table 15: Winery Wastewater Treatment Methods with Corresponding Efficiencies[123]

Category	*Methods*	*COD Removal*
Physical chemical	*- precipitation* *- sedimentation* *- coagulation* *- electrocoagulation*	*9%* *20-40%* *35%* *47%*
Biological	*- membrane bioreactor* *- conventional activated -sludge process* *- anaerobic batch reactor*	*94%-97%* *98%* *98%* *80%-97%*
Advanced oxidation processes	*- TiO2* *- with Fe* *- with ozone*	*84%* *93% (98% afterstripping)* *84%*

The large quantity of industrial effluents produced daily, containing chemicals toxic to human health and the environment, has led researchers worldwide to develop highly efficient, cost-effective, and energy-saving wastewater treatment technologies for both industrial and domestic use.

Advanced Oxidation Processes (AOPs) have garnered particular interest as they generate enough hydroxyl radicals to oxidize most complex chemicals present in effluent water. This category includes Fenton and similar processes, hydrodynamic and acoustic cavitation, photocatalysis, and combined treatments. Using AOPs can significantly improve the degradation efficiency of refractory organic compounds. However, the Fenton process requires the addition of many hazardous chemicals (such as H_2O_2, H_2SO_4, and NaOH) and produces sludge.[152]

Among these, cavitation has attracted the attention of many researchers and has been used in various sectors, including disinfection, sludge treatment, degradation of polymers, organic compounds, pesticides, and textile dyes. Additionally, in wastewater treatment, it can be used in combination with other reagents or chemical technologies to reduce chemical consumption and improve energy efficiency, thus achieving low-cost operation.[153]

4.5.4 Acoustic and Hydrodynamic Cavitation

Cavitation is the phenomenon of nucleation, growth, and implosion of vapor or gas-filled cavities within a short period, usually milliseconds, made possible when the local liquid pressure drops to the saturation pressure at a given temperature. Initially, it was considered a harmful phenomenon because it caused corrosion, noise, and vibrations in equipment, damaging pumps, valves, pipes, and propellers.[154]

These disadvantages can be suppressed or reduced with appropriate measures, such as selecting high-pressure-resistant materials, controlling pressure and flow velocity, and better designing pipes and devices. When a cavitation bubble explodes, it generates an enormous implosion force that causes local temperature spikes, which can reach 500-1500 K, and pressure, which can reach 100-5000 atmospheres. Additionally, there can be physicochemical effects that induce numerous changes: under extreme conditions, water molecules can decompose into various species with high oxidizing potential, including hydroxyl radicals (-OH), OOH, and H_2O_2.[9]

Based on the type of generation, cavitation can be divided into four categories: optical cavitation (OC), particle cavitation (PC), acoustic cavitation (AC), and hydrodynamic cavitation (HC) [21].In the field of wastewater treatment, AC and HC have been most studied.

AC is due to pressure variations caused by the passage of ultrasonic waves in the liquid at rest; generally, multiple frequencies are used simultaneously, in the range of 20 kHz-1 MHz. Ultrasonic waves are generated by the vibration of the container walls holding the liquid or by the vibration of an object submerged in the liquid. This type of process is widely used in chemical synthesis, polymer material

degradation, and the petrochemical industry. However, high energy consumption and the limited cavitation zone restrict its development.[23]

HC shows better characteristics in terms of energy efficiency and equipment simplicity. In hydrodynamic cavitation, bubbles are generated by the passage of liquid through a device with a section constriction (throttle valve, perforated plate, Venturi tube) located along the conduit through which the liquid flows. As the liquid passes through the constriction, there is an increase in kinetic energy and a corresponding decrease in static pressure, in [155]accordance with Bernoulli's equation 5:

$$\frac{1}{2}\rho v^2 + \rho g h + P = constant \qquad Equation\ 5$$

where:

ρ= liquid density

(v) = liquid velocity

The goal of this process is to ensure that the constriction section brings the static pressure close to or below the liquid's saturation pressure at the operating temperature, thus generating microbubbles, whose sizes can range from a few nanometers to a few millimeters, which grow in the divergent part of the Venturi and then implode and collapse where the pressure exceeds the saturation pressure.[155]

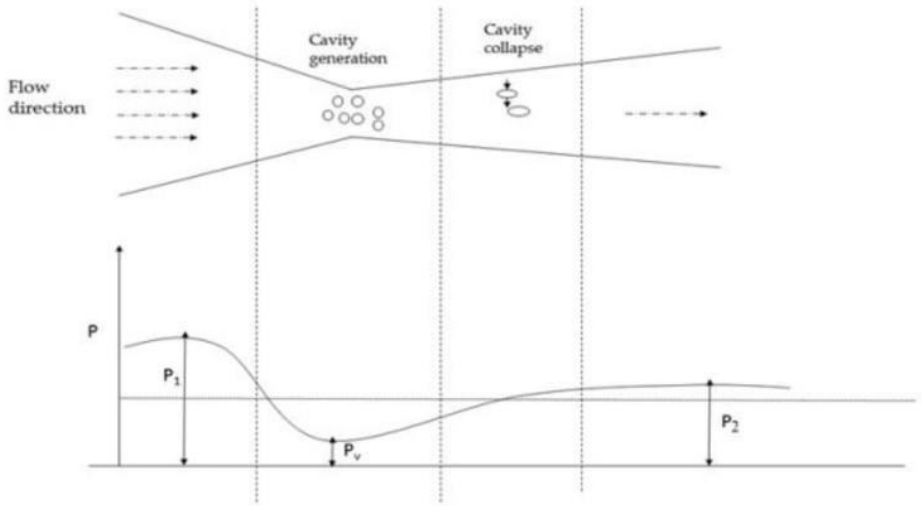


Figure 14:Various stages of cavitation events with a pressure profile in the hydrodynamic cavitation reactor

The explosion of cavitation bubbles, in addition to temperature and pressure spikes, can cause, under extreme conditions, the decomposition of water molecules into various species with high oxidizing potential, including hydroxyl radicals, whose formation reactions are as follows:

$$H_2O \rightarrow \cdot OH + \cdot H \qquad \textit{Equation 6}$$

$$H_2O + \cdot H \rightarrow \cdot OH + H_2 \qquad \textit{Equation 7}$$

$$\cdot O + H_2O \rightarrow 2 \cdot OH \qquad \textit{Equation 8}$$

In the case of a Venturi tube, bubble formation begins in the convergent phase, then grows through the throat section. Downstream of the Venturi, bubble collapse is accompanied by fluid expansion, causing inevitable pressure losses between the upstream and downstream of the cavitation medium.[64]

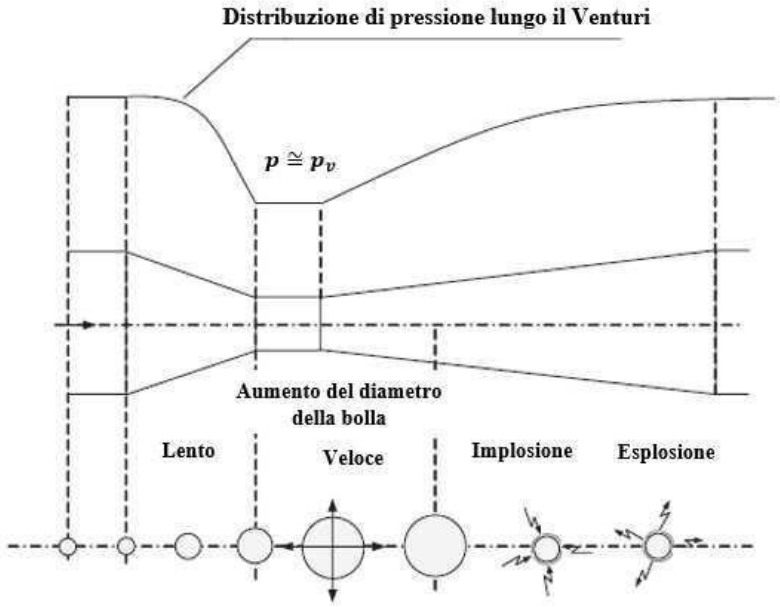


Figure 15:Formation and collapse of bubbles in a Venturi tube

The intensity of the implosion mainly depends on the turbulence level downstream of the cavitation reactor; in the case of the Venturi tube, this level is low, and in some cases, bubbles may undergo continuous oscillations (pressure peaks of 2-20 bar).[62]

To describe the HC phenomenon, a dimensionless parameter, the cavitation number (Cv), is used, defined as:

$$Cv = \frac{p_2 - p_v}{0.5 \cdot \rho \cdot v_0^2} \qquad \textit{Equation 9}$$

where:

(p_2) = downstream pressure of the cavitation device

(p_v) = vapor pressure of the liquid at the operating temperature

(v_0) = average liquid velocity in the constriction

ρ= liquid density

By tuning this parameter, we can achieve maximum efficiency for our HC process. The Cv at which cavitation onset occurs is known as Cavitation Inception (Cv_i), ideally equal to one ($Cv_i = 1$). However, it has been found that even with a cavitation number greater than one, for example, in the range of 2 to 4, cavitation can occur due to the presence of dissolved gases or impurities that act as weak points in the liquid for cavitation development: the addition of air, gas, or solid particles improves the density of the number of cavities generated but also results in a consequent decrease in collapse conditions. Analyzing the phenomenon, it has been noted that the point where cavitation is maximum is in the Cv range between 0.1-1.[39]

According to Jain et al., the Cv varies depending on the plant geometry and flow conditions, parameters that must be adjusted so that the cavitation number falls within the range of 0.15-0.25. Focusing on parameter tuning, it has been seen that as the inlet pressure (P1) increases, the Cv decreases, and the number of cavities generated increases due to a higher flow velocity through the throat section, further lowering static pressure and favoring the formation of the necessary turbulence for radical species formation[48]Focusing on parameter tuning, it has been observed that as the inlet pressure (P1) increases, the Cv decreases and the number of cavities generated increases due to a higher flow velocity through the throat section, which further lowers the static pressure and favors the formation of the turbulence necessary for the formation of radical species [25].

Continuing to lower the cavitation number will reach a point where the efficiency of the phenomenon will begin to decrease because the inlet pressure in the convergent section will generate many bubbles that will start to coalesce, forming

a large cavitational bubble, or cavity cloud, which will be carried away with the liquid without collapsing, thus reducing the generation of ˙OH radicals.

The condition of cavity cloud formation is defined as choked cavitation. The maximum cavitational intensity is obtained at a Cv slightly higher than that of choked cavitation [26].

The hydrodynamic cavitation phenomenon, therefore, depends on the number of cavities generated and the intensity of their collapse, parameters controllable through Cv tuning.[156]

4.5.5 . THE FENTON PROCESS

In 1894, Henry J. Fenton observed that hydrogen peroxide (H_2O_2), in the presence of iron salts ($FeSO_4$) and in an acidic environment, generated hydroxyl radicals (OH), extremely useful in the treatment of industrial discharges due to their high reactivity.[157]

There are several scientific studies and interpretations, sometimes conflicting, about the actual sequence of reactions that constitute the Fenton process. However, it can be considered that the mixture of H_2O_2 and iron salts (ferrous ions Fe^{2+}) as a catalyst exhibits its oxidizing action towards organic substances through the production of ·OH radicals, according to the reaction

The Fenton process involves the reaction of hydrogen peroxide (H_2O_2) with ferrous ions (Fe^{2+}) to produce hydroxyl radicals (·OH), which are highly reactive and can oxidize organic substances. The key reactions in the Fenton process are as follows:[158]

Formation of Hydroxyl Radicals:

$$Fe^{2+} + H_2O_2 \rightarrow Fe^{3+} + \cdot OH + OH^- \qquad \textit{Equation 10}$$

Regeneration of Ferrous Ions:

$$Fe^{3+} + H_2O_2 \rightarrow Fe^{2+} + \cdot OOH + H^+ \qquad \textit{Equation 11}$$

These reactions illustrate the catalytic cycle where ferrous ions are oxidized to ferric ions (Fe^{3+}) and then reduced back to ferrous ions, allowing the continuous production of hydroxyl radicals

Fenton and Photo-Fenton Process

The Fenton process is a very interesting technique for the treatment of textile wastewater because H_2O_2 is an environmentally friendly oxidant and iron, in addition to being very abundant, also has low toxicity. The Fenton process also features easy equipment, easy maintenance, and low cost; its non-selective nature allows the removal of a wide range of contaminants with a drastic reduction in toxicity ([159]

$$Fe^{2+} + H_2O_2 \rightarrow Fe^{3+} + \cdot OH + OH^- \qquad \textit{Equation 12}$$

The highly reactive radicals · OH can, in turn, react with the dyes present in the wastewater, causing their oxidation. The Fe^{3+} ion can be recycled through the relatively slow reaction:

$$Fe^{3+} + H_2O_2 \rightarrow Fe^{2+} + HO_2 + H^+ \qquad \textit{Equation 13}$$

The Photo-Fenton reaction further improves the degradation of organic pollutants through direct photolysis or by increasing the production of · OH, according to the following reactions:

$$Fe^{3+} + H_2O_2 \rightarrow Fe(HO_2)^{2+} + H^+ \qquad \textit{Equation 14}$$

$$Fe(HO_2)^{2+} + hv \rightarrow Fe^{2+} + \cdot OH \qquad \textit{Equation 15}$$

In cases where partial oxidation of organic contaminants also leads to the formation of toxic intermediates (even more harmful than the original compounds), it is necessary to apply further treatment to the resulting effluent before its final disposal into the aquatic environment

4.5.5.1. PHOTOCATALYSIS

Photocatalysis is an advanced oxidation process initiated by the combined action of light and water, mimicking the process of chlorophyll photosynthesis in absorbing and transforming pollutants into non-harmful compounds.

For this process to occur, the presence of a catalyst is necessary: the best are solid semiconductors, and among them, the most used is titanium dioxide (T), a white

crystalline powder that is economical and particularly efficient when irradiated by UV rays.

Semiconductors have a particular electronic structure, characterized by a full valence band (VB) and an empty conduction band (CB), making them particularly sensitive in photo-induced Redox processes. The energy difference between the lowest level of the VB and the highest level of the CB is called the "Energy gap" (Eg) and is the minimum light energy required to make a material a good conductor.

If a semiconductor like TiO_2 is irradiated with photons of energy greater than its Eg, an electron from its valence band can overcome the energy gap and be promoted to the conduction band. The vacancies of metal oxides, with high oxidizing power, can react with absorbed water forming a hydroxyl radical ($^{\bullet}OH$); the electrons promoted to the conduction band have a strong reducing power and react with the oxygen in the air forming the superoxide ion (O_2^-). Both formed species are highly reactive and capable of oxidizing most organic contaminants, decomposing them into CO_2 and H_2O, similar to what happens with chlorophyll photosynthesis.[160]

The photocatalytic process is used in various engineering applications, thanks to its antibacterial and anti-pollution effects, which is why many companies are investing in this new green technology [28]. However, its limitations lie in the high band gaps, strong instability, and difficult recovery after treatment [21].

H_2O_2/UV

This is a photolytic process, where the production of radical species is obtained from the photolysis reaction of H_2O_2 in fact, hydrogen peroxide is activated by UV as an external energy source, as shown by the equation:

$$H_2O_2 \xrightarrow{UV} 2 \cdot OH \qquad \textit{Equation 16}$$

The photolysis of hydrogen peroxide effectively oxidizes most natural compounds. The rate of photolysis of H_2O_2 specifically depends on the incident power or intensity. Sunlight can also be used as a radiation source, but the photolysis rate may be lower compared to UV light. The oxidizing capacity of UV/H_2O_2 can be attributed to the formation of the reactions describing UV/H_2O_2 are as follows:[13]

Initiation (direct photolysis of H_2O_2 produces OH radicals):

$$H_2O_2 \xrightarrow{UV} 2 \cdot OH \qquad \textit{Equation 17}$$

$$H_2O_2 + HO_2^{\bullet} \rightarrow \cdot OH + H_2O + O_2 \qquad \textit{Equation 18}$$

Propagation (of radicals):

$$H_2O_2 + \cdot OH \rightarrow HO_2^{\bullet} + H_2O \qquad \textit{Equation 19}$$

Termination:

$$HO_2^{\bullet} + HO_2^{\bullet} \rightarrow H_2O_2 + O_2 \qquad \textit{Equation 20}$$

$$\cdot OH + \cdot OH \rightarrow H_2O_2 \qquad \textit{Equation 21}$$

$$\cdot OH + HO_2^{\bullet} \rightarrow H_2O + O_2 \qquad \textit{Equation 22}$$

Light energy works to accelerate the degradation reaction, as most organic contaminants absorb UV energy in the range of 200-300 nm.

4.5.5.2 Combined Treatments

Although hydrodynamic cavitation has unique advantages in wastewater treatment, it alone is not efficient and economical enough to satisfactorily degrade target compounds. Combining HC with other AOPs can significantly increase degradation efficiency [29].

To evaluate the efficiency of the hybrid process, the value of the synergistic index SI must be considered, defined as:[161]

$$SI = \frac{k(HC+AOP)}{k(HC)+k(AOP)} \qquad \textit{Equation 23}$$

where $k(\mathrm{HC} + \mathrm{AOP})$indicates the reaction rate constant of the combined process, while $k(\mathrm{HC}) + k(\mathrm{AOP})$ indicate the reaction rate constants of the individual processes. Usually, if SI > 1, the removal efficiency of the hybrid process is greater than that of the individual processes.

The first combination analyzed is that between HC and hydrogen peroxide (H_2O_2), a weak acid with a relatively high oxidation potential that depends on pH (1.80 V at pH=0; 0.87 V at pH=14). It does not decompose spontaneously and generates ·OH radicals in the reaction medium [31]. Under HC conditions, H_2O_2 decomposes

into ·OH with an oxidation potential of 2.8V, leading to the degradation of contaminants.

Although the addition of H_2O_2 can increase the degradation yield of the cavitation process, it is important to use the optimal amount relative to the pollutant content, as excessive use can worsen the process efficiency [21].

Another widely studied combination is that between HC and Fenton: in this case, H_2O_2 is catalyzed by Fe^{2+} to generate a high amount of ·OH that can interact with most organic compounds to degrade them.

However, the wastewater treatment process with Fenton is accompanied by the production of large amounts of sludge, which is a major drawback for its application. Additionally, the Fenton process needs to be carried out at a pH

4.5.6 Innovative Treatments of Textile Wastewater

Recent studies have shown that cavitation is promising for wastewater treatment due to its ability to efficiently degrade many pollutants . Cavitation is the phenomenon where vapor zones form within a fluid, which subsequently implodes. This occurs when there is a local pressure drop to the vapor pressure of the liquid. The liquid, under saturation conditions, undergoes a phase change from liquid to gas, resulting in the formation of vapor-containing bubbles (cavities). The first step of cavitation is the so-called[162]

Nucleation, which is the origin of microscopic spaces that can form nuclei for the growth of macroscopic bubbles that will collapse later. There are two types of nucleation: homogeneous, which occurs when thermal motions within the liquid temporarily create microscopic voids that can later form the necessary nuclei for the growth of macroscopic bubbles, and heterogeneous, which is favored by the presence of microparticles dispersed in the primary fluid or caused by the roughness of the walls of the conduit containing the fluid. The second phase is bubble expansion, where growth is essentially due to the difference between the pressure inside the bubble (which can be assumed to be equal to the vapor pressure) and the

pressure in the surrounding liquid. The final step is bubble collapse and implosion, where bubble growth stops, collapse begins and culminates in an implosion that can cause damage.[163]



Figure 16: Phases of Cavitation

The devices used include an orifice, a valve, or a venturi. When the liquid flows through the constriction of the device, pressure and kinetic energy are exchanged, and the liquid velocity increases at the expense of the local pressure decrease; Figure 1.10 shows the example of the venturi.[62], [64]

[34]

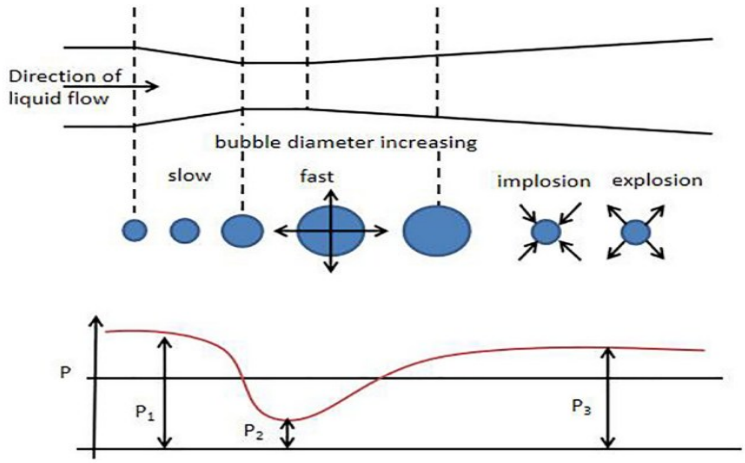


Figure 17: Venturi Tube - Hydrodynamic Cavitation

(P1/P3 static pressure before/after the throat, P2-static pressure in the throat, P vapor pressure of the liquid [113]

In the treatment of textile wastewater, hydrodynamic cavitation (produced by pressure variation in a flowing liquid caused by velocity variation in the system) is used compared to acoustic cavitation, whose reactors have low scale-up potential

and lower energy efficiency [164] The effectiveness of hydrodynamic cavitation in degrading organic pollutants depends greatly on various operating conditions such as the inlet pressure of the orifice (cavitation device), the cavitation number, the orifice hole size, and the physicochemical properties of the liquid. For this reason, experiments are conducted at different operating pressures to optimize the cavitation device to achieve maximum degradation [165] The extreme conditions induced by hydrodynamic cavitation lead to the formation of radicals and · OH from the decomposition of water vapor, as shown in the reaction below, and non-condensable gases within the cavities [166]

$$H_2O \overset{HC}{\rightarrow} \cdot OH + H \cdot \qquad \textit{Equation 24}$$

$$2 \cdot OH + H \cdot \rightarrow H_2O_2 \qquad \textit{Equation 25}$$

These species can produce the oxidation of dissolved pollutants. Although hydrodynamic cavitation has shown good applicability for wastewater treatment, the degradation of complex pollutants using only HC is difficult due to insufficient oxidation capacity. For this reason, innovative treatment studies have been conducted to increase treatment efficiency by using hydrodynamic cavitation in combination with other oxidants such as ozone, Fenton reagent, and hydrogen peroxide. In any combination, it is important to optimize the conditions, particularly the load of chemical oxidants. Below are some examples of combining hydrodynamic cavitation with oxidizing agents:[167]

4.5.6.1 HC + H_2O_2

Hydrogen peroxide mainly acts as an additional source of hydroxyl radicals as it undergoes dissociation under cavitation conditions. The combination of HC with H_2O_2 increases the amount of hydroxyl radicals generated due to dissociation induced by extreme temperature conditions, ultimately intensifying degradation. However, any excess H_2O_2 can also react with free radicals as represented in Eq 26 and make them unavailable for the main degradation reaction.[168]

$$H_2O_2 + \cdot OH \rightarrow HO_2 + H_2O \quad \textit{Equation 26}$$

It can therefore be stated that as H_2O_2 loads increase, degradation would be favored only up to an optimal value beyond which the beneficial effects of adding extra

oxidant would not be observed. A study in the literature observed the COD degradation efficiency of the effluent as a function of the molar concentration of H_2O_2, varying it from 0.1M to 0.9M (the molar ratio between H_2O_2 and COD varied from 1:6.5 to 1:0.72); Figure 1.11 shows how, beyond the optimal value of 0.7M, the COD degradation yield decreases because the residual excess of H_2O_2 reacts with the generated hydroxyl radicals and reduces the availability of radicals for oxidation, resulting in a lower COD reduction for an increase in H_2O_2 load beyond the optimal[72]

4.5.6.2HC + O_3

Ozonation, despite being promising, has some shortcomings: non-selective reaction of pollutant oxidation, which slows down most reactions; formation of intermediate products; low and unstable solubility of ozone in water, which limits the mass transfer process and reduces ozone utilization. The synergistic effect of hydrodynamic cavitation and ozone can alleviate many of the problems of the ozonation process, such as ozone selectivity and low solubility in water. The mechanical effect of cavitation creates turbulence that effectively eliminates mass transfer resistance between ozone and the liquid and increases ozone solubility, reducing the amount of ozone required by about one-third to half to lower costs and treatment requirements. Additionally, the chemical effect of cavitation substantially increases the yield of hydroxyl radicals and provides an alternative oxidation mechanism: pyrolysis, which produces substances with a high redox potential to react with pollutants and increases contaminant removal. The reactions that occur are summarized as follows[113]

$$O_3 \overset{HC}{\rightarrow} O_2 + O(^3P) \qquad \textit{Equation 27}$$

$$H_2O \overset{HC}{\rightarrow} \cdot H + \cdot OH \qquad \textit{Equation 28}$$

$$O(^3P) + H_2O \rightarrow 2 \cdot OH \qquad \textit{Equation 29}$$

$$Pollutant + \cdot OH \rightarrow Oxidations\ products \qquad \textit{Equation 30}$$

$$Pollutant + O_3 \rightarrow Oxidations\ products \qquad \textit{Equation 31}$$

4.5.6.3 PHOTOCHEMISTRY OF AQUEOUS PAHS

The interaction of PAHs with light in water has received significant attention. This occurs through two main processes:

Direct Photolysis: PAHs absorb light directly, causing their transformation or breakdown. This process is straightforward when the absorption spectrum and quantum yield are known[169]

Indirect Photolysis: Light is absorbed by photosensitizers like humic substances, flavins, PAHs themselves, and mineral surfaces. These produce reactive species such as singlet oxygen, which can transform PAHs [170]

PAHs in water can absorb solar radiation, especially around 313 and 366 nm, facilitating their degradation [171] Photo transformation by singlet oxygen forms oxygenated products like diones and endoperoxides, often more biodegradable than PAHs, affecting high-molecular-weight [172]

Natural degradation of organic compounds by solar radiation exceeds released pollutants in many regions. UV photolysis treats water with PAHs, using low-pressure mercury lamps for chlorinated aromatics and hazardous substances, and medium to high-pressure mercury lamps for various pollutants[173]

Understanding PAH photochemistry in water shows sunlight and UV radiation's role in degradation, aiding PAH-contaminated water remediation.

Photochemical processes begin when a molecule absorbs a photon. The functional groups that absorb photons are called chromophores, which include double bonds, carbonyls, and aromatic systems [174]

When organic molecules absorb light, they are converted to an electronically excited state, meaning the molecule attains a higher potential energy than its ground state. The absorption ranges for some chromophores are as follows:

- Simple alkene: 190-200 nm
- Acyclic diene: 220-250 nm
- Cyclic diene: 250-270 nm

- Styrene: 270-300 nm
- Saturated ketones: 270-280 nm
- α, β-Unsaturated ketones: 310-330 nm
- Aromatic ketones/aldehydes: 280-300 nm
- Aromatic compounds: 250-280 nm

When a molecule absorbs radiation, several outcomes are possible:

1. **Vibronic relaxation:** The molecule quickly reaches the new energy minimum structure for the excited state, releasing energy into the solvent.
2. **Intersystem crossing:** The molecule transitions to triplet states by spin inversion, reaching a new energy minimum through vibrational relaxation.
3. **Emission of light:** The molecule returns to the ground state, emitting light (e.g., fluorescence, phosphorescence).
4. **Quenching of the excited state:** Energy is transferred to another molecule.
5. **Radiationless deactivation:** The molecule returns to the ground state through vibrational (thermal) deactivation without light emission, transferring energy to the solvent or environment.
6. **Photochemical reaction:** A chemical reaction occurs as a result of the absorbed energy [172], [175]

Photochemical reactions are significant in the environmental fate of PAHs. Direct photolysis can lead to the breakdown of PAHs when they absorb sunlight, particularly UV radiation. This process is influenced by factors such as the intensity of sunlight, the presence of other substances that can act as photosensitizers, and the specific properties of the PAHs involved.

Indirect photolysis involves the interaction of PAHs with reactive species generated by photosensitizers. These reactive species, such as singlet oxygen, can further degrade PAHs into more biodegradable forms. This process is crucial in natural waters where sunlight and photosensitizers like humic substances are present.[172]

The efficiency of photodegradation varies among different PAHs. For instance, PAHs with more aromatic rings tend to be more resistant to photodegradation due to their stable structure. However, once they are broken down, the resulting products are often more susceptible to further degradation by other environmental processes.[176], [177]

In addition to natural photodegradation, artificial UV photolysis is used in water treatment to remove PAHs and other hazardous substances. This method involves using UV lamps to irradiate contaminated water, promoting the breakdown of pollutants. Combined oxidation processes, such as H_2O_2/UV and O_3/UV, enhance the effectiveness of UV photolysis by generating additional reactive species that aid in the degradation of PAHs.

Overall, photochemical processes play a vital role in the transformation and removal of PAHs from the environment, contributing to the reduction of their persistence and toxicity.[175], [177]

5. MATERIALS AND METHODS

5.1 MATERIALS AND METHODS

This section provides a brief overview of the chemicals, equipment, and analytical procedures used in the study.

5.2 CAVITATION SYSTEM

5.2.1 CHEMICALS

The studies conducted on the treatment of textile and winery wastewater, as well as the degradation of dyes, a consistent set of chemicals was utilized to facilitate the advanced oxidation processes and Fenton reactions. Chemicals including heptahydrate iron sulfate, sulfuric acid (95–97% p.a.), and sulfuric acid (wt.%), were used to adjust the pH of the solution. Methylene blue (MB; C16H18N3ClS; molecular weight:319.85 $g \cdot mol^{-1}$) were procured from sigma Aldrich. Hydrogen peroxide (30%) and sodium hydroxide were sourced from Panreac and EKA, respectively. Their application across various experimental setups aimed to optimize the degradation of organic pollutants and achieve significant reductions in chemical oxygen demand (COD). By employing these chemicals, the studies ensured consistency and comparability in the treatment processes, ultimately enhancing the efficiency and effectiveness of wastewater treatment.

5.2.2 EXPERIMENTAL SETUP AND PROCEDURE

The schematic diagram of the HC reactor setup used in this study is shown in Figure 19A Venturi is the cavitation device. The reactor configuration and Venturi details were previously reported in our previous research.[168] All experiments were carried out with a fixed effluent volume of 1 L. The temperature of the solution (T = 20°C) was maintained constantly by circulating cooling water through the jacket.

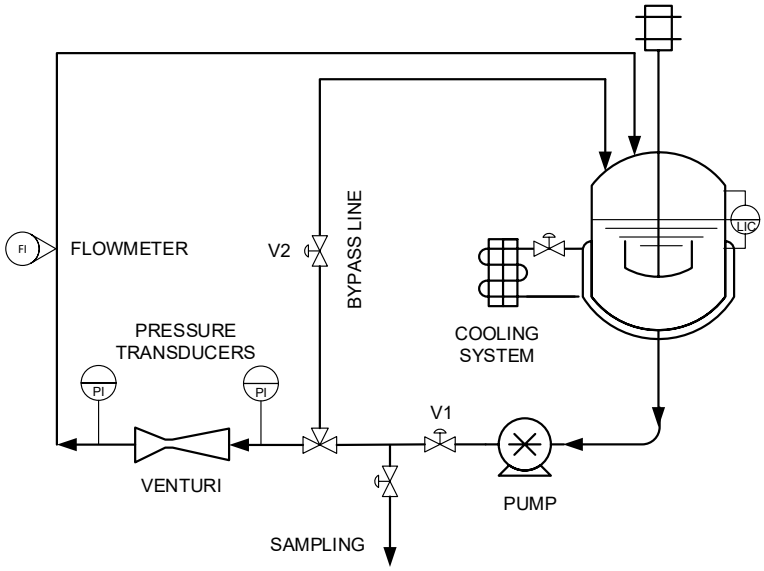


Figure 18:Lab-scale experimental apparatus.

All the experiments were performed at 0.45 MPa as the optimum operating pressure for HC, as established in earlier work[14]. Periodically, samples were collected at the bottom of the holding tank to check the extent of COD reduction. All the experiments were performed at the pH of the effluent (pH of 2). As per the literature review, the degradation of various organic pollutants is favored at an acidic condition; hence, no pH adjustments were made [14] Typically, the acidic condition is favorable for the generation of hydroxyl radicals and restraining the recombination of hydroxyl radicals into hydrogen peroxide [178]. For better process efficiency, experiments were performed using hydrogen peroxide and ozone along with HC to evaluate the effect of a combined process: HC + H_2O_2, HC + O_3, and HC + H_2O_2 + O_3. A commercial ozonator (Triogen LAB2B, power: 230V-1PH-50HZ) supplied ozone with a capacity of 180 watts. The sparger of the ozone layer was fixed in the feed tank. Hydrogen peroxide (H_2O_2 30% wt.) was purchased from VWR Chemicals International.

5.2.2.1 DYE REMOVAL FROM AQUEOUS SOLUTION

The experimental plan consists of three sections: hydrodynamic cavitation (HC) experiments, oxidation process only with ozone (Ozone experiments), and the hybrid process: HC + ozone (Hybrid process: HC + Ozone). The HC experiments focused on the effect of inlet pressure on dye degradation, with an initial solution concentration of 5 mg/L at pH 2 and a treatment time of 60 minutes. The decolorization yield was analyzed by varying the initial solution concentration and pH while maintaining the pressure and pH. The ozone experiments were divided into two sets, varying the effect of ozone flow and pH on dye degradation. The hybrid process was then studied, analyzing decolorization yields as a function of initial solution concentration and pH. The degradation process was repeated under the same conditions, combining hydrodynamic cavitation applied at the optimum pressure. The results of these experiments provide valuable insights into the optimal treatment conditions for dye degradation.

5.2.2.2 Textile wastewater treatment

The first experiment was conducted with hydrogen peroxide only, varying its concentration (0.1-0.9 mol/L). The second experiment was conducted with ozone alone with a feeding rate of 7.5mg/L to investigate the effect of ozone on color degradation and COD reduction. In the last experiments, the HC has been tested under fixed conditions of pressure and peroxide concentration (P=4.5 bar, pH=2, 0.3 mol/L of H_2O_2 and 7.5 mg/L of ozone). The optimal O_3 feeding rate was according to a previous study by the same research group [168], and the concentration of peroxide was fixed at the optimal value of 0.3 M. For all the experiments with H_2O_2, with or without HC, the main parameter used to evaluate the effectiveness of the process was the chemical oxygen demand (COD) of the samples measured before and after the treatment.

Ozone Generating Module: An ozone generating module (Triogen LAB2B, power: 230V-1PH-50HZ) was fed with dry air input of 4-10 L/min. The maximum ozone output was 4 gm/h. The Triogen LAB2B consists of a ceramic dielectric with 316 stainless steel electrodes within an aluminum-finned outer heatsink housing. The module end caps are manufactured from PTFE with stainless steel tubing connectors to PVDF

External inlet/outlet connectors. The shrouded housing has thermostatic protection to stop ozone production if the module temperature rises due to the failure of the cooling fan.

5.2.2.3 Winery wastewater treatment

The Fenton oxidation process was conducted under the following conditions: at room temperature and pH 3.5, utilizing 40 mL reactors agitated in an orbital shaker (Heidolph–Reax 20 shaker at 16 rpm). The pH of the effluent was adjusted to 3 using H2SO4 solution. Once a specific dose of iron ($FeSO_4 \cdot 7H_2O$) was added, the reaction commenced upon the introduction of H_2O_2 into the system. Sodium hydroxide was introduced after 1 hour of reaction to terminate the process, facilitating the precipitation of iron hydroxides and the depletion of residual H_2O_2. After 2 hours of treatment, 5 mL of sample was taken to analyse the COD and, subsequently, 20% calcium hydroxide was added to raise the pH between 7 and 8, obtaining precipitation of the iron. The mixture was subsequently filtered using a vacuum pump and the filtrate was analyzed.

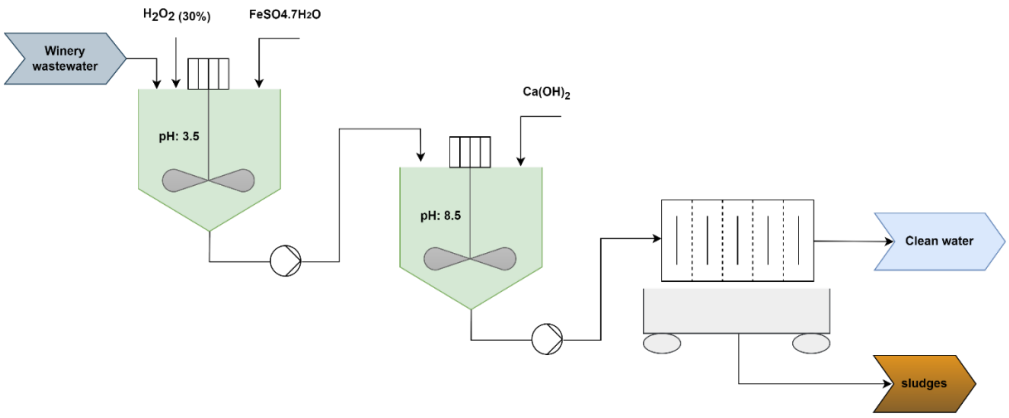


Figure 19:Process flowsheet diagram for winery wastewater treatment.

The table below provides a comprehensive summary of the materials, experimental apparatus, and conditions used in three different studies focused on treating various types of wastewaters. In the study titled "Application of Hybrid Oxidative Processes Based on Cavitation for the Treatment of Methyl Blue Solutions," the researchers utilized materials such as Methylene Blue, sodium hydroxide, sulfuric acid, and distilled water. The experimental setup included a hydrodynamic cavitation system

and an ozone generating module. The experimental conditions involved varying inlet pressures (0.81 to 5.5 bar), initial dye concentrations (5 to 25 mg/L), and solution pH (2 to 8). The ozone process evaluated flow rates (7 to 8.2 mg/L) and the effect of pH on dye degradation. The hybrid process combined hydrodynamic cavitation with ozone, testing initial dye concentrations (10 to 100 mg/L).

The second study, "Water Reuse in the Textile Industry with Membranes and Advanced Oxidation Processes," focused on treating textile wastewater using chemicals for pH adjustment and advanced oxidation processes (AOPs). The experimental apparatus included a membrane filtration system (ultrafiltration and reverse osmosis) and AOPs (ozone, hydrogen peroxide, and UV radiation). The conditions involved ultrafiltration to remove suspended solids, reverse osmosis for further purification, and the application of ozone and hydrogen peroxide with UV radiation to oxidize organic pollutants. The hybrid process combined membrane filtration with AOPs to enhance treatment efficiency.

The study on textile wastewater treatment explores the integration of hydrodynamic cavitation (HC) with advanced oxidation processes (AOPs) to treat real textile dye effluent. Conducted using a lab-scale apparatus with a Venturi tube, the experiments tested various combined processes, including HC/H_2O_2, HC/O_3, HC/O_3//H_2O_2, and O_3/H_2O_2. The HC/O_3//H_2O_2 process achieved the highest COD reduction of 93%, followed by HC/H_2O_2 at 88%, H2O2 alone at 84%, HC/O_3 at 74%, and O_3 alone at 70%. The study highlights the significant synergetic effect of the HC/O_3//H_2O_2process and concludes that integrating HC with catalytic ozonation is a promising approach for treating textile wastewater, demonstrating both technical and economic feasibility for industrial applications.

In the study **"Enhancing Fenton Process Efficiency for Winery Wastewater Treatment,"** the materials used included heptahydrate iron sulfate, sulfuric acid, hydrogen peroxide, and sodium hydroxide. The experimental setup comprised 40 mL reactors, an orbital shaker, and analytical instruments such as a spectrophotometer, TOC and COD analyzers, and a vacuum pump. The experimental conditions were set at room temperature with a pH of 3.5 and a reaction period of 1 hour. The hydrogen peroxide process involved adjusting the pH using sulfuric acid, adding iron sulfate followed by hydrogen peroxide,

and terminating the reaction with sodium hydroxide. The hybrid process combined cavitation with hydrogen peroxide, evaluating the impact of the $[H_2O_2]/[Fe^{2+}]$ ratio and hydrogen peroxide concentration on the Fenton process efficiency.

This summary encapsulates the diverse methodologies and conditions employed in these studies to optimize wastewater treatment processes, highlighting the innovative approaches and combinations of techniques used to achieve efficient pollutant degradation.

Table 16:Table Summary of Experimental Conditions for Treating Wastewaters

Study	Materials	Experimental Apparatus	pH0	Iron source	[Fe]0 (mg dm-3)	[H2O2]0 (mg dm-3)	Pressure (bar)	Ozone flow rate(g/L)
Treatment of Methyl blue	Methylblue (MB)	HC SYSTEM	2-8	-	0	0	0.85-5.5	-
	Sodium hydroxide (NaOH)	Ozone Generating Module	2-8	-	0	0		7.5-8
	Sulfuric acid (H_2SO_4)	HC+ozone	2-8	-	0	0	0.85-5.5	7.5-8
water reuse in the Textile Industry with Membranes and Advanced Oxidation Processes	- Textile Wastewater Sulfuric acid (H_2SO_4)	Advanced Oxidation Processes (O_3, H_2O_2, UV)	2-8					
Application of Ozone and Hydrogen Peroxide Coupled with Hydrodynamic Cavitation for Real Textile Industrial Water Treatment	Real textile dye effluent	HC System, Venturi tube, Ozone Generating Module, H_2O_2	2	-	[0.3-0.9]	4.5		7.5
Enhancing Fenton Process Efficiency for Winery Wastewater Treatment		- reactors		[Fe(C2O4)3]$^{3-}$				
		Winerywastewater	6.5-7	[Fe(C2O4)3]$^{3-}$		0.03-0.5		
		TOC and COD analyzers		-				

5.2.3 ANALYTICAL PROCEDURE

The UV-VIS spectrophotometer (Cary 1E, UV Visible spectrophotometer Varian) was used to analyze the color of the effluents before and after treatments. The total organic carbon (TOC) and the chemical oxygen demand (COD) were determined using the TOC and COD analyzer. The COD analysis, and TOC were test cuvettes (HACH LCK114 and

LCK381, respectively). Total solids (TSS) were determined by drying the effluent sample in an oven at 104 degrees Celsius (UF160) for 24 h.

The spectrophotometric methods based on cuvette for determining ammonium and nitrate chloride in real textile wastewater were assessed. The methods are based on detecting the 340 to 900 nm wavelength range in ready-to-use cuvettes (bar-coded reagent cuvettes).



Figure 20:Spectrophotometer used for the evaluation of chlorides, phenols, and sulfates

The experiments have been performed for a maximum treatment time of 60 min, sampling every 10 min for the wastewater analysis.

The decolorization value (ΔAbs) was calculated by Eq. (32)

$$Degradation\ rate\ [\%\ ] = \left(\frac{Abs_0 - Abs}{Abs_o}\right) \times 100 \qquad Equation\ 32$$

In Eq. (32), Abs_0 and Abs correspond to the values before and after the treatment processes, at the λ_{max}, respectively. In Eq. (33), COD_{in} and COD_{out} correspond to the Chemical Oxygen Demand values before and after treatment processes, respectively.[176]

$$COD\ reduction\ [\%] = \left(\frac{COD_{in} - COD_{out}}{COD_{in}}\right) \times 100 \qquad Equation\ 33$$

5.3 FENTON AND SOLAR PHOTO-FENTON SYSTEM

5.3.1 CHEMICALS

The pollutants, anthracene (ANT, $C_{14}H_{10}$; 178.23 g mol^{-1}) and benzo[a]pyrene (BaP, $C_{20}H_{12}$; 252.31 g mol^{-1}), were sourced from Sigma-Aldrich. Sodium dodecyl sulfate (SDS, 90%), also provided by Sigma Aldrich, was used as a surfactant. Hydrogen peroxide (H_2O_2, 35%) from Thermo Scientific served as the oxidant. Sodium oxalate monohydrate (99.5%) and iron (III) sulfate hydrate (97%), both from Sigma Aldrich, were used to formulate the ferrioxalate complex. Iron (II) sulfate heptahydrate from Thermo Scientific and sulfuric acid (H_2SO_4, 98%) from Sigma Aldrich were employed in the Fenton tests. Titanium (IV) oxysulfate solution, obtained from Sigma Aldrich, was used to quantify H_2O_2. Phenanthroline, acetic acid, ammonium acetate, and L-ascorbic acid, all from Sigma Aldrich, were used for total iron determination. Sodium tetraborate, methylene blue solution, phenolphthalein (Sigma Aldrich), and chloroform (VWR) were used for SDS quantification. HPLC-grade acetonitrile (Fisher) and phosphoric acid (Sigma-Aldrich) were used as mobile phase in HPLC determinations. All stock solutions were prepared using high-purity water from a Millipore Direct-Q system (resistivity>18 MΩ cm at 25 ºC). [179]

5.3.2 EXPERIMENTAL SETUP AND PROCEDURE

The synthetic emulsion was treated using Fenton and photo-Fenton processes. Fenton experiments were conducted in batch mode using a 500 ml amber reagent glass bottle to minimize the influence of light exposure and immersed in a bath for temperature control. A solar light simulator with a cylindrical borosilicate glass flat-plate reactor with external recycling (360 mL, 10 cm length) was used for solar photo-Fenton experiments[157] Fig22The reactor featured a quartz window to ensure effective UV-Vis radiation transmission. The light source was an Oriel 67005 solar simulator, equipped with an air mass filter (AM 1.5 G, ASTM E 892 standard) and a liquid attenuation filter (Water Optical Filter, 1.5 Inch Series) provided by Newport Corp. The experimental conditions were set at 240 W of light intensity and 10 cm between the light source and the reactor, simulating the average

solar radiation in Madrid (40˚30′ N, 3˚40′ E, Spain) on a clear September day. The spectrum of the simulated solar light irradiated through the reactor quartz window is shown in , Figure 23The emulsion (2 L), containing contaminants, catalyst and oxidant, was recirculated (30 L h^{-1}) using a liquid pump (NF 300 KT, Liquiport). A circulating-thermostatic system (Temperature controller, PolyScience) maintained a consistent temperature throughout the reaction.[127]

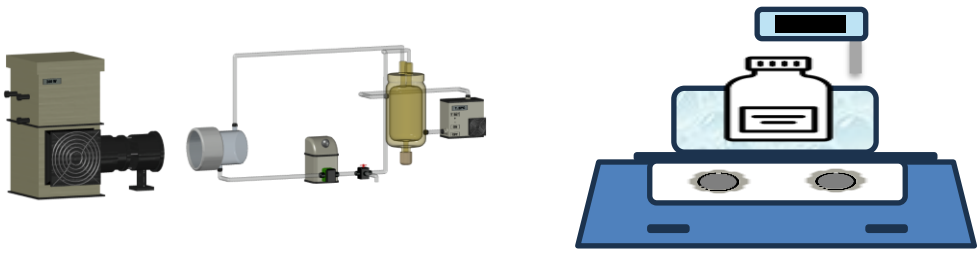


Figure 21: Scheme of the experimental set-up Fenton and Solar photo-Fenton.

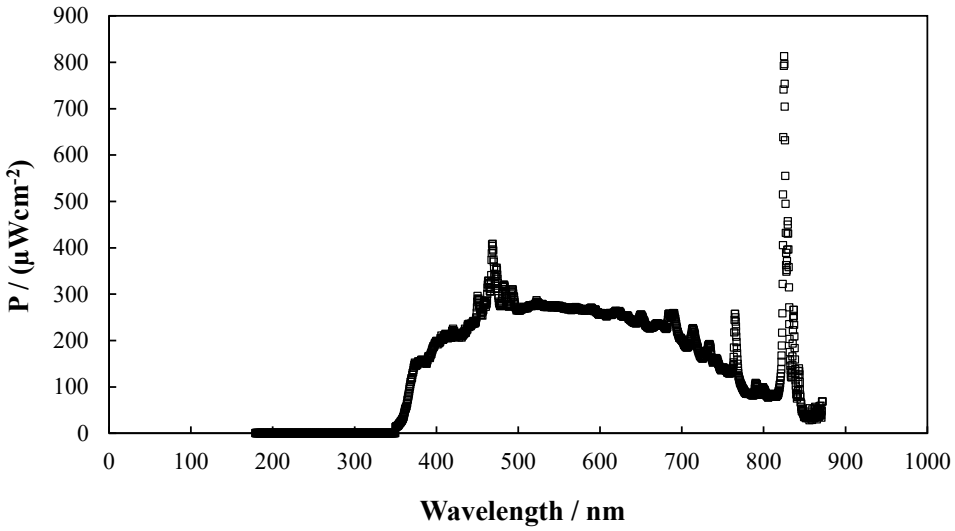


Figure 22:Simulated solar light received in the reactor

The oxidation experiments, including both Fenton and photo-Fenton tests, were performed by sequentially adding the synthetic emulsion, the catalyst, and the oxidant to the reactor. The study examined the effects of hydrogen peroxide concentrations (ranging from 60 to 240 mg dm^{-3}) and catalyst concentrations (ranging from 2.5 to 10 mg dm^{-3}) in both systems, along with control experiments.

Hydrogen peroxide concentrations were based on the conservative assumption that one mole of hydroxyl radicals is generated per mole of H_2O_2. For complete mineralization of 5 mg dm^{-3} of BaP and ANT to water and carbon dioxide, the required H_2O_2 concentrations were calculated to be 60.63 and 63.03 mg dm^{-3}, respectively. Three levels of H_2O_2 concentration were tested: stoichiometric (120 mg dm^{-3}), double (240 mg dm^{-3}), and half (60 mg dm^{-3}) to assess their impact. These concentrations are much lower than those used in direct Fenton treatment of PAH-contaminated soils, thus reducing reaction severity and costs.

The iron concentrations were selected based on the Spanish government's environmental discharge limits (10 mg dm^{-3}), using 10, 5, and 2.5 mg dm^{-3}. In Fenton tests (pH 3), ferrous iron dissolved in acidified water (H_2SO_4) was used as a catalyst, while in photo-Fenton tests (pH 6.5-7), a ferrioxalate complex was used. An oxalate/iron molar ratio of 10:1 ensured complete iron solubilization in the emulsion.

Experiments were conducted for 360 minutes at room temperature in triplicate, with deviations of less than 5%. The experimental conditions are summarized in Table 17

Table 17:Experimental conditions for treating contaminated emulsions (4500 mg dm^{-3} of SDS and 5 mg dm^{-3} of BaP and ANT).

Exp. (E)	Test	Light source	pH_0	Iron source	$[Fe]_0$ (mg dm^{-3})	$[H_2O_2]_0$ (mg dm^{-3})
1	Control	-	6.5-7	-	0	0
2	Control	-	6.5-7	-	0	120
3	Control	-	3	$FeSO_4$	5	0
4					5	60
5	Fenton	-	3	$FeSO_4$	5	120
6					5	240
7					2.5	120
5	Fenton	-	3	$FeSO_4$	5	120
8					10	120
9	Control	-		$[Fe(C_2O_4)_3]^{3-}$	5	0
10	Control	-	6.5-7	$[Fe(C_2O_4)_3]^{3-}$	5	120
11	Control	Solar		-	0	0
12					5	60
13	Photo-Fenton	Solar	6.5-7	$[Fe(C_2O_4)_3]^{3-}$	5	120
14					5	240
15					2.5	120
13	Photo-Fenton	Solar	6.5-7	$[Fe(C_2O_4)_3]^{3-}$	5	120
16					10	120

5.3.3 ANALYTICAL PROCEDURE

A Shimadzu TOC-V analyzer with an image de l'**icône NFC**: infrared detector was used to quantify the soil total organic carbon (TOC) content. TC was measured through oxidative combustion at 714 ºC. Inorganic carbon (IC) was determined at 200 ºC after adding phosphoric acid (35%) to the soil sample. The concentration of metals in the soil was quantified using a microwave plasma atomic emission spectrometer (4100 MP-AES, Agilent). Following the EPA 3051A guidelines, soil samples were predigested in a microwave extraction system (Milestone Ethos One) using nitric acid (70%) and hydrochloric acid (37%). The oven conditions were set to increase the temperature at 32°C min^{-1} until reaching 175°C, which was then maintained for 4.5 min . Soil pH was determined using a Basic 20-CRISON pH electrode in a soil/water suspension (1:2).[180]

The concentration of PAHs in the soil (after extraction with methanol (V_L/W = 2 mL g^{-1}) 180 min US, 40ºC [39]) and in the emulsions (measured directly) were determined by HPLC, equipped with an Agilent 1100 series-coupled DAD detector and a Poroshell 120 EC-C18 2.7 µm (3.0 x 150 mm) column, at 40 ºC. The mobile phase (0.5 mL min^{-1}) consisted of acetonitrile (HPLC-grade) and 0.1% phosphoric

acid (60:40%, v:v). An injection volume of 20 µL was employed. A 250 nm and 300 nm wavelength were used for ANT and BaP determination, respectively. [114]

The concentration of H_2O_2 in the emulsions (and in the soil natural oxidant demand (NOD) determination) was quantified by measuring the concentration of the complex formed between H_2O_2 and Ti^{4+}, using titanium (IV) oxysulfate solution. The concentration of this complex was then analyzed spectrophotometrically at 410 nm . Total iron in the emulsions was measured following ISO 6332 guidelines. This colorimetric method involves adding 1 mL of 1,10-phenanthroline, 1 mL of acetic acid (7.32 g dm^{-3}), and ammonium acetate (250 g dm^{-3}) to 4 ml of the sample. The resulting solution was analyzed spectrophotometrically at 510 nm to quantify ferrous iron (Fe^{2+}). Ferric iron (Fe^{3+}) was subsequently determined at 510 nm by adding L-ascorbic acid . [181]

The concentration of inorganic ions in the emulsions was determined by ion chromatography (IC). Ions were measured using a Metrohm 930 Compact IC Flex connected to a conductivity detector and a Metrosep A Supp 5 250/4.0 column. The mobile phase (0.7 cm^3 min^{-1}) consisted of Na_2CO_3 (3.2 mM) and $NaHCO_3$ (1 mM). The injection volume was 20 µL. Conductivity and pH were measured using a HI991301 pH/EC/TDS Meter supplied by Hanna.[114]

SDS concentration was determined by a spectrophotometric method based on forming an ionic pair between the anionic surfactant and methylene blue . A buffer was prepared with 10 mM sodium tetraborate ($Na_2B_4O_7 \cdot 10H_2O_2$). First, 200 µL of the buffer was added to 5 ml of the SDS-containing sample. Then, 30 µL of methylene blue solution (0 – 2.5 mg dm^{-3}) and 50 µL of phenolphthalein were added to the buffer-SDS complex. After mixing for 5 min, the anionic surfactant–cationic dye complex was extracted with chloroform (4 mL), and the extract was measured at 650 nm (Spectroquant® Prove 300 UV/VIS Spectrophotometer, Merck Millipore).[114] The total Organic Carbon (TOC) of the emulsions was measured using a Shimadzu TOC-V analyzer by oxidative combustion at 714 ºC, coupled with a CO_2 infrared detector. The Critical Micelle Concentration (CMC) of the emulsions (before and after oxidation treatments) was determined using a Force Tensiometer (Tensíio KRÜSS WO04779).

In conclusion, the materials and methods employed for the treatment of hydrocarbons, winery effluents, and textile wastewater were meticulously designed to ensure effective and environmentally safe oxidation processes. By carefully selecting the concentrations of hydrogen peroxide and catalysts, and adhering to regulatory limits, the experiments were conducted under controlled conditions that balance efficiency and environmental safety.

6. EXPERIMETAL RESULTS

This section presents the findings from the experimental treatments conducted on various wastewater samples, including textile and winery effluents. The results are systematically categorized to provide a clear and comprehensive understanding of the outcomes.

Section 6.1 focuses on the results related to dyes and textiles treatments, further divided into dyes results (6.1.1) and textiles results (6.1.2). The experiments utilized advanced oxidation processes (AOPs) such as hydrodynamic cavitation (HC) combined with hydrogen peroxide (H_2O_2) and ozone (O_3). The optimal conditions for each treatment were determined, highlighting significant reductions in chemical oxygen demand (COD) and color.

Section 6.2 details the outcomes of winery wastewater treatments. The study evaluated the efficiency of the Fenton process, a widely used AOP, for reducing organic content in winery effluents. Using a three-level full-factorial design, the optimal conditions for COD removal were identified as $[H_2O_2]$ = 0.5 mol/L and $[H_2O_2]/[Fe^{2+}]$ = 2.5, achieving up to 85% COD reduction. The results underscore the potential of the Fenton process for industrial wastewater treatment, contributing to sustainable wastewater management.

Section 6.3 covers the results from hydrocarbons treatments, analyzing the effectiveness of different methods in breaking down hydrocarbons and assessing factors such as degradation rates and environmental impact.

Section 6.4 explores the potential for water reuse, focusing on the treatment and recycling of wastewater for industrial applications. The study highlights the benefits of integrating advanced oxidation processes with traditional treatment methods to achieve high-quality water suitable for reuse. The findings demonstrate significant reductions in contaminants, making the treated water viable for various industrial purposes, thereby promoting sustainability and reducing the environmental footprint.

Each section aims to elucidate the effectiveness and implications of the respective treatments, contributing valuable insights to the field. The comprehensive analysis provided in this chapter will serve as a foundation for further research and practical applications in the respective areas of study.

6.1 DYES AND TEXTILES TREATMENTS RESULTS

6.1.1 DYES RESULTS

The results and discussion section of this study provides a comprehensive analysis of the degradation of Methyl Blue (MB) dye using hydrodynamic cavitation (HC) and ozone (O_3) processes, both individually and in combination. This section aims to elucidate the effectiveness of these methods under various operational conditions, including different pressures, ozone dosages, pH levels, and initial dye concentrations.[182]

The experiments were designed to identify the optimal parameters for each process, ensuring maximum degradation efficiency. The findings are discussed in detail, highlighting the synergistic effects observed in the hybrid HC and O_3 process, which significantly enhances the degradation rates compared to the individual methods. Additionally, the energy consumption and cost-effectiveness of each process are evaluated to provide a practical perspective on their industrial applicability.

6.1.1.1 HC RESULTS

3.1.1. Effect of the inlet pressure

The oxidizing capacity of HC depends on inlet pressure and cavitation number (Cv) defined as follows:[183]

$$C_v = \frac{P_2 - P_v}{0.5\rho v_0^2} \quad \textit{Equation 34}$$

Where P2 is the pressure measured downstream of the Venturi tube (Pa), Pv is the vapor pressure of the aqueous solution (Pa), ρ is the aqueous solution density (kg/m3), and vo is the flow velocity (m/s). Cv is a dimensionless number used to describe cavitation conditions. Cavitation occurs when Cv ≤ 1 in the ideal conditions, but in some cases, it could also happen for values greater than 1, for example, when there are dissolved gases or suspended solids that act as cavitation nuclei. For our HC system, the Cv number is 0.5 – 0.27 for 0.3-0.6 bar, respectively. The details about Cv values are reported in a previous work [14].

The pressure effect was studied in the Pmin=0.81 bar to 5.5 bar to determine the optimum pressure. The results (Fig. 22) show an increase (from 4% to around 33%) in the degradation rate of MB as a function of the inlet pressure. Beyond 4.5 bar, a decrease in the degradation rate has been noticed, reaching about 17% and 21% at 5 and 5.5 bar, respectively. Thus, the pressure that will be considered an optimal parameter for the next series of experiments will be 4.5 bar. This trend is in line with what has been reported in the scientific literature; more in detail, the more pressure increases, the more significant number of radicals that are generated, but beyond the optimal pressure, the incomplete collapse occurs, followed by a decrease in degradation rate [184] . Using a single orifice, Patil and Gogate [4] studied the impact of inlet pressure in the operating range of 1–8 bar on the degradation of methyl parathion. It was found that at greater pressures, the rate of growth reduces from 1 bar to the ideal value of 4 bar. An increase in cavitational activity at higher operating pressures can be the cause of the observed rise in degradation as the pressure climbs from 1 to 3 bar. When operational pressures are raised, the cavity collapses more quickly and violently, producing a stronger pressure pulse.

Kumar et al. [185] investigated the degradation of methyl blue dye at various inlet pressures ranging from 1 to 10 bar. They reported that a decolorization of about 32% was observed at the optimal pressure of 5 bar. Similar observations have been noticed during this investigation as compared to earlier results. When the input pressure was increased beyond the optimal value, a reduction in the rate of degradation of MB dye was detected. Thus, the cavitation number increased linearly

with input pressure, demonstrating that cavity formation becomes easier as inlet pressure increases [45]. However, an undesirable consequence could be produced by the rapidity with which cavities form when inlet pressure monotonically increases, resulting in cavity clouds with much lower cavitational collapse intensity [186]. Figures 23-24 report the results of this series of experiments.

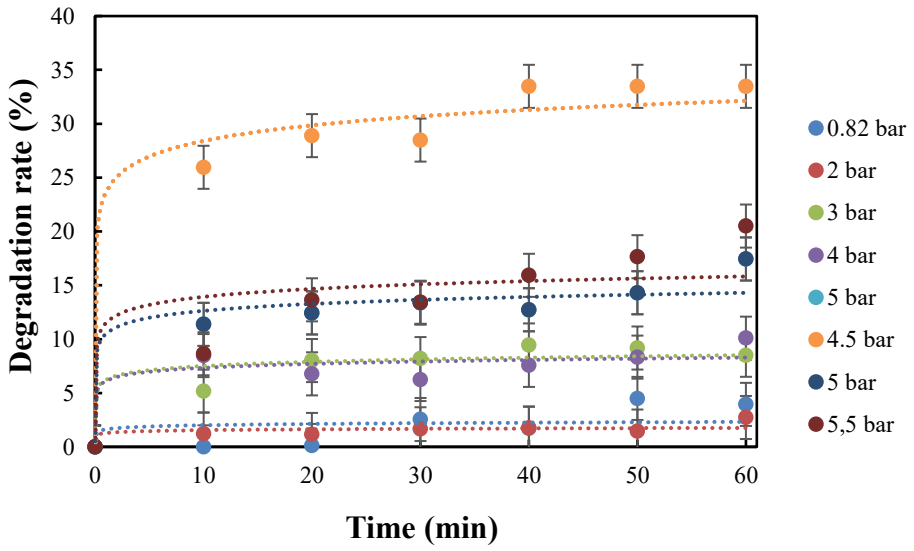


Figure23:Effect of the inlet pressure on MB decolorization (C0 = 5 mg/L, V = 1 L, pH = 2, T = 20°± 2°C)

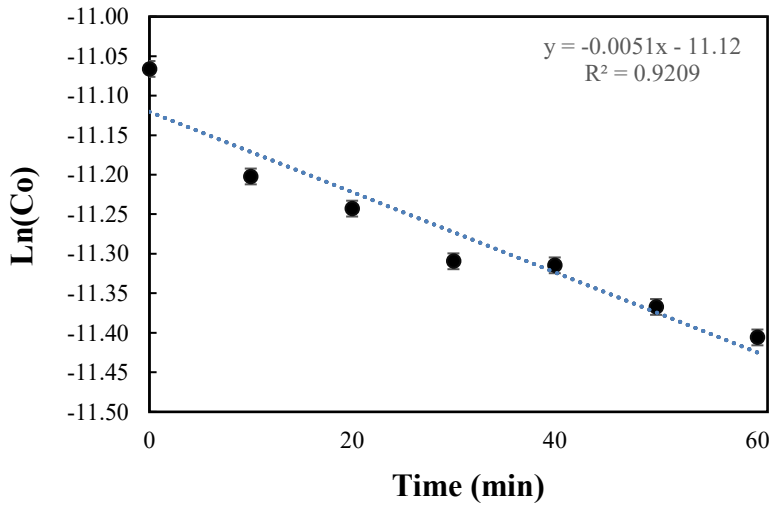


Figure 24: Kinetic analysis for the experiment conducted at 4.5 bar.

The data have been used to estimate the kinetic constants using the pseudo-first-order kinetic model, following the Eqs. (35) -(36)

$$-\ln\left(\frac{C_0}{C_t}\right) = kt \qquad \textit{Equation 35}$$

$$C = C_o\ exp[-kt] \qquad \textit{Equation 36}$$

$$lnC = -kt + \ln C_o \qquad \textit{Equation 37}$$

where C (mol/L) is the concentration of MB, t is time, and k is the kinetic constant.

Fig. 23shows the kinetic analysis for the experimental test performed at 4.5 bar. The data fitted through Eq. (35) and the slope described the kinetic constant. The same study has also been conducted for the other experiments. The minimum kinetic constant rate obtained at 0.82 bar was 0.0009 min-1, and the maximum at 4.5 bar was equal to 0.005 min-1. The degradation yields were compared with the results obtained in a previous campaign of tests [184], in which the degradation of another dye was studied, the methyl orange (Fig. 24).

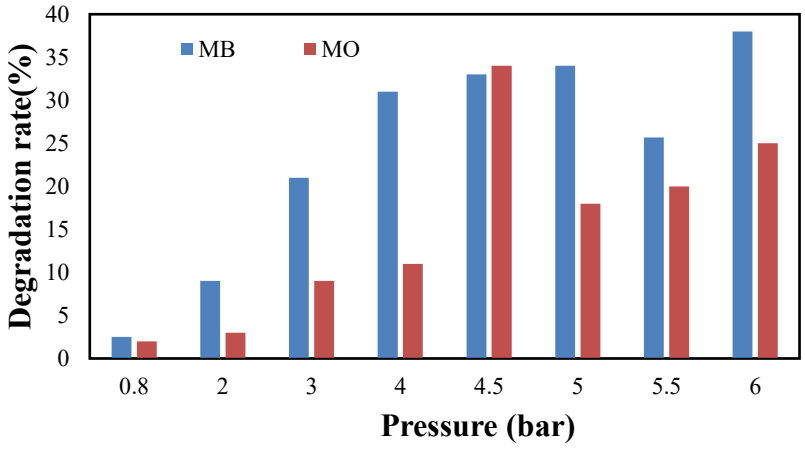


Figure 25:Comparison between methyl orange (MO) and methyl blue (MB).

It is possible to observe that the optimal inlet pressure to maximize the production of the radicals is 4-4.5 bar. It mainly depends on the geometrical structure of the Venturi tube; the difference in yields between the two dyes lies in the chemical structure, since methyl blue is more difficult to degrade with respect to methyl orange [14]. Effect of initial dye concentration

The concentration of the dye is an important parameter to be considered in the study. The experiments were performed with HC only at Poptimal =4.5 bar with a variation of MB concentration from 2.5 to 25 mg/L at pH=2 for one hour of treatment time, with sampling every 10 min. As a result, the degradation yield

decreased by increasing the initial concentration from 2.5 mg/L to 25 mg/L. This is since, above a specific concentration, considered as critical, the number of generated radicals is fixed with a higher substrate loading. In Fig 6, the experimental results of the decolorization tests showed that when the concentration increased from 2.5 mg/L to 25 mg/L, the degradation rate decreased from 56% to 2.5%.

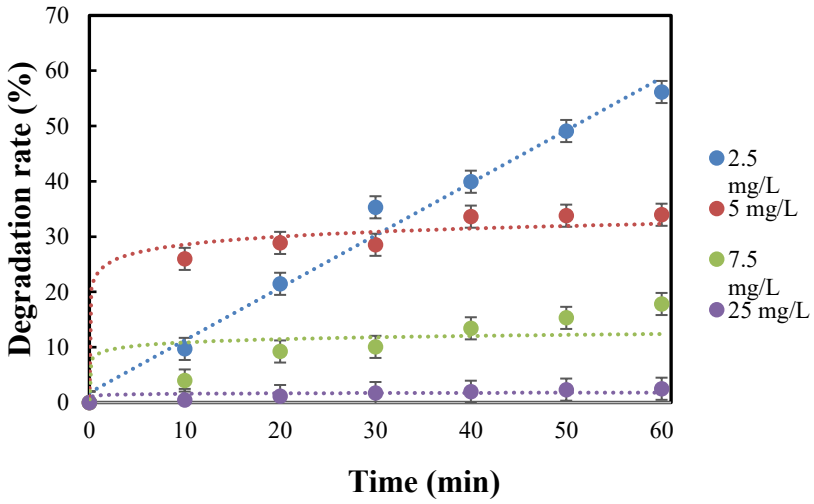


Figure 26: Effect of the initial solution concentration (in ppm) on the degradation of MB (Pin = 4.5 bar; V = 1 L; pH = 2; T = 20 ± 2 ℃)

6.1.1.2. OZONE EXPERIMENTAL RESULTS

6.1.1.2.1 EFFECT OF O3 DOSAGE

Ozone has a strong oxidation potential [187]. It has been reported that ozone could be an effective remediation for dye mineralization. Methyl blue decolorization tests carried out through ozonation were carried out by varying the O3 dosage at the levels 8.2 mg/L, 8 mg/L, 7.5 mg/L, 7 mg/L (4 L/min, 6L/min, 8L/min, 10 L/min, respectively) with C_0 equal to 10 mg/L at pH=2, to identify the optimal dosage of ozone under the investigated conditions.

The results obtained are reported and compared in Fig 26. For the initial O_3 concentration equal to 8.2 mg/L and 8 mg/L, the decolorization of MB obtained in 20 min was equal to 81% and 95%, respectively. For an amount of ozone equal to 7.5 mg/L, the degradation yield reached 99% in about 20 min.

In the case of an initial concentration of O_3 equal to 8.2 mg/L and 8 mg/L, a complete discoloration of the methyl blue was obtained in a time equal to 30

minutes. Thus, increasing the O_3 feed rate can reduce the treatment time. A dosage of 8 L/min of ozone was adopted for the subsequent experiments, as it resulted in the optimal flow value.

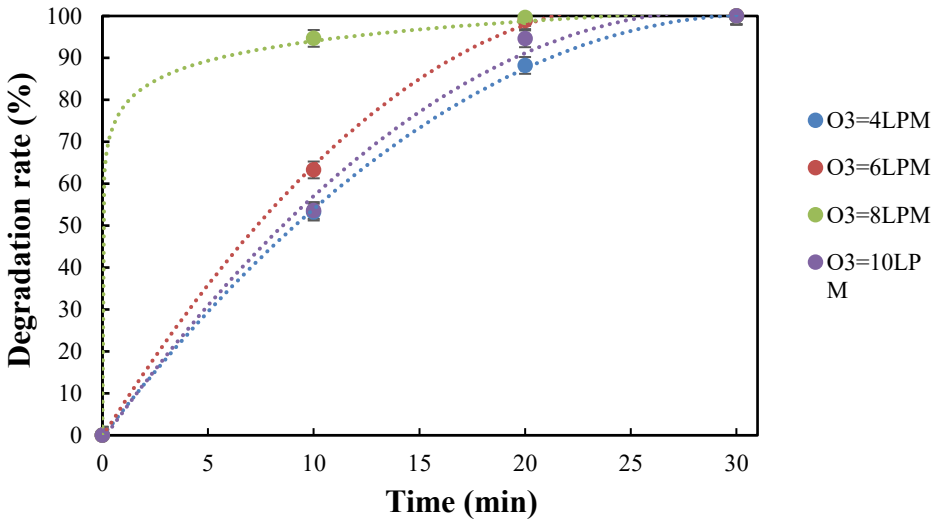


Figure 27:Effect of O3 dosage on the degradation of MB (C0=10mg/L; V = 1 L; pH = 2; T = 20 ± 2 ℃).

3.2.2 Effect of the initial pH

The pH is a conducting parameter in our experiments. The initial pH was studied in the range of 2-8 with 7.5 mg/L of O3 feeding rate at C0= 10 mg/L. Fig. 8 shows the effect of pH in the degradation, with the degradation rate that reached the maximum at pH=2. These results showed that an acidic medium is a favorable condition for degrading dyes [165]. This result has been reported by several authors and was explained by the fact that in the acidic medium, the dye molecule is in a molecular state with high hydrophobicity. The recombination of ·OH is prevented. Therefore, a high amount of hydroxyl radicals is generated, which enhances the degradation of dye. Wang et al[188] reported that the greater degradation rate under acidic circumstances is due to two factors: (I) under acidic conditions, the production of hydroxyl radicals (OH) in the HC system is more beneficial because it precludes ·OH recombination; at the same time, the oxidation potential of ·OH in acidic conditions is greater than that in alkaline ones. [168], [189] (II) the enhancement of degradation rate is mostly determined by whether the dye molecules are in the molecular or ionic states. In acidic solutions, MB tends to exist in the molecule

state. Because of the molecule's hydrophobicity, MB is mostly found near the gas-liquid interface between the cavity and water [190].

MB occurs in an ionic form in alkaline circumstances, then becomes hydrophilic and mostly exists in solution. Due to the short half-life, only about 10% of the generated ·OH diffuses into the main body of the solution. Based on these experimental results, the following experiments were carried out under the condition of solution pH = 2.0.

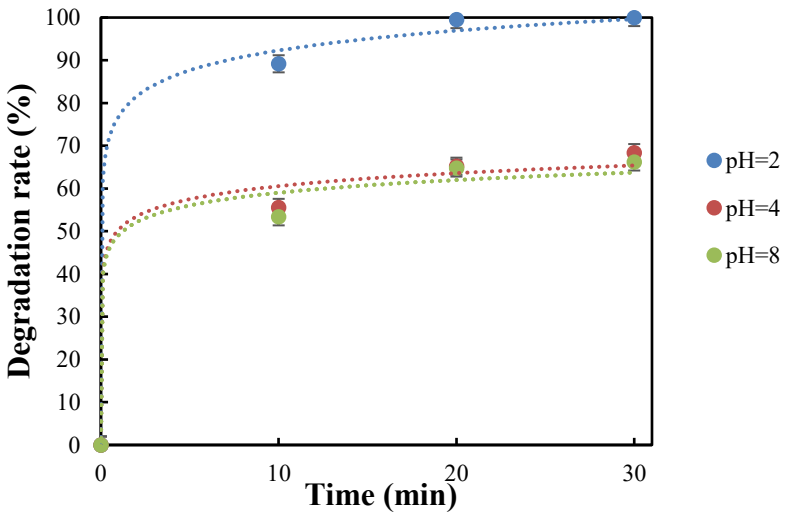


Figure 28:Effect of pH on the degradation of MB
(C0=10 mg/L; O3=8 LPM; V = 1 L; pH = 2; T = 20 ± 2 ℃)

The scope of the first series of experiments is to evaluate the efficiency of O3 alone at different initial solution concentrations before the combination with the hybrid process. In this current investigation, the feeding rate was equal to 8 L/min of ozone. The inlet pressure was fixed at 4.5 bar and the pH=2 while the concentration of MB was varied from 10 mg/L to 100 mg/L. The results are presented in Fig. 27. It can be seen that after 1h of treatment with O3 alone, the degradation rate reached 99.6% for an initial concentration of 25 mg/L. For the other concentrations, the rate varied between 99.3%, 85%, and 84.7% for 50, 75, and 100 mg/L, respectively. [168]

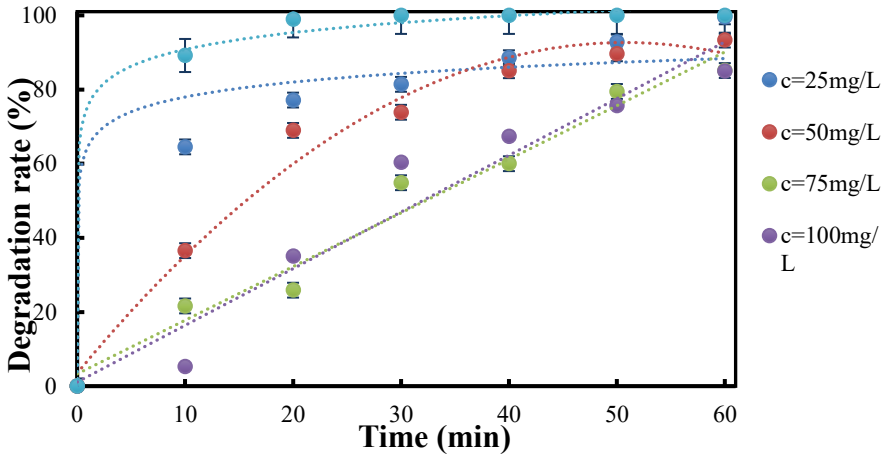


Figure 29: Effect of O_3 on the degradation of MB at high concentration (Pin=4.5 bar; O3=8 LPM; V = 1 L; pH = 2; T = 20± 2 ℃)

6.1.1.3 Factorial Plan

The experimental results were reorganized according to a factorial plan with three factors and multiple levels to identify the effect of the quantities studied in the various experiments. In particular, the following factors were dye concentration, factor A (10-50-100 ppm); time of treatment, factor B (10-30-60 min); and the type of treatment, factor C (only ozone- ozone/hydrodynamic cavitation). The degradation yields were used for the statistical analysis of the data. The significance of the factors and interactions was determined by the F-test method with 95% confidence levels. The third-order interaction was used to estimate the experimental error. Tables 19 20 summarizes the experimental data [14]

Table 18:Factorial plan and experimental results

	B – time					
	10	*min*	*30*	*min*	*60*	*Min*
	C - Treatment		*C - Treatment*		*C – Treatment*	
A, ppm	*O3*	*O3/HC*	*O3*	*O3/HC*	*O3*	*O3/HC*
10	*89.2*	*89.2*	*100*	*100*	*100*	*100*
50	*36.6*	*65*	*73.9*	*86.4*	*93.3*	*93.6*
100	*5.26*	*28.5*	*60.4*	*73*	*85*	*85.9*

Table 19: Analysis of the variance

	Sum Square (SS)	*Freedom degree (df)*	*Mean Square = SS/df*	*F value = MS/MSE*	*P value*	*Significance (%)*
A	*4823.49*	*2.00*	*2411.75*	*108.45*	*7.62E-05*	*99.99*
B	*5335.71*	*2.00*	*2667.85*	*119.96*	*5.95E-05*	*99.99*
AB	*1748.33*	*4.00*	*437.08*	*19.65*	*2.93E-03*	*99.71*
C	*337.48*	*1.00*	*337.48*	*15.17*	*1.15E-02*	*98.85*
AC	*170.40*	*2.00*	*85.20*	*3.83*	*9.80E-02*	*90.20*
BC	*212.21*	*2.00*	*106.10*	*4.77*	*6.93E-02*	*93.07*
	12627.61					
Err	*111.20*	*5.00*	*22.24*			
TOT		*18*				

The results of the ANOVA show that Factors A (dye concentration), B (time) and C (type of the treatment) influence the dye oxidation process. The AB interaction is also significant. Figure 29shows the graphs for the three effects and the AB interaction for practical interpretation of the experiment.

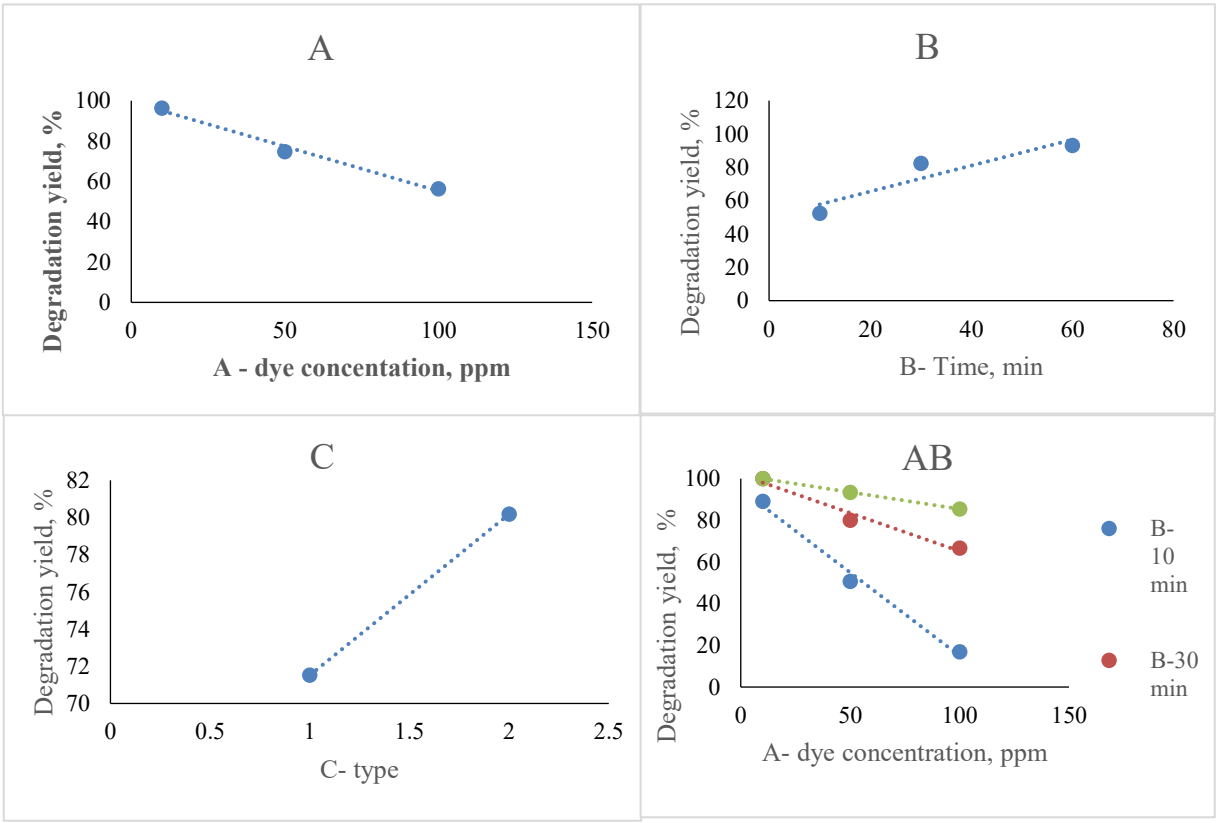


Figure 30: Main effect and interaction

It is possible to observe that the factors B (time) and C (type of the process) had a positive effect: an increase in the variable, in the specific case of the factor C, the use of the combined treatment O_3 and HC, shifts the mean deviation from the target toward the increase (thus increases the degradation yield). Instead, an increase in factor A (dye concentration) had a negative effect on the degradation process.

6.1.1.4HC COMBINED WITH O_3

Coupling ozone and hydrodynamic cavitation are beneficial in reducing the dose of O_3 and, subsequently, the operative costs[182]. Moreover, the secondary pollution problem is prevented by decomposing the residual ozone into oxygen . As a result, the generation of more hydroxyl radicals (·OH) and the enhancement of ozone dissolution in the effluent is achieved. Results obtained from O_3 treatment combined with HC are presented below (Fig. 11). The combined process results in a 30-minute degradation of 2-4% more than O3 alone and substantially better than HC alone. This can be explained by the increased synergistic effect that results from the interaction of HC and O_3. The HC improves the gas-liquid mass transport, which supports ozone's oxidation potential. As a result, MB achieves its maximum oxidation capacity [113], [191]. The optimization of HC in terms of inlet pressure and cavitation number and the combination with ozone could be an effective solution to reduce the treatment time on the one hand and save energy on the other hand. The degradation rate reaches 99% under the hybrid process.

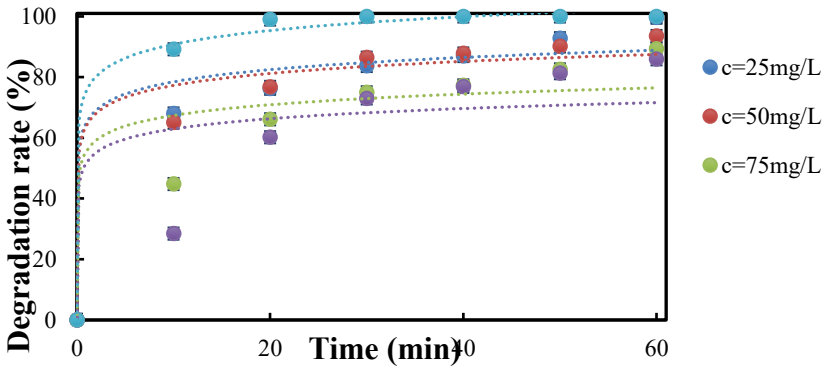


Figure 31: Effect of HC combined with O3 on the degradation of MB (Pin=4.5 bar; O3=8 LPM; V = 1L; pH = 2; T = 20± 2 ℃)

The result obtained in Fig.10 can be explained by the fact that the degradation rate constantly rose noticeably when HC and O_3 interacted as the amount of O_3 increased, indicating good synergy between O_3 and HC. There are two primary

causes. On the one hand, HC may promote gas-liquid mass transfer, bringing ozone into direct contact with organic contaminants. Ozone may efficiently oxidize MB contaminants due to its high oxidation potential of 2.08 V. On the other hand, the oxidative capacity of MB molecules is further increased by the decomposing of ozone into a more reactive form of ·OH when HC is present.

The synergist effect for the experiment HC and ozone for the experiment with 20 ppm of dye was 1.6. For other test experiments conducted for an initial solution concentration greater than 10 ppm, the degradation yields are near zero, so the effect was not calculated. A value greater than 1 confirms the positive impact of the combined process.

The work involves enhancing experimental technical factors such as inlet pressure, beginning concentration, pH, and combinations of HC with ozone, as well as exploring MB degradation at high concentrations. The following are the appropriate process parameters: 4.5 bar inlet pressure, initial pH = 2.0, and initial solution concentration = 10 mg/L. Table21 also provides a comparison of various studies relating to dye degradation employing HC in hybrid configuration, showing the specifics of the cavitation devices and the significant outcomes. [113]

Table 20: Comparison with other studies of MB Degradation using hydrodynamic cavitation.

Sr. No.	***Reference***	***Degradation method***	***Optimum conditions and operating parameter***	***Results***
1.	*Wang et al [35]*	*HC (orifice plate.) Ozone, $Na_2S_2O_8$.*	*1. Pressure=3 bar 2. pH = 2 3. Oxidant: O_3=012g/h 4. $Na_2S_2O_8$= 0.05g/l*	*decolorization in 60 min O_3 (0.12 g/h) =92.55% HC + O_3= (0.12 g/h) 99.3 % HC alone =21.8%*
2.	*Kumar et al. [28]*	*HC (circular venturi), hydrogen peroxide, photocatalysis (TiO2)*	*1. Pressure=5 bar 2. pH = 2 3. Oxidant: H_2O_2 = 1:20 4. TiO_2 = 200 mg/l*	*1. decolorization in 60 min HC=15.32% , H2O2=23.58%,, HC+H_2O_2=99.64%,HC=9.46%, HC+ H_2O_2=18.41%, HC + TiO2 =12.68% . 2. decolorization in 120 min. HC=32.32%, TiO_2 =26.52%, HC + TiO2 = 64.58%.*

6.1.1.5 Energy and cost estimation for MB degradation

From an industrial point of view, it is crucial to consider the costs of the process. The following compares different methods for treating solutions with varying concentrations of dyes [48]. More in detail, only the operative cost related to the energy consumption for the degradation of the 95% dye has been included. The time was calculated by using the following eq.38:

$$t95\% = 2.996 \; x \; k \qquad \textit{Equation 38}$$

where k is the kinetic constant of the degradation.

The energy consumption (kWh) was estimated by equation eq. 39:

$$E = \frac{P_E\,(kW) \; x \; t_{95\%} \;\; (h)}{treatment \; volume \; (m3)} \qquad \textit{Equation 39}$$

PE is the power consumed for the treatment.

Where PE for the HC experiments are equal to electrical consumption of the pump as in eq.40:

$$P_E = \frac{\Delta P \; (Pa) \cdot Q \; (\frac{m3}{s})}{\eta} \qquad \textit{Equation 40}$$

ΔP is the pressure drop, Q is the volumetric flow and η is the efficiency (for hypothesis of 50%).

For ozone experiments, the energy consumption was fixed to 105 Watts, as reported in the technical manual of the ozonizer. Table 22reports the results of this analysis. The energy cost has been estimated multiplied by the PE by the actual price in Italy (0.35 €/kWh). The highest cost is for the single process of hydrodynamic cavitation, which has long treatment times to reach 95% degradation. For example, treating 10 ppm of dye by cavitation alone takes nearly 28 hours of treatment time. The time and cost are greatly reduced by using ozone alone or the combined process.[59], [188]

Table 21:Energy consumption for the degradation of 95% of dye solutions

Dye concentration	*HC*	*Ozone (8 L/min)*	*HC and ozone*	*Cost for energy (€)*	*Cavitation yield (mg of dye degraded/J) **
10 ppm	*Yes*	*No*	*No*	*620*	*9.57E-06*
10 ppm	*No*	*Yes*	*No*	*6*	*1.75E-05*
10 ppm	*Yes*	*Yes*	*Yes*	*20*	*1.90E-05*
25 ppm	*-*	*Yes*	*No*	*50*	*1.04E-04*
25 ppm	*-*	*No*	*Yes*	*50*	*6.63E-05*
50 ppm	*-*	*Yes*	*No*	*49*	*1.15E-04*
50 ppm	*-*	*No*	*Yes*	*87*	*8.34E-05*
75 ppm	*-*	*Yes*	*No*	*69*	*8.92E-05*
75 ppm	*-*	*No*	*Yes*	*105*	*7.49E-05*
100 ppm	*-*	*Yes*	*No*	*68*	*1.00E-04*
100 ppm	*-*	*No*	*Yes*	*110*	*7.47E-05*

(*calculated at 30 min)

In most cases, the cost for the hybrid process is more expensive (for the same degradation) because in this case, there are two energy cost items, the one related to ozonator consumption and the one related to pump consumption. As regards the cavitation yields, the hybrid process appears to have a higher yield only when working with low concentrations of dye. As the MB concentration increases under the conditions investigated, there is no obvious benefit in using the combined process, the most significant positive effect indeed being attributable to the presence of ozone.[192]

6.1.2 TEXTILES RESULTS

The treatment of textile wastewater presents significant environmental challenges due to the presence of high levels of chemical oxygen demand (COD), total organic carbon (TOC), and persistent synthetic dyes. This study investigates the effectiveness of advanced oxidation processes (AOPs), specifically hydrodynamic cavitation (HC) combined with ozone (O_3) and hydrogen peroxide (H_2O_2), in degrading these pollutants. The results demonstrate substantial improvements in pollutant reduction, highlighting the synergistic effects of combined treatments. This section discusses the experimental findings, including the characterization of wastewater, treatment efficiencies, kinetic studies, and economic analyses, providing a comprehensive evaluation of the proposed methods for industrial application.

6.1.2.1 CHARACTERIZATION OF THE WASTEWATER

Table 22 shows the characteristics of the textile effluent. The most likely pollutants are dyes, detergents, and chlorinated compounds.

Table 22:Characteristics of effluent

Parameter	*Value*	*Unit*
pH	***7,16***	***-***
Color	***0,78***	***Abs***
Total suspended solids (TSS)	***1030-220***	***mg/L***
Chemical oxygen demand	***140.2***	***mg/L***
Total Organic carbon TOC	***65***	***mg/L***
Biochemical oxygen demand	***12***	***mg/L***
Azote	***16.9***	***mg/L***
Ammonium	***0.0077***	***mg/L***
Chloride	***140***	***mg/L***
Nitrate	***6.162***	***mg/L***
Cationic surfactants	***0.182***	***mg/L***
Nonionic surfactants	***2.565***	***mg/L***

6.1.2.2 HYDRAULIC CHARACTERISTICS OF THE SYSTEM

Fig. 32 shows the hydraulic characteristics of the laboratory apparatus. For input pressures above 0.45MPa, the conventional cavitation number (Cv), defined as follows, showed a minor drop. [63]

$$C_v = \frac{P_2 - P_v}{0.5\rho v_0^2} \qquad \text{Equation 41}$$

Where P2 is the pressure measured downstream of the Venturi tube (MPa), Pv is the vapor pressure of the aqueous solution (MPa), ρ is the aqueous solution density (kg/m3), and vo is the flow velocity (m/s). Cv is a dimensionless number used to describe the cavitation conditions. The cavitation number decreases with increasing inlet pressure, indicating that cavity creation becomes easier as inlet pressure ris[150]. However, an adverse effect could be caused by the rapidity with which cavities form when inlet pressure monotonically increases, creating cavity clouds

with significantly lower cavitation collapse intensity [193]. Furthermore, given the increase in energy consumption caused by increasing pressure, optimal operating inlet pressure must be calculated to reduce the energy consumption and cost [41, 42].

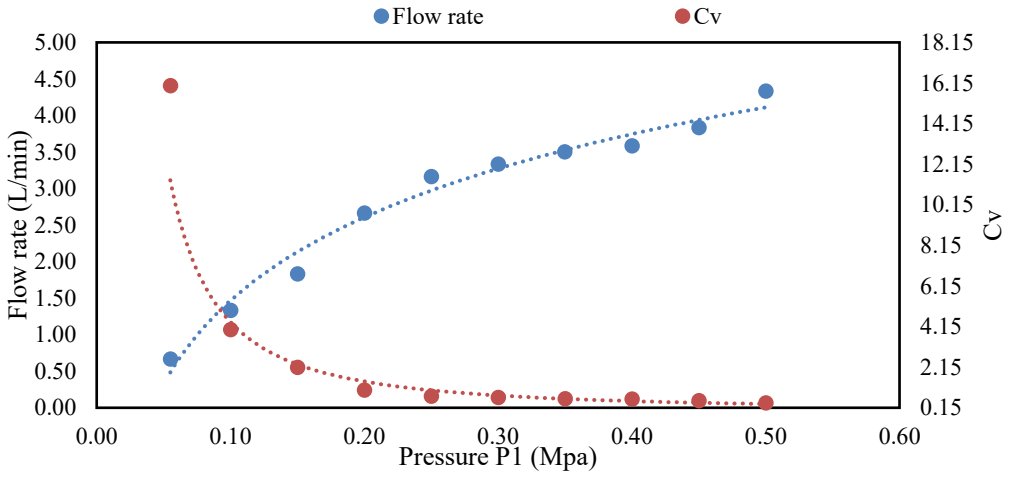


Figure 32:the Hydraulic curve

6.1.2.3 Treatment of textile effluents with using H_2O_2

The results of the first experiments under the following operative conditions (H_2O_2=0.3 mol/L, pH=2) showed a reduction of 84% and 55% of COD and TOC, respectively. Table 24 shows the characterization of the effluent after H2O2 addition. These results almost agree with several studies on COD reduction via the oxidation process purification of wasted caustic wastewater found in the literature. The total percentage of COD removed from spent caustic was greater than 99.5%. [194].The proportion of COD removed at pH 2.5 in the traditional hydrogen peroxide oxidation method was 89%. The COD elimination percentage at the same pH for the advanced oxidation procedure with the Fenton reagent was 96.4%. [151]

Table 23 :Characteristics of effluent after H2O2 treatment

Parameter	*Value*	*Unit*	*Average Reduction [%]*
color	***0.35***	***Abs***	***55***
Total Suspended Solids	***1032***	***mg/L***	***53***
Chemical Oxygen Demand	***23***	***mg/L***	***84***
Nitrogen	***10.9***	***mg/L***	***36***
Ammonium	***0.0056***	***mg/L***	***27***
Chloride	***70***	***mg/L***	***50***
Nitrate	***3.12***	***mg/L***	***49***
Cationic surfactants	***0.087***	***mg/L***	***52***
Nonionic surfactants	***1.123***	***mg/L***	***56***

6.1.2.4 TREATMENT OF TEXTILE EFFLUENTS WITH USING HC COMBINED WITH H_2O_2

Further research was conducted to evaluate the combined performance of HC + H_2O_2 on pollutant degradation after the individual performance of HC and peroxide alone for color and COD reduction. The tests with the hybrid process were carried out at a pressure of 4.5 bar and a solution pH=2. The H_2O_2 molar ratio was changed from 0.1 mol/L to 0.9 mol/L. The textile dye degradation rate constant was calculated using Equation 1. The data has also been used to define the decolourization kinetics also been used to define the decolourization kinetics, which follows a first-order law (Equation 42). Figure 3 reports, as an example, the results of the experiment conducted with 0.3 mol/L hydrogen peroxide.

$$ln\left(\frac{C_0}{C_t}\right) = kt \quad \textit{Equation 42}$$

where C is the concentration of textile wastewater, t is time, and k is the kinetic constant. [195]The first-order reaction fit the data adequately since the regression coefficient, R2, was greater than 0.9. Based on the slope of the line, the decolorization rate constant, k, was calculated to be 0.022 min-1.

Table 24 :the kinetic constant for different approaches.

Treatment	*k*	*Unit*
HC	***0.006758***	***min^{-1}***
H_2O_2	***0.013356***	***min_{-1}***
HC + 0.1 M H_2O_2	***0.01708***	***min^{-1}***
HC + 0.3 M H_2O_2	***0.02268***	***min^{-1}***
HC + 0.7 M H_2O_2	***0.02035***	***min^{-1}***
HC + 0.9 M H_2O_2	***0.01593***	***min^{-1}***

After 60 minutes of treatment, the UV-vis absorption spectra of textile dye treatment using hydrodynamic cavitation combined with hydrogen peroxide for varied molar ratios are shown in Fig. 34. Maximum decolorization was observed at 0.3 mol/L. As a result of this investigation, 0.3 mol/L was found to be the optimal concentration for textile wastewater decolorization. Increasing concentration from 0.1 to 0.3 mol/L improves the decolorization; however, the degradation of color shows a declining tendency above 0.3 mol/L.

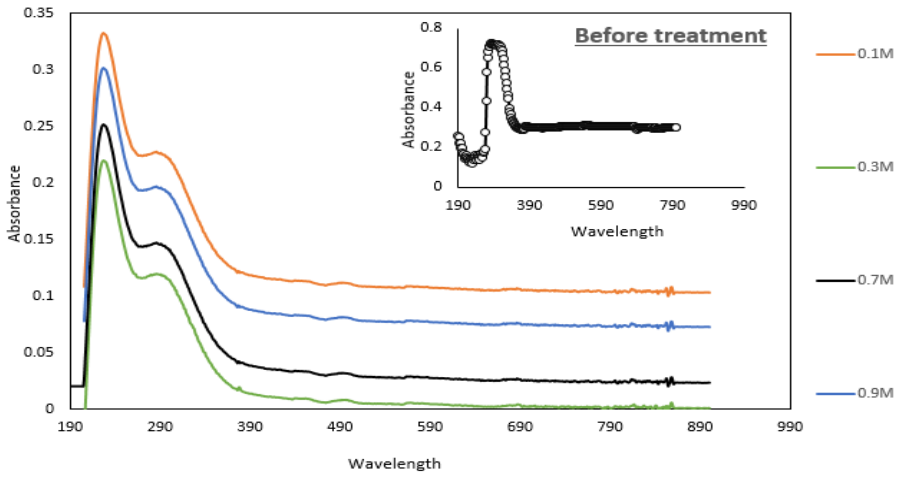


Figure 33:UV-vis spectra of textile wastewater degradation before and after HC +H_2O_2 treatments

Figure 34reports the reduction in COD and color overtime for different **H_2O_2** molar ratios. The HC coupled with hydrogen peroxide can reduce COD by about 88%. Furthermore, this method is successful at color reduction, achieving a percentage of 75 % in the case of an H2O2 molar ratio of 0.3 mol/L.

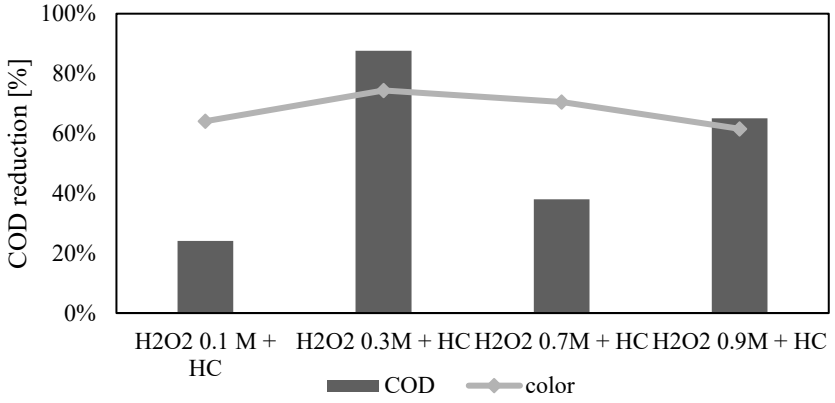


Figure 34:Extent of COD and Color reduction obtained in the presence of oxygen peroxide
(Experimental conditions: pressure= 4.5 bar, pH = 2, Temperature = 25 ± 2 ◦C).

Table 25 shows the reduction of chloride cationic surfactant, and COD for each H_2O_2 dosage. For the combined process, the rate of COD reduction rose as H_2O_2 loading increased. As Khajeh et al. [167] demonstrated, even ions in solution can be strongly reduced: they can chemically interact with OH· radicals, resulting in the following reductions: cationic surfactant 55%, Cl 50 % $^-$, NO_3^- 52%, SO_4^2 49%, PO_4^{3-} 90.6%.

Table 25:Characteristics of effluent after HC+H_2O_2 treatment

Parameter	***Concentration***				***Units***
HC+ H_2O_2	***0.1mol/L***	***0.3mol/L***	***0.7mol/L***	***0.9mol/L***	***-***
COD	***106***	***23***	***86.85***	***48***	***mg/L***
Cl^-	***70***	***70***	***70***	***70***	***mg/L***
NO_3^-	***9.5***	***3***	***8.69***	***8.98***	***mg/L***
PO_4^{3-}	***0.286***	***0.207***	***0.311***	***0.233***	***mg/L***
SO_4^{2-}	***172.5***	***114***	***178***	***224***	***mg/L***
Cationic surfactants	***0.091***	***0.083***	***0.091***	***0.09***	***mg/L***
Nonionic surfactant	***0.59***	***0.272***	***0.231***	***0.26***	***mg/L***
Color	***0.28***	***0.2***	***0.23***	***0.3***	***Abs***

This effect can be explained by the fact that when H_2O_2 is added, more OH radicals are produced, aiding in the oxidation process. However, if H_2O_2 is added in higher quantities above a specific concentration, the produced OH radicals are scavenged by a recombination process, decreasing the degradation reaction [167]. Higher amounts of hydrogen peroxide may also reduce the cavitation intensity since vaporous cavities are formed in this situation.

The efficiency of the process will be determined by the amount of hydroxyl radicals produced by the cavitation bubbles and the reactivity of these radicals within and outside the bubbles by the various organic/inorganic species present in the wastewater sample [170] However, excessive H_2O_2 concentration resulted in hydroxyl radical scavenging, and hence, the COD reduction and degradation rate decreased at 0.7 and 0.9 mol/L of H_2O_2. At these conditions, the COD reduction were 24%, 34% and 65 %, (0.1mol/L, 0.7 mol/L, 0.9mol/L of H_2O_2), respectively. When HC is combined with H_2O_2, the following primary reactions occur [49]

$$H_2O_2 \xrightarrow{cavitation} 2 \cdot OH \qquad \textit{Equation 43}$$

$$\cdot OH + pollutant \rightarrow produced\ mineralized \qquad \textit{Equation 44}$$

However, introducing an excess of H_2O_2 results in the following reactions.

$$\cdot OH + \cdot OH \xrightarrow{cavitation} H_2O_2 \qquad \textit{Equation 45}$$

$$\cdot OH + H_2O_2 \xrightarrow{cavitation} H_2O + H_2O \qquad \textit{Equation 46}$$

$$\cdot OH + \cdot O_2 \xrightarrow{cavitation} H_2O \cdot + O \cdot \qquad \textit{Equation 47}$$

$$H_2O \cdot + H_2O \cdot \xrightarrow{cavitation} H_2O_2 + O_2 \qquad \textit{Equation 48}$$

according to Gore et al, Reactive orange 4 (RO4) dye degradation was found to be accelerated by the addition of H_2O_2 to the HC [69].

They reported a decrease in the rate of RO4 dye degradation above the 1:30 molar ratio of H_2O_2 addition. This investigation also showed that the H_2O_2 dosage can be optimized to enhance the degradation rate of ternary dye utilizing the HC in aqueous media.

6.1.2.5 TREATMENT OF TEXTILE EFFLUENTS USING OZONE AND COMBINED TREATMENTS

Ozonation is a promising approach for textile wastewater treatment because it can convert refractory organics into intermediates, improving wastewater biodegradability. However, ozonation cannot accomplish total mineralization, which has become an inescapable limitation in its use. [196]Dias et al. and Sun et al. found that ozonation had a good effect on chroma treatment (up to 99%), but the removal rate of chemical oxygen demand (COD) was insufficient [197]. In the current study, different ozonation-based approaches were investigated. The first experiments were conducted with ozone alone with a feeding rate of 7.5 mg/L and pH=2 to investigate the effect of ozone on color degradation and COD reduction. It has been found that the COD and color reduction in the individual ozonation process were 69.57% and 63.46%, respectively, as shown in Fig. 36.The ozone was [198]coupled to HC and H_2O_2 under fixed conditions of pressure and hydrogen peroxide concentration (P=4 bar, pH=2, 0.3 mol/L of H_2O_2) to mineralize and accelerate the ozone decomposition fully, creating OH radicals . The treatment time was reduced to 20 minutes due to combining the two processes, which increased the radical number. Numerous studies have demonstrated that the ozonation method with H_2O_2 and UV light added a good degradation effect on textile wastewater. The combination of cavitation and ozonation can be an effective strategy for increasing the formation of OH radicals as well as the dissolution of ozone in the effluent, resulting in greater application of injected ozone[199]. The major condition for a higher ozone dissolving rate in wastewater is improved mass transfer via cavitation. Incorporating HC into individual ozonation increased COD reduction in the current investigation, with real COD reductions of 73.8% and 69.575%, respectively. The use of cavitation promoted COD reduction by improving the conversion

of molecular ozone to OH radicals. Some previous research has proven similar outcomes for combining cavitation with ozone. The degradation rate occurred three times faster for HC/O_3. Adding H_2O_2 to the effluent could accelerate ozone decomposition, resulting in an increased generation of OH radicals. It was discovered that H_2O_2 increased the COD reduction of textile water from 73.8% for HC + Ozone to 83% for H_2O_2 +Ozone. It can be explained that the modification of the beginning mechanism of ozone decomposition (from OH to H_2O) may increase the production of OH radicals from ozone (Eq. (49)). Typically, the ozonation process generates two OH radicals from three decomposed ozone molecules. In contrast, the O_3/H_2O_2 process generates one OH radical from each destroyed ozone molecule. The O_3/H_2O_2 process's potent oxidation capacity can also improve COD reduction in conventional wastewater treatment plant effluent [198]

$$H_2O_2 + O_3 \rightarrow 2 \cdot OH + 3O_3 \qquad \textit{Equation 49}$$

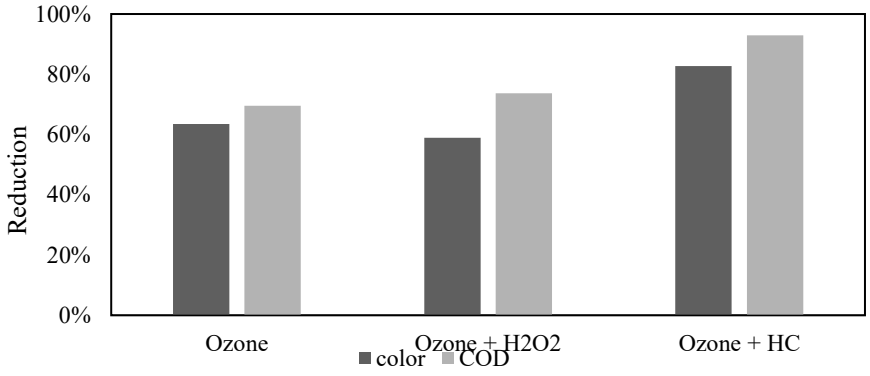


Figure 35: Extent of COD and color reduction obtained for HC+H_2O_2 and HC+Ozone (Experimental conditions: pH = 2, Temperature = 25 ± 2 ◦C, Ozone flow rate = 7.5 mg/L [H_2O_2] = 0.3 mol/L, pressure = 4.5 bar)

6.1.2.6 Treatment of textile effluents using the combination of HC /H_2O_2/O_3

An investigation was carried out to enhance the degradation rate using the combined process $HC+O_3+H_2O_2$. According to our previous study, the optimal O3 feeding rate was (7.5mg/L), and the concentration of peroxide was fixed at the optimal value of 0.3 M.The combined process has been found to increase the generation of OH radicals, which causes

a reduction in COD (9.83 mg/L). This reduction increases to 5 times with the addition of O3. Thus, the combination of ozone, peroxide, and cavitation lead to 95% of COD reduction, as shown in Fig 36. The COD was significantly decreased from 140 mg/L to 7 mg/L [200].

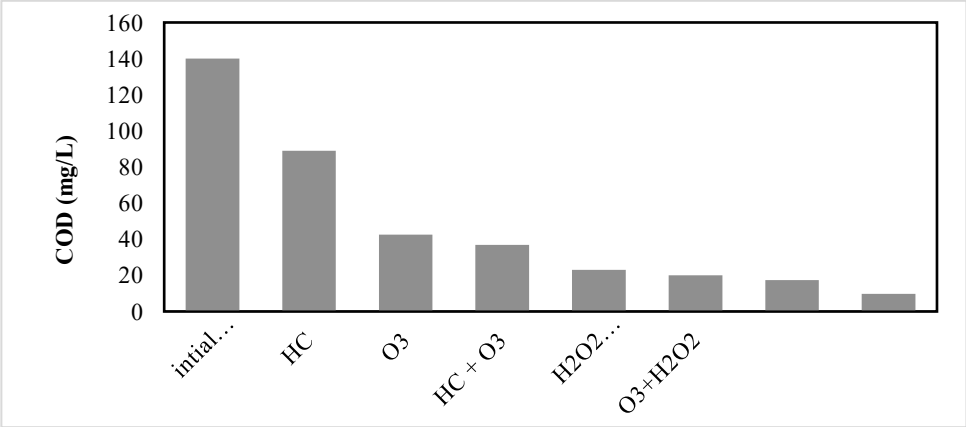


Figure 36:COD concentration as a function of the treatment

For the HC/O_3/H_2O_2, the rate constant k increased from 0.0227min -1 and 0.0299 min -1 (O_3 /H_2O_2 and HC/O_3 approaches, respectively) to reach the value k =0.39 min -1. Rosal and coworkers [59] discovered that the generation of intermediates increased more for HC/O_3/H_2O_2 than the other approaches, indicating that HC/O3/H2O2 oxidized more recalcitrant intermediates into end products. The cavitational events at the ozone dispersion site may have accelerated the dissociation of ozone, resulting in a higher number of OH radicals. The rate constant k changed, indicating that the intermediates generated during the approach of cavitation combined with O3/H_2O_2 were resistant to oxidation. Overall, the combination of cavitation and HC/O_3/H_2O_2 achieved more COD reduction than the O_3 /H_2O_2 and HC/O_3 approaches.

Synergistic effect

The synergistic effect has been calculated to compare the different processes under investigation. The color removal rate of textile wastewater by single H_2O_2 or HC + H_2O_2 was over 88% in 10 minutes, but the removal rate by HC alone was lower than 33%, indicating that HC without a strong oxidant could not be able to eliminate the contaminant effectively in a short time.

The pseudo-first-order rate constants of textile wastewater HC/O_3, HC/ H_2O_2, and HC/ H_2O_2/O_3 were 0.022, 0.029, and 0.39 min -1, respectively.

The obtained k values show that the hybrid HC/ H_2O_2 /O_3 process is superior to the binary integrated processes for wastewater. The synergistic index (f) of HC/ H_2O_2/O_3 calculated using k values by Eq. (50-52)

$$f = \frac{K_{HC/H2O2}}{K_{HC}+K_{H2O2}} = \frac{2.2\times10^{-2}}{0.675\times10^{-2}+1.3\times10^{-2}} = 1.11 \quad \textit{Equation 50}$$

The HC + H_2O_2 treatment had a synergetic coefficient of 1.11, indicating that the combined treatment improved the mass transfer of H_2O_2, produced more micro-bubbles, and OH·, and thus effectively degraded more contaminants [59].

The synergistic effects were 5.53 and 7.40, for HC/O_3 and HC/ H_2O_2/O_3, respectively indicating a significant synergy compared to the cumulative effect of separate processes.

$$f = \frac{K_{HC/O3}}{K_{HC}+K_{O3}} = \frac{2.2\times10^{-1}}{0.675\times10^{-2}+3.3\times10^{-2}} = 5.53 \quad \textit{Equation 51}$$

$$f = \frac{K_{HC/H2O2/O3}}{K_{HC}+K_{O3}+K_{H2O2}} = \frac{0.39}{0.675\times10^{-2}+3.33\times10^{-2}+1.3\times10^{-2}} = 7.40 \quad \textit{Equation 52}$$

Similar literature reports can also confirm the findings of this study. Rajoriya et al. [49] evaluated the effect of combining HC and O_3 (1-5 g/h) on textile wastewater treatment. When the ozone flow rate was 3 g/h, the combined technique removed 48% and 22.72% of

TOC and COD, respectively. It has a synergy index of 1.42, indicating a positive synergistic impact.

Wang et al. [201] investigated the degradation effect of combining HC and O_3 treatment of dyeing wastewater. The results revealed that degradation was low when using HC or O_3 alone. However, the combination of HC + O_3 could completely degrade the dye wastewater within 10 minutes, significantly improving the textile wastewater degradation efficiency. The higher synergistic index (f) value for HC/O_3/H_2O_2 could be attributed to the better decomposition of ozone in the presence of H_2O_2 generating a greater amount of OH· radicals. This demonstrates that the combination strategy presented in this study has a substantial synergistic effect and can boost textile wastewater degrading efficiency.

6.1.2.7 Cost and Energy estimation for wastewater treatment

Another significant parameter is the cavitation yield which is calculated using Eq. (35)

$$Cavitation\ yield\left[\frac{mg/L}{J}\right] = \frac{amount\ of\ dye\ degraded}{\frac{P_E \times t}{V}} \qquad \textit{Equation 53}$$

Where P_E is the power consumed for the treatment (kW), t is the treatment time (h) and V is the treated volume (m^3)

This yield may be defined as the quantum of dye (mg) reduced per unit of energy delivered into the system (J). In the current study, the cost of treating textile wastewater is based on the cavitational yield and the cost of oxidants used during the treatment (Table 28).

The energy costs associated with different oxidation processes, including HC/H_2O_2, HC/O3, HC/O_3/H_2O_2, O3/H_2O_2, and standalone H_2O_2 or ozone treatments, with the goal of achieving a 90% degradation rate.

The energy cost per kWh was set at 0.23€, while the costs of H_2O_2 per liter were set at (0.9€) [192]. Compared to other methods, HC/O_3/H_2O_2 treatment was quite

energy and cost-efficient. The cost of the HC-based strategy is much lower, with projected costs of 50.45€, 19.87 €, and 12.62€ per liter for HC/O_3, HC/H_2O_2, and HC/O_3/H_2O_2, respectively. for the HC experiments PE is equal to electrical consumption of the pump as in eq.16:

$$P_E = \frac{\Delta P\,(Pa)\cdot Q\,(\frac{m3}{s})}{\eta} \qquad \textit{Equation 54}$$

ΔP is the pressure drop, Q is the volumetric flow and η is the efficiency.

Table 26:Estimation of cost for various approaches coupled with HC

Method	*COD reduction (%)*	*cv (10-6) (mg/l J)*	*Energy consumption (kWh/m3)*	*Cost of treatment (€/m3)*
HC alone	***36.4***	***1.5***	***0.03***	***35.62***
O_3 alone	***69.57***	***-***	***0.18***	***47.63***
H_2O_2	***83.71***	***-***	***-***	***9***
HC+ O_3	***73.71***	***3.7***	***0.10***	***50.45***
HC+ H_2O_2	***87.61***	***3.4***	***0.03***	***19.87***
HC+ H_2O_2 +O_3	***92.98***	***9***	***0.06***	***12.6***

Thanekar et al. [202]explored Naproxen degradation using HC/O_3 and achieved 40% degradation at a cost of 0.21€/L. Similarly, Gujar et al. [62] used O_3 and US/O3 to treat wastewater from the cellulosic fiber manufacturing sector, with estimated costs of 78.42 and 59.80/L, respectively. It is also critical to understand that treatment costs are highly dependent on the effluent and hybrid treatment strategy used, illustrating the significance of the current analysis for wastewater treatment.

6.1.2.8 PROCESS ANALYSIS

The following section discusses process analysis for real wastewater treatment. The commercial software SuperPro Designer has been used to perform this study. Two cases were investigated: the existing traditional process (first scenario), and an innovative process involving the addition of the hydrodynamic cavitation (HC) combined with the advanced oxidation process HC+O_3+H_2O_2 (second scenario).

The textile company has provided the data for the traditional process. Incorporating hydrodynamic cavitation in the existing industrial process could be an innovative approach for efficiently treating textile effluent.[202]

Both processes aim to produce high-quality water that may be reused for industrial applications, particularly in the textile industry.Figure 37. depicts the suggested process flow diagrams for both scenarios.

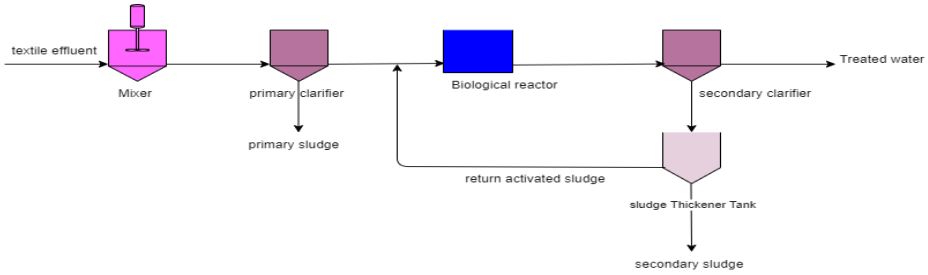


Figure 37 :Process analysis for the traditional process

The traditional process involves, after mixing, a primary clarifier. After that, the industrial wastewater is sent to the biological section which includes an aerobic reactor and a sludge thickener. This operation sequence provides for COD, color, and BOD reduction. The innovative process is introduced before the biological section, with centrifugation to remove solid particles and the combined hydrodynamic cavitation treatment. To simulate the HC, the optimal experimental conditions have been considered (P=4.5 bar, pH = 2, Temperature = 25 ± 2 ◦C, Ozone flow rate = 7.5 mg/L [$\mathbf{H_2O_2}$] = 0.3 mol/L).

The effluent then passes through a pump, which raises the liquid pressure inside the cavitation reactor to 4.5 bar, the optimal pressure for maximal degradation rate yield.

Table 27:Comparison between traditional and innovative process

	Initial concentration[mg/L]	***Final concentration Traditional process***	***Final concentration Innovative Process***	***Advantage (%)***
COD	***140.2***	***124.67***	***6.45***	***84%***
BOD_5	***12***	***7.92***	***0.73***	***90%***
TOC	***65***	***41***	***2.27***	***94%***

This analysis compared the current treatment train with a new plant configuration in which HC was incorporated into the traditional process. According to Table 5, the traditional process reduced the COD of the effluent by 11 %, whereas for the innovative approach, the COD was reduced by 95%, illustrating the efficacy of the combined operation. The TOC reduction is enhanced from 36% to 96%, as well as the BOD_5 reduction, which increased significantly from 20% to 92.7%.

Overall, textile wastewater treatment was achieved efficiently by applying HC in conjunction with ozone and hydrogen peroxide for increased COD, TOC, and BOD_5 reduction without sludge formation. Because of the low treatment cost and a greater extent of COD reduction, HC combined with catalytic ozonation has shown the potential for industrial usage . [14]

6.2 WINERY TREATMENTS RESULTS

6.2.1 . RESULTS AND DISCUSSION

6.2.1.1 CHARACTERIZATION OF WINERY WASTEWATER:

The effluent utilized in these investigations was directly collected from the winery wastewater treatment plant (WWTP) of a winery industry "La Quercia Vini" winery (Morro D'Oro, Teramo).Experimental activities aimed at studying the treatment of winery effluents were conducted in the Chemical Plants laboratory of the University of L'Aquila Before undergoing any treatment, the winery effluent was examined

and characterized through spectrophotometric analysis , to estimate the concentration of any contaminants and to perform a check against the limit values imposed by the relevant regulations.

The TOC and COD analysers were used to determine total organic carbon (TOC) and chemical oxygen demand (COD). The chemicals utilized in the COD and TOC analyses were test cuvettes (LCK114 and LCK381, respectively). Total solids (TSS) have been determined by drying the effluent sample in an oven at 104 degrees Celsius (UF160) for 24 hours.

The cuvette-based spectrophotometric methods for detecting ammonium and nitrate chloride in real textile wastewater were evaluated. The methods detect wavelengths ranging from 340 to 900 nm in ready-to-use cuvettes (bar-coded reagent cuvettes). The results obtained are reported in Table30.

Table 28:Characteristics of effluent.

Parameter	***Range***	***Unit***
pH	*7*	**-**
Chemical oxygen demand	***1200***	***mg/L***
Total Organic carbon TOC	***42.4***	***mg/L***
Biochemical oxygen demand	***428.22***	***mg/L***
Phenols	***1***	***mg/L***
Ammonium	***0.15***	***mg/L***
Chloride	***12.9***	***mg/L***
Nitrate	***1.29***	***mg/L***
Sulfates	***36.7***	***mg/L***
Total Nitrogen	***5.46***	***mg/L***

6.2.1.2. Experimental Results and Model Development

To assess the impact of $[H_2O_2]/[Fe^{2+}]$ and $[H_2O_2]$ on the efficiency of the Fenton process, a three-level full-factorial design of experiments (3^k) was employed. The studied ranges of process parameters were as follows: 0.03, 0.27, 0.5 mol/L (hydrogen peroxide

concentration) and 0.83, 1.66 ,2.5 (H_2O_2/Fe^{2+} molar ratio). Table 29 presents the applied levels for each independent factor. Fenton's method was utilized to minimize COD levels and mitigate the impact of WW discharge on natural water courses and municipal wastewater treatment plants.

Table 29:Independent Variable Actual and Coded Values Used for Two-Factor, Three-Level.

Independents variables	***Units***	***Symbols***	***Coded Level***		
			-1	***0***	***1***
Hydrogen peroxide [H_2O_2]	***(mol/L)***	***X_1***	***0.03***	***0.027***	***0.5***
Molar Ratio [H_2O_2]/ [Fe^{2+}]	***Add***	***X_2***	***0.83***	***1.66***	***2.5***

H_2O_2 and Fe^{2+}were chosen as independent variables because they are operational features that have been shown to have a significant impact on the performance of the Fenton-like process. Based on previous determinations of the ideal values for the Fenton reaction, the range of Fe^{2+} was defined with the goal of achieving a minimum range of H_2O_2/Fe^{2+} [152] We looked at the connections between process responses and independent variables. Combining least-squares regression and a quadratic model to identify ideal operating conditions of the general form [203], [204]

$$Y_i = \beta_0 \sum_{i=1}^{k} \beta_i X_i + \sum_{i=1}^{k} \beta_{ii} {X_i}^2 + \sum_{i=1}^{k-1} \sum_{j=2}^{k} \beta_{ij} X_i X_j + C \quad \text{Equation 55}$$

Yi is the predicted response, β_0, β_i, β_ii, and β_ij are coefficients illustrating the intercept, linear, quadratic, and cross-factor interaction effects, Xi and Xj are independent variables, k is the number of factors, and Cis is the residual term. The Design Expert version 13.0.8.0 software program was used to conduct design experiments (DOE), developing quadratic model equations using least squares

regression and Analysis of Variance (ANOVA) to a 95% confidence interval (= 0.05), and navigating the three-dimensional (3D) response surface.

The overall goal was to assess the viability of utilizing a Fenton treatment method to reduce organic loadings in WWTP's downstream liquid treatment train (Figure 1). As a result, COD removal rate (Y1) is chosen as the primary response variables.

Equation illustrates the quadratic models developed to predict the response parameters in terms of the coded independent variables reaction time (X1), H2O2, (X2(Molar Ratio [H_2O_2]/ [Fe^{2+}].[125]

$$Y = 63.74 + 36X_1 + 1.56X_2 - 0.00691X_1X_2 + 0.0291 \cdot$$

$$X_1{}^2 0.0219 X_2{}^2 \quad \text{Equation 56}$$

Table 30 summarizes the values that were observed and predicted for the three response variables. Table 31 provides the ANOVA findings for the overall models and individual terms. Coefficients with p-values < 0.05 were considered statistically significant, while those with p > 0.10 were not.[205]

Table 30.Observed and predicted COD removal for the two factors used to assess performance of the Fenton-like process for the treatment of actualWWpre-treated via centrifugation.

Run order	***Independent variables***		***COD Removal (%) Y1***		***residual***	***Standard Order***
	X1	***X2***	***Observed***	***Estimated***		
1	***0.03***	***0.833***	***66.12***	***62.13***	***3.99***	***6***
2	***0.27***	***0.833***	***74.75***	***78.58***	***3.82***	***8***
3	***0.5***	***0.833***	***83.03***	***81.26***	***1.78***	***7***
4	***0.03***	***1.66***	***67.40***	***67.32***	***0.09***	***3***
5	***0.27***	***1.66***	***76.04***	***79.29***	***-3.24***	***9***
6	***0.5***	***1.66***	***84.32***	***80.71***	***3.62***	***4***
7	***0.03***	***2.5***	***68.72***	***65.12***	***3.60***	***1***
8	***0.27***	***2.5***	***77.36***	***80.47***	***-3.11***	***2***
9	***0.5***	***2.5***	***85.64***	***84.25***	***1.39***	***5***
10	***0.27***	***1.66***	***79.53***	***74.05***	***3.84***	***10***
11	***0.27***	***1.66***	***79.61***	***74.05***	***3.48***	***11***

*Table 31.**ANOVA results for the development of quadratic models to predict COD removal.***

Source of variation	*Sum of square*	*Degrees of freedom*	*Mean Square*	*F*	*Significance*
A, H2O2 (mol/L)	*516.30*	*2*	*258.15*	*83274.66667*	*99.8%*
AL	*444.68*	*1*	*444.68*	*143445.3333*	*99.8%*
AQ	*71.62*	*1*	*71.62*	*23104*	*99.6%*
B [H2O2]/ [Fe2+]	*10.78*	*2*	*5.39*	*1738.666667*	*98.3%*
BL	*10.33*	*1*	*10.33*	*3333.333333*	*98.9%*
BQ	*0.45*	*1*	*0.45*	*144*	*94.7%*
AB	*11.92*	*4*	*2.98*	*961.3333333*	*97.6%*
ABL	*0.41*	*2*	*0.20*	*65.33333333*	*91.3%*
ABQ	*11.52*	*2*	*5.76*	*1857.333333*	*98.4%*
MSEerrorr	*0.0031*				
R^2	*0.9579*				
Adjusted R^2	*0.9439*				
Adeq Precision	*15.3438*				

4. Analysis and Discussion

After 60 minutes of reaction, the COD removal was consistently greater than 50% regardless of the operating conditions. The highest elimination rate of 85.7% was attained when $[H_2O_2]$ = 0.5 $molL^{-1}$ and $[H_2O_2/Fe^{2+}]$ = 1.66 were employed. Examining the study design allows us to develop a simple model for calculating the response variable's value, COD elimination. Equation (56) illustrates the relationship between the independent and variable variables as well as their interactions and effects. The adjusted square correlation between the experimental and projected COD values was 94%, with an R2 of 0.95.[204]

Increasing H_2O_2 concentration had a positive effect on COD degradation. COD is eliminated mostly at the start of the process. The study using 0.27M H_2O_2 did not effectively lower COD levels. The experiment using 0.5 M of H_2O_2 had the maximum COD removal rate, reaching 85% for pre-treated WW T. The amount of H_2O_2 used directly influences oxidation, and consequently COD elimination rates. The Fenton reagent effectively destroys refractory organic compounds in pretreated WW. Increased H_2O_2 levels result in higher COD conversion due to increased hydroxyl radical generation.

In Figure38, the 3D surface depicts COD abatement as a function of the independent factors. The highest COD elimination rates are observed for central peroxide-iron ratio values across the full peroxide concentration range. Statistical analysis shows that the H_2O_2/Fe^{2+} ratio and hydrogen peroxide concentration had a significant impact on COD removal over the evaluated range of independent variables ($p < 0.05$). [203]
This is due to Fe^{2+} ions' catalytic involvement in the Fenton process, which promotes H_2O_2 breakdown and results in more effective COD reduction. Analysing the design of experiments yields a simplified model for estimating the value of COD removal. The connection of the response variable and the independent factors

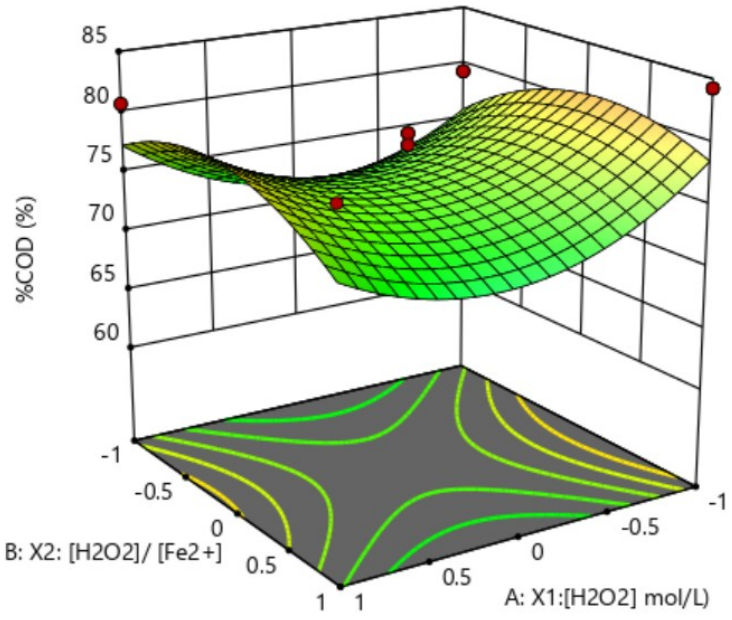


Figure 38:Response surface for COD removal as a function of [H2O2] and [H2O2/Fe2+].

Comparing the experimental COD values with the model-predicted values, a reasonable agreement was found with an adjusted square correlation of 97% and a coefficient of determination (R2) of 0.99, as demonstrated in Fig 39.

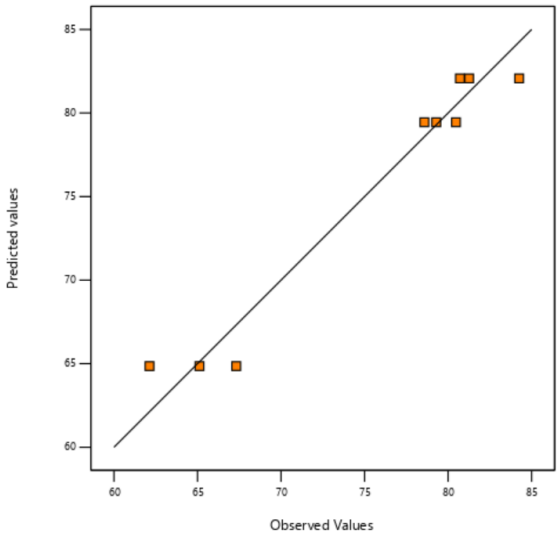


Figure 39: Comparison between experimental and model predicted values for CODremoval.

The quadratic terms for X_1 and X_2 indicate the optimal value for each parameter among the investigated ranges. Figures 38 and 39 show optimal COD at the midpoint of investigated parameter ranges: H_2O_2 (X_1) of 0.5 mol/l and 2.5[H_2O_2/Fe^{2+}].(X_2)Optimal H_2O_2, in H_2O_2-based AOPs is widely acknowledged for its role as a radical scavenger

As a result, the degree of oxidation, and hence COD elimination, is directly proportional to the amount of H_2O_2 utilized. The Fenton reagent effectively degrades refractory organic materials in pre-treated WW.

The rise in COD conversion with the increase of H_2O_2 can be explained by the creation of a bigger amount of hydroxyl radicals and, thus, a greater extension of oxidation processes.

The greater H_2O_2 concentration (0.5M) resulted in a final COD of 94 mg L^{-1}. This results in a 98% COD conversion relative to the initial WW value, which falls below the legal limit set by European regulations (150 mg L^{-1}).Increasing H2O2 can be explained by the formation of a bigger amount of hydroxyl radicals, and hence a greater extension of oxidation reactions.[204]

6.3 HYDROCARBONS TREATMENTS RESULTS

6.3.1 SOIL CHARACTERIZATION

The clean soil was made up of industrial aggregates that could be easily broken down into smaller particles (< 2 mm). It mainly consisted of fine silts and clays. The soil had a near-neutral pH, an inorganic carbon content (bicarbonate) of 189.36 ± 3.89 g kg^{-1}, and an organic carbon content of 17.87 ± 1.21 g kg^{-1}, likely due to humic acid-type compounds. The Natural Oxidant Demand (NOD) for H_2O_2 was measured over 48 hours by mixing the reference soil with 40 g dm-3 of the oxidant (VL/W=2 ml g^{-1}). The NOD was over 120 g of H_2O_2 per kg of soil, mainly because of the high carbonate content. This high, unproductive H_2O_2 consumption shows that using this oxidant directly is not suitable for soils like this, highlighting the need to wash the soil to remove pollutants before treating the washing solution.[206]

The metal concentrations in the soil are listed in Table Appendix , with calcium and copper being the most common, along with small amounts of silicon, magnesium, and potassium. After spiking and ageing the soil, the contaminant levels were 35.12 ± 3.15 mg dm^{-3} of ANT and 14.64 ± 1.20 mg dm^{-3} of BaP. Other soil characteristics (metals, TOC, IC, pH, etc.) remained unchanged after this process [207]

6.3.2 . SURFACTANT SOIL WASHING

Soil washing was performed with initial SDS concentrations of 2500, 3500, 5000, 6500, 7500, 8500, and 10000 mg dm^{-3}. The adsorption of SDS onto the soil (denoted as q, in grams of SDS per kilogram of soil) was measured using a spectrophotometric method applied to the aqueous phase. The results were then plotted against concentration. of SDS in the washing emulsions Figure 42adisplays the results for (SDSemulsion). [208]The residual PAH concentrations in the soil and emulsions were measured, achieving a pollutant mass balance of over 90% for all SDS concentrations. Partition coefficients (Kd), which represent the ratio of each PAH's concentration in the soil ([PAHi]soil) to that in the aqueous phase ([PAHi]aq) at equilibrium (24 hours), were calculated using Eq. 57. Figure 42b

illustrates the dependence of partition coefficients for ANT and BaP on the SDS concentration.[209]

$$K_d = \frac{[PAH_i]_{soil}}{[PAHH_iJ_{aq}} \qquad \textit{Equation 57}$$

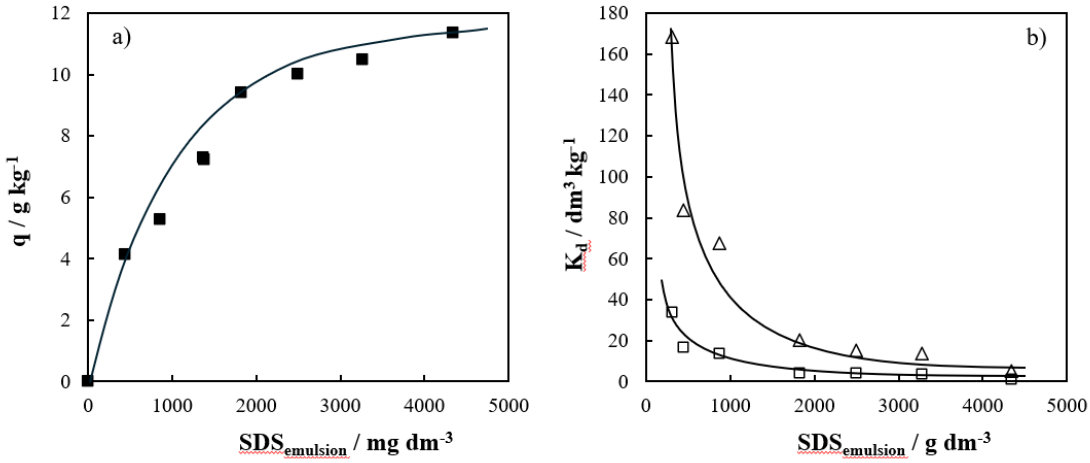


Figure 40: a) Adsorption isotherm of SDS in the contaminated soil and, b) K_d of ANT (triangles) and BaP (squares) after soil washing with SDS (V_L/W = 2 mL g^{-1}, 24 h).

Soil washing resulted in some surfactant adsorption, with a non-linear SDS partition between soil and liquid phases (Figure 42aa), reaching asymptotic values, as commonly reported for anionic surfactants. SDS adsorption increased from 4.10 to 11.60 g kg^{-1} of soil as the initial SDS concentration rose from 2500 to 10000 mg dm^{-3} (final SDS in the aqueous phase from 500 to 4500 mg dm^{-3}, respectively). Soil physicochemical and mineralogical properties, particularly kaolinite content, influence surfactant adsorption. Various results have been published regarding SDS adsorption on soils (1.8 g SDS kg^{-1} [SDS]0 = 5000 mg dm-3 to 11 g SDS). kg^{-1}, $[SDS]_0$ = 10000 mg dm^{-3}). The authors concluded that the type and concentration of contaminants also affect the SDS adsorption. [181]

Despite some surfactant loss due to adsorption, surfactants are crucial for remediating PAH-contaminated soils by significantly enhancing PAH solubility, which is otherwise low in water (e.g., ANT solubility = 0.044 mg dm^{-3} and BaP = 0.0038 mg dm^{-3}). Without surfactants, a partition coefficient (Kd) over 1300 dm3 kg^{-1} for the pollutants would slow down soil remediation. As shown in Figure 42b, adding SDS greatly increased PAH solubilization, reducing the Kd for both

pollutants and improving contaminant removal. When SDS concentration in the aqueous phase exceeded 4000 mg dm^{-3}, the PAH partition coefficient remained constant, with ANT (5.05 dm3 kg^{-1}) being five times higher than BaP (1.03 dm3 kg^{-1}).

The iron concentration in the wash emulsion, determined by colorimetry, was negligible, which is relevant since iron is a catalyst in Fenton-type processes for treating these emulsions. Considering SDS partitioning between soil and aqueous phase and the increase in PAH solubility with SDS concentration in the emulsion at the tested VL/W ratio, the soil was washed with an initial SDS concentration of 10000 mg dm^{-3}. This resulted in an emulsion with 4341.72 mg dm^{-3} SDS, well above the CMC of 1800 mg dm^{-3}, and 6.15 mg dm^{-3} ANT and 4.31 mg dm^{-3} BaP. The remaining pollutant concentrations in the soil were 19.05 mg kg-1 for ANT and 5.38 mg kg^{-1} for BaP. Thus, 51% of total PAHs were extracted under the tested conditions (VL/W = 2 mL g−1, 24 h), suggesting that successive cycles are needed for complete remediation. Additionally, SDS adsorption would likely decrease in subsequent washings, reducing surfactant requirements.[210]

6.3.3 TREATMENT OF POLLUTED EMULSION

Using the Kd values from the soil washing experiments, a synthetic polluted emulsion was created with 4500 mg dm^{-3} of SDS, 5 mg dm^{-3} of ANT, and 5 mg dm^{-3} of BaP.

6.3.3.1 FENTON PROCESS: EFFECT OF OXIDANT AND CATALYST DOSAGE

Control experiments were performed to evaluate the stability of pollutants in the emulsion under three conditions: emulsion without reagents , with the oxidant (H_2O_2) , and with the catalyst (Fe) . The reaction mixture was gently agitated in the dark, and PAH concentrations were monitored over 6 hours. Figure 43shows the normalized concentrations of ANT and BaP at the end of the experiments.[136]

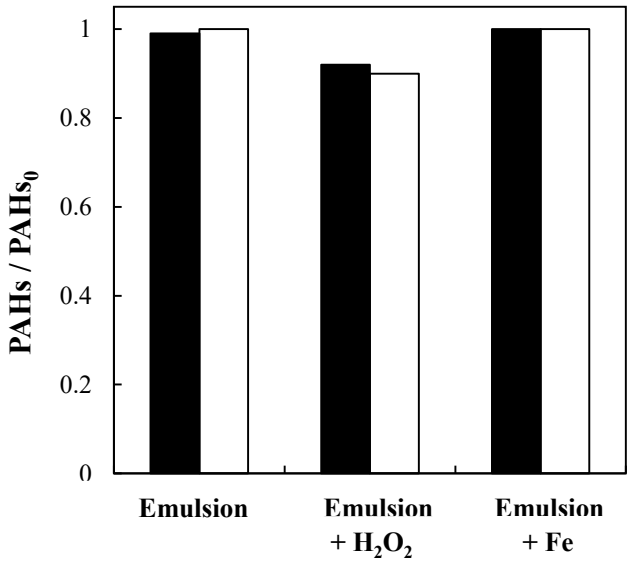


Figure 41:Normalized concentration of PAHs ([SDS]$_0$ = 4500 mg dm^{-3}, [ANT]$_0$ = 5 mg dm^{-3}, [BaP]$_0$ = 5 mg dm^{-3}) without reagents, in the presence of H_2O_2 (120 mg dm^{-3}), and Fe (5 mg dm^{-3}) (E1-E3). Black bars: ANT; white bars: Ba, pH=7.

The concentration of PAHs in the emulsion remained stable (E1), ruling out the possibility of PAHs volatilization at room temperature. Similarly, no significant change in the concentration of PAHs was detected when iron was added to the emulsion (E3).[211] However, the addition of H_2O_2 led to a slight decrease in the concentrations of ANT and BaP (<10%), likely due to the oxidation potential of H_2O_2 (E^0 = 0.87 V) . The minimal degradation of contaminants under these conditions highlights the need to activate the oxidant to generate more reactive species, such as hydroxyl radicals (E^0 = 2.80 V) , generated in the Fenton process. The effectiveness of this process The effectiveness of PAH degradation was evaluated using different doses of hydrogen peroxide (E4, E5, and E6) and catalyst (E7, E5, and E8). Figures 3a and 3b show the conversion of ANT and BaP over time with 60, 120, and 240 mg H_2O_2 dm^{-3}, respectively.[207]

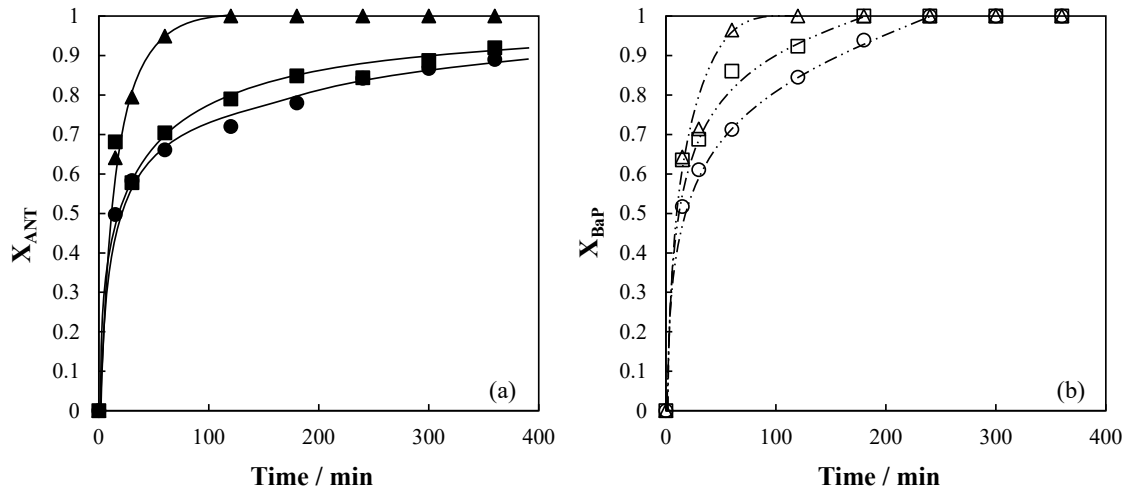


Figure 42:Influence of H_2O_2 concentration (60 (●), 120 (■), and 240 mg dm^{-3} (▲)) on the degradation of PAHs in the emulsion by Fenton process (E4-E6). $[SDS]_0$ = 4500 mg dm^{-3}; $[ANT]_0$ = 5 mg dm^{-3}; $[BaP]_0$ = 5 mg dm^{-3}; $[Fe]_0$ = 5 mg dm^{-3}, pH=3.

The pollutants were progressively degraded over time using lower oxidant concentrations than those reported for direct Fenton Reagent application on soil or non-ionic surfactants. Figures 44a and 44b show rapid conversion in the first 60 minutes, followed by a slower degradation rate. This could be due to hydroxyl radicals competing to oxidize intermediate organic compounds and the parent compounds (ANT and BaP). Higher oxidant dosages resulted in faster PAH degradation. Specifically, with H2O2 concentrations of 60, 120, and 240 mg dm^{-3}, complete BaP degradation was achieved after 120, 180, and 240 minutes, respectively (Figure 44b). Complete ANT degradation was achieved in 120 minutes at the highest oxidant dose (Figure 44a). As H_2O_2 concentration increases , more hydroxyl radicals are generated, leading to faster pollutant degradation. [212]

The impact of catalyst concentrations on PAH removal was assessed using the stoichiometric oxidant dosage for pollutant mineralization (120 mg H_2O_2 dm^{-3}). Figure 45 shows the degradation of PAHs with 2.5, 5, and 10 mg Fe dm-3. Increasing iron concentration improved contaminant degradation, with BaP degrading faster than ANT at all iron levels. Complete degradation of BaP and ANT was achieved after 120 and 300 minutes, respectively, with 10 mg Fe dm^{-3}. Similar trends were seen with lower catalyst dosages (5 and 2.5 mg Fe dm^{-3}). With 10 mg Fe dm^{-3}, BaP was fully degraded in about 180 minutes (Figure 45a), and over 80% of ANT was removed after 360 minutes (Figure 45b). Iron facilitated the catalytic cycle of H_2O_2 decomposition, generating hydroxyl radicals , which oxidize organic

contaminants during the Fenton reaction. Thus, higher iron concentrations may boost hydroxyl radical production and enhance PAH removal rates.[213]

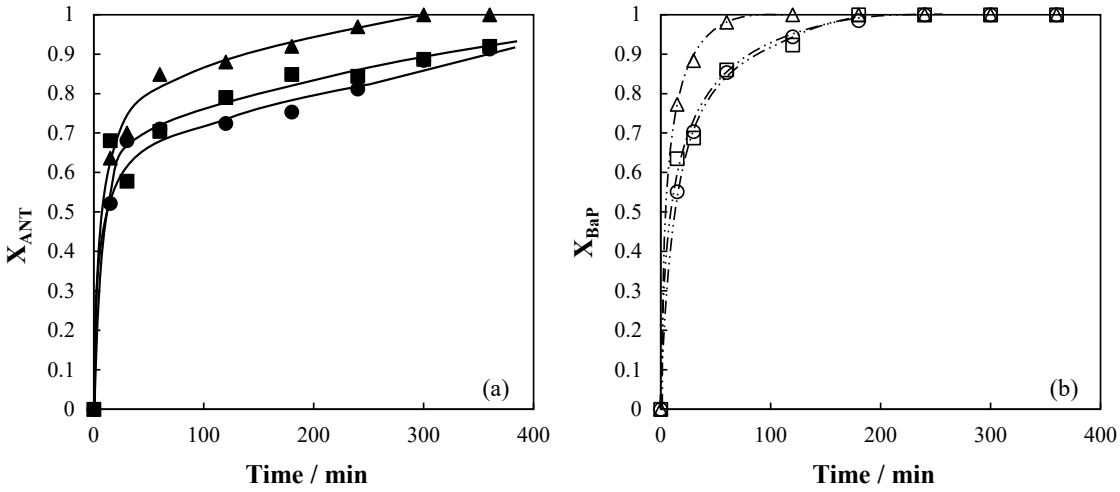


Figure 43: Influence of iron concentration (2.5 (●), 5 (■), and 10 mg dm^{-3} (▲)) on the degradation of PAHs in the emulsion in the Fenton process (E5, E7-E8). $[SDS]_0$ = 4500 mg dm^{-3}; $[ANT]_0$ = 5 mg dm^{-3}; $[BaP]_0$ = 5 mg dm^{-3}; $[H_2O_2]_0$ = 120 mg dm^{-3}, pH=3.

Regarding reagent consumption, the oxidant, catalyst, and pH evolution were monitored during the reactions (data not shown). Despite the initial oxidant concentration, H_2O_2 consumption remained below 30% at 6 hours under all tested conditions . In contrast, the dissolved iron concentration showed significant change, as the pH remained around 3 throughout the 6-hour experiment, preventing iron precipitation.[214]

6.3.3.2 Solar photo-Fenton process: effect of oxidant and catalyst dosage

The photo-Fenton process was evaluated for treating PAH-contaminated emulsions at neutral pH to overcome the challenges of the acidic pH required in the traditional Fenton process. Using a ferrioxalate complex as an activator prevents iron precipitation under circumneutral pH conditions. This complex is formed from iron (III) and oxalate (Eq. 58). Additionally, under solar light irradiation, Fe^{3+} (from the ferrioxalate complex) is reduced to Fe^{2+} (Eq. 59), facilitating the catalytic decomposition of hydrogen peroxide to generate hydroxyl radicals (Fenton reactions).[215]

$$Fe^{3+} + 3C_2O_4^{2-} \rightleftarrows [Fe^{III}(C_2O_4)_3]^{3-} \qquad \textit{Equation 58}$$

$$[Fe^{III}(C_2O_4)_3]^{3-} \xrightarrow{h\nu} Fe^{2+} + 2C_2O_4^{2-} + C_2O_4^{\bullet-}$$ *Equation 59*

First, a series of control experiments were conducted to assess the chemical stability of the PAHs under different conditions: in the presence of the ferrioxalate complex , with both ferrioxalate and H_2O_2 , and under solar light irradiation . The remaining concentrations of PAHs after 6 hours of treatment are shown in Figure appendix. In the absence of light, the ferrioxalate complex had a negligible effect on PAH degradation . Similarly, with H_2O_2 and the ferrioxalate complex , minimal degradation of ANT and BaP (<10%) was achieved at neutral pH (Figure SM2). Under these conditions, the ferrioxalate complex does not generate Fe2+, minimizing the catalytic decomposition of H_2O_2 to hydroxyl radicals at circumneutral pH. The slight PAH degradation observed may be due to the oxidation potential of H_2O_2, as seen in control test .[216]

Organic pollutants can also be degraded through direct light irradiation within a specific spectrum range. The potential of solar light irradiation to degrade the target

The potential of solar light irradiation to degrade PAHs was evaluated . First, the absorption spectra of ANT and BaP were determined, showing a broad absorption spectrum primarily in the UV range from 190 to 450 nm (Figure SM3). Since the solar reactor emits from 350 nm (Figure SM1), these compounds could be partially degraded under solar light. About 15% of the total radiation from the solar photoreactor falls within the 350 to 450 nm range.[217]

The evolution of PAH concentrations during photolysis with solar light showed a slight decrease, with ANT and BaP concentrations reduced by approximately 12% and 22% after 6 hours, respectively . This modest degradation highlights the benefit of combining solar radiation with other technologies like the Fenton process.[218]

The key operating variables in the solar photo-Fenton oxidation treatment (oxidant and iron dosages) were evaluated. Figures 46a and 47b present the conversion of ANT and BaP at initial oxidant concentrations from 60 to 240 mg H_2O_2 dm^{-3}, respectively

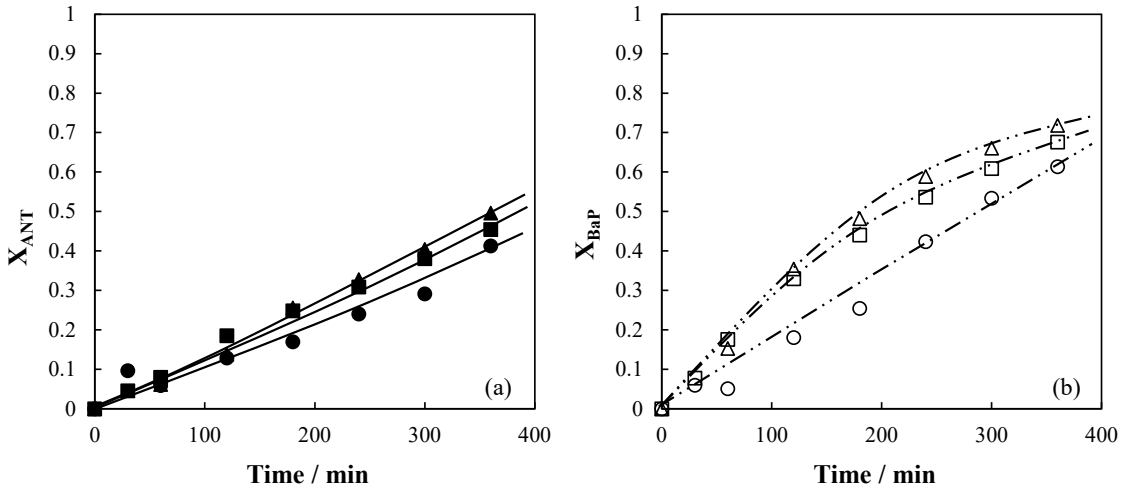


Figure 44:Influence of H_2O_2 concentration (60 (●), 120 (■) and 240 mg dm^{-3} (▲)) on the degradation of PAHs in the solar Photo-Fenton process (E12-E14). $[SDS]_0$ = 4500 mg dm^{-3}; $[ANT]_0$ = 5 mg dm^{-3}; $[BaP]_0$ = 5 mg dm^{-3}; $[Fe]_0$ = 5 mg dm^{-3}, pH=7.

A clear positive effect of the solar photo-Fenton process compared to direct photolysis was observed, with final PAH degradations increasing by approximately 30%. A slight increase in the degradation rate of the pollutants was noted as the oxidant concentration increased. ANT degradation ranged from 28% to 39% (Figure 46a) and BaP from 51% to 59% (Figure 46b) when using oxidant concentrations from 60 to 240 mg H_2O_2 dm^{-3}. These results also confirm the preferential degradation of BaP over ANT during the solar photo-Fenton process at neutral pH.[219]

The limited improvement in PAH degradation with increased oxidant dosage could be attributed to unproductive reactions among oxidants and radicals as the oxidant concentration increases.

The effect of iron concentration was evaluated, maintaining the stoichiometric oxidant concentration for PAH mineralization. PAH conversions over time with iron concentrations ranging from 2.5 to 10 mg dm-3 are shown in Figure 47.[136]

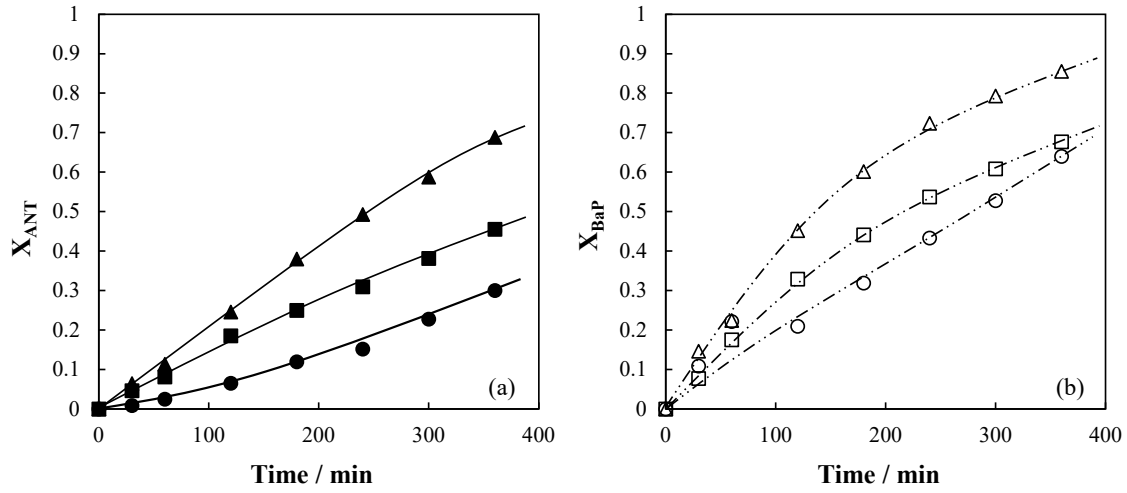


Figure 45: Influence of iron concentration (2.5 (●), 5 (■), and 10 mg dm^{-3} (▲)) on the degradation of PAHs in the solar photo-Fenton process (E15, E13, E16). $[SDS]_0$ = 4500 mg dm^{-3}; $[ANT]_0$ = 5 mg dm^{-3}; $[BaP]_0$ = 5 mg dm^{-3}; $[H_2O_2]_0$ = 120 mg dm^{-3}, pH=7.

The results showed that increasing the iron dosage from 2.5 to 10 mg dm-3 led to a rise in ANT degradation from 30% to 69% over 6 hours (Figure 47a). Similarly, BaP degradation improved significantly from 64% to 86% with the same increase in iron dosage (Figure 47b). These findings indicate that PAH degradation in the photo-Fenton process is more influenced by the catalyst than the initial oxidant concentration. This is likely due to the higher production of Fe^{2+} in the solution, which increases the generation of hydroxyl radicals. Therefore, using higher iron concentrations or extending the reaction time would enhance PAH degradation.[220]

Regarding reagent consumption, the evolution of H_2O_2, Fe^{2+}, oxalate concentration, and pH was monitored during the solar photo-Fenton tests (data not shown). H_2O_2 consumption was below 25% under all tested conditions , slightly lower than in the corresponding Fenton tests. Additionally, there was negligible variation in total iron concentration, as the oxalate concentration (more than 75% of the initial oxalate) was sufficient to sustain the formation of the ferrioxalate complex. Finally, a neutral pH between 6 and 7 was maintained throughout the 6-hour experiments, which is advantageous for the application of the process.[221]

6.3.3.3. Comparison of Fenton and solar photo-Fenton processes

The data from PAH removal during the Fenton and solar photo-Fenton processes were fitted to a pseudo-first order kinetic model (Eq. 60). The results, including kinetic constants and correlation coefficients, are summarized in Table 35.

$$Ln(C_0/C) = k \cdot t \qquad \textit{Equation 60}$$

where, C_0 represents the initial concentration of PAHs (5 mg dm^{-3}), C is the PAHs concentration (mg dm^{-3}) at a given time, k is the kinetic constant (h^{-1}), and t is the reaction time (h).[222]

Table 32:Pseudo-first order kinetic constants calculated for the degradation of PAHs with the Fenton and photo-Fenton processes at different oxidant and catalyst doses.

		Fenton				**Solar photo-Fenton**			
H2O2 (mg dm-3)	**Fe (mg dm^{-3})**	**k_{ANT} (h^{-1})**	**R^2**	**k_{BaP} (h^{-1})**	**R^2**	**k_{ANT} (h^{-1})**	**R^2**	**k_{BaP} (h^{-1})**	**R^2**
60	**5**	0.4325	0.9148	0.9798	0.9623	0.0712	0.9392	0.1435	0.9758
120	**5**	0.4838	0.8872	1.4943	0.9236	0.0973	0.9985	0.1897	0.9997
240	**5**	2.9640	0.9897	3.1795	0.9882	0.1048	0.9905	0.2152	0.9991
120	**2.5**	0.4474	0.8928	1.4801	0.9795	0.0508	0.9711	0.1542	0.9844
120	**5**	0.4838	0.8872	1.4943	0.9236	0.0973	0.9985	0.1897	0.9997
120	**10**	0.9279	0.9634	4.1234	0.9895	0.1785	0.9921	0.3169	0.9992

As expected, the kinetic constants for PAH degradation increased with higher concentrations of both oxidant and catalyst in both technologies. The fit to a first-order reaction was less accurate when using data from the Fenton reagent at pH 3. In contrast, a better fit to a pseudo-first-order reaction and more reliable kinetic constants were obtained from experiments using Solar Photo-Fenton. In this treatment, changes in catalyst concentration had a greater influence on the variation

of the kinetic constants than the hydrogen peroxide dosage. BaP exhibited higher kinetic constants than ANT under all operating conditions[222]

BaP exhibited higher kinetic constants than ANT under all operating conditions. Ultimately, the Fenton process showed approximately twice the degradation kinetics compared to the solar photo-Fenton process, suggesting that the Fenton process may offer a faster alternative for PAH degradation, albeit with the drawback of requiring an acidic pH.

Figure 48summarizes the total PAH degradation achieved (%) by the end of the experimental time for both technologies. As shown, BaP was completely degraded by the Fenton process under all tested conditions. For ANT, the stoichiometric amount of oxidant (120 mg H_2O_2 dm^{-3}) and a catalyst dosage of at least 5 mg dm^{-3} of Fe were necessary.[223]

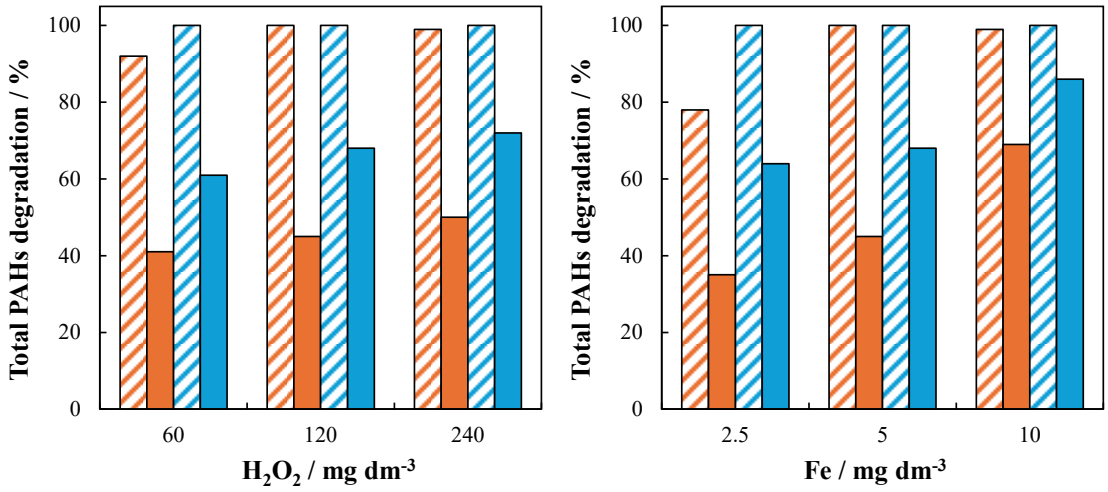


Figure 46:PAHs degradation at 6 h by Fenton and solar photo-Fenton with varying oxidant and catalyst dosages. ANT: orange bars; BaP: blue bars. Fenton: stripped bars; solar photo-Fenton: full bars

Under similar conditions, the solar photo-Fenton process yielded more moderate results, with ANT removal ranging from 35% to 70% and BaP removal from 60% to 85% across the various operating conditions studied.Overall, the Fenton process consistently achieved higher final The degradation rates for both ANT and BaP were higher in the Fenton process compared to the solar photo-Fenton process

under all tested conditions. Notably, BaP degraded faster than ANT at various oxidant and catalyst dosages in both technologies. Previous studies have suggested that PAH characteristics influence degradation efficiencies in Fenton oxidation. Typically, low molecular weight PAHs (2-3 rings) like ANT are considered less recalcitrant and easier to degrade than high molecular weight PAHs (4-6 rings) like B[208]. This typical pattern contrasts with the results observed in this study. However, other research using different technologies, such as activated persulfate, has reported the opposite behavior—a higher degradation rate associated with an increased number of rings . Furthermore, BaP has been reported to have a higher affinity for hydroxyl radical oxidation than other PAHs with a similar or even lower number of rings, possibly due to BaP's higher ionization potential [224]. In this context, the degradation kinetics of PAHs seem to be primarily influenced by both the molecular structure and the technology employed for their degradation.

6.3.3.4. Reuse of treated emulsions

The hydroxyl radicals generated during Fenton and photo-Fenton processes are not selective and can degrade both the target contaminants and the surfactants in the emulsion [135]. Recovering surfactants from emulsions treated with oxidation processes is crucial both economically and environmentally. Surfactants are used in large concentrations to enhance the solubility of hydrophobic contaminants, and their recovery can significantly reduce operational costs by enabling their reuse in subsequent treatment cycles.

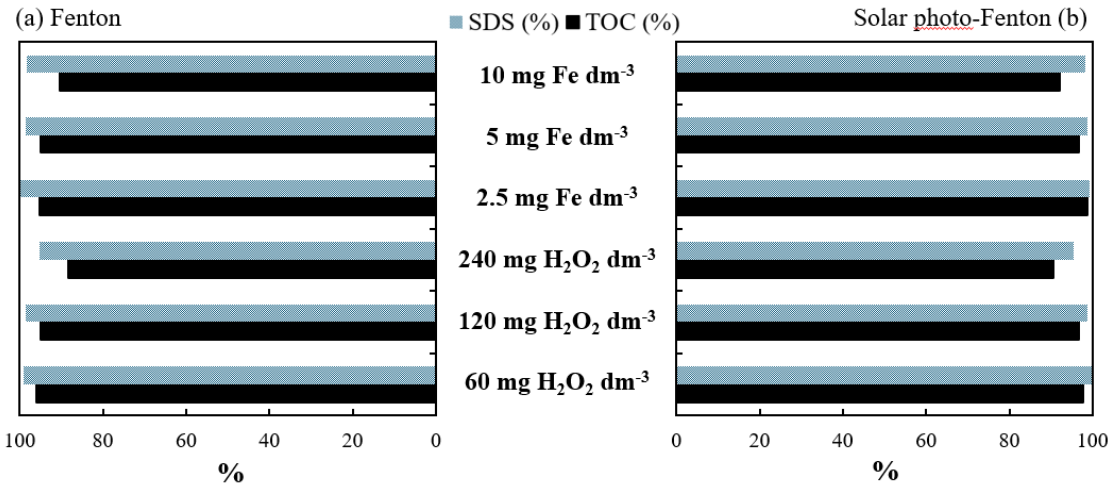
In this context, the concentration of SDS in the emulsion was indirectly measured for both processes by quantifying sulfate or sulfonate groups (the anionic part of SDS) using the methylene blue test, while the integrity of the alkyl chain (the hydrophobic portion of the surfactant) was assessed through total organic carbon (TOC) analysis. The surfactant activity of SDS depends[215].

The functionality of SDS depends on both the sulfonate groups and the alkyl chain, making the integrity of both crucial. Figure 8 shows the results for sulfonate groups (SDS) and TOC at the end of the reaction time under different conditions for the Fenton and solar photo-Fenton processes.

The sulfonate groups of SDS remained nearly intact after the oxidation processes under all tested conditions, indicating that the anionic part, essential for its surfactant function, is resistant to the oxidative environment. [179]Conversely, TOC depletion was minimal. Only at the highest hydrogen peroxide concentration (240 mg H_2O_2 dm^{-3}) was a slight decrease observed in SDS concentration (4% for both processes) and TOC (11% for Fenton and 9% for photo-Fenton). This slight decrease can be attributed to the higher concentration of hydroxyl radicals generated with increased oxidant dosage. Despite this, the mineralization of the SDS emulsion was negligible, suggesting that the alkyl chain remained largely intact, and the surfactant's overall integrity was preserved after both Fenton and photo-Fenton treatments. Although some oxidation of the alkyl chain might have occurred, low levels of surfactant mineralization were achieved.[225]

The surfactant capacity of the treated emulsions under medium conditions (120 mg dm^{-3} H_2O_2 and 5 mg dm^{-3} Fe) was evaluated by comparing the critical micelle concentration (CMC) of the initial emulsion (4500 mg dm^{-3} SDS and 10 mg dm^{-3} PAHs) with those of the resulting emulsion after Fenton and photo-Fenton treatments. This comparison assessed whether the surfactant's ability to form micelles remained unchanged from the initial to the treated emulsion, indicating if its functional integrity was preserved after the oxidation treatments. The surface tension of the treated emulsions and the CMC values obtained after the Fenton and photo-Fenton tests were equivalent (variations <10%) to those of the initial emulsion (1925 ± 126 mg dm^{-3}), confirming the high stability of the surfactant capacity of SDS after the oxidation treatment. Therefore, the treated emulsion could be reused in subsequent soil washing. In this regard, the presence of H_2O_2 in the emulsions would not pose a problem due to the low content and quick decomposition.[225]

upon contact with soil. For Fenton treatment, acidifying the emulsion after the soil washing step may be necessary due to the high carbonate content of the soil. Both technologies showed promising results, allowing the treated emulsion to be reused for solubilizing PAHs in successive processes.[226]



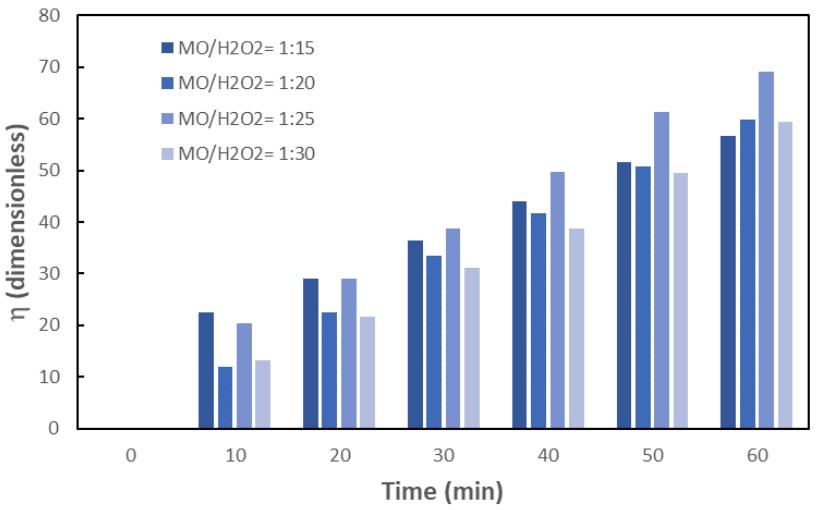
.Figure 47:Surfactant capacity of the emulsion (SDS and TOC) after the (a) Fenton and (b) solar-Fenton processes at different oxidant and catalyst doses. CMC values remain unchanged after oxidation treatment.

6.4 WATER REUSE RESULTS

The previously described experimental apparatus was used to conduct cavitation tests on various dyes, both in standalone and hybrid configurations. Here, we present aggregated results for two contaminants, methyl orange (MO) and methylene blue (MB), focusing on the effect of inlet pressure (0.2-0.5 MPa) using HC in a standalone configuration[19]. The results are expressed in terms of removal efficiency, defined as:

$$\eta = \frac{C_0 - C_t}{C_0}$$

the figure bellow illustrates the positive effect of inlet pressure on all tested contaminants. As pressure increases, the removal rate also increases, reaching a maximum efficiency at pressures between 0.3-0.4 MPa, beyond which efficiency starts to decline. This trend is consistent with literature findings for other compounds, where increased HC efficiency in removal can be attributed to enhanced OH radical production due to intensified cavitation activity at higher pressures. However, beyond certain pressure values, this positive effect diminishes, and efficiencies begin to decrease. Figure 3 shows the degradation efficiency of the tested compounds as a function of the cavitation number.[227]



The plot of hydraulic curve can be divided into three regions, separated by a transition zone. On the right side, there is a region where no cavitation occurs because the cavitation number (Cv) exceeds unity for inlet pressures below 0.3 MPa, resulting in very low degradation efficiencies (below 3%) for all tested compounds. In the central zone, the cavitation number (Cp) falls below unity as the upstream pressure increases due to the greater kinetic energy of the circulating liquid. To ensure cavitating conditions, experiments are conducted at inlet pressures well above 0.2 MPa and Cv < 0.8. In this zone, as pressure increases and Cv decreases, degradation efficiencies for all tested compounds increase up to a maximum before starting to decline. This phenomenon, known as choked cavitation, characterizes the left region of the plot. It was observed that cavitation for Cv < 0.4 is located on the decreasing branch of the curves and is characterized by many cavities merging to form vapor bubbles without collapsing to produce radicals useful for the oxidation reaction. in the choked cavitation zone degradation efficiencies decrease significantly. this confirm that there is range of Cv in which cavitation experiments have to be carried of cv in which cavitation experiments have to be carried out in for the specific device independently, the range is 0.3 – 0.6 MPa. However, by reading of Figs 2 and 3, it appears that for all tested molecules, the removal efficiencies with using only cavitation after 60 min of treatment time are in the range 30%-35% at the optimal pressure values (MO, MB). For the same contaminant MO, experimental results carried out in hybrid configurations with

adding hydrogen peroxide in the same experimental apparatus have shown that the degradation efficiencies grow up significantly .AS for example, Fig shows the degradation efficiency of MO in the cavitation device with different concentration of H_2O_2 added in solution [228]

As can be seen from the analysis of FIG 4, the value of MO/ H_2O_2 molar ratio equal to 1:25 with a treatment time 60 min appears to be as the optimal dosage. The worsening of performance at higher hydrogen peroxide concentration is due to recombination of OH radicals, as possible negative outcome of the oxidant which may react with the hydroxyl radicals thus decreasing the radicals present in the solution, destined to degrade methyl orange.[83]

Moreover , the efficiency of hydrodynamic cavitation process in the presence of the metals (iron and nickel) and hydrogen peroxide (0.005%v/V) of hydrogen peroxide , iron (20 mg/L) and nickel (10 mg/L)= 0.4MPa , was tested ,showing that combining HC, H_2O_2 and metals, the degradation yields were near to 90% , meaning that the presence of iron induced an advanced Fenton process which improved the efficiency of the entire process of cavitation

6.5 . PROCESS ANALYSIS

Another goal of the thesis was to conduct a process study to investigate the technical feasibility of the treatment processes under investigation. The analysis was carried out for two types of effluents: textile and pharmaceutical. For the latter, no experimental studies were conducted, but technical data from a real plant, Takeda Italia, were collected.

The following part discusses the process analysis for real-world wastewater treatment. The commercial software SuperPro Designer was utilized to conduct this investigation. Two scenarios were investigated: the existing traditional method (first scenario) and a new technique that integrated hydrodynamic cavitation (HC) with the advanced oxidation process HC+O3+H2O2 (second scenario). The textile firm gave data for the traditional process. Incorporating hydrodynamic cavitation into existing industrial processes could be a novel

technique to efficiently treating textile wastewater.

6.5.1 TEXTILE WASTEWATER

Process Analysis is discussed below, considering a real wastewater, whose average characteristics are reported in section of textile treatment .it is a real wastewater taken from textile industry, which operates in Abruzzo region.

Two different cases were investigated: one involving hydrodynamic cavitation HC process alone, the second adding a mixture of H_2O_2 +Ni+Fe before HC occurs. The aim of both plants is the production of a high -quality water reusable for industrial purposes, in particular in textile industry

Fig 48 a and b shows the process flow diagram proposed for both cases.

The two schemes share the following steps .the stream n.1 ,which is the dyeing wastewater effluent produced by the textile industry and characterized , undergoes a screening operation ,which is able to reduce the biochemical oxygen demand (BOD) and the total suspended solids (TSS) values .the most efficient fine screen devises are the rotary drums ,which are often used to replace primary sedimentation.Typical data about removal percentage spam with 25%-50% for BOD and 25-45% for TSS [229] . considering a mean value, the BOD of stream n.2 decreases from 10 mg/L until 6.3 mg/L.

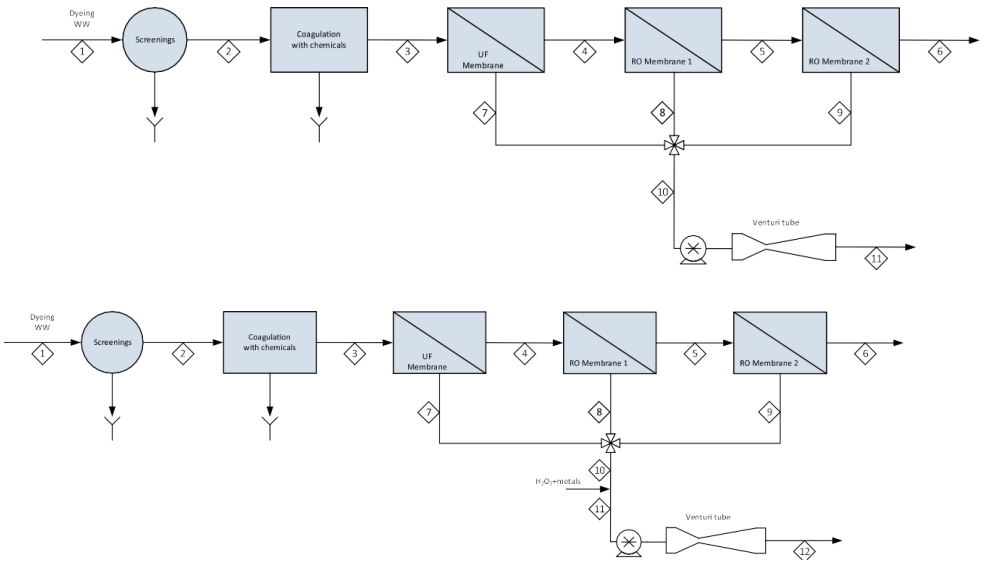


Figure 48:(a) Process analysis with hydrodynamic cavitation alone and (b)q process analysis with hydrodynamic cavitation preceded by adding a solution of H2O2 +metals*

Subsequently, the effluent is subjected to a coagulation process with chemicals. different substances can be added to the wastewater, ferric chloride, ferric chloride with lime and ferric sulphate with lime. Anyway, if they are correctly dosed, if the mixing is efficient and the process is properly controlled, TSS may be reduced from 80% to 90%, while BOD from 50% to 80% [230], [231]. Again, considering the mean values, the BOD and TSS of Stream

Reduce respectively to 2.2 and 146 mg/L. These preliminary steps are followed by tangential membrane sections, which consist of three different stages : the first is an ultrafiltration process (UF), while the next two are both reverse osmosis (RO). During the UF step the incoming effluent named n.3 is divided into permeate and retentate streams. Here it is crucial to make the correct choise of the module, in terms of material and MWCO, the dyes inside wastewater usually show a rejection of about 97%, if the membrane material is made of polysulfone with MWCO greater than 700 Da.Simultaneously, this configuration permits us to reach an interesting reduction of both chemical oxygen demand (COD;75%-80%) and total organic carbon TOC (50%-60%). Finally, UF realizes the almost total rejection of residual TSS and surfactant amounts. Consequently, stream n.4, that is the permeate stream of UF membrane, shows these characteristics: COD 28 mg/L, TOC 29 mg/L, TSS 0 mg/L, TOTAL SURFACTANT 0 mg/L.Ro is the most selective tangential membrane process. A typical performance summary is shown in table 33.

Table 33:Typical performance summary for reverse osmosis process

Parameter	***Average Reduction [%]***	***References***
COD	***94***	***[31]***
BOD	***30-60***	***[32]***
TOC	***90-98***	***[26]***
Cl^-	***98.9***	***[33]***
NO_3^-	***84-86***	***[26]***
SO_4^{2-}	***99.8***	***[31]***
PO_4^{3-}	***99***	***[32]***
Colour	***90-96***	***[26]***

With the average reduction showed above the n.5 permeate stream is a good quality water, except for Cl^- concentration as its value still too high (1.54 mg/L). This is the reason why the second RO membrane module is necessary, by which not only the Cl^- concentration decreases to very low value (0.0169 mg/L), but also other parameters improve further, to obtain a high -quality effluent water that can be reused for industrial purposes or even discharged in superficial water .its characteristics are reported in table 36 . the three retentate streams n.7 ,8 and 9 are mixed all together and they undergo a different treatment , as shown in fig 5a and b . referring to fig 50.a the stream n 10 is treated in hydrodynamic cavitation reactor, with proper value of pressure and time as defined in the experimental section (inlet pressure p= 0.4 MPa, treatment time t=60 min).

The HC alone is able to reduce TOC amount to 87% [80]and the COD almost by 15% [168]. Furthermore ,, this process is effective on colour reduction reaching a percentage decrease between 30%-35% , in case of pressure range between 0.3-0.4 MPa .Even ions in solutions May be strongly lowered , as showed by [167] etall: they can chemically interact with OH^- radicals ,giving rise to the following perecentage reductions :Cl^- 69.5%, NO_3- 94.3% , SO_4^{2-} 98.6%, PO_4^{3-} 90.6%.

Table 34reports the characteristics of stream n.11. There are some critical values in terms of TSS,$Cl.^-$ and colour which make this stream not suitable to be reused even for textile industrial applicatioms .A further process is necessary ,for example an adsorption on active carbon to improve the effluent and make him suitable for water reuse

Table 34:The characteristics of stream

Parameter	***Concentration Stream n.6***	***Concentration Stream n.11***	***Concentration Stream n.12***
COD,mg/L	***0.10***	***7***	***119***
BOD,mg/L	***0.66***	***1.53***	***1.53***
TSS,mg/L	***0.00***	***146***	***146***
TOC,mg/L	***0.10***	***8.53***	***8.37***
Cl^-,mg/L	***0.0169***	***43***	***140***
NO_3^-,mg/L	***0.14***	***0.33***	***6.01***
SO_4^{2-},mg/L	***0.000690***	***2.4***	***172.6***
Total surfactant ,abs	***0.00***	***4.0***	***4.0***
PO_4^3 ,abs	***0.0000253***	***0.024***	***0.253***
Colour ,abs	***0.00***	***4.0***	***4.0***

Better performances may be obtained if hydrodynamic cavitation process is performed in presence of both hydrogen peroxide and metals .Authors using 0.005 %v/v of H_2O_2 together with 20 mg/L of iron and 10 mg/L of nickel ,with an inlet pressure of 0.4 MPa , reached a colour degradation yield of about 90% .This satisfactory results was due not only to presence of hydrogen peroxide which favours the formation of more OH^- free radicals , that are available to degrade organic substances . In addition , the presence of metals promotes the reaction with oxygen, to produce further OH- radicals ,which react with the dye allowing to achieve such a degradation yield .further benefits were also found by Agarkoti et al. who added H_2O_2 and metals inside the wastewater before HC occurs ,achieving a COD reduction yield until 95% with proper Fe/H_2O_2 ratio .Table 34 shows the characteristics of stream n.12 of Fig 48b.

Looking at table 36 its is possible to notice that stream n.12 of Fig .50b is highly improved if compared with stream n.11 of Fig 50a in terms of colour ,TOC and COD reduction .Anyway there is still a critical value which is the concentration of chlorine ion (43mg/l Table 34).Another step of HC , optimized to remove Cl^- ,will be able to make also this stream suitable for textile industrial reuse reaching the target of zero waste discharge process ZLD.

6.5.2 PHARMACEUTICAL WASTEWATER OF TAKEDA

Introduction

The pharmaceutical industry plays an indispensable role in global health and well-being by providing essential medications for the treatment and prevention of diseases. However, the manufacturing processes in this industry generate wastewater containing a variety of pollutants, including residual pharmaceuticals, solvents, heavy metals, and organic compounds. These pollutants can have significant impacts on the environment and human health if not properly treated.

Treating pharmaceutical wastewater presents unique challenges due to the complexity and variability of the pollutants present. Conventional wastewater treatment methods are often inadequate for removing these pollutants, necessitating the development and optimization of advanced treatment technologies.

Simulation is crucial in the design, evaluation, and optimization of pharmaceutical wastewater treatment plants. By employing mathematical and computer models, engineers can simulate the behaviour of different treatment processes, assess their effectiveness, and identify optimal conditions for maximum pollutant removal. Simulation also allows for the exploration of various design and operational scenarios, helping to minimize costs and the environmental impact of wastewater treatment.

Pharmaceutical companies such as Takeda prioritize comprehensive wastewater management to address a variety of pollutants originating from their manufacturing processes. These include nitrogen compounds like ammonia nitrogen and nitrates, which can exert oxygen demand in water bodies if not properly treated, potentially violating environmental standards. Additionally, pollutants such as Chemical Oxygen Demand (COD), Biochemical Oxygen Demand (BOD), Total Organic Carbon (TOC), and Total Suspended Solids (TSS) are critical concerns. High levels of COD indicate the presence of organic pollutants that can deplete oxygen, while elevated BOD suggests a greater organic load that may harm aquatic ecosystems. TOC measurements are crucial as organic compounds can act as nutrients, contributing to eutrophication if discharged untreated. Excessive TSS can impair water quality by reducing clarity and impacting aquatic habitats. By employing advanced physical, chemical, and biological treatment processes, pharmaceutical firms strive to mitigate these pollutants to meet regulatory standards, minimize environmental impact, and demonstrate their commitment to sustainable wastewater management practices and environmental stewardship.

The primary objective of this study is to provide a thorough understanding of the challenges and opportunities related to pharmaceutical wastewater treatment and to demonstrate the crucial role of simulation in the design and operation of efficient and sustainable treatment systems.

The simulated plant employs a combination of advanced treatment technologies to effectively remove pollutants from pharmaceutical wastewater. These technologies include:

Advanced Oxidation: Advanced oxidation processes, such as the Fenton process, are used to decompose refractory organic pollutants into less harmful by-products.

The Fenton process utilizes a combination of hydrogen peroxide and iron to generate highly reactive hydroxyl radicals that can oxidize a wide range of organic pollutants.

Membrane Filtration: Membrane filtration, such as ultrafiltration and reverse osmosis, is used to remove suspended solids, colloidal matter, and dissolved pollutants from the wastewater. These processes use semi-permeable membranes to physically separate pollutants from the water.

Biological Treatment: Biological treatment processes, such as activated sludge and membrane bioreactors (MBR), are used to remove biodegradable organic matter from wastewater. These processes employ microorganisms to break down organic matter into carbon dioxide, water, and biomass.

By integrating these advanced treatment technologies, the simulated plant aims to achieve a high level of pollutant removal and produce an effluent that complies with environmental standards

6.5.2.1 THE TAKEDA WASTEWATER TREATMENT PROCESS (WWT)

The Takeda Process is a single-sludge system designed to enhance the removal of pollutants from wastewater. It consists of three zones in series: an anoxic zone, a biological treatment zone, and an ultrafiltration zone. The process operates as follows: The first zone is an anoxic zone where denitrification occurs, designed to remove nitrogen compounds from the wastewater. The second zone is a biological treatment zone where microorganisms break down organic matter in the wastewater. The third zone is an ultrafiltration zone where suspended solids, colloidal matter, and high molecular weight solutes are removed from the wastewater. Mixed liquor is recycled from the ultrafiltration zone back to the anoxic zone at a rate of four to six times the influent flow rate. Return activated sludge is also recycled from the clarifier back to the anoxic zone. This process aims to achieve high levels of pollutant removal and produce an effluent that meets environmental standards.

In the real Takeda's Wastewater Treatment Plant (WWTP), there are two tanks where the logic of alternating cycles is implemented. In these tanks, an oxidation/nitrification phase alternates in sequence with a reductive phase

denitrification. This alternating cycle enhances the efficiency of nitrogen removal and overall treatment performance. However, for simplification purposes, this sketch does not include these details as it shown in the The P&I of Takeda Plant (appendix A)

Case 2: Integration of Hydrodynamic Cavitation In this case, the Takeda Process is enhanced by integrating hydrodynamic cavitation after the ultrafiltration zone while keeping the same system configuration. Hydrodynamic cavitation involves the formation, growth, and implosive collapse of vapor bubbles in a liquid, which generates intense local energy and enhances the breakdown of pollutants. The first zone remains an anoxic zone for denitrification. The second zone remains a biological treatment zone for the breakdown of organic matter. The third zone remains an ultrafiltration zone for the removal of suspended solids and colloidal matter. After ultrafiltration, the wastewater undergoes hydrodynamic cavitation to further enhance the removal of pollutants. Mixed liquor is recycled from the hydrodynamic cavitation zone back to the anoxic zone at a rate of four to six times the influent flow rate. Return activated sludge is also recycled from the clarifier back to the anoxic zone. This integrated process aims to achieve even higher levels of pollutant removal and produce an effluence that exceeds environmental standards

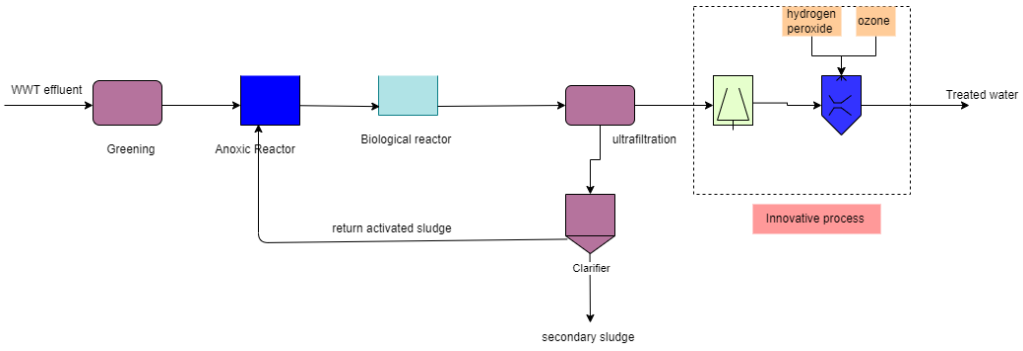


Figure 49 : The Takeda process

6.5.2.2 Takeda Wastewater Treatment Process Simulation using SuperPro Designer

The Super Pro Design software (version 9.0 was used for the simulation presented within this article), by Intelligent Inc. USA, is a computer simulator tool package

that tracks the behaviour of chemicals in individual and combinations of unit operations. Within this software database, various chemicals are provided, and also it has the allowance to insert new ones. As it has a variety of procedure operations with different kinds of equipment, can be easily used for the design and simulation of a working plant in either batch or continuous operation mode. Based on the all the chemical reactions involved within a process, this software allows the mass and energy balance estimation for all streams of the process, estimates purchase costs, and reports stream and equipment data, as well as capital and manufacturing costs. A compressive description of the software and also its way of operating various processes are fond in the user's guide of each version of this tool.

An existing wastewater treatment plant, modelled in SuperPro Designer, is designed to handle an average flow of 2400 m^3/day. The equipment and dimensions are as follows:

- **Anoxic Reactor (AXR-101)**: unit with a volume of 3,444,320.07 L, constructed from concrete. This reactor plays a crucial role in reducing the nitrogen content in wastewater through anoxic conditions.
- **Aeration Basin (AB-101)**: unit with a volume of 5,740,092.43 L, constructed from. The aeration basin is essential for promoting the growth of aerobic bacteria, which helps in breaking down organic matter.
- **Clarifier (CL-101)**: unit with a surface area of 2.78 m^2, constructed from concrete. The clarifier helps in the separation of solids from the liquid, ensuring clearer effluent.
- **Ultrafilter (UF-101)**: 86 units, each with a surface area of 49.83 m^2, constructed from SS316. These ultrafilters are used to remove fine particles and microorganisms from the wastewater.
- **Centritech Centrifuge (CF-101)**: 17 units, each with a capacity of 99.15 L/h, constructed from SS316. The centrifuges are used for dewatering sludge, reducing its volume and making it easier to handle.

- **Mixers (MX-101 and MX-102)**: 2 units, with capacities of 515,060.52 kg/h and 71,050.12 kg/h respectively, constructed from CS. These mixers ensure thorough mixing of wastewater with treatment chemicals or other additives.
- **Flow Splitter (FSP-101)**: 1 unit with a capacity of 444,064.45 kg/h, constructed from CS. The flow splitter evenly distributes the flow of wastewater to different treatment units.
- **Centrifugal Pump (PM-101)**: 1 unit with a power of 12.73 kW, constructed from SS316, This pump is used to move wastewater through the treatment process.
- **Generic Boxes (GBX-101 and GBX-102)**: 2 units, each with a capacity of approximately 71,050 kg/h, constructed from CS. These generic boxes serve as placeholders for various treatment stages or storage units.

This setup, as represented in SuperPro Designer, ensures efficient processing and treatment of wastewater, leveraging a combination of advanced filtration, mixing, and separation technologies. The integration of these units allows for the effective removal of contaminants, ensuring that the treated water meets environmental standards

The following stoichiometry and kinetic constants in the aeration basin and aerobic digester are:

The following stoichiometry and kinetic constants in the anoxic reactor and biological oxidation processes are:

Anoxic Reactor

a) **Denitrification** (the stoichiometry is on a mass basis):

$$62.00NO3 + 34.60DomWas \rightarrow 33.40CO2 + 13.20N2 + 42.60H2O + 7.40Xvssh$$

Reaction Type: Monod, **Ks**: 0.44 mg/L, **k**: 0.02 h^{-1}

Biological Oxidation

Substrate (DomWaste) Degradation (the stoichiometry is on a mass basis):

$$0.10NH3 + 1.00DomWaste + 1.40O2 \rightarrow 0.90CO2 + 0.80H2O + 0.80Xvssh$$

Reaction Type: Monod, **Ks**: 5 mg/L, **k**: 0.066 h^{-1}

Nitrification (the stoichiometry is on a mass basis):

$$7.50NH3 + 1.80CO2 + 24.60O2 \rightarrow 25.20NO3 + 7.70H2O + 1.00Xvssh$$

Reaction Type: Monod, **Ks**: 1.4 mg/L, **k**: 0.04 h^{-1}

Degradation of X-vss-h (the stoichiometry is on a mass basis):

$$1.15O2 + 1.05Xvssh \rightarrow 0.10NH3 + 1.45CO2 + 0.45H2O + 0.20Xvssi$$

Reaction Type: First-order, **k**: 0.002 h^{-1}

Degradation of X-vss-n (the stoichiometry is on a mass basis):

$$15O2 + 1.05Xvssn \rightarrow 0.10NH3 + 1.45CO2 + 0.45H2O + 0.20Xvssi$$

Reaction Type: First-order: 0.002 h^{-1}

These reactions and kinetic constants are crucial for modeling and optimizing the performance of the wastewater treatment processes in SuperPro Designe

Integration of Hydrodynamic Cavitation

The process studied in the laboratory was simulated in SuperPro Designer and integrated into the process currently used at Takeda. The data for the incoming stream of textile wastewater are similar to the simulation of the current plant. After the ultrafiltration module and using a mixer (MX-102), it is combined with hydrogen peroxide and ozone at the optimal concentrations found through experimentation. The simulated process flow diagram is shown in the Appendix A: The flowsheet of Takeda's wastewater treatment plant

The output stream continues its path in the plant, while another stream containing solids must be disposed of. The stream is then sent to a pump (PM-101) that raises the liquid pressure to 4.5 bar, which is the optimal pressure for maximum degradation yield in the cavitation reactor. Once the appropriate operating

conditions are reached, the incompressible fluid is sent to a generic box (GBX-102), which corresponds to the hydrodynamic cavitation reactor. The reactions that occur are as follows:

- **Water Splitting**: As it passes through the constriction of the cavitation reactor, vapor bubbles are created that implode violently, causing the water to split (yield set at 2%):
  - $H_2O \rightarrow H\cdot + OH\cdot$ Eq (4.8)
- **Radical Formation from H_2O_2 and Ozone** (also with a yield of 2%):
  - $H_2O_2 \rightarrow 2\,OH\cdot$
  - $O_3 \rightarrow O + O_2$
  - $O_2 + H_2O \rightarrow 2\,OH\cdot$

Wastewater Degradation: The highly reactive radicals react with the pollutant particles in the wastewater, forming degradation products that are more easily degraded by bacteria in secondary treatments:

$$1\,WWT + 1\,OH \rightarrow 1\,prod\ degradation$$

- **Final Degradation**: The degradation products react with OH radicals to form carbon dioxide and water with a yield of 82%.
  - $Prod\ degradation + OH\cdot \rightarrow CO_2 + H_2O$

6.5.3 RESULTS AND DISCUSSION

A process analysis is discussed below. Considering a real wastewater from Takeda, whose average characteristics are reported in Tab.35

Table 35: Characteristics of effluent

Parameter	Value	Unit
pH	***5.5-10***	**-**
Total suspended solids (TSS)	***1274.32***	***mg/L***
Chemical oxygen demand COD	***2508***	***mg/L***
Total Organic carbon TOC	***758.57***	***mg/L***
Biochemical oxygen demand BOD_5	***1029.31***	***mg/L***
Ammonium	***20.77***	***mg/L***
Chloride	***49.43***	***mg/L***
Nitrate	***37.33***	***mg/L***

Two different cases were reported: one the standard process existing ,the second involves the integration of Hydrodynamic cavitation adding the Hydrogen peroxide and the ozone to enhance the radicals production. The wastewater treatment process for pharmaceutical manufacturing (Stream S101) effluents begins with screening operation which able to reduce the BOD and total suspended solid (TSS) and anoxic reactor, followed aerobic reactor followed by and ultrafiltration (UF) stages. Initially, Stream S101 exhibits high levels of key parameters: TOC (758.3 mg/L), COD (2508 mg/L), BOD5 (1029.32 mg/L), TSS (1274 mg/L), and TS (1304 mg/L). After standard treatment, Stream S-110 shows significant percentage reductions: TOC (99.29% reduction), COD (99.41% reduction), BOD5 (99.24% reduction), TSS (99.16% reduction), and TS (91.45% reduction) (Table 34). To further enhance water quality, hydrodynamic cavitation (HC) is integrated after UF, resulting in Stream S-126 where all parameters are completely degraded to zero (Table 2). This HC process achieves 100% degradation rates for TOC, COD, BOD5, TSS, and TS, indicating thorough removal of contaminants. These results underscore the efficacy of integrated treatment approaches in achieving high-quality effluent suitable for reuse or environmentally responsible discharge, aligning with sustainability

objectives and regulatory requirements

Table 36: Concentration of Parameters Before and After Treatment

Parameter	Stream S101 (mg/L)	Stream S110 (mg/L)	Stream S126 (mg/L)
TOC	758.3	5.4	0
COD	2508	14.83	0
BOD5	1029.32	7.84	0
TSS	1274	10.65	0
TS	1304	111.43	0

Table 37: Degradation Rates Achieved Through Hydrodynamic Cavitation (HC)

Parameter	Stream S110 (mg/L)	Stream S126 (mg/L)	Average Degradation Rate (%)
TOC	5.4	0	99.29
COD	14.83	0	99.41
BOD5	7.84	0	99.24
TSS	10.65	0	99.16
TS	111.43	0	91.45

Enhanced performance can be achieved if the hydrodynamic cavitation process is conducted in the presence of both hydrogen peroxide and ozone. Researchers, using 2 kg/h of H_2O_2 together with 0.10 kg/h of ozone, with an inlet pressure of 0.4 MPa, achieved a complete degradation. This impressive result is attributed not only to the presence of hydrogen peroxide, which facilitates the formation of additional OH- free radicals that degrade organic substances, but also to the presence of ozone. Ozone promotes the reaction with oxygen, generating further OH- radicals, which react with the dye, resulting in such a achieving complete COD degradation. This detailed approach highlights not only the substantial reduction in pollutant concentrations through conventional treatment methods but also emphasizes the critical role of advanced technologies like hydrodynamic cavitation in achieving near-complete removal of contaminants. The findings underscore the potential for such integrated systems to meet stringent environmental standards, support sustainable water management practices, and contribute to the preservation and protection of water resources.

6.5.3.1 Operational Costs (OPEX)

The Operating Costs (OPEX) of the wastewater treatment plant represent the annual expenses required for its operation. These costs are crucial for the financial planning and sustainability of the facility. The main components of the OPEX are detailed below:

1. Electricity Costs: Energy costs are determined by assessing the power consumption of all installed equipment, including pumps, compressors, mixers, and other machinery [1].

The consumption is calculated by multiplying the installed power of each equipment by its average annual operating hours [1].

Key energy-consuming areas include the equalization unit, the biological compartment, the ultrafiltration unit, and the sludge line [2-4].

The compressors for oxidation and MBR are the largest consumers of energy [2, 3].

The total annual energy consumption for the plant is 6,359.91 kWh/g, with a cost of 0.07 €/kWh, leading to an annual electricity cost of approximately €162,495.00 [4].

2. Sludge Disposal Costs:

The cost of sludge disposal depends on the nature of the sludge, with an assumption of assimilability to urban waste in this case [5].The daily production of wet sludge is estimated to be 4.8 m^3/day [5].

Based on a typical urban waste disposal cost of €120/m^3, the annual cost for sludge disposal is approximately €180,000.00 [5].

3. Chemical Reagent Costs:Chemical reagents are used for various purposes, including conditioning the influent, improving sludge dewaterability, and cleaning the ultrafiltration membranes [6].The chemicals used include hydrochloric acid, nutrient mix, citric acid, sodium hypochlorite, and polyelectrolyte [6, 7].The costs for these chemicals are calculated based on their annual consumption and unit cost [6].

The total annual cost for chemical reagents is approximately €103,820.00 [7].

4. Plant Supervision and Management Costs:

The plant is designed to be highly automated and self-regulating, with most equipment having active backups [7]. Control and remote monitoring are provided through a PLC and SCADA system [7].

The automated systems and remote monitoring allow for a reduction in the required personnel for operation, therefore, the plant requires only minimal daily inspections [7].

The annual cost for personnel is estimated to be €22,000.00, based on a daily commitment of two hours by an operator and a substitute [7].

Total Annual Operating Costs (OPEX):

The total annual operating cost of the plant is the sum of electricity, sludge disposal, chemical reagents, and personnel costs [8].The summarized annual OPEX is approximately €468,315.00 [8]The operational costs of the treatment plant are a significant consideration, encompassing energy consumption, sludge disposal, chemical usage, and personnel costs.[93], [227]

Energy Consumption: The plant's energy consumption is detailed, with major consumers including pumps, compressors, and the ultrafiltration system. The total annual energy cost is estimated at €162,495. In summary, the OPEX is composed of various components, with electricity and sludge disposal as the most significant costs. The chemical and personnel costs are also important contributors. The plant's design emphasizes automation and efficiency to minimize operational costs while ensuring effective wastewater treatment.

Concluding comments

This report presents the findings of a process analysis on the integration of membrane processes and hydrodynamic cavitation for treating industrial wastewater of Takeda (WWT). Based on the degradation efficiency WWT in an experimental setup with a Venturi orifice, an integrated treatment cycle is simulated. In this cycle, dyeing wastewater is pre-treated, filtered through a membrane operation, and subjected to an advanced oxidation process (AOP) with hydrodynamic cavitation in a hybrid configuration. The material balance across

different stages of the treatment train demonstrates that integrating membranes and hydrodynamic cavitation in a hybrid configuration (cavitation with H_2O_2 and ozone treatment) results in clean water that can be reused as process water and a concentrated stream that, after tertiary treatment, can be safely discharged**.**

7. CONCLUSIONS

This doctoral research has successfully developed and evaluated a range of effective treatment methods for the removal of organic pollutants (i.e dyes, phenols, hydrocarbons) from several types of industrial wastewater, mainly textile and winery effluents.The literature review provided an in-depth analysis of various treatment methods. Physicochemical techniques such as adsorption, membrane filtration, coagulation-flocculation, and ion exchange were thoroughly examined. Advanced oxidation processes (AOPs), including photocatalysis, chemical oxidation, and electrochemical treatment, were also explored for their potential in waste treatment. Additionally, biological methods, such as microbial degradation and enzymatic approaches, were discussed for their effectiveness in breaking down pollutants.

For hydrocarbon treatment, the research focused on bioremediation, phytoremediation, and chemical methods. These approaches were evaluated for their efficiency and practicality in real-world applications. The treatment of textile and winery waste was explored through the innovative use of hydrodynamic cavitation. This method was highlighted for its application, results, and advantages, demonstrating its potential as a viable treatment option.

The experimental methods section detailed the materials and methods used, study areas, experimental set-up, and analytical methods for data processing. This rigorous approach ensured the reliability and validity of the research findings.

The results and discussion chapter presented comprehensive data on the removal efficiencies of dyes and hydrocarbons. Comparative analysis of different treatment methods revealed significant insights into their effectiveness. The impact of hydrodynamic cavitation on textile and winery waste treatment was particularly noteworthy, showcasing its potential to address these specific types of waste.

The integration of hydrodynamic cavitation with other advanced oxidation processes, such as hydrogen peroxide and ozone, demonstrated significant improvements in the degradation of dyes. The combined processes achieved higher removal efficiencies compared to individual treatments, highlighting the synergistic effects of these methods. For instance, the combination of HC/O_3/H_2O_2 achieved the highest COD reduction of 93%, followed by HC/H_2O_2, H_2O_2 alone, HC/O3, and O3 alone. This indicates the potential of these integrated approaches for industrial wastewater treatment.

For the winery A factorial experiment was conducted to assess the impact of hydrogen peroxide load and hydrogen peroxide iron ratio on COD reduction. Although COD elimination rates were used as response variables, the study found that they do not correctly indicate the reaction's extent. This could be related to the solubilization of COD fractions during Fenton-like treatment, which, when paired with sample handling techniques before parameter analysis, impacts removal rates. The rate of oxidation and, by extension, COD removal is directly influenced by the amount of H_2O_2 utilized. In pretreated WW, the Fenton reagent efficiently eliminates refractory organic contaminants

The process analysis for textile conducted in this study compared the traditional wastewater treatment processes with innovative approaches incorporating hydrodynamic cavitation. The results demonstrated significant improvements in pollutant removal efficiencies and cost-effectiveness. The innovative process achieved a 95% reduction in COD, illustrating the efficacy of the combined operation. The TOC and BOD5 reductions were also significantly enhanced, indicating the potential for these methods to produce high-quality effluent suitable for reuse in industrial applications.

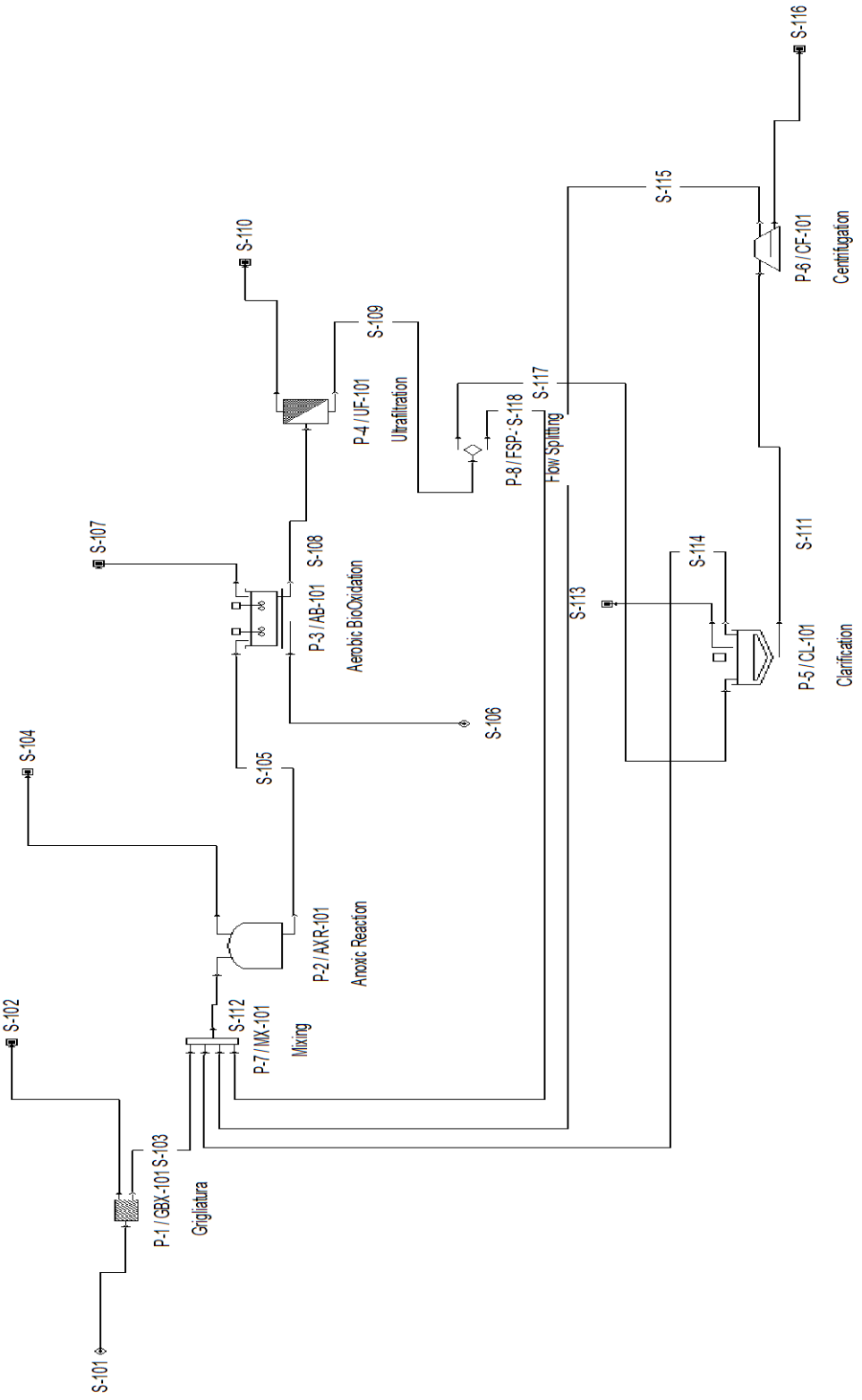
Additionally, the Takeda wastewater treatment plant's process analysis highlighted the effectiveness of integrating hydrodynamic cavitation with advanced oxidation processes. The plant's comprehensive multi-stage process, including equalization, fine screening, pH correction, hydrodynamic cavitation, nutrient dosing, extended aeration, and MBR technology, ensures high purification efficiency and compliance with environmental standards. The detailed cost analysis further supports the economic feasibility of these innovative treatment methods.

Despite the successes achieved, the research faced several challenges. These included optimizing treatment conditions and scaling up the processes for practical applications. Addressing these challenges is crucial for the future implementation of these methods on a larger scale.

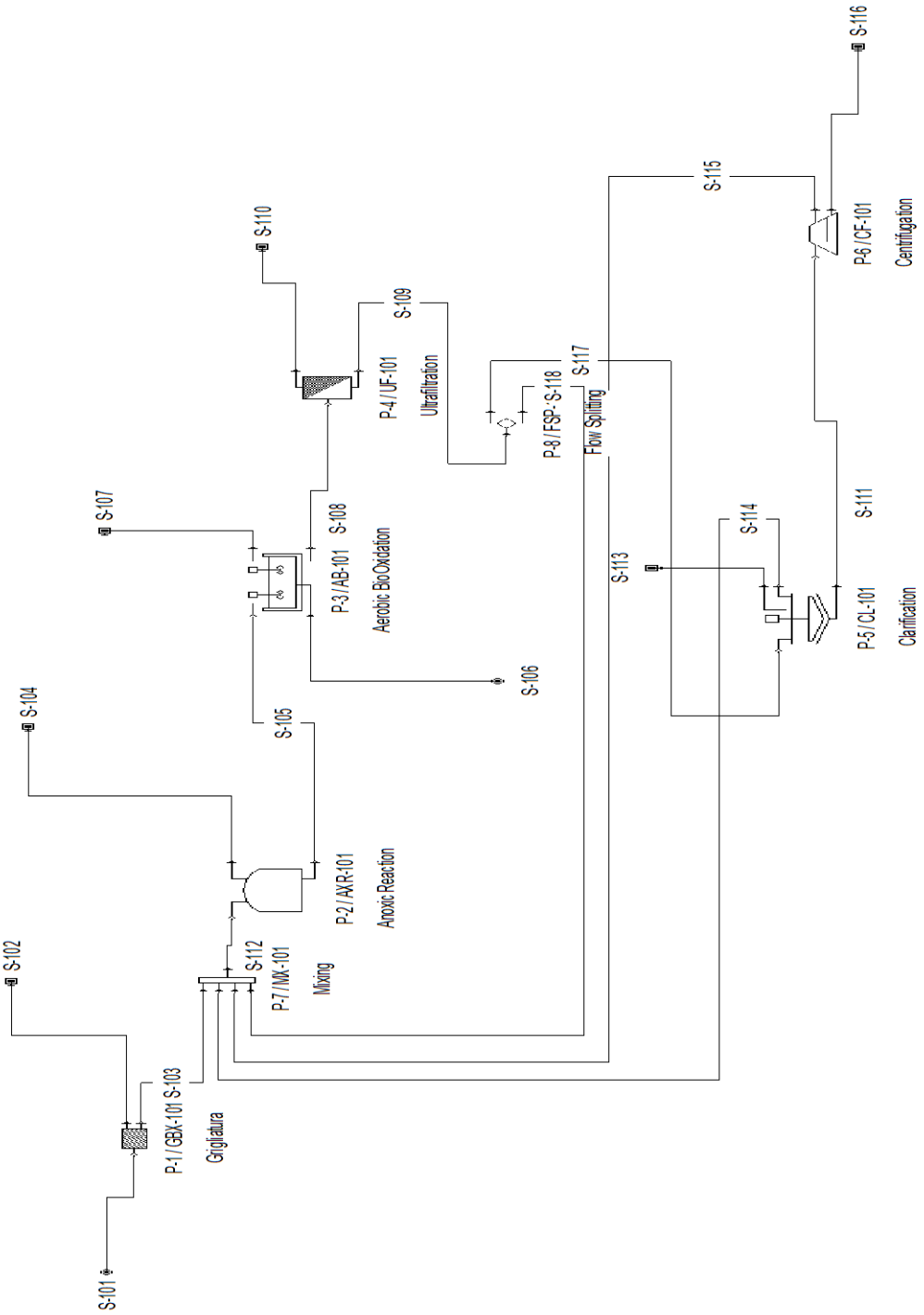
Future research directions include further refinement of the treatment methods developed in this study. There is also a need to explore the integration of these methods into existing waste management systems to enhance their efficiency and sustainability. Additionally, investigating the long-term environmental impacts and economic feasibility of these treatment methods will be essential for their widespread adoption.

APPENDIX A

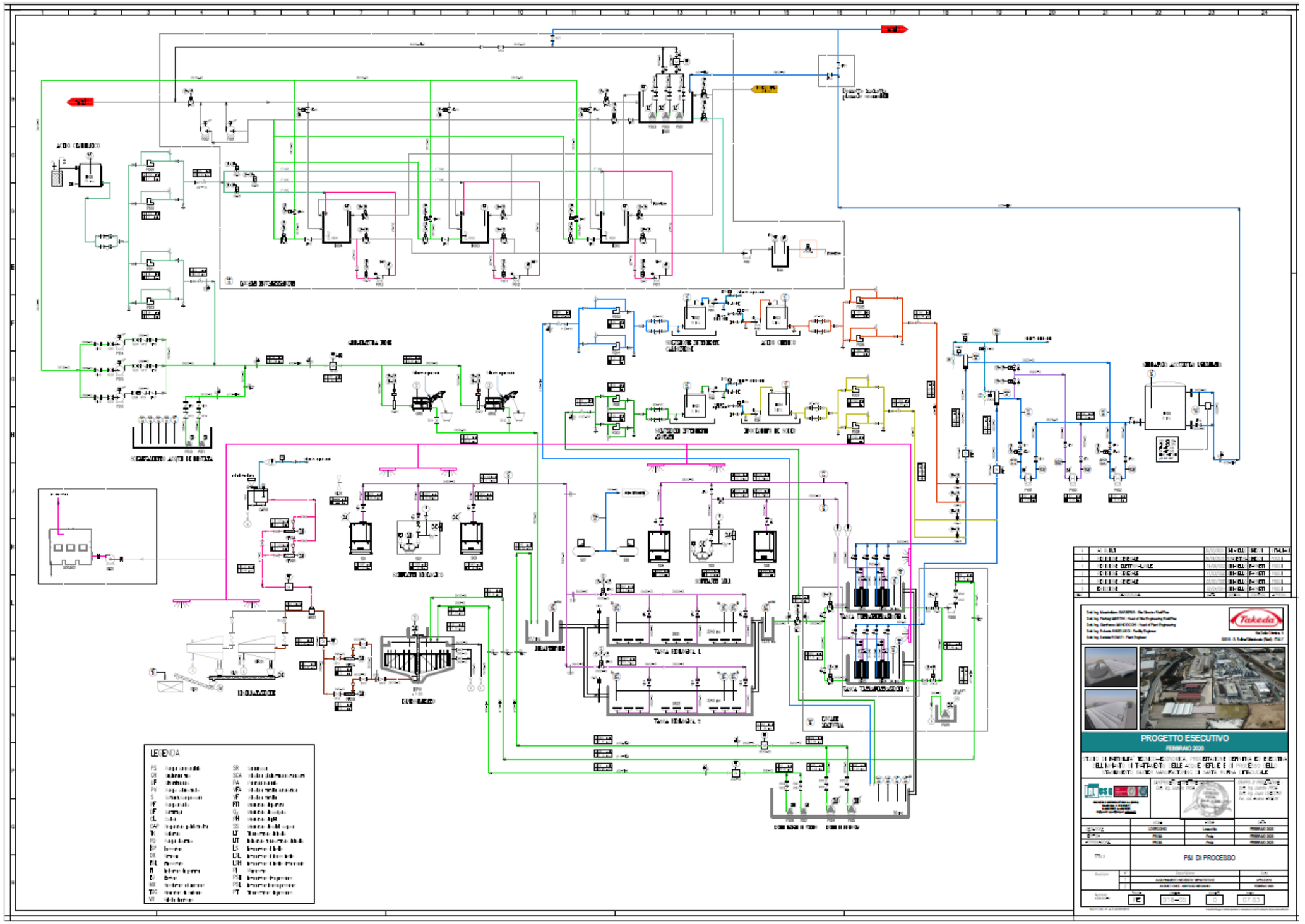
The flowsheet of Takeda's wastewater treatment plant



The flowsheet of Takeda's wastewater treatment plant with cavitation



The P&I of Takeda Plan


LEGENDA
PROGETTO ESECUTIVO
FEBBRAIO 2020
P&I DI PROCESSO

ADDENDUM B

Estimation of cost and energy required for textile effluent using HC [44]:

Effluent solution volume = 1 L

Volumetric flow rate V= 283 l/ h = 0.000078 m^3/sec

Inlet pressure: P_{in}=450000Pa

Outlet pressure: P_{out}=101325Pa

Treatment time = 60 min = 3600 s

Power dissipation in the system = Flow rate (m^3/s) × ΔP= (450000-101325) ×0.000078 = 27.19W (Pressure drop in Pa)

The energy dissipated per unit volume = Power dissipated per unit volume × Treatment time (s) =97907.94 J/L=27.2 kWh/m^3

Considering cost of 1 kWh energy consumption = 0.23 €

Energy consumption in 60 min by ozone generator for HC (180 W) =0.180kWh/m^3
Cost of ozone for 1L effluent solution (HC) = 0.180 ×0.23 = 0.0414 €
Cost of optimum H_2O_2dosage = 0.9 €/L

BIBLIOGRAPH

[1] gupta et al2021, “Recent advances on the removal of dyes from wastewater using various adsorbents: A critical review”.

[2] S. N. L. A. M. G. D. P. S. C. S. C. V. C.G. Lopresto, “Calabrò, Enzymatic transesterification of waste vegetable oil to produce biodiesel, Ecotoxicology and Environmental Safety, Volume 121,”.

[3] E. H., I. M. H. , M. K. , & K. S. R. M. (2020). Ezechi, “A comparative evaluation of two electrode systems on continuous electrocoagulation of boron from produced water and mass transfer resistance. Journal of Water Process Engineering, 34, 101133.”.

[4] gogate et al 2021, “[HTML] Cavitation based treatment of industrial wastewater: A critical review focusing on mechanisms, design aspects, operating conditions and application to real …”.

[5] A. Mukherjee, A. Mullick, R. Teja, P. Vadthya, A. Roy, and S. Moulik, “Performance and energetic analysis of hydrodynamic cavitation and potential integration with existing advanced oxidation processes: A case study for real life greywater treatment,” *Ultrason Sonochem*, vol. 66, no. September 2019, p. 105116, 2020, doi: 10.1016/j.ultsonch.2020.105116.

[6] B. Wang, H. Su, and B. Zhang, “Hydrodynamic cavitation as a promising route for wastewater treatment – A review,” *Chemical Engineering Journal*, vol. 412, no. November 2020, p. 128685, 2021, doi: 10.1016/j.cej.2021.128685.

[7] G. , L. M. , & A. G. (2020). Mancuso, “A critical review of the current technologies in wastewater treatment plants by using hydrodynamic cavitation process: principles and applications. Journal of Environmental Health Science and Engineering, 18, 311-333.”.

[8] R. , D. M. , D. F. P. , P. D. , V. N. , V. G. , & de C. B. Hamidi, " Recent developments and future outlooks of hydrodynamic cavitation as an intensification technology for renewable biofuels production. Journal of Environmental Chemical Engineering, 110819.".

[9] M., U. A. , P. I. , B. N. , & E. H. M. Omelyanyuk, "Optimization of Rotational Hydrodynamic Cavitation Reactor Geometry. Fluids, 9(10).".

[10] V. K., C. D. K. , D. R. H. , T. N. H. , K. J. , C. S. W. , . . . & N. D. D. Nguyen, "Review on pretreatment techniques to improve anaerobic digestion of sewage sludge. Fuel, 285, 119105.".

[11] P., L. D. , Z. C. , P. Q. , W. L. , & L. Y. Zhou, "Comparison of different sewage sludge pretreatment technologies for improving sludge solubilization and anaerobic digestion efficiency: A comprehensive review. Science of The Total Environment, 171175.".

[12] J. , H. Y. , X. C. , & H. H. (2018). Shi, "Biological coupling process for treatment of toxic and refractory compounds in coal gasification wastewater. Reviews in Environmental Science and Bio/Technology, 17, 765-790.".

[13] C. Agarkoti, P. R. Gogate, and A. B. Pandit, "Coupling of acoustic/hydrodynamic cavitation with ozone (O3), hydrogen peroxide (H2O2), magnesium oxide (MgO) and manganese dioxide (MnO2) for the effective treatment of CETP effluent," *Sep Purif Technol*, vol. 284, no. November 2021, p. 120281, 2022, doi: 10.1016/j.seppur.2021.120281.

[14] V. Innocenzi, A. Colangeli, and M. Prisciandaro, "Methyl orange decolourization through hydrodynamic cavitation in high salinity solutions," *Chemical Engineering and Processing - Process Intensification*, vol. 179, no. June, p. 109050, 2022, doi: 10.1016/j.cep.2022.109050.

[15] A., Y. A. , B. H. A. , S. N. S. , B. M. R. , A. I. , . . . & C. S. (2021). Giwa, "Recent advances in advanced oxidation processes for removal of contaminants from water: A comprehensive review. Process Safety and Environmental Protection, 146, 220-256.".

[16] S. F. , M. M. , N. S. , C. A. T. , R. N. , U. M. A. , . . . & S. P. L. (2021). Ahmed, " Recent developments in physical, biological, chemical, and hybrid treatment techniques for removing emerging contaminants from wastewater. Journal of hazardous materials, 416, 125912.".

[17] N. H. et T. Gökçe. INCE, " Reactive dyestuff degradation by combined sonolysis and ozonation. Dyes and pigments, 2001, vol. 49, no 3, p. 145-153.".

[18] C. and S. D. ZAHARIA, " Textile organic dyes-characteristics, polluting effects and separation/elimination procedures from industrial effluents-a critical overview. IntechOpen, Rijeka, 2012.".

[19] V. P. M. , C. M. , et al. INNOCENZI, " Comparison of performances of hydrodynamic cavitation in combined treatments based on hybrid induced advanced Fenton process for degradation of azo-dyes. Journal of environmental chemical engineering, 2019, vol. 7, no 3, p. 103171.".

[20] G. (2017). Mancuso, " Enhancement of wastewater and sludge treatment processes by hydrodynamic cavitation.".

[21] O. (2022). Muminov, "TYPES OF CAVITATION, CAUSING VIBRATION IN ENGINEERING AND WATER SUPPLY SYSTEMS. Science and innovation, 1(A7), 732-737.".

[22] X., L. J., J. L. , W. G. , Z. S. , Y. J. Y. , & C. S. (2020). Sun, "A review on hydrodynamic cavitation disinfection: The current state of knowledge. Science of the Total Environment, 737, 139606.".

[23] A., & A. F. (1986). Karimi, "Comparison of erosion mechanisms in different types of cavitation. Wear, 113(3), 305-322.".

[24] J., B. M., R. S. , G. S. , S. V. K. , & P. A. B. (2017). Carpenter, "Hydrodynamic cavitation: an emerging technology for the intensification of various chemical and physical processes in a chemical process industry. Reviews in Chemical Engineering, 33(5), 433-468.".

[25] Y. T. , P. A. B. , & M. V. S. (1999). Shah, “ Cavitation reaction engineering. Springer Science & Business Media.”.

[26] X. , Y. W. , X. X. , J. L. , X. X. , W. G. , . . . & C. S. (2021). Sun, “Effect of the cavitation generation unit structure on the performance of an advanced hydrodynamic cavitation reactor for process intensifications. Chemical Engineering Journal, 412, 128600.”.

[27] H. , Z. Y. , & Z. J. (2022). Zheng, “ Recent developments in hydrodynamic cavitation reactors: Cavitation mechanism, reactor design, and applications. Engineering, 19, 180-198.”.

[28] J. P. , & M. J. M. (2006). Franc, “ Fundamentals of cavitation (Vol. 76). Springer science & Business media.”.

[29] P. S. K. M. S. et P. A. B. KUMAR, “ Experimental quantification of chemical effects of hydrodynamic cavitation. Chemical Engineering Science, 2000, vol. 55, no 9, p. 1633-1639.”.

[30] C. E. (2014). Brennen, “Cavitation and bubble dynamics. Cambridge university press.”.

[31] B. , & S. H. (2024). Jia, “ Non-Spherical Cavitation Bubbles: A Review. Fluids, 9(11), 249.”.

[32] D. , L. Ž. , P. J. , P. R. , & D. M. (2021). Podbevšek, “ Experimental evaluation of methodologies for single transient cavitation bubble generation in liquids. Experiments in fluids, 62, 1-28.”.

[33] I. , E. D. G. , G. A. , & F. D. K. (2014). Tzanakis, “ Incubation pit analysis and calculation of the hydrodynamic impact pressure from the implosion of an acoustic cavitation bubble. Ultrasonics Sonochemistry, 21(2), 866-878.”.

[34] H. (2024). Choi, “ Evolution and control of venturi cavitation under different liquid conditions ”.

[35] G. , L. M. , & A. G. (2020). Mancuso, “ A critical review of the current technologies in wastewater treatment plants by using hydrodynamic

cavitation process: principles and applications. Journal of Environmental Health Science and Engineering, 18, 311-333.”.

[36] S. (2018). Lee, “ System configuration and control using hydraulic transformers (Doctoral dissertation, University of Minnesota).”.

[37] S. , & B. Y. (2008). Arrojo, “A theoretical study of hydrodynamic cavitation. Ultrasonics Sonochemistry, 15(3), 203-211.”.

[38] D. , S. V. K. , & M. S. (2020). Panda, “Controlled hydrodynamic cavitation: A review of recent advances and perspectives for greener processing. Processes, 8(2), 220.”.

[39] A. (2023). Vijayan, “ Characterization of cavitation zone in cavitating venturi flows: Challenges and road ahead. Physics of Fluids, 35(11).”.

[40] H. , Z. Y. , & Z. J. (2022). Zheng, “ Recent developments in hydrodynamic cavitation reactors: Cavitation mechanism, reactor design, and applications. Engineering, 19, 180-198.”.

[41] S. , & B. Y. (2008). Arrojo, “ A theoretical study of hydrodynamic cavitation. Ultrasonics Sonochemistry, 15(3), 203-211.”.

[42] A. M. , A. B. K. , J. T. , & A. M. A. S. (2024). Yeneneh, “ Hydrodynamic Cavitation and Advanced Oxidation for Enhanced Degradation of Persistent Organic Pollutants: A Review. Sustainability, 16(11), 4601.”.

[43] Y. , Z. X. , L. C. , Z. L. , W. W. , C. G. , & D. J. (2024). Chen, “Mass transfer enhancement and flow field simulations for a Venturi bubble generator with multiple inlet tubes. Nuclear Engineering and Design, 424, 113249.”.

[44] D. , D. C. C. , & B. J. J. R. (2015). Bertoldi, “Experimental investigation of two-phase flashing flows of a binary mixture of infinite relative volatility in a Venturi tube. Experimental Thermal and Fluid Science, 64, 152-163.”.

[45] M. , P. M. , L. A. , & M. D. (2014). Capocelli, “ Hydrodynamic cavitation of p-nitrophenol: a theoretical and experimental insight. Chemical Engineering Journal, 254, 1-8.”.

[46] P. , K. S. , & M. V. S. (2012). Kumar, “ Flow regime maps and optimization thereby of hydrodynamic cavitation reactors. AIChE Journal, 58(12), 3858-3866.”.

[47] A. , A. J. A. , & S. J. F. (2012). Ducoin, “An experimental analysis of fluid structure interaction on a flexible hydrofoil in various flow regimes including cavitating flow. European Journal of Mechanics-B/Fluids, 36, 63-74.”.

[48] A. (2023). Vijayan, “Characterization of cavitation zone in cavitating venturi flows: Challenges and road ahead. Physics of Fluids, 35(11).”.

[49] C. E. (2014). Brennen, “ Cavitation and bubble dynamics. Cambridge university press.”.

[50] M. T. , V. J. A. , P. B. W. , & B. P. A. (2021). Khoo, “ Nucleation and cavitation number effects on tip vortex cavitation dynamics and noise. Experiments in Fluids, 62, 1-19.”.

[51] M. , Z. G. , P. M. , L. K. , & C.-D. O. (2022). Ge, “ Intensity and regimes changing of hydrodynamic cavitation considering temperature effects. Journal of Cleaner Production, 338, 130470.”.

[52] M. T. , V. J. A. , P. B. W. , & B. P. A. (2021). Khoo, “Nucleation and cavitation number effects on tip vortex cavitation dynamics and noise. Experiments in Fluids, 62, 1-19.”.

[53] Y. , Q. Z. , W. D. , W. G. , W. Y. , L. S. , & P. G. (2017). Zhang, “ Fundamentals of cavitation and bubble dynamics with engineering applications. Advances in Mechanical Engineering, 9(3), 1687814017698321.”.

[54] J. P. , & M. J. M. (2006). Franc, “ Fundamentals of cavitation (Vol. 76). Springer science & Business media.”.

[55] P. R. , & P. A. B. (2000). Gogate, “ Engineering design methods for cavitation reactors II: hydrodynamic cavitation. AIChE journal, 46(8), 1641-1649.”.

[56] M. , Z. M. , D. M. , K. T. , H. E. , K. B. , & Š. B. (2013). Petkovšek, “Rotation generator of hydrodynamic cavitation for water treatment. Separation and purification technology, 118, 415-423.”.

[57] M. , G.-B. T. , G.-A. I. , H. E. , K. T. , K. A. K. , . . . & K. B. (2016). Dular, “Use of hydrodynamic cavitation in (waste) water treatment. Ultrasonics sonochemistry, 29, 577-588.”.

[58] P. C. , B. J. , W. J. , & V. T. T. J. C. (2015). Pennings, “ Dynamics of isolated vortex cavitation. Journal of Fluid Mechanics, 778, 288-313.”.

[59] J. Wang *et al.*, “Degradation of acid red 73 wastewater by hydrodynamic cavitation combined with ozone and its mechanism,” *Environ Res*, vol. 210, no. January, p. 112954, 2022, doi: 10.1016/j.envres.2022.112954.

[60] C. Agarkoti, P. D. Thanekar, and P. R. Gogate, “Cavitation based treatment of industrial wastewater: A critical review focusing on mechanisms, design aspects, operating conditions and application to real effluents,” *J Environ Manage*, vol. 300, no. September, p. 113786, 2021, doi: 10.1016/j.jenvman.2021.113786.

[61] M. T. , A. T. , N. S. , G. M. , & K. A. (2020). Gevari, “ Direct and indirect thermal applications of hydrodynamic and acoustic cavitation: A review. Applied Thermal Engineering, 171, 115065.”.

[62] A. , & R. V. V. (2019). Simpson, “ Modeling hydrodynamic cavitation in venturi: Influence of venturi configuration on inception and extent of cavitation. AIChE Journal, 65(1), 421-433.”.

[63] A. , S.-P. T. , P. M. , & D. M. (2017). Šarc, “The issue of cavitation number value in studies of water treatment by hydrodynamic cavitation. Ultrasonics sonochemistry, 34, 51-59.”.

[64] Y. S. , H. D. H. , C. H. , J. H. , & C. S. H. (2017). Kim, “ Experimental study on Venturi-type natural ventilator. Energy and Buildings, 139, 232-241.”.

[65] G. , L. M. , & A. G. (2017). Mancuso, “A swirling jet-induced cavitation to increase activated sludge solubilisation and aerobic sludge biodegradability. Ultrasonics sonochemistry, 35, 489-501.”.

[66] M. (2021). Bis, “ Current research trends in the application of hydrodynamic cavitation in environmental engineering. Advances in Environmental Engineering Research in Poland, 167-178.”.

[67] A. S.-P. T. P. M. et al. ŠARC, “ The issue of cavitation number value in studies of water treatment by hydrodynamic cavitation. Ultrasonics sonochemistry, 2017, vol. 34, p. 51-59.”.

[68] J. , L. B. K. , S. R. , M. N. , S. M. P. , M. S. , . . . & B. B. (2023). Mukherjee, “ Advanced oxidation process for the treatment of industrial wastewater: A review on strategies, mechanisms, bottlenecks and prospects. Chemosphere, 140473.”.

[69] M. M. , S. V. K. P. D. V. , et al. GORE, “ Degradation of reactive orange 4 dye using hydrodynamic cavitation based hybrid techniques. Ultrasonics sonochemistry, 2014, vol. 21, no 3, p. 1075-1082.”.

[70] S. M. , & G. P. R. (2019). Joshi, “ Intensification of industrial wastewater treatment using hydrodynamic cavitation combined with advanced oxidation at operating capacity of 70 L. Ultrasonics Sonochemistry, 52, 375-381.”.

[71] X. , & Z. Y. (2009). Wang, “Degradation of alachlor in aqueous solution by using hydrodynamic cavitation. Journal of hazardous materials, 161(1), 202-207.”.

[72] M. , & P. A. B. (2002). Sivakumar, “Wastewater treatment: a novel energy efficient hydrodynamic cavitational technique. Ultrasonics sonochemistry, 9(3), 123-131.”.

[73] V. K. , P. A. B. , S. K. P. S. , & A. S. (2012). Saharan, “Hydrodynamic cavitation as an advanced oxidation technique for the degradation of acid red 88 dye. Industrial & Engineering Chemistry Research, 51(4), 1981-1989.”.

[74] S. M. Joshi and P. R. Gogate, "Intensification of industrial wastewater treatment using hydrodynamic cavitation combined with advanced oxidation at operating capacity of 70 L," *Ultrason Sonochem*, vol. 52, no. December 2018, pp. 375–381, 2019, doi: 10.1016/j.ultsonch.2018.12.016.

[75] G. , L. M. , L. M. , & A. G. (2016). Mancuso, "Decolourization of Rhodamine B: A swirling jet-induced cavitation combined with NaOCl. Ultrasonics Sonochemistry, 32, 18-30.".

[76] R. , & S. T. P. (2004). Pietroforte, "ASCE Journal of Construction Engineering and Management: Review of the years 1983–2000. Journal of construction engineering and management, 130(3), 440-448.".

[77] J. , & S. R. Y. (1996). W. reclamation and reuse criteria in the US. W. S. and T. 33(10-11), 451-462. Crook, "Crook, J., & Surampalli, R. Y. (1996). Water reclamation and reuse criteria in the US. Water Science and Technology, 33(10-11), 451-462.Water reclamation and reuse criteria in the US. Water Science and Technology, 33(10-11), 451-462.".

[78] T. (Ed.). (1998). Asano, " Wastewater reclamation and reuse: water quality management library (Vol. 10). Crc Press.".

[79] V. (2013). Novotny, " Water–energy nexus: retrofitting urban areas to achieve zero pollution. Building Research & Information, 41(5), 589-604.".

[80] D. on E. L. S. W. S. T. B. & C. on the A. of W. R. as an A. to M. F. W. S. Needs. (2012). National Research Council, "Water reuse: potential for expanding the nation's water supply through reuse of municipal wastewater. National Academies Press.".

[81] E. (2004). Friedler, " Quality of individual domestic greywater streams and its implication for on-site treatment and reuse possibilities. Environmental technology, 25(9), 997-1008.".

[82] L. , Z. G. , T. H. , & B. C. (2007). Hernandez Leal, " Characterisation and biological treatment of greywater. Water Science and Technology, 56(5), 193-200.".

[83] F. , W. K. , & O. R. (2009). Li, “Review of the technological approaches for grey water treatment and reuses. Science of the total environment, 407(11), 3439-3449.”.

[84] B. , H. T. R. , N. B. , H. A. D. , G. H. E. , C. J. E. , . . . & B. J. C. (2018). Morelli, “Critical review of eutrophication models for life cycle assessment. Environmental science & technology, 52(17), 9562-9578.”.

[85] M. , F. P. , R. C. , & H. K. (2012) Usman, “ Application of magnetite-activated persulfate oxidation for the degradation of PAHs in contaminated soils. Chemosphere, 87(3), 234-240.”.

[86] D. G. , & N. V. (2018). U. Randall, “The liquid gold of wastewater. Journal of Environmental Chemical Engineering, 6(2), 2627-2635.”.

[87] A. N. , H. M. R. , & T. Z. (2009). Bdour, “Perspectives on sustainable wastewater treatment technologies and reuse options in the urban areas of the Mediterranean region. Desalination, 237(1-3), 162-174.”.

[88] Unicef. (2015)., “ Trends in maternal mortality: 1990 to 2015: estimates by WHO, UNICEF, UNFPA, World Bank Group and the United Nations Population Division.”.

[89] A. B. , & H. D. W. (1971). Bishop, “Water reuse systems analysis. Journal of the Sanitary Engineering Division, 97(1), 41-57.”.

[90] M. E. , & D. J. A. (1974). Mulvihill, “Optimal timing and sizing of a conjunctive urban water supply and waste water system with nonlinear programing. Water Resources Research, 10(2), 170-175.”.

[91] A. G. , R. J. J. , S. C. , & O. J. M. (1992). Perez, “Aroma components and free amino acids in strawberry variety Chandler during ripening. Journal of Agricultural and Food Chemistry, 40(11), 2232-2235.”.

[92] D. E. , & S. T. L. (1979). Pingry, “Integrated water management with reuse: A programing approach. Water Resources Research, 15(1), 8-14.”.

[93] S. J. (2017). Judd, “Membrane technology costs and me. Water research, 122, 1-9.”.

[94] L. , G.-G. S. , B. J. , & M. M. T. (2017). Lijó, “The environmental effect of substituting energy crops for food waste as feedstock for biogas production. Energy, 137, 1130-1143.”.

[95] K. A. , S. M. K. , B. A. , K. A. A. , & S. S. (2014). Vakil, “Characterization of greywater in an Indian middle-class household and investigation of physicochemical treatment using electrocoagulation. Separation and Purification technology, 130, 160-166.”.

[96] A. M. , S. J. , & G. S. (2017). Valek, “ Quantification of the urban water-energy nexus in México City, México, with an assessment of water-system related carbon emissions. Science of the Total Environment, 590, 258-268.”.

[97] M. , A.-A. T. , M. H. R. , & A.-G. S. G. (2018). Mannan, “Quantifying the energy, water and food nexus: A review of the latest developments based on life-cycle assessment. Journal of Cleaner Production, 193, 300-314.”.

[98] W. C. , & S. A. L. (Eds.). (2013). Burns, “ Climate change geoengineering: Philosophical perspectives, legal issues, and governance frameworks. Cambridge University Press.”.

[99] B. , S. J. P. , K. A. , & S. N. (2016). Singh, “ Bioactive compounds in banana and their associated health benefits–A review. Food chemistry, 206, 1-11.”.

[100] V. C. , V.-O. S. B. , H.-G. A. , M.-R. I. , & O.-L. M. T. (2018). Eze, “Kinetic modelling of microalgae cultivation for wastewater treatment and carbon dioxide sequestration. Algal Research, 32, 131-141.”.

[101] S. H. , L. K. S. , S. S. , R. A. , G. C. A. , & I. S. I. (2018). Lee, “Wastewater treatment and electricity generation from a sunlight-powered single chamber microbial fuel cell. Journal of Photochemistry and Photobiology A: Chemistry, 358, 432-440.”.

[102] M. A. D. C. , C. M. D. A. , & C. A. L. B. (2024). Lemos, “Application of linear and non-linear methods in estimating fugitive emissions by using flux chamber at the Jockey Club Controlled Landfill in Brasília/DF. Engenharia Sanitaria e Ambiental, 29, e20240006.”.

[103] W. , W. R. , & Z. J. B. (2014). Mo, “Energy–water nexus analysis of enhanced water supply scenarios: a regional comparison of Tampa Bay, Florida, and San Diego, California. Environmental science & technology, 48(10), 5883-5891.”.

[104] T. , A. A. , J. D. , van der S. P. , & V. K. (2011). Thi Hoang Duong, “Urban water management strategies based on a total urban water cycle model and energy aspects–case study for Tel Aviv. Urban Water Journal, 8(2), 103-118.”.

[105] A. Libutti et al., “Agro-industrial wastewater reuse for irrigation of a vegetable crop succession under Mediterranean conditions,” Agric Water Manag, vol. 196, pp. 1–14, Jan. 2018, doi: 10.1016/J.AGWAT.2017.10.015. ”.

[106] T. A. A. B. B. E. J. and G. T. A. N. Angelakis, “Water reuse: From ancient to modern times and the future,” Frontiers in Environmental Science, vol. 6, no. MAY. Frontiers Media S.A., May 11, 2018. doi: 10.3389/fenvs.2018.00026. ”.

[107] M. T. D. H. V. M. M. V. and V. M. M. Procházková, “Industrial wastewater in the context of European Union water reuse legislation and goals,” J Clean Prod, vol. 426, p. 139037, Nov. 2023, doi: 10.1016/J.JCLEPRO.2023.139037. ”.

[108] P. R. Gogate and G. S. Bhosale, “Comparison of effectiveness of acoustic and hydrodynamic cavitation in combined treatment schemes for degradation of dye wastewaters,” Chemical Engineering and Processing: Process Intensification, vol. 71, pp. 59–69, Sep. 2013, doi: 10.1016/J.CEP.2013.03.001. ”.

[109] N. H. Ince and G. Tezcanli-Güyer, “Impacts of pH and molecular structure on ultrasonic degradation of azo dyes,” Ultrasonics, vol. 42, no. 1–9, pp. 591–596, Apr. 2004, doi: 10.1016/J.ULTRAS.2004.01.097. ”.

[110] S. , M. S. , & E. H. A. (2020). Benkhaya, “A review on classifications, recent synthesis and applications of textile dyes. Inorganic Chemistry Communications, 115, 107891.”.

[111] P. V. , Z. M. et O. M. A. NIDHEESH, “ An overview on the removal of synthetic dyes from water by electrochemical advanced oxidation processes. Chemosphere, 2018, vol. 197, p. 210-227.”.

[112] M. B. K. M. E. O. and H. A. A. Aleboyeh, “Prediction of azo dye decolorization by UV/H2O2 using artificial neural networks,” Dyes and Pigments, vol. 77, no. 2, pp. 288–294, Jan. 2008, doi: 10.1016/J.DYEPIG.2007.05.014. ”.

[113] B. Wang, T. Wang, and H. Su, “A dye-methylene blue (MB)-degraded by hydrodynamic cavitation (HC) and combined with other oxidants,” *J Environ Chem Eng*, vol. 10, no. 3, p. 107877, 2022, doi: 10.1016/j.jece.2022.107877.

[114] E. , et al. Jurado, “ Simplified spectrophotometric method using methylene blue for determining anionic surfactants: Applications to the study of primary biodegradation in aerobic screening tests. Chemosphere, 2006. 65(2): p. 278-285.”.

[115] F. Mashkoor and A. Nasar, “Magsorbents: Potential candidates in wastewater treatment technology – A review on the removal of methylene blue dye,” *J Magn Magn Mater*, vol. 500, no. January, p. 166408, 2020, doi: 10.1016/j.jmmm.2020.166408.

[116] C. R. G. N. T. J. and K. V. M. P. H. Nakhate, “Engineering aspects of catalytic ozonation for purification of real textile industry wastewater at the pilot scale,” Journal of Industrial and Engineering Chemistry, vol. 69, pp. 77–89, Jan. 2019, doi: 10.1016/J.JIEC.2018.09.010. ”.

[117] R. Kant, “Textile dyeing industry an environmental hazard,” *Nat Sci (Irvine)*, vol. 04, no. 01, pp. 22–26, 2012, doi: 10.4236/ns.2012.41004.

[118] “ Tecnotessile, 2007”.

[119] M. , N. J. , B. S. , C. S. , & T. S. K. (2021). Behera, “A review on the treatment of textile industry waste effluents towards the development of efficient mitigation strategy: An integrated system design approach. Journal of Environmental Chemical Engineering, 9(4), 105277.”.

[120] M. , & N. T. (2016). Ford, “Legislating for control: the trade union act 2016. Industrial Law Journal, 45(3), 277-298.”.

[121] “Istat, Italia, & Direzione generale della statistica. (1918). Annuario statistico italiano. Tip. Elzeviriana.”.

[122] L. H. and W. T. S. H. Latessa, “Characteristics and practical treatment technologies of winery wastewater: A review for wastewater management at small wineries,” J Environ Manage, vol. 342, p. 118343, Sep. 2023, doi: 10.1016/J.JENVMAN.2023.118343. ”.

[123] M. T. M. M. V. M. and D. H. V. Miklas, “Winery Wastewater Treatment Technologies: Current Trends and Future Perspective,” Chem Eng Trans, vol. 94, pp. 847–852, 2022, doi: 10.3303/CET2294141. ”.

[124] J. R. R. L. M. G.-F. and R. M. Q.-F. P. M. Reis, “Optimization of Fenton process conditions in winery wastewaters treatment followed by ion exchange process to recover iron,” Journal of Industrial and Engineering Chemistry, Aug. 2023, doi: 10.1016/J.JIEC.2023.08.050. 110”.

[125] V. C. , & I. R. E. (2023). Niculescu, “An overview on management and valorisation of winery wastes. Applied Sciences, 13(8), 5063.”.

[126] T. G. , C. A. , F. F. , P. S. , G. F. H. , F. A. , & V. M. (2022) Ambaye, “ Remediation of soil polluted with petroleum hydrocarbons and its reuse for agriculture: Recent progress, challenges, and perspectives. Chemosphere, 293, 133572.”.

[127] A. B. , et al. Patel, “ Polycyclic Aromatic Hydrocarbons: Sources, Toxicity, and Remediation Approaches. Frontiers in Microbiology, 2020. 11.”.

[128] F. , D. R. H. , G. G. , T. B. Y. , B. A. A. , & A. A. K. (2021). Jahedi, “Polycyclic aromatic hydrocarbons in PM 1, PM 2.5 and PM 10 atmospheric

particles: identification, sources, temporal and spatial variations. Journal of Environmental Health Science and Engineering, 19, 851-866.”.

[129] D. A. , B. M. , B. A. T. , B. F. , B. F. , C. Y. , . . . & W. T. G. (2023). Dale, “ PHANGS–JWST First Results: The Influence of Stellar Clusters on Polycyclic Aromatic Hydrocarbons in Nearby Galaxies. The Astrophysical Journal Letters, 944(2), L23.”.

[130] X. , C. S. , Z. Z. , P. X. , & H. Q. (2017). Huang, “ Characteristics of hydrocarbons in sediment core samples from the northern Okinawa Trough. Marine Pollution Bulletin, 115(1-2), 507-514.”.

[131] Y. , D. D. , Q. K. , S. J. , & C. Z. (2022). Wei, “Ecological risk assessment of heavy metal pollutants and total petroleum hydrocarbons in sediments of the Bohai Sea, China. Marine Pollution Bulletin, 184, 114218.”.

[132] T. , N. R. , H. D. , G. T. , I. M. , B. F. , . . . & K. U. (2021). Muddemann, “Improving the treatment efficiency and lowering the operating costs of electrochemical advanced oxidation processes. Processes, 9(9), 1482.”.

[133] X. , W. H. , Z. F. W. , H. G. C. , & M. S. K. (2013). Zhang, “Attributing intensification of precipitation extremes to human influence. Geophysical Research Letters, 40(19), 5252-5257.”.

[134] C. , et al. Dai, “Review on the contamination and remediation of polycyclic aromatic hydrocarbons (PAHs) in coastal soil and sediments. Environmental Research, 2022. 205.”.

[135] J. K. , H. E. A. and G. R. Nicol. Saxe, “Fenton oxidation of polycyclic aromatic hydrocarbons after surfactant-enhanced soil washing. Environmental engineering science, 2000. 17(4): p. 233-244.”.

[136] M. , et al. Smara, “ Efficiency of Hydrogen Peroxide and Fenton Reagent for Polycyclic Aromatic Hydrocarbon Degradation in Contaminated Soil: Insights from Experimental and Predictive Modeling. Processes, 2024. 12(3).”.

[137] X. S. C. C. L. et al. LIU, " Decoloration of methylene blue by heterogeneous Fenton-like oxidation on Fe3O4/SiO2/C nanospheres in neutral environment. Materials Chemistry and Physics, 2018, vol. 213, p. 231-238.".

[138] M. A. (2012). Nkansah, " Environmental Remediation: Removal of polycyclic aromatic hydrocarbons.".

[139] A. T. Lawal, "Polycyclic aromatic hydrocarbons. A review. Cogent Environmental Science, 2017. 3(1).".

[140] J. , et al. Yan, "Photomutagenicity of 16 polycyclic aromatic hydrocarbons from the US EPA priority pollutant list. Mutation Research/Genetic Toxicology and Environmental Mutagenesis, 2004. 557(1): p. 99-108.".

[141] S. A. , L. C. S. and M. M. S. Wise, " Analytical Methods for Determination of Polycyclic Aromatic Hydrocarbons (PAHs) — A Historical Perspective on the 16 U.S. EPA Priority Pollutant PAHs. Polycyclic Aromatic Compounds, 2015. 35(2-4): p. 187-247.".

[142] P. R. F. et P. Nichola. PUSPITA, "Efficiency of sequential ozone and UV-based treatments for the treatment of secondary effluent. Chemical Engineering Journal, 2015, vol. 268, p. 337-347.".

[143] I. , & H. J. I. (2013). Lee, "The effects of waste-activated sludge pretreatment using hydrodynamic cavitation for methane production. Ultrasonics Sonochemistry, 20(6), 1450-1455.".

[144] H. J. , N. D. X. , & B. J. H. (2008). Kim, " The performance of the sludge pretreatment system with venturi tubes. Water Science and Technology, 57(1), 131-137.".

[145] M. C. , S. C. , G. F. , & P. B. (2007). Trouilhé, "Physical and chemical water requirements of the white-clawed crayfish (Austropotamobius pallipes) in western France. Aquatic Conservation: Marine and Freshwater Ecosystems, 17(5), 520-538.".

[146] Z. Rajah, M. Guiza, R. R. Solís, N. Becheikh, F. J. Rivas, and A. Ouederni, "Clopyralid degradation using solar-photocatalytic/ozone process with olive

stone activated carbon," *J Environ Chem Eng*, vol. 7, no. 1, p. 102900, 2019, doi: 10.1016/j.jece.2019.102900.

[147] M. S. Hossain, P. Sarker, M. S. Rahaman, F. F. Ahmed, M. R. Shaibur, and M. Khabir Uddin, "Biological Treatment of Textile Wastewater by Total Aerobic Mixed Bacteria and Comparison with Chemical Fenton Process," *Pollution*, vol. 8, no. 4, pp. 1418–1433, 2022, doi: 10.22059/POLL.2022.340753.1408.

[148] L. B. K. F. M. et al. BILIŃSKA, "Catalytic ozonation of textile wastewater as a polishing step after industrial scale electrocoagulation. Journal of environmental management, 2020, vol. 265, p. 110502.".

[149] G. , L. M. , & A. G. (2017). Mancuso, " A swirling jet-induced cavitation to increase activated sludge solubilisation and aerobic sludge biodegradability. Ultrasonics sonochemistry, 35, 489-501.".

[150] C. G. P. R. , et P. A. B. AGARKOTI, "Comparison of acoustic and hydrodynamic cavitation based hybrid AOPs for COD reduction of commercial effluent from CETP. Journal of Environmental Management, 2021, vol. 281, p. 111792.".

[151] A. M. S. B. H. S. Z. et al. GHOLAMI, "Highly efficient treatment of petrochemical spent caustic effluent via electro-Fenton process for COD and TOC removal: optimization and experimental. Biomass Conversion and Biorefinery, 2023, p. 1-17.".

[152] M. A. Hassaan and A. El Nemr, "Advanced Oxidation Processes for Textile Wastewater Treatment," *International Journal of Photochemistry and Photobiology*, vol. 2, no. 3, pp. 85–93, 2017, doi: 10.11648/j.ijpp.20170203.13.

[153] A. Buthiyappan, A. R. Abdul Aziz, and W. M. A. Wan Daud, "Recent advances and prospects of catalytic advanced oxidation process in treating textile effluents," *Reviews in Chemical Engineering*, vol. 32, no. 1, pp. 1–47, 2016, doi: 10.1515/revce-2015-0034.

[154] V. V. , B. V. M. , N. S. , S. V. P. , & S. A. T. (2022). Ranade, “Hydrodynamic Cavitation: Devices, Design and Applications. John Wiley & Sons.”.

[155] M. A. R. A. A. M. and A. B. P. V. K. Saharan, “Effect of geometry of hydrodynamically cavitating device on degradation of orange-G,” Ultrason Sonochem, vol. 20, no. 1, pp. 345–353, Jan. 2013, doi: 10.1016/J.ULTSONCH.2012.08.011. ”.

[156] T. A. , J. J. A. M. , B. C. A. , C. E. , & T. C. E. (2020). Bimestre, “Theoretical modeling and experimental validation of hydrodynamic cavitation reactor with a Venturi tube for sugarcane bagasse pretreatment. Bioresource technology, 311, 123540.”.

[157] C. Walling, “Fenton’s Reagent Revisited. Accounts of Chemical Research, 1975. 8(4): p. 125-131.”.

[158] R. Tanveer, A. Yasar, A. ul B. Tabinda, A. Ikhlaq, H. Nissar, and A. S. Nizami, “Comparison of ozonation, Fenton, and photo-Fenton processes for the treatment of textile dye-bath effluents integrated with electrocoagulation,” *Journal of Water Process Engineering*, vol. 46, Apr. 2022, doi: 10.1016/J.JWPE.2021.102547.

[159] M. Z. and C. A. M.-H. S. O. Ganiyu, “Heterogeneous electro-Fenton and photoelectro-Fenton processes: A critical review of fundamental principles and application for water/wastewater treatment,” Appl Catal B, vol. 235, pp. 103–129, Nov. 2018, doi: 10.1016/J.APCATB.2018.04.044. ”.

[160] U. J. , et al. Ahile, “A review on the use of chelating agents as an alternative to promote photo-Fenton at neutral pH: Current trends, knowledge gap and future studies. Science of the total environment, 2020. 710: p. 134872.”.

[161] A. Mukherjee, A. Mullick, P. Vadthya, S. Moulik, and A. Roy, “Surfactant degradation using hydrodynamic cavitation based hybrid advanced oxidation technology: A techno economic feasibility study,” *Chemical Engineering Journal*, vol. 398, no. May, p. 125599, 2020, doi: 10.1016/j.cej.2020.125599.

[162] K. Fedorov *et al.*, “Synergistic effects of hybrid advanced oxidation processes (AOPs) based on hydrodynamic cavitation phenomenon – A review,” *Chemical Engineering Journal*, vol. 432, no. October 2021, p. 134191, 2022, doi: 10.1016/j.cej.2021.134191.

[163] A. S. and T. T. I. Lapchuk, “Application of hybrid advanced oxidation and adsorption processes for pharmaceutical wastewater treatment,” The Treatment of Pharmaceutical Wastewater: Innovative Technologies and the Adaptation of Treatment Systems, pp. 247–275, Jan. 2023, doi: 10.1016/B978-0-323-99160-5.00008-4. ”.

[164] P. et G. Parag. THANEKAR, “ Application of hydrodynamic cavitation reactors for treatment of wastewater containing organic pollutants: Intensification using hybrid approaches. Fluids, 2018, vol. 3, no 4, p. 98.”.

[165] M. S. Kumar, S. H. Sonawane, and A. B. Pandit, “Degradation of methylene blue dye in aqueous solution using hydrodynamic cavitation based hybrid advanced oxidation processes,” *Chemical Engineering and Processing: Process Intensification*, vol. 122, no. September, pp. 288–295, 2017, doi: 10.1016/j.cep.2017.09.009.

[166] M. Khajeh, E. Taheri, M. M. Amin, A. Fatehizadeh, and J. Bedia, “Combination of hydrodynamic cavitation with oxidants for efficient treatment of synthetic and real textile wastewater,” *Journal of Water Process Engineering*, vol. 49, no. September, p. 103143, 2022, doi: 10.1016/j.jwpe.2022.103143.

[167] M. A. M. M. F. A. et al. KHAJEH, “ Synergetic degradation of atenolol by hydrodynamic cavitation coupled with sodium persulfate as zero-waste discharge process: Effect of coexisting anions. Chemical Engineering Journal, 2021, vol. 416, p. 129163.”.

[168] K. I. V. et P. Marina. AYEDI, “ Combined Hydrodynamic Cavitation-based Processes as an Efficient Treatment Approach for Real Textile Industrial Wastewater. Chemical Engineering Transactions, 2023, vol. 100, p. 181-186.”.

[169] I. Khan *et al.*, “and Photodegradation,” 2022.

[170] M. Y. , H. G. M. R. et al. GHALY, “ Photochemical oxidation of p-chlorophenol by UV/H2O2 and photo-Fenton process. A comparative study. waste management, 2001, vol. 21, no 1, p. 41-47.”.

[171] K. , & S. G. (2024). Mokrzyński, “Photoreactivity of polycyclic aromatic hydrocarbons (PAHs) and their mechanisms of phototoxicity against human immortalized keratinocytes (HaCaT). Science of the Total Environment, 924, 171449.”.

[172] R. M. , & S. M. E. (1999). Pagni, “The photochemistry of PAHs and PCBs in water and on solids. Environmental photochemistry, 139-179.”.

[173] J. (2016). Ping, “Development of photolysis enhanced oxidation technologies for the removal of polycyclic aromatic hydrocarbons from offshore produced water (Doctoral dissertation, Memorial University of Newfoundland).”.

[174] J. (2008). Jacob, “The significance of polycyclic aromatic hydrocarbons as environmental carcinogens. 35 years research on PAH—a retrospective. Polycyclic Aromatic Compounds, 28(4-5), 242-272.”.

[175] M. A. (2012). Nkansah, “Environmental Remediation: Removal of polycyclic aromatic hydrocarbons Dissertation.”.

[176] S. , L. C. , P. A. , C. V. V. , F. E. , B. M. J. , . . . & P. V. J. (2011). Sanches, “Direct photolysis of polycyclic aromatic hydrocarbons in drinking water sources. Journal of Hazardous Materials, 192(3), 1458-1465.”.

[177] G. , & H. M. (2019). Eker, “Effect of UV wavelength, temperature and photocatalyst on the removal of PAHs from industrial soil with photodegradation applications. Environmental technology.”.

[178] S. Rajoriya, S. Bargole, S. George, and V. K. Saharan, “Treatment of textile dyeing industry effluent using hydrodynamic cavitation in combination with advanced oxidation reagents,” *J Hazard Mater*, vol. 344, pp. 1109–1115, 2018, doi: 10.1016/j.jhazmat.2017.12.005.

[179] S. , et al. Dini, “The Physicochemical and Functional Properties of Biosurfactants: A Review. Molecules, 2024. 29(11): p. 2544.”.

[180] G. Eisenberg, “Colorimetric Determination of Hydrogen Peroxide. Industrial & Engineering Chemistry Analytical Edition, 1943. 15(5): p. 327-328.”.

[181] S. and K. C. Khilar. Paria, “A review on experimental studies of surfactant adsorption at the hydrophilic solid–water interface. Advances in Colloid and Interface Science, 2004. 110(3): p. 75-95.”.

[182] K. , I. V. , & P. M. (2024). Ayedi, “Application of hybrid oxidative processes based on cavitation for the treatment of methyl blue solutions. Sustainable Water Resources Management, 10(2), 92.”.

[183] G. A. et S. Hiroshi. ISMAIL, “Review on effect of different type of dyes on advanced oxidation processes (AOPs) for textile color removal. Chemosphere, 2022, vol. 291, p. 132906.”.

[184] S. Das, A. P. Bhat, and P. R. Gogate, “Degradation of dyes using hydrodynamic cavitation: Process overview and cost estimation,” *Journal of Water Process Engineering*, vol. 42, no. May, p. 102126, 2021, doi: 10.1016/j.jwpe.2021.102126.

[185] A. N. P. V. , et K. M. KUMAR, “Suresh. Composite wastewater treatment by aerated electrocoagulation and modified peroxi-coagulation processes. Chemosphere, 2018, vol. 205, p. 587-593.”.

[186] S. I. N. Zapata *et al.*, “Hydrodynamic Cavitation as a Clean Technology in Textile Industrial Wastewater Treatment,” *Chem Eng Trans*, vol. 86, no. October 2020, pp. 277–282, 2021, doi: 10.3303/CET2186047.

[187] G. L. P. H. et L. K. Victor. YIN, “An ozone/hydrogen peroxide/microwave-enhanced advanced oxidation process for sewage sludge treatment. Journal of Environmental Science and Health, Part A, 2007, vol. 42, no 8, p. 1177-1181.”.

[188] X. , W. J. , G. P. , G. W. , & W. C. (2009). Wang, " Degradation of rhodamine B in aqueous solution by using swirling jet-induced cavitation combined with H2O2. Journal of Hazardous Materials, 169(1-3), 486-491.".

[189] V. Innocenzi, M. Prisciandaro, M. Centofanti, and F. Vegliò, "Comparison of performances of hydrodynamic cavitation in combined treatments based on hybrid induced advanced Fenton process for degradation of azo-dyes," *J Environ Chem Eng*, vol. 7, no. 3, p. 103171, 2019, doi: 10.1016/j.jece.2019.103171.

[190] B. , S. H. , & Z. B. (2021). Wang, "Hydrodynamic cavitation as a promising route for wastewater treatment–A review. Chemical Engineering Journal, 412, 128685.".

[191] S. Raut-Jadhav, M. P. Badve, D. V. Pinjari, D. R. Saini, S. H. Sonawane, and A. B. Pandit, "Treatment of the pesticide industry effluent using hydrodynamic cavitation and its combination with process intensifying additives (H2O2 and ozone)," *Chemical Engineering Journal*, vol. 295, pp. 326–335, 2016, doi: 10.1016/j.cej.2016.03.019.

[192] C. G. P. R. , et P. A. B. AGARKOTI, " Coupling of acoustic/hydrodynamic cavitation with ozone (O3), hydrogen peroxide (H2O2), magnesium oxide (MgO) and manganese dioxide (MnO2) for the effective treatment of CETP effluent. Separation and Purification Technology, 2022, vol. 284, p. 120281.".

[193] S. R. M. M. M. G. V. , et al. MALAVASI, " Numerical method to provide cavitation index for control valves. In : Pressure Vessels and Piping Conference. American Society of Mechanical Engineers, 2013. p. V004T04A003.".

[194] S.-H. et W. H.-Shan. SHEU, " Treatment of olefin plant spent caustic by combination of neutralization and Fenton reaction. Water research, 2001, vol. 35, no 8, p. 2017-2021.".

[195] N. , S. V. , A. K. , et al. NIRMALA, " Removal of toxic metals from wastewater environment by graphene-based composites: A review on

isotherm and kinetic models, recent trends, challenges and future directions. Science of The Total Environment, 2022, vol. 840, p. 156564.”.

[196] S. B. S. G. S. et al. RAJORIYA, “Treatment of textile dyeing industry effluent using hydrodynamic cavitation in combination with advanced oxidation reagents. Journal of Hazardous Materials, 2018, vol. 344, p. 1109-1115.”.

[197] M. M. L. M. , N. B. et al. DIAS-MACHADO, “ Treatment of cork boiling wastewater using chemical oxidation and biodegradation. Chemosphere, 2006, vol. 64, no 3, p. 455-461.”.

[198] V. K. , P. D. V. , G. P. R. , et al. SAHARAN, “ Advanced oxidation technologies for wastewater treatment: an overview. Industrial wastewater treatment, recycling and reuse, 2014, p. 141-191.”.

[199] G. , G. K. R. , B. A. J. , et al. SUN, “ Treatment of agricultural wastewater in a combined tidal flow-downflow reed bed system. Water Science and Technology, 1999, vol. 40, no 3, p. 139-146.”.

[200] J. L. et V. G. Urs. ACERO, “Characterization of oxidation processes: ozonation and the AOP O3/H2O2. Journal-American Water Works Association, 2001, vol. 93, no 10, p. 90-100.”.

[201] J. C. H. Y. R. et al. WANG, “Intensified degradation of textile wastewater using a novel treatment of hydrodynamic cavitation with the combination of ozone. Journal of Environmental Chemical Engineering, 2020, vol. 8, no 4, p. 103959”.

[202] S. K. Gujar, P. R. Gogate, P. Kanthale, R. Pandey, S. Thakre, and M. Agrawal, “Combined oxidation processes based on ultrasound, hydrodynamic cavitation and chemical oxidants for treatment of real industrial wastewater from cellulosic fiber manufacturing sector,” *Sep Purif Technol*, vol. 257, no. October 2020, p. 117888, 2021, doi: 10.1016/j.seppur.2020.117888.

[203] S. , M. M. , & C. P. K. (2012). Ghafoori, “ Free-radical-induced degradation of aqueous polyethylene oxide by UV/H2O2: experimental design, reaction

mechanisms, and kinetic modeling. Industrial & engineering chemistry research, 51(46), 14980-14993.".

[204] A. A. , & S. A. (2016). Zorpas, "Multi-criteria analysis of sustainable environmental clean technologies for the treatment of winery's wastewater. International Journal of Global Environmental Issues, 15(1-2), 151-168.".

[205] M. B. , & M. M. (2008). Johnson, "Aqueous metronidazole degradation by UV/H2O2 process in single-and multi-lamp tubular photoreactors: kinetics and reactor design. Industrial & engineering chemistry research, 47(17), 6525-6537.".

[206] S. , et al. Kuppusamy, "Remediation approaches for polycyclic aromatic hydrocarbons (PAHs) contaminated soils: Technological constraints, emerging trends and future directions. Chemosphere, 2017. 168: p. 944-968.".

[207] F. , et al. Pardo, "Optimization of the application of the Fenton chemistry for the remediation of a contaminated soil with polycyclic aromatic hydrocarbons. Journal of Chemical Technology and Biotechnology, 2016. 91(6): p. 1763-1772.".

[208] M. , et al. Cheng, " Hydroxyl radicals based advanced oxidation processes (AOPs) for remediation of soils contaminated with organic compounds: A review. Chemical Engineering Journal, 2016. 284: p. 582-598.".

[209] B. N. , et al. Giménez, "Reaction kinetics formulation with explicit radiation absorption effects of the photo-Fenton degradation of paracetamol under natural pH conditions. Environmental Science and Pollution Research, 2021. 28(19): p. 23946-23957. ".

[210] A. and V. Isac. Sychiov, " Iron compounds and mechanisms of homogeneous catalysis of O-2 and H2O2 activation, as well as oxidation of organic substrates. Uspekhi Khimii, 1995. 64(12): p. 1183-1209.".

[211] C. , et al. Trellu, "Remediation of soils contaminated by hydrophobic organic compounds: How to recover extracting agents from soil washing solutions? Journal of hazardous materials, 2021. 404: p. 124137.".

[212] Y. , et al. Gou, “ Insights into the effects of Fenton oxidation on PAH removal and indigenous bacteria in aged subsurface soil. Environmental Pollution, 2022. 298.”.

[213] A. , et al. Mojiri, “ Comprehensive review of polycyclic aromatic hydrocarbons in water sources, their effects and treatments. Science of the Total Environment, 2019. 696.”.

[214] C. M. , A. R. and A. S. Dominguez, “ Selective removal of chlorinated organic compounds from lindane wastes by combination of nonionic surfactant soil flushing and Fenton oxidation. Chemical Engineering Journal, 2019. 376: p. 120009.”.

[215] S. and M. R. Mehrasbi. Safa, “Investigating the photo-Fenton process for treating soil washing wastewater. Journal of Environmental Health Science and Engineering, 2019. 17: p. 779-787.”.

[216] L. O. , et al. Conte, “Solar-assisted oxidation of organochlorine pesticides in groundwater using persulfate and ferrioxalate. Environmental Pollution, 2024. 343.”.

[217] L. O. , et al. Conte, “Vis LED Photo-Fenton Degradation of 124-Trichlorobenzene at a Neutral pH Using Ferrioxalate as Catalyst. International Journal of Environmental Research and Public Health, 2022. 19(15): p. 9733.”.

[218] P. K. , et al. Singa, “Photo-Fenton process for removal of polycyclic aromatic hydrocarbons from hazardous waste landfill leachate. International Journal of Environmental Science and Technology, 2021. 18(11): p. 3515-3526.”.

[219] R. , et al. Garcia-Cervilla, “Partition of a mixture of chlorinated organic compounds in real contaminated soils between soil and aqueous phase using surfactants: Influence of pH and surfactant type. Journal of Environmental Chemical Engineering, 2021. 9(5): p. 105908.”.

[220] A. R. , et al. Ribeiro, “An overview on the advanced oxidation processes applied for the treatment of water pollutants defined in the recently launched Directive 2013/39/EU. Environment international, 2015. 75: p. 33-51.”.

[221] E. and J. B. Neyens, " A review of classic Fenton's peroxidation as an advanced oxidation technique. Journal of Hazardous Materials, 2003. 98(1): p. 33-50.".

[222] L. , et al. Ge, "Aquatic Photochemistry of Fluoroquinolone Antibiotics: Kinetics, Pathways, and Multivariate Effects of Main Water Constituents. Environmental Science & Technology, 2010. 44(7): p. 2400-2405.".

[223] L. , et al. Ge, "Aqueous photochemical degradation of hydroxylated PAHs: Kinetics, pathways, and multivariate effects of main water constituents. Science of The Total Environment, 2016. 547: p. 166-172.".

[224] P. C. , et al. Marinosa, " Real soil treatment by chemical oxidation: Hydrogen peroxide application. Recent Advances in Fluid Mechanics and Heat&Mass Transfer, Florence, Italy, 2011.".

[225] M. and D. B. Tiwari, "Tripathy, Soil contaminants and their removal through surfactant-enhanced soil remediation: a comprehensive review. Sustainability, 2023. 15(17): p. 13161.".

[226] A. , et al. Santos, "Mineralization lumping kinetic model for abatement of organic pollutants using Fenton's reagent. Catalysis Today, 2010. 151(1-2): p. 89-93.".

[227] K. I. V. M. D. C. G. P. Marina. AYEDI, " Water reuse in the textile industry with integrated treatments: membranes and advanced oxidation processes. Journal of Desalination and Water Treatment, 2023, Vol.309, p. 158–164".

[228] M.Prisciandaro et al., "M. Prisciandaro and V. Innocenzi, 'Chapter 5 Advanced wastewater oxidation processes and their role in water reuse for a circular economy,' 2023, doi: 10.1016/B978-0-323-95280-4.00015-1. ".

[229] M. J. , & R. T. (Eds.). (2016). Taherzadeh, "Resource recovery to approach zero municipal waste. CRC Press.".

[230] J. , S. J. , C. S. , C. S. , & D. E. (2015). Dasgupta, "Remediation of textile effluents by membrane based treatment techniques: a state of the art review. Journal of environmental management, 147, 55-72.".

[231] M. (1998). Cheryan, “Ultrafiltration and microfiltration handbook. CRC press.”.

[232] M. S. A. M. S. M. N. A. K. and A. H. K. A. S. Masood, “Current situation of pharmaceutical wastewater around the globe,” The Treatment of Pharmaceutical Wastewater: Innovative Technologies and the Adaptation of Treatment Systems, pp. 19–52, Jan. 2023, doi: 10.1016/B978-0-323-99160-5.00013-8. ”.

[233] R. R. A. P.-M. J. A. et al. ROSAL, “Removal of pharmaceuticals and kinetics of mineralization by O3/H2O2 in a biotreated municipal wastewater. Water research, 2008, vol. 42, no 14, p. 3719-3728.”.

[234] M. K. C. A. T. et al. ANTONOPOULOU, “ An overview of homogeneous and heterogeneous photocatalysis applications for the removal of pharmaceutical compounds from real or synthetic hospital wastewaters under lab or pilot scale. Science of the total environment, 2021, vol. 765, p. 144163.”.

[235] G. F. J. N. H. Z. et al. ASGARI, “ Catalytic ozonation of industrial textile wastewater using modified C-doped MgO eggshell membrane”.

ACKNOWLEDGEMENTS

"***Nothing in life is to be feared, it is only to be understood. Now is the time to understand more, so that we may fear less."***

Marie Curie

To my dear mother Zaineb

Affable, honourable, kind: You represent for me the symbol of goodness par excellence, the source of tenderness, and the example of dedication that has never ceased to encourage and pray for me. Your prayer and blessing have been of great help to me in successfully completing my studies.

I dedicate this work to you as a testimony of my deep love. May God, the Almighty, preserve you and grant your health, long life, and happiness.

To my dear father Ali

No dedication could express the love, esteem, dedication, and respect I have always had for you. Nothing in the world is worth the efforts made day and night for my education and well-being. This work is the fruit of your sacrifices that you have made for my education and training.

To my sisters

As a testimony of the attachment, love, and affection I have for you. Despite the distance, you are always in my heart. I thank you for your unparalleled hospitality and your sincere affection. I dedicate this work to you with all my wishes for happiness, health, and success.

To my brother Maatoug

I dedicate this work to you with all my wishes for happiness, health, and success.

To My friend Barbara Malsegna ‘’Habibi ‘’deserves a special mention for her constant support. I am truly grateful for your friendship and support. Thank you for being there for me every step of the way.

Numerous thanks are owed to those who have supported and inspired me throughout my studies, here at the University of L'Aquila.

I would first like to thank my advisor, Professor Marina Prisciandaro, for her wonderful guidance, continuous support, and motivation throughout my PhD career, which enabled me to accomplish one of the important milestones in my career. With respect to his profound understanding in Chemical and Environmental Engineering, I was able to gain a deeper understanding in wastewater treatment and have developed a greater appreciation for the field.

I am also thankful to my co-supervisor Professor Valentina Innocenzi for her valuable guidance, support, and suggestions throughout the research work.

I would like to give my special thanks Professor Aurora Santos and Miguel Carbone, for their selfless support during my PhD journey in Madrid. Lastly, I am thankful to everyone who has helped me along the way.

Karima

Tesi redatta con il sostegno finanziario del programma

FSE-REACT-EU, PON “Ricerca e Innovazione” 2014-2020 (D.M. 1061/2021)

Asse IV “Istruzione e ricerca per il recupero – REACT-EU”

Azione IV.5 “Dottorati e Contratti di ricerca su tematiche green”

